STUK-A188 May 2002

Nuclear fuel particles in the environment – characteristics, atmospheric transport and skin doses

R. Pöllänen

STUK – Radiation and Nuclear Safety Authority
University of Helsinki, Department of Physics

ACADEMIC DISSERTATION
To be presented, with the permission of the Faculty of Science of the University of Helsinki, for public criticism in the Small Auditorium E204 at Physicum on May 28th 2002, at 12 o'clock a.m.

STUK • SÄTEILYTURVAKESKUS • STRÅLSÄKERHETSCENTRALEN
RADIATION AND NUCLEAR SAFETY AUTHORITY

SEVERAL PAGES OF THIS PUBLICATION ARE INTENTIONALLY LEFT OUT, DUE TO THE FACT THAT THESE PARTS ARE OUT OF INIS SUBJECT SCOPE

The conclusions presented in the STUK report series are those of the authors and do not necessarily represent the official position of STUK.

ISBN 951-712-528-3 (print)
ISBN 951-712-529-1 (pdf)
ISSN 0781-1705

Edita Prima Oy, Helsinki 2002

Sold by:
STUK—Radiation and Nuclear Safety Authority
P.O. Box 14 FIN-00881 HELSINKI Finland
Tel. +358 9 759 881

PÖLLÄNEN, Roy. Nuclear fuel particles in the environment - characteristics, atmospheric transport and skin doses. STUK-A188. Helsinki 2002. 64 p. + app. 90 p.

ISBN 951-712-528-3
ISSN 0781-1705

Keywords Nuclear fuel particle, hot particle, radionuclide, atmospheric transport, activity, skin dose.

SUMMARY

In the present thesis, nuclear fuel particles are studied from the perspective of their characteristics, atmospheric transport and possible skin doses. These particles, often referred to as 'hot' particles, can be released into the environment, as has happened in past years, through human activities, incidents and accidents, such as the Chernobyl nuclear power plant accident in 1986. Nuclear fuel particles with a diameter of tens of micrometers, referred to here as large particles, may be hundreds of kilobecquerels in activity and even an individual particle may present a quantifiable health hazard.

The detection of individual nuclear fuel particles in the environment, their isolation for subsequent analysis and their characterisation are complicated and require well-designed sampling and tailored analytical methods. In the present study, the need to develop particle analysis methods is highlighted. It is shown that complementary analytical techniques are necessary for proper characterisation of the particles. Methods routinely used for homogeneous samples may produce erroneous results if they are carelessly applied to radioactive particles.

Large nuclear fuel particles are transported differently in the atmosphere compared with small particles or gaseous species. Thus, the trajectories of gaseous species are not necessarily appropriate for calculating the areas that may receive large particle fallout. A simplified model and a more advanced model based on the data on real weather conditions were applied in the case of the Chernobyl accident to calculate the transport of the particles of different sizes. The models were appropriate in characterising general transport

properties but were not able to properly predict the transport of the particles with an aerodynamic diameter of tens of micrometers, detected at distances of hundreds of kilometres from the source, using only the current knowledge of the source term. Either the effective release height has been higher than reported previously or convective updraft may have influenced the transport. Models applicable to large particle dispersion in a turbulent atmosphere should be further developed.

The health threat from large nuclear fuel particles differs from that of uniform contamination. In contact with human tissue such as skin, a highly active beta-emitting particle may cause a large but localised dose to the tissue, whereas at distances of more than about one centimetre from the source the dose is negligible. Large particles are poorly inhalable because of their size. They may be deposited in the upper airways but are not easily transported deep into the lungs. Instead, deposition onto the surface of skin is of more relevance with respect to acute deterministic health effects. In the present work, skin doses are calculated for particles of different sizes and different types by assuming the particles are deposited on the body surface. The deposition probability as a function of the number concentration of the particles in air is not estimated.

The doses are calculated at the nominal depth of the basal cell layer and averaged over a square centimetre of the skin. Calculated doses are compared with the annual skin dose limit for the public (50 mGy at a depth of 0.07 mm and averaged over 1 cm^2). After the Chernobyl accident the most active nuclear fuel particles detected in Europe, hundreds of kilometres from the source, would have been able to produce a skin dose exceeding this limit within one hour when deposited onto skin. However, the appearance of deterministic effects necessitates skin contact lasting more than one day.

The health hazards of nuclear fuel particles must be taken into account in estimating the consequences of a severe nuclear accident and planning countermeasures to protect the rescue workers and the general public.

PÖLLÄNEN, Roy. Ydinpolttoainehiukkaset - ominaisuudet, kulkeutuminen ilmakehässä ja ihoannos. STUK-A188. Helsinki 2002. 64 s. + liitt. 90 s.

ISBN 951-712-528-3
ISSN 0781-1705

Avainsanat Ydinpolttoainehiukkanen, kuuma hiukkanen, radionuklidi, kulkeutuminen ilmakehässä, aktiivisuus, ihoannos.

YHTEENVETO

Väitöskirjassa tutkitaan ydinpolttoinehiukkasia - niiden ominaisuuksia, kulkeutumista ilmakehässä ja mahdollisia ihoannoksia. Näitä ns. kuumia hiukkasia voi vapautua ympäristöön ihmisten toiminnan sekä erilaisten tapahtumien ja onnettomuuksien seurauksena kuten esimerkiksi Tshernobylin onnettomuudessa vuonna 1986. Suuret, halkaisijaltaan kymmenien mikro-metrien ydinpolttoainehiukkaset, voivat olla aktiivisuudeltaan satoja kilobecquerellejä ja jopa yksittäiset hiukkaset voivat aiheuttaa välittömiä säteilyhaittoja.

Yksittäisten ydinpolttoainehiukkasten havainnointi ympäristöstä, hiukkasten eristäminen analyysejä varten sekä hiukkasten ominaisuuksien luonnehdinta eivät ole suoraviivaisia, vaan edellyttävät hyvin suunniteltua näytteenottoa ja räätälöityjä analyysimenetelmiä. Tutkimuksessa tuodaan esille menetelmäkehityksen tarve sekä osoitetaan, että toisiaan täydentävien analyysimenetelmien käyttö on välttämätöntä radioaktiivisten hiukkasten ominaisuuksien kartoittamiseksi. Homogeenisille näytteille tarkoitetut menetelmät rutiininomaisesti sovellettuna voivat tuottaa virheellisiä tuloksia ja voivat siten vaikuttaa vääristävästi hiukkasten aiheuttaman terveyshaitan arviointiin.

Tutkimuksessa osoitetaan, että suuret ydinpolttoainehiukkaset kulkeutuvat ilmakehässä toisin kuin pienet hiukkaset ja kaasumaiset aineet. Kaasumaisten aineiden trajektorit eivät siten välttämättä ole riittäviä arvioitaessa onnettomuudessa vapautuvien radioaktiivisten aineiden kulkeutumista ja aluetta, jonne kuumat hiukkaset voivat kantautua. Sekä yksinkertaistettua että kehittynyttä, todellisiin säätietoihin perustuvaa laskentamallia sovellettiin erikokoisten hiukkasten kulkeutumiseen

Tshernobylin onnettomuudesta. Mallit kykenivät varsin hyvin ennustamaan suurten hiukkasten kulkeutumista, mutta aerodynaamiselta halkaisijaltaan jopa kymmenien mikrometrien hiukkasten löytymistä useiden satojen kilometrien etäisyydeltä päästölähteestä ei pystytty kunnollisesti selittämään olemassaolevan tiedon perusteella. Joko vapautumiskorkeus on ollut aiemmin raportoitua suurempi tai konvektiiviset pystysuuntaiset virtaukset ovat vaikuttaneet kulkeutumiseen. Leviämismalleissa todettiin olevan kehittämisen tarvetta erityisesti turbulenttisen dispersion ja suurten hiukkasten kulkeutumisen osalta.

Ydinpolttoainehiukkasten aiheuttama uhka poikkeaa tasaisen kontaminaation tapauksesta. Kudoksen kanssa kosketuksessa oleva beetasäteilyä lähettävä hiukkanen voi aiheuttaa suuren mutta erittäin paikallisen säteilyannoksen, kun taas kauempana, noin yli senttimetrin päässä, annos on vähäinen. Kokonsa takia suuret ydinpolttoainehiukkaset eivät hengitysilman mukana kulkeudu syvälle keuhkoihin, vaan jäävät esimerkiksi ylähengitystiehyeisiin. Akuutteja säteilyseurauksia tarkasteltaessa hiukkasten depositio ihoon ja tätä kautta saatava säteilyannos onkin varteenotettava altistusreitti. Työssä laskettiin mahdollisia ihoannoksia erityyppisille ja erikokoisille ydinpolttoainehiukkasille olettaen hiukkasten olevan kiinnittyneenä ihon pintaan. Deposition todennäköisyyttä hiukkasten lukumääräpitoisuuden funktiona ei arvioitu.

Ihoannokset laskettiin tyvisolukerroksen nimellissyvyydelle ja keskiarvoistettuna neliösenttimetrin pinta-alalle. Laskennallisten annosten suuruutta verrattiin väestön ihoannosrajaan (50 mGy vuodessa ihon neliösenttimetriä kohden syvyydelle 0,07 mm). Tshernobylin onnettomuuden jälkeen aktiivisimmat Euroopasta, satojen kilometrien etäisyydeltä päästöpaikasta löydetyt ydinpolttoainehiukkaset olisivat voineet jopa alle tunnissa aiheuttaa tämän rajan ylityksen deponoiduttuaan ihon pintaan. Deterministisen terveyshaittojen ilmaantumiseen olisi kuitenkin vaadittu kuitenkin yli vuorokauden kestävä ihokontakti.

Ydinpolttoainehiukkasten aiheuttama terveysuhka täytyy ottaa huomioon arvioitaessa mahdollisen vakavan ydinonnettomuuden säteilyseurauksia ja suunniteltaessa suojelutoimenpiteitä pelastustyöntekijöille ja väestölle.

CONTENTS

ORIGINAL PUBLICATIONS

The present thesis is based on the following original publications, which are referred to in the text as roman numerals I – VIII. In addition, the results of the licentiate thesis (Pöllänen 1997) in particular and other publications of the disputant mentioned in the reference list are also taken into account.

I Toivonen H, Pöllänen R, Leppänen A, Klemola S, Lahtinen J, Servomaa K, Savolainen A L, Valkama I. A nuclear incident at a power plant in Sosnovyy Bor, Russia. Health Physics 1992; 63: 571 - 573.

II Pöllänen R, Toivonen H. Skin doses from large uranium fuel particles - application to the Chernobyl accident. Radiation Protection Dosimetry 1994; 54: 127 - 132.

III Pöllänen R, Toivonen H. Transport of large uranium fuel particles released from a nuclear power plant in a severe accident. Journal of Radiological Protection 1994; 14: 55 - 65.

IV Pöllänen R, Toivonen H. Skin dose calculations for uranium fuel particles below 500 μm in diameter. Health Physics 1995; 68: 401 - 405.

V Pöllänen R, Valkama I, Toivonen H. Transport of radioactive particles from the Chernobyl accident. Atmospheric Environment 1997; 31: 3575-3590.

VI Pöllänen R. Highly radioactive ruthenium particles released from the Chernobyl accident: particle characteristics and radiological hazard. Radiation Protection Dosimetry 1997; 71: 23 - 32.

VII Pöllänen R, Ikäheimonen T K, Klemola S, Juhanoja J. Identification and analysis of a radioactive particle in a marine sediment sample. Journal of Environmental Radioactivity 1999; 45: 149 - 160.

VIII Pöllänen R, Klemola S, Ikäheimonen T K, Rissanen K, Juhanoja J, Paavolainen S, Likonen J. Analysis of radioactive particles from the Kola Bay area. Analyst 2001; 126: 724 - 730.

This work was conducted in the Laboratory for Airborne Radioactivity at STUK - Radiation and Nuclear Safety Authority in 1992 – 2001. The disputant is the sole author of publication VI and, except for publication I, the leading writer of other publications. In publication I, the disputant performed nuclide ratio calculations and contributed the preparation of the paper.

The disputant designed publications II, III and IV together with the co-author, and was responsible for the calculations and the overall preparation of the papers.

Intense co-operation with Finnish Meteorological Institute (FMI) was a prerequisite for achieving the results of the atmospheric transport calculations in publication V. The disputant designed the research, performed dose calculations, made the review of particles from the Chernobyl accident, and interpreted the results. FMI performed atmospheric transport calculations.

Close collaboration with other co-authors of publications VII and VIII was necessary in characterising the properties of radioactive particles. The disputant designed the research and prepared the papers as well as performed the identification and isolation of the particles. The disputant took the need and use of other analytical methods under advisement and interpreted the results. A notable part of experimental particle characterisation was performed by co-authors.

1 INTRODUCTION

Radioactive particles considered in the present thesis are tiny pieces of artificial radioactive material, mainly nuclear fuel particles, dispersed into the environment because of different human activities. Radioactive particles are considered here as aggregates of radioactive atoms that give rise to inhomogeneous distribution of radionuclides significantly different from that of the natural background particles of the sample. Nuclear fuel particles are those originating from nuclear fuel. Although particle size may vary considerably mainly large fuel fragments, diameter from a few micrometers up to tens of micrometers and often referred to as 'hot particles', are of special concern here. Radioactive particles smaller than about 1 μm in diameter and generated by various nucleation/condensation processes are not treated.

There exists no widely accepted definition for the concept of a 'hot particle'. It is often used in the meaning that the particle is highly active; sometimes it is used for particles having high specific activity. Khitrov *et al.* (1994) have suggested the following definition: a hot particle is a particle with any radionuclide or composition with size up to 50 - 80 μm and activity over 4 Bq. The National Council on Radiation Protection and Measurements (NCRP 1999) states that "hot particles are considered to be > 10 μm but < 3000 μm in any dimension. Hot particles smaller than 10 μm may be treated as general contamination...". Radioactive particles originating from atmospheric nuclear tests are historically referred to as hot particles. This concept was later attributed to fuel fragments originating from the Chernobyl accident.

Hot particles have been frequently identified after past nuclear incidents as shown e.g. by Salbu (2000): "A significant fraction of radionuclides released by nuclear events, for instance nuclear weapon tests, nuclear reactor accidents, and fires involving nuclear installations is associated with particles. Furthermore, effluents from nuclear reactors and reprocessing plants under normal operating conditions contain radionuclides in particulate and colloidal form. Radioactive particles are also observed in the vicinity of radioactive waste dumped at sea." Hot particles are also regularly detected in normally operating nuclear power plants. The NCRP (1999) concluded that "hot particles associated with nuclear facilities have been mostly an 'inplant' problem associated with nuclear reactors, but the possibility that hot particles

could inadvertently escape to the outside environment cannot be entirely dismissed".

Although the presence and release of hot particles into the environment from past nuclear incidents are widely documented, they are often considered as a unique and "rare form of radioactivity" (Kutkov *et al.* 1995) and treated something like a scientific curiosity (Sandalls *et al.* 1993) which may lead to an underestimation of their significance. The particulate nature of radioactive substances is not necessarily taken properly into account in environmental monitoring and consequence analyses of nuclear accidents. In traditional consequence analyses 'radioactivity' (not necessarily particles) is assumed to be released, transported, dispersed, and deposited on a target area. Existing monitoring systems are rather designed to detect 'radioactivity' than individual particles; and in laboratory analyses the radioactive species are often considered as 'becquerels' more or less evenly distributed in a sample. As regards the abovementioned issues, the results of the present thesis give a new perspective and ideas for subsequent studies.

The role of hot particles in estimating the significance of radioactive releases is far from clear. Vajda (2001) concluded that "there is still a lack of knowledge to fully understand the processes of hot particle formation, transport, migration, bioavailability and health hazards". The aim of the present thesis is to study nuclear fuel particles from the perspective of health hazards. The studies focuses on

- the characterisation of nuclear fuel particles,
- their transport and dispersion in the atmosphere and
- the estimation of possible skin doses.

The hazard cannot be considered hypothetical. At the time of the Chernobyl accident, six persons were near the plant at different distances in the direction to which the radioactive plume was moving (Barabanova and Osanov 1990). They were exposed to fallout particles which covered their skin and the ground. The person who received the highest γ-dose had very severe and widespread β-radiation burns (the β-dose was more than 20 times higher than the γ-dose). At the time of the accident, he was 1 km from the plant and remained there for an hour. He was covered with black dust and died 17 d after the exposure. Except for one person with the smallest dose, other victims in this area also died. No beta burns were reported in distant areas.

Highly active particles (activity of ^{137}Cs up to 10^8 Bq), originating from the disposal site of manipulated nuclear fuel of the material test reactor, were observed in the Dounreay, Scotland (COMARE 1999). COMARE performed risk estimation for ingested radioactive particles and arrived at the conclusion that "the particles, if encountered, present a hazard to health, and the hottest particles could induce serious acute radiation effects. Whilst the probability of encountering a particle is small, it is not negligible."

Since nuclear fuel particles may pose a health hazard, there is a need to develop methods for atmospheric transport and dispersion that take into account realistic weather conditions and the particulate nature of the release plume. As shown in publication V, nuclear fuel particles may present a potential health threat far from the source. Particles may be transported hundreds of kilometres in the atmosphere and, depending on wind conditions during the transport, also to other areas than gaseous species.

The health hazard caused by nuclear fuel particles is different compared with uniform contamination. Even if their number concentration in air is low, it is possible some individuals will receive a highly active particle deposited for example on the skin. Consequently, only a small fraction of the tissue may be exposed at levels that may cause severe health damage. Since the activity of a particle may be more than 1 MBq, the dose in its immediate vicinity may be very large. Risk estimations have been performed for inhalable hot particles from Chernobyl (e.g. Hofmann *et al.* 1988) but some of the particles detected after past nuclear incidents were much more than 10 μm in aerodynamic diameter and, consequently, are poorly inhaled (NCRP 1999). Instead, when deposited on the skin they may produce a notable skin dose within a short time (Publication VI). This fact is often disregarded in assessing the significance of large radioactive particles (see e.g. Garland and Nicholson, 1991).

The health threat that large nuclear fuel particles may pose is determined by particle properties such as composition, activity and size and their concentration in the environment. In practice, quantitative risk estimation may be useless owing to the very large uncertainties related to particle release, characteristics, appearance, and bioavailability. In the present thesis, rather an identification of short-term hazards than a detailed risk analysis is performed using the Chernobyl accident and nuclear fuel fragments originating from it as an example. A proper understanding of the nature of the

hazard caused by highly active particles may facilitate designing the countermeasures that are needed in future nuclear incidents.

2 NUCLEAR FUEL PARTICLES IN THE ENVIRONMENT

Radioactive particles were distributed worldwide as a result of atmospheric nuclear tests mainly in 1950s and 1960s (see e.g. Salbu 2000, Vajda 2001). Local contamination due to nuclear bomb debris occurred as a result of aircraft crashes in Thule, Greenland, in 1968 (Moring *et al.* 2001) and Palomares, Spain, in 1966 (Romero 2001). The uncontrolled re-entry of nuclear-powered satellites into the atmosphere, such as Cosmos 954 in Canada in 1978 (Gummer *et al.* 1980), led to the dispersion of highly active particles into the environment.

The nuclear fuel particles considered in the present study may be generated in severe nuclear accidents and released into the environment, as occurred in the Chernobyl accident. The release of nuclear fuel particles cannot be considered unique to severe nuclear accidents only. After the Sosnovyy Bor incident in Russia 1992 nuclear fuel particles were detected in air samples collected along the coast of the Gulf of Finland (publication I, Paatero and Hatakka 1997). In addition, particulate radioactive materials have been detected in the environment after the releases from reprocessing plants, such as in Tomsk in 1993 (Hyder *et al.* 1996). Particles have been observed in aquatic environments (Salbu 2000) and in the areas in which the storage of nuclear fuel and radioactive waste exists (publication VIII).

Nuclear fuel particles have been also detected in nuclear power plants during their normal operation. NCRP (1999) reviewed in-plant radioactive particles found in U.S.A. Comprehensive surveys in nuclear power plants revealed the presence of fuel type particles as well as those composed of activation products. Although the review concentrated on the particles found in nuclear power plants NCRP concluded that "hot particles can occur in research reactor facilities and other nuclear facilities". Highly active particles are treated as an occupational safety problem rather than as a hazard to the public. However, "minimising the production and release of hot particles are clearly the preferred control methods, but the possibility of such events occurring cannot be ignored" (NCRP 1999). Mandjukov *et al.* (1994) concluded that "the presence of hot particles in the NPPs seems to be the rule rather than the

exception." However, "radioactive particles, tens of μm or more in diameter, are unlikely to be emitted directly from nuclear facilities with exhaust gas cleansing systems, but may arise in the case of an accident or where resuspension from contaminated surfaces is significant" (Garland and Nicholson, 1991).

Although highly active particles have been frequently detected after past nuclear incidents, their appearance and distribution even in the vicinity of the release site is generally not known. Published deposition maps of radionuclides such as ^{137}Cs, based for example on an environmental survey using mobile radiation detection systems, do not necessarily reflect the distribution of hot particles. Their presence must be verified using a well-defined sampling and sample analysis programme (Fig 1).

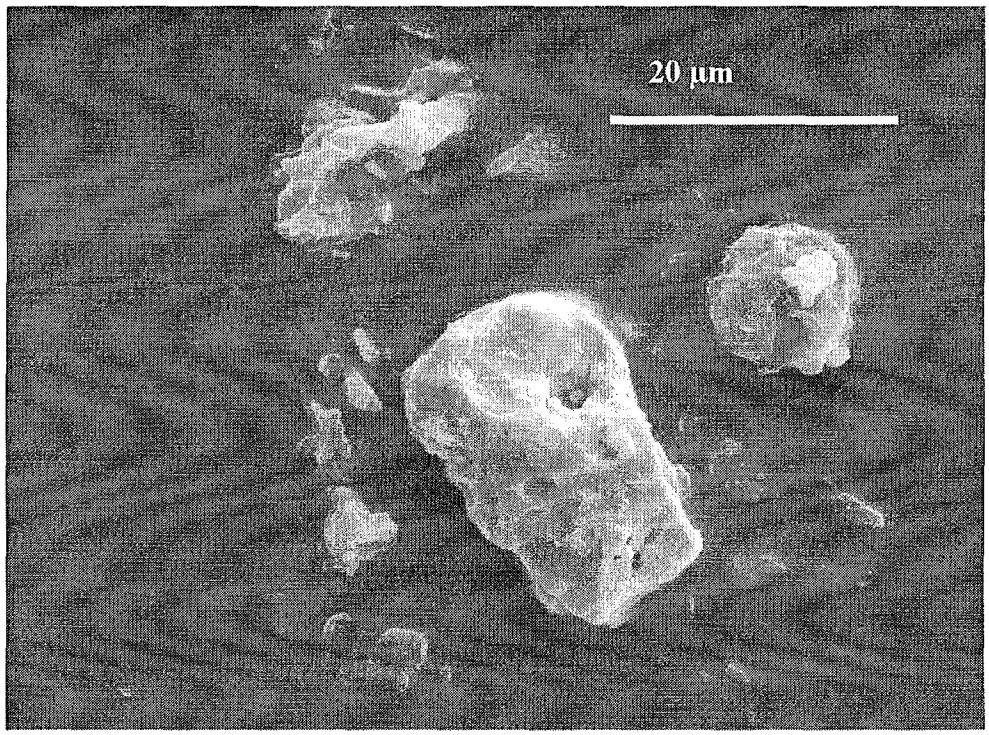

Figure 1. *Nuclear fuel particle (large object in the middle) detected in a marine sediment sample (publication VII).*

Despite the fact that more than a hundred scientific papers dealing with radioactive particles in the environment have been published (see for example the reference list by Pöllänen (1997)), the particle data from past nuclear incidents is far from complete owing to sparse sampling and the difficulties in analysing particle properties. Usually only a limited number of individual particles have been identified and, subsequently, characterised by different analytical means. Nevertheless, the number of identified radioactive particles especially from the Chernobyl accident is large enough to facilitate their classification into different groups. This makes it possible to understand the processes of particle formation and release.

2.1 Formation and release of particles from nuclear fuel

The characteristics of nuclear fuel particles reflect the properties of the source material and provide detailed information of their origin, formation, transport, reactivity, transformation reactions, and environmental impact (Jambers *et al.* 1995). The radionuclide composition of nuclear fuel particles characterises the nuclear fuel and different physical processes occurring during irradiation; elemental composition refers to the mechanisms during particle formation. The particle may contain nuclides that are already present in the source material except when nuclides from other sources are attached to the particle during transport or generated through radioactive decay.

In a severe nuclear accident, radioactive materials emitted from nuclear fuel and released into the environment may be in the form of gases, vapours and particles of different sizes. Soon after the release, the gaseous materials may be converted into solid species because of radioactive decay (for example ^{87}Kr $\rightarrow$ ^{87}Rb). High temperature may lead to the emission of volatile materials such as I, Cs, or their compounds and lead to the subsequent generation of small (diameter less than 1 μm) radioactive particles via nucleation, condensation, and coagulation. The nuclide composition of these 'condensation-type' particles deviates from that of nuclear fuel. After the Chernobyl accident, nuclides such as ^{103}Ru, ^{131}I, ^{132}Te, ^{134}Cs and ^{37}Cs were generally detected in these particles.

Energetic events may lead to the fragmentation of nuclear fuel, as occurred in the Chernobyl accident. Particles generated through mechanical fuel disintegration are usually large (diameter larger than 1 μm) and their nuclide

composition resembles that of the source material. This does not necessarily mean that each particle has the same composition because the source material is usually somewhat inhomogeneous. In the Chernobyl accident, 'U-type' fuel fragments with composition similar to nuclear fuel on the average were released into the environment. In addition, 'Ru-type' particles composed mainly of elements such as Ru, Rh, Mo, Tc and Pd were released from the damaged plant. These particles were often identified as the metallic precipitates present in irradiated nuclear fuel (publication VI). However, their formation/release mechanisms are still unclear. Mechanical emission is an obvious mechanism to explain the characteristics of some of the Ru-type particles found in the environment (publication VI).

Complex physical-chemical phenomena may affect the composition of fuel fragments if the temperature during the particle formation/emission is high. The elements or compounds, which have sufficiently high vapour pressure, may be easily vaporised from the particles that are then depleted with respect to these materials. U-type fuel fragments from the Chernobyl accident were generally depleted with respect to elements such as I and Cs.

2.2 Nuclear fuel particles from the Chernobyl accident

Nuclear fuel particles from the Chernobyl nuclear power plant were identified in several European countries. Pöllänen (1997) summarised those findings in which single particles or their detailed properties were analysed (also publication V). The particles were found in air filters or were collected from different surfaces. The method and the time of collection and the location of sampling have a crucial effect on the detectable characteristics of the particles. At the time of the Chernobyl accident, only a few laboratories were aware of the occurrence of nuclear fuel particles and thus their findings were clustered and sparse. Particles were systematically collected in only a few locations, not over wide areas, and the characteristics of only a few hundred radioactive particles have been reported in literature. The reported range of values of the number of deposited particles and especially the number concentrations in air is wide (Tables I and II) because of difficulties in locating the particles, different threshold values in detecting the particles, different analysis methods, and different timing of the estimates.

Table I. *Number of deposited hot particles per square meter (Pöllänen 1997). Some authors have not reported the detection threshold (in terms of activity). In this case the reported detection limit is denoted as a question mark.*

Reference	Location	Reported detection threshold	m^{-2}
Rytömaa *et al.*, 1986	Open areas in Finland	1 Bq	up to 10000 (mean<1000)
Robertson 1986,	Stockholm	?	5 - 8
Perkins *et al.*, 1989	Öland	?	< 1
Kerekes *et al.*, 1991	Stockholm, Gotland, Gävle	90...220 Bq	~ 0.2
Devell 1988	Studsvik	100 - 200 (^{141}Ce) Bq	1
Osuch *et al.*, 1989	North-eastern Poland	50 Bq	0.007 - 1.9
Broda 1987	Mikolajki	100 Bq	0.1
Petryaev *et al.*, 1990	40 - 250 km from the plant	?	10^{5} - 10^{3}
Wahl *et al.*, 1989	Konstanz	1 - 10 Bq	170
		10 - 50 Bq	38
		> 50 Bq	3
Kritidis *et al.*, 1988	Athens	1-10 Bq (7.5.1986)	130
		10-100 Bq (7.5.1986)	13
		100-1000Bq (7.5.1986)	1.3
Lindner *et al.*, 1992	4 km from the plant	d_p < 5 μm	> 10000
		d_p > 5 μm	5000
Viktorova and Garger 1990	5 km from the plant	?	50000
	90 km from the plant	?	15000
Khitrov *et al.*, 1994	20 km from the plant	2 × background	50 - 60
	40 km from the plant	2 × background	30 - 40
(Sandalls *et al.*, 1993)	60 km from the plant	2 × background	10
	Kiev	2 × background	1 - 2

A simple order-of-magnitude-estimate of the number of deposited U-type particles per unit area can be achieved as follows: by assuming that the amount of nuclear fuel released into the environment in the form of particles is 7000 kg (Sandalls *et al.* 1993) and by assuming that the equivalent volume diameter of the particles is 10 μm and their density 10500 kg m^{-3}, the number of released particles is then approximately 10^{15}. The sum activity of relatively

long-lived isotopes is 1300 Bq per particle (see Table IV, decay time 10 d). If particles are deposited within a zone of 30 km in radius the number of deposited particles per square meter is on the average 450 000 m^{-2} (which refers to the activity of about 500 MBq m^{-2}). This approximate estimate is by a factor of ten higher than the numbers reported near the Chernobyl nuclear power plant (Table I).

Table II. *Number concentration of hot particles in ambient air (Pöllänen 1997).*

Reference	Location	Time	Detection threshold (Bq)	m^{-3}
Toivonen *et al.*, 1988	Helsinki	28.4.1986	10 (May 1987)	0.08
Mattsson *et al.*, 1986	Helsinki	28 - 30.4.1986	50	0.0011 - 0.020
	Nurmijärvi	27 - 30.4.1986	50	0.0022 - 0.022
Sinkko *et al.*, 1987	Nurmijärvi	27 - 28.4.1986	?	0.019 - 0.08
Lujanas *et al.*, 1994	Vilnius	28 - 29.4.1986	?	10000
		29.4 - 1.5.1986	?	4 - 866
Kolb 1986	Brunswick	1.5 - 9.5.1986	1 - 15	0.0002
Wahl *et al.*, 1989	Konstanz	May 1986	1 - 10	0.068
			10 - 50	0.015
			> 50	0.0011
Balashazy *et al.*, 1988	Budapest	29.4 - 8.5.1986	10 (2.7.1986)	5×10^{-5}

Large-scale fallout from the Chernobyl accident was spatially heterogeneous, i.e. the territorial distribution of nuclides such as ^{95}Zr, ^{141}Ce, ^{144}Ce, ^{134}Cs and ^{137}Cs varied widely (Arvela *et al.* 1990; Jantunen *et al.* 1991, Mietelski and Was 1995). Smaller inhomogeneities with elevated amounts of radioactive materials were also identified (Luokkanen *et al.* 1988); these 'hot spots' were a few kilometres in diameter. In Lithuania, a small number of hot spots (several tens of square metres in area) were found on the ground (Lujanas *et al.* 1994). Near the Chernobyl power plant, hot spot areas with a marked occurrence of radioactive particles were detected (IAEA, 1991). In Poland, spots as small as 30 cm in diameter were identified (Broda 1987).

The local distribution of nuclear fuel particles was extremely inhomogeneous. The relative occurrence of U-type and Ru-type particles differs. This observation suggests that they were not released in the same way or their transport was different. It is possible that the particles deposited in Poland originated from a different part of the reactor compared to those which were transported to Scandinavia. This was deduced by different depletion of Cs and different isotope ratios of $^{103}Ru/^{106}Ru$ and ^{144}Ce (Broda 1987). Large objects may be transported hundreds of kilometres from the plant. For example, Broda *et al.* (1989) reported even 600 µm particles in Poland, suggesting that the bulk of these particles comprised fragments of the reactor graphite moderator. Radioactive particles were also found in human tissue.

The content of nuclear fuel particles, their size and isotopic composition depend on the distance from the Chernobyl nuclear power plant. The nuclear fuel particle contribution in the 30-km zone around the plant was at least 65 % of the total activity (Tcherkezian *et al.* 1994). The territorial distribution of nuclear fuel particles and condensable particles differ. The proportion of condensation particles is estimated as 60 % and 98 % at distances up to 25 and 60 km from the NPP (Pavlotskaya et al. 1994). Within 10 km from the plant, less than 3 % were attributed to condensed particles and more than 95 % to fuel particles (Salbu et al. 1994).

3 CHARACTERISATION OF RADIOACTIVE PARTICLES

The prerequisites for achieving proper results in particle analysis are the awareness of the possible existence of hot particles in the environment, well-designed sampling procedures and the capability of identifying and isolating particles from the sample. In addition, the availability of proper equipment for particle analysis is necessary, as is a well-trained and experienced staff that is able to apply the methods normally used in bulk analyses to the analysis of individual particles.

The analysis of individual particles complements conventional bulk analysis. However, the measured properties of individual particles are not necessarily sufficient in estimating the relevant characteristics of the particles, their transport in the environment, and the possible threats to health. Sometimes calculative methods must be applied. This is especially the case when the appropriate methods of analysis are not available or they are used too late: nuclear fuel particles have been identified and analysed typically weeks or even years after the accidents, preventing the detection of short-lived nuclides. In addition, the particles were usually analysed with gamma-ray spectrometers only. Although nuclides with low gamma yield or pure beta emitters as well as those with low activity were not generally detected, they may essentially contribute to possible health hazards (publication VI).

Particle analysis can be divided into the following phases:

- Identification of the possible presence of individual radioactive particles in a sample; estimation of their number in the sample and, possibly, the activity of individual particles.
- Isolation and separation of the radioactive particles from the sample that may contain billions of inactive uninteresting background particles.
- Analysis of particle characteristics using different methods.
- Interpretation of the analysis results and comparison with calculated particle properties.

3.1 Sampling, identification, and isolation

Standard radiation monitoring techniques may provide information about areas with elevated amount of contamination (hot spots) but they are not necessarily appropriate for the identification of individual hot particles. Sampling techniques are needed. Direct identification of the presence of hot particles in the environment requires devices that are able to scan the inhomogeneities of the contamination (e.g. Khitrov *et al.* 1994).

The procedures for particle sampling (method, time and location) and analysis (method and time of analysis) determine those properties of the particles that are possible to detect. Especially the sampling distance from the plant and the time and methods of analyses make a notable contribution in obtaining a representative sample of radioactive particles. For example, coarse particles cannot be detected far from the plant owing to their short residence time in air and short-lived nuclides cannot be detected if sampling and analyses are performed too late.

A range of sampling and sample manipulation techniques exists for different types of sample materials (Vajda 2001). For example, airborne radioactive particles are usually collected using air filtration or deposition samplers. Without particle isolation/separation, average quantities, such as activity concentrations in air, are then obtained. However, the size distribution of the particles can be measured using impactors. Single particles from other types of samples can be identified as deposited onto different surfaces or incorporated in the matrix of a bulk sample (publications VII and VIII).

The presence of non-volatile nuclides, such as ^{154}Eu (publication VII), detected by traditional bulk sample analysis may give a hint of the presence of hot particles. Another possibility for making a preliminary identification of the presence of hot particles in the samples is to perform repeated mixing of the samples and subsequent counting (Bunzl 1998). Sample splitting into smaller subsamples and their analysis is another option. In addition, autoradiography (Pöllänen *et al.* 1996) or imaging plate techniques (Moring *et al.* 2001; Zeissler *et al.* 1998) are appropriate methods that also provide data on the particle distribution in a sample (Fig. 2).

A prerequisite for analysing the properties of individual particles is isolation and further separation of the particles in question from the sample. The advantages of isolation are apparent: by analysing individual particles, it is

possible to achieve results that are otherwise not possible owing to the interference of non-relevant bulk particles in the sample. Adhesive tapes are often used in the isolation (publications VII and VIII). The identification and analysis of individual hot particles may sometimes be possible without manual particle isolation using scanning electron microscopy or secondary ion mass spectrometry. A sufficiently large number of hot particles must then be present in the sample and the physical size of the sample should be small enough.

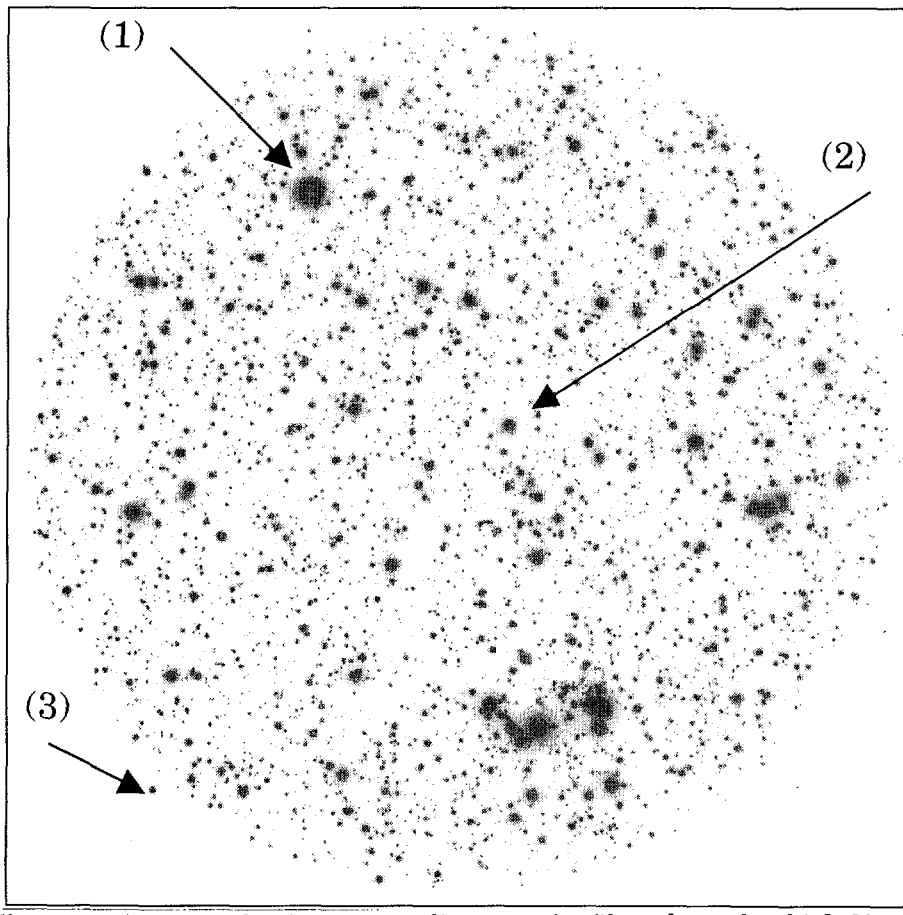

Figure 2. *An example of an autoradiogram of a filter through which 25 m^3 air has passed (Pöllänen et al. 1996). The sample containing activation-type radioactive particles was collected in a nuclear power plant. The film exposure time was 10 d. The total activity of the filter was about 0.5 kBq. Three particles were separated from the filter and analysed using a gamma-ray spectrometer and nuclides ^{54}Mn, ^{58}Co, ^{59}Fe, ^{60}Co and ^{95}Zr were identified. The sum activity of these nuclides in the particles 1, 2 and 3 were 25 Bq, 12 Bq and 0.7 Bq, respectively.*

3.2 Analysis methods

A range of assay methods is needed for the complete characterisation of hot particles. The information that can be obtained in analysing the particles depends on the method of analysis. The information collected from the inactive nuclides of the particle may be as valuable as that obtained from radioactive nuclides. In forensic analyses, the particle characteristics may function as a fingerprint of their origin. For example, the comprehensive analyses of the hot particle detected in the marine sediment sample from Gotland deep (publication VII) were of fundamental importance in estimating the particle's origin.

The scientific and technical challenges of hot particle manipulation and analysis are associated with the small size of the particles and their identification from (inactive) non-interesting background particles. Different techniques have specific limitations of their own, which may lead to difficulties in determining the optimum method for analysing the particle in question. However, if they are appropriately used, the results of their analysis may complement each other. Special emphasis must be placed on the order of different analysis methods. The order depends on the type of information needed in each case (Table III).

Vajda (2001) classified hot particle analysis techniques into nuclear analytical techniques and microanalytical techniques. The main advantages of using nuclear analytical techniques compared to microanalytical ones are their sensitivity and relatively simple use. Radiation emitted by radioactive materials in the sample is 'passively' registered whereas microanalytical techniques need stimulation, typically a particle beam ejected into the specified object to be analysed, before detecting the response signal. This means that in microanalytical techniques the hot particle in question must be usually unequivocally identified before the analysis. In nuclear analysis techniques, the particle does not necessarily have to be identified provided the background particles in the sample do not contain significant amounts of the same radionuclides as the particle itself.

Nuclear analytical techniques commonly used in particle analysis, and also utilised in publications VII and VIII, are autoradiography or similar types of imaging systems, and α, β and γ-ray spectrometry. The outcome of these methods is the nuclide composition of the particles and in the case of

autoradiographic/imaging techniques, the particle distribution in the sample. Other methods, such as different types of dose rate meters, are used especially during sample manipulation.

Table III. *Methods of analyses used in the present thesis (publications VII and VIII).*

Method of analysis	Purpose	Property to be measured
Autoradiography	Identification, localisation, and isolation of radioactive particles.	Number of radioactive particles, total beta activity of a particle.
Gamma-ray spectrometry	Presence and amount of gamma-emitting radionuclides in a particle/sample.	Activity of gamma-emitting radionuclides.
Beta spectrometry	Presence and amount of beta-emitting radionuclides in a particle/sample.	Activity of beta-emitting radionuclides (entire or dissolved particle).
Alpha spectrometry	Presence and amount of alpha-emitting radionuclides in a particle/sample.	Activity of alpha-emitting radionuclides (entire or dissolved particle).
Scanning electron microscopy with X-ray analysis	Visualisation and elemental composition of radioactive particles.	Particle size, concentration of elements.
Secondary ion mass spectrometry	Visualisation and nuclide composition of a radioactive particle.	Concentration of nuclides.
Infrared spectrometry	Material characterisation.	Chemical composition.

Microanalytical techniques are frequently used in material sciences but their applications to radioactive particles are rare. The small size of the particles, the absence of suitable standards and difficulties in determining the interaction volume (the volume from which measurable information can be achieved) make it difficult to obtain quantitative results. Depending on the type of beam used, the information may come from the surface of the particle or from the deeper parts. The key characteristics of the hot particles that can be detected using microanalytical techniques are their element (or sometimes

nuclide) composition and structure. In addition, the chemical composition, crystal structure, oxidation state etc. may be obtained.

Since most microanalytical techniques require special and usually very expensive equipment, co-operation between different research centres is often necessary. Their use in particle analysis is also very expensive because of the amount of manual work with respect to the number of analysed particles is often very small (publications VII and VIII). A notable drawback of most microbeam techniques is the need to operate under vacuum, which may cause the loss and transformation of volatile and unstable compounds.

Different types of electron microscopes are widely used in particle analysis. They use an electron beam to excite the atoms in the target sample. Characteristic X-rays as well as secondary electrons, backscattered electrons, transmitted electrons, or diffracted electrons are detected. Scanning electron microscopy with an energy dispersive X-ray spectrometer is used in the present analyses (publications VII and VIII). Equipment using other types of beams, such as X-rays, protons, sychroton radiation etc. was not available.

Mass spectrometers are used to determine the elemental and nuclide composition of bulk materials, but applications to particle analysis are scarce. In mass spectrometry, the samples (or the target in question) are decomposed and ionised and then ejected into the unit which separates the ions with different mass-to-charge ratios. Mass spectrometers can be used in hot particle analysis provided the particle in question can be separated from the bulk sample (publication VIII). Other techniques, such as infrared spectroscopy (publication VIII), are very seldom used in particle analysis.

3.3 Calculation of particle characteristics

The characteristics of nuclear fuel particles can be predicted in certain situations. In order to estimate particle properties, the primary assumption is that nuclear fuel particles reflect the characteristics of nuclear fuel. Another assumption is that the proportions of certain elements remain unchanged during particle formation and release. This, of course, is not valid for gaseous (or volatile) species. The third assumption is that other materials are not significantly agglomerated/condensed into an existing nuclear fuel particle or materials are not evaporated, i.e. particle composition does not change remarkably during transport and deposition. However, when particles are

deposited on the ground their weathering leads to mobilisation and the possible intake of the radionuclides incorporated in the particles.

The characteristics of nuclear fuel particles as well as their abundance in various media must be known in order to estimate their potential health effects and risks. The dose calculations cannot be fully performed using the information gathered merely from particles detected in the environment since particle sampling and detection may not be necessarily representative and the analytical methods may not be necessarily adequate for estimating all the relevant properties of the particles (publication VI). Sometimes prompt activity analyses of the particles are not possible because of the tedious procedures needed for particle sampling, isolation, and analysis. Calculative methods are needed.

An approach based on fuel inventory calculations is used to supplement characteristics that cannot be obtained from measurements. A typical example of this procedure is that the activity of a relatively short-lived nuclide is calculated from the activity of a more long-lived nuclide of the same element, provided the decay time and burnup of the fuel from which the particle has been originated are known.

The amount of (radioactive) materials in a reactor core, the 'inventory', is estimated using the ORIGEN2 (Croff 1983) computer code designed to calculate the different characteristics of nuclear fuel. It calculates numerically the concentrations of different elements and nuclides in the nuclear fuel. The main phenomena considered in ORIGEN2 are nuclear fission, neutron-induced transmutation, and radioactive decay. A set of ORIGEN2 calculations for different reactor types was performed as a function of fuel burnup and decay time. The results of the calculations are stored in a database that is used to estimate the characteristics of irradiated fuel and particles.

Since the output of ORIGEN2 is very large and the code itself does not include the possibilities to treat all this information in a modern way, a tool for data management, known as OTUS, was developed (Pöllänen *et al.* 1995). Inventory data were calculated for PWR (VVER-440), BWR (Swedish type) and RBMK (Chernobyl) reactors using simplified operation histories (Pöllänen 1997), i.e. reactor power was assumed to be constant during the irradiation, and fuel outages were taken into account except for the RBMK reactor. The database contains the concentrations of the elements and nuclides present in the reactor fuel. The activity of a specified nuclide per unit volume of the reactor fuel in

question is obtained multiplying fuel density by activity concentration (Fig. 3). Since the specific power used in the calculations was assumed to be constant during irradiation, the calculated concentrations are rather indicative than true estimates of the amount of materials present in the reactor fuel.

The Chernobyl accident showed that the isotopic composition of U-type particles generally reflects the core inventory (Osuch *et al.* 1989). The proportions of certain elements in a nuclear fuel fragment, e.g. Zr and Ce, are similar to those in nuclear fuel. The proportions of their nuclides are determined only by the burnup and cooling time (decay time) of the specified reactor fuel provided that isotopes of the same element behave similarly during particle formation and release. In addition, the activities per unit volume may differ by a factor of about two in different NPP reactor types (Pöllänen 1997).

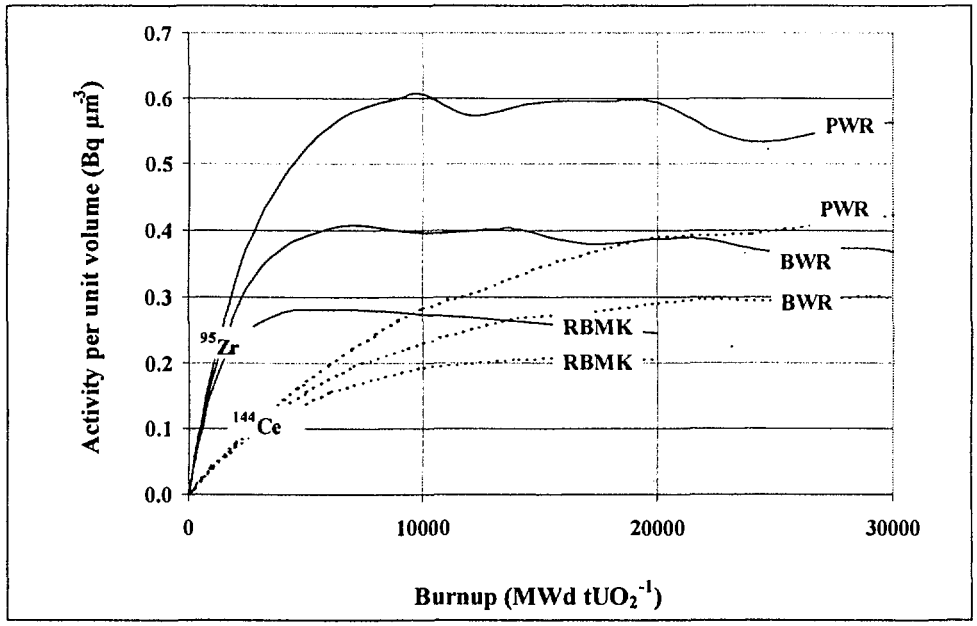

Figure 3. *An example of the activity per unit volume (Bq μm^{-3}) of ^{95}Zr and ^{144}Ce in PWR (VVER440), BWR and RBMK (Chernobyl) fuel as a function of fuel burnup. Activities are shown up to the average burnup of exhausted fuel (Pöllänen 1997).*

The particle size estimation from nuclide-specific activities is based on the assumption that the nuclide ratios of non-volatile elements are not changed during the fuel fractionation processes (e.g. Piasecki *et al.* 1990, Jaracz *et al.* 1990). Pöllänen (1997) calculated the equivalent volume diameter of Chernobyl particles from the known activity per unit volume of a nuclide (or from the sum activity of several nuclides). Particle sizes were estimated separately for U-type and Ru-type particles because their activities per unit volume were different.

Activity ratios are of special importance. In general, the activity ratios can be used in two ways:

1) If two different isotopes of the same element, e.g. ^{141}Ce and ^{144}Ce, are detected in a particle then it is possible to estimate the burnup of the fuel from which the particle has originated. This was applied by Pöllänen (1997) in making hot particle size estimation detected in the environment for which the sizes were not reported in the original publications. The method was also used in publication VII.
2) If the burnup and decay time of the fuel is known then it is possible to estimate the activity of the nuclides (e.g. ^{90}Sr) that cannot be detected using a gamma-ray spectrometer. This was applied in publication VI where the activities of short-lived nuclides, not reported in the original papers, were estimated.

For homogeneous particles, the activity is directly proportional to particle mass which, in turn, is proportional to the cube of particle linear dimension. Particle size (volume or equivalent volume diameter) is often determined using electron microscopy, which in addition to activity analysis allows determining the activities of various nuclides per unit volume of the particle. On the other hand, particle size can be estimated using gamma-ray analysis only, if activity per unit volume is known.

4 ATMOSPHERIC TRANSPORT

In atmospheric transport and dispersion, large nuclear fuel particles pose different problems compared with small radioactive particles and gaseous species (publications III and V). In the atmosphere, they behave differently and they are not distributed within a release plume in the same way. Soon after their release, the large particles (aerodynamic diameter $d_a \gtrsim 20$ μm) leave the main aerosol stream mainly by sedimentation. In weather types where wind speed and direction change significantly with height, large particles and gaseous species or small particles may be transported separately. It is even possible that in some areas the fall-out contains mainly large particles, neither gaseous species nor small particles.

In addition to the sedimentation, atmospheric turbulence contributes notably on the deposition of large particles. Particles with a sedimentation velocity greater than 1 m s^{-1} ($d_a \gtrsim 200$ μm) fall so fast that turbulent dispersion is no longer important (Van der Hoven 1968). For particles of a few μm in aerodynamic diameter, turbulent dispersion is certainly an important deposition mechanism but a question arises over the net effect of the sedimentation and the turbulent dispersion for particles of sizes between these limits. The threshold value of the sedimentation velocity, at which settling becomes important, depends on the magnitude of the velocity of turbulent motions in the air (Garland and Nicholson 1991).

Despite the uncertainties associated with the role of sedimentation and turbulent dispersion, it is important to discover the areas that may receive the fall-out of highly active particles in a severe nuclear accident. However, gravitational settling of particles as a deposition process in real time long-range dispersion models in operational use is often excluded (Bartnicki *et al.* 2001). For the purposes of emergency preparedness, it is crucial to establish the maximum transport range of particles that may produce an acute health hazard, although they are of special concern near the release site. The transport range is defined as the distance from the point of release to the point of deposition (Pöllänen *et al.* 1995, publication III). Range estimates are based on the time difference between the release and deposition. During this time, the particles, originally lifted up to the effective release height, are transported over a distance determined by the wind velocity. Only dry

deposition is considered (also in publications III and V). A user-friendly computer code using simplified atmospheric conditions was developed to estimate the transport range of large particles (Pöllänen *et al.* 1995). The code, known as TROP, is intended mainly for use in emergency preparedness but it can also be used for research purposes.

TROP does not take into account varying wind conditions during transport and, thus, it cannot be fairly used in operational situations. The transport of large particles must be connected to the prevailing weather (Fig. 4). A long-range transport, dispersion and dose model, TRADOS[1], was developed for real-time calculations in realistic atmospheric conditions (Valkama and Salonoja 1993). The transport and dispersion of the particles is described by 3-dimensional trajectories and the resultant vertical velocity is the sum of the sedimentation velocity and the velocity of ascending or descending airflow.

The code uses numerical weather prediction model data to calculate trajectories. Weather parameters for different altitudes are stored routinely four times a day in a database that contains weather parameters, such as wind components, air temperature, relative humidity etc. The size and density of the particles as well as their effective release height are required as trajectory model input. However, in operational use, these quantities may be very uncertain and the calculated fallout areas are then only suggestive.

Particle trajectories were calculated for the Chernobyl accident in publication V and in Valkama *et al.* (1995). The effective release height of the particles and the atmospheric phenomena related to their transport were investigated by comparing particle findings in the environment with the locations given by particle trajectories. Since the size of the nuclear fuel particles detected in the environment is usually not documented, it was estimated using calculative means.

Unlike air parcel trajectories, the trajectories of large particles terminate when they hit the ground. However, the point of deposition cannot be determined accurately because of atmospheric turbulence. TRADOS is unable to take turbulence into account and the conclusion that the maximum effective release height must either have been considerably higher than previously reported or particles may have been lifted up to higher altitudes in deep convective cells (publication V) must be further validated. Valkama and

[1] SILAM computer code has replaced TRADOS, which is no longer in operational use.

Pöllänen (1996) concluded that convective lifting might have affected the dispersion and deposition of radioactive particles from the Chernobyl accident (Fig. 5) but the effects of atmospheric turbulence on the transport of large particles is still an open question. A novel computer code known as SILAM is under development (Valkama and Ilvonen, 2000) and it may validate the conclusions presented above.

The Norwegian Meteorological Institute has taken into account the ideas presented in publication V and simulated the transport of the large particles in the Chernobyl accident (Bartnicki *et al.* 2001). They verified that large particles could travel long distances before being deposited (publication V).

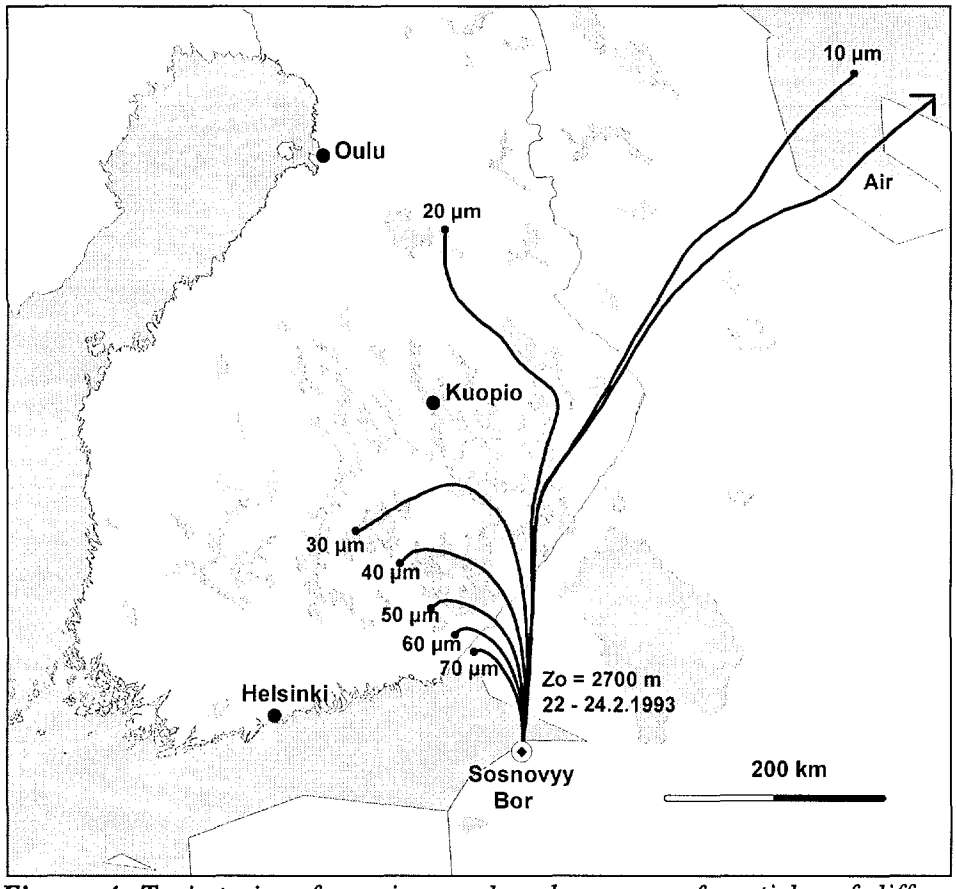

Figure 4. *Trajectories of an air parcel and a group of particles of different aerodynamic diameters released hypothetically from Sosnovyy Bor (Pöllänen et al. 1993). The release height is 2700 m. The average wind velocity along the particle trajectories is between 3.5 to 6 m* s^{-1}*. The transport situation refers to the days Feb 22-24, 1993.*

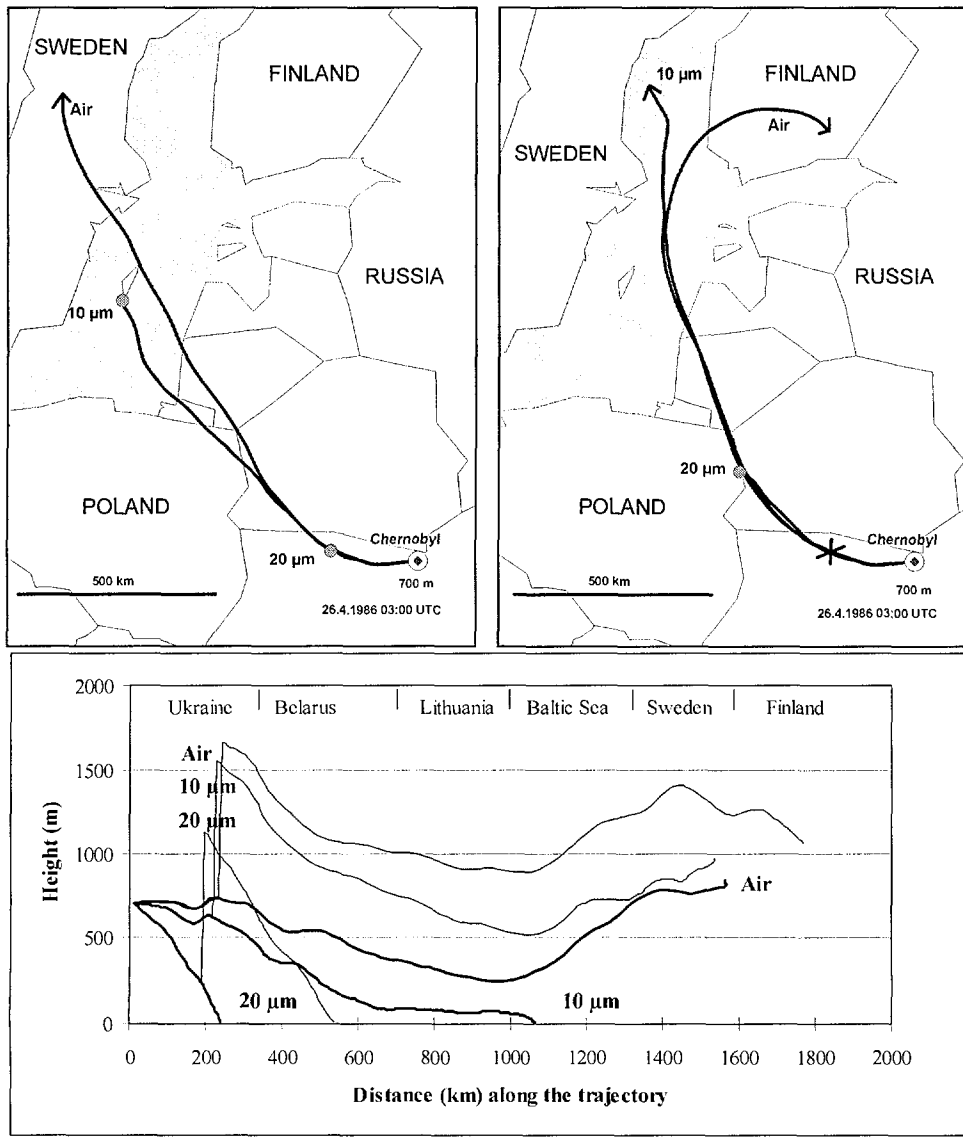

Figure 5. *Trajectories of an air parcel and particles 10 µm and 20 µm in aerodynamic diameter originating from Chernobyl NPP on April 26, 1986 at 03:00 UTC (Valkama and Pöllänen 1996). The effective release height is 700 m. On the left above, convective uplift is not assumed, whereas air parcel and particles on the right above experience an uplift of 1000 m. The location of the updraft is shown as a cross near Chernobyl. The heights of the trajectories are presented below. The thin lines refer to air parcel and particles that experience updraft whereas the thick lines represent those that experience no vertical uplift.*

5 CALCULATION OF SKIN DOSES

As regards the health hazards associated with large nuclear fuel particles, the skin doses are of special importance. The particles are poorly respirable because of their size and as a source of external radiation, they can often be treated in the same way as homogeneous contamination. As deposited into the environment, the mobility and bioavailability of the radioactive material incorporated in the particles are different compared to contamination that is more homogeneous. The uptake of radionuclides via ingestion of contaminated food or water and their subsequent absorption in the body are also different. Although above-mentioned matters must be taken into account in the consequence analyses of nuclear accidents, and are worth further research, they are not considered here. Instead, the most prominent feature of large nuclear fuel particles with respect to health threats, the possibility of producing acute deterministic radiation effects, is studied.

5.1 Ionising radiation and skin

Beta particles of various energies and low energy gamma rays are of greatest concern and importance in radiation protection of the skin. Damage that may be caused by more penetrating X and gamma rays will generally be limited by dose limits to other organs. Radiation doses from alpha particles may be high in the superficial layers of the skin without a notable dose in the deeper layers. This is due to the very low penetration of alpha particles. Exposure to very high doses over a very small area poses a particular problem.

The characteristics of the skin (Fig. 6) and its response to ionising radiation considerably affect the health hazard caused by highly active particles. The mechanisms of radiation effects on the skin are studied in numerous experimental investigations. However, the primary aim of most of these studies is related to radiotherapy, i.e. relatively large areas of the skin are irradiated with X or gamma rays. Specific radiation protection problems, such as skin irradiation with highly radioactive particles, cannot be necessarily explained by extrapolation from results of these experiments. The ionising radiation emitted from radioactive particles may induce deterministic effects and cancer of the exposed skin. A review of these effects as well as dosimetric

quantities and skin dose limits (chapter 5.2), based on ICRP (1990 and 1991), are presented in the following.

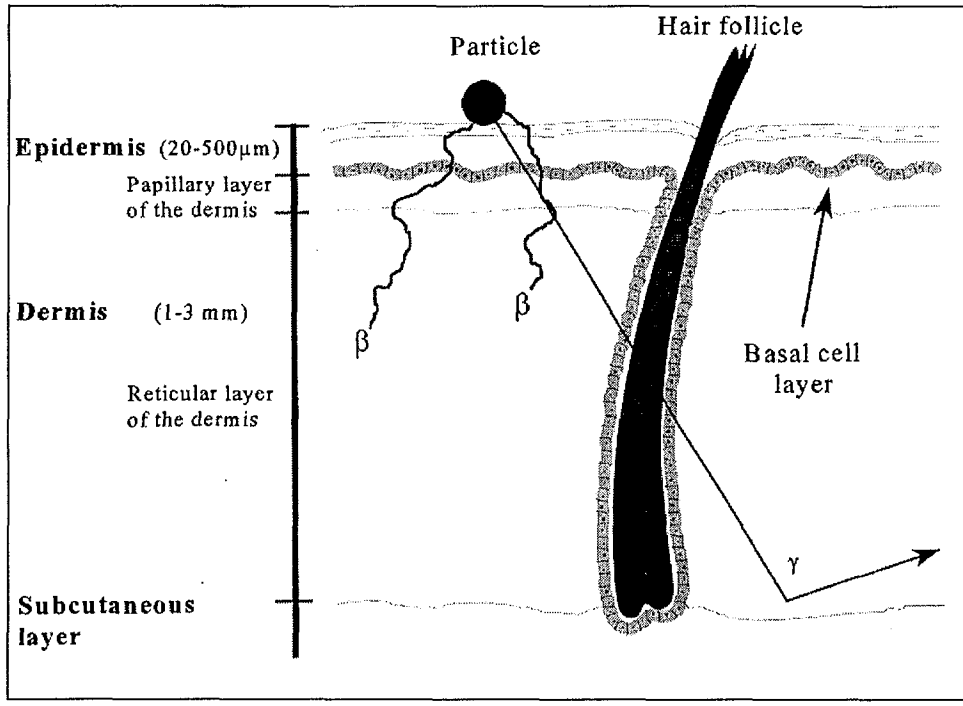

Figure 6. *Schematic cross-section of skin on which a radioactive particle is deposited (Pöllänen 1997). The routes of beta particles and photons originating from the particle are shown schematically. As a comparison for the thicknesses of the skin layers marked above, the distances in water at which 90% of the beta energy of ^{144}Ce, ^{90}Sr and ^{106}Rh is absorbed are 0.28 mm, 0.79 mm and 7.9 mm, respectively.*

Deterministic radiation-induced changes in the skin show several distinct phases of damage. Their severity depends on irradiation conditions, such as the type, energy, and intensity of the radiation and exposure time, and type and area of the exposed skin. The main phases of the damage are:

- Reddening of the skin (an early transient erythema) seen within a few hours of irradiation, which usually subsides after 1 - 2 d.
- Loss of the basal cells leads to the main erythematous reactions: keratinisation of the skin after moderate doses (dry desquamation), loss of the epidermis after high doses (moist desquamation) or hair loss may

result after 3 - 6 weeks. A skin wound (secondary ulceration) may develop if moist desquamation is severe.

- Late phase erythema is associated with blood vessel damage (dermal ischemia) and possible necrosis of skin between 8 - 20 weeks or more after irradiation.
- Late skin damage such as the thinning of dermal tissues after 6 months (atrophy), dilatation of superficial dermal capillaries (telangiectasia) and necrosis.

Nuclear fuel particles are of special radiological concern because of their small size ($\lesssim$1 mm) and high activity. When deposited on the skin they may produce very high and localised doses (Fig. 7). The nuclide composition of the particles may vary greatly, i.e., the particles may contain alpha emitters, low- and high-energy beta emitters, as well as gamma-ray emitters. The energy of alphas and very low-energy betas is absorbed in the epidermis above basal cell layer whereas gammas and high-energy betas may penetrate deep ($\gtrsim$ 1 cm) in the skin.

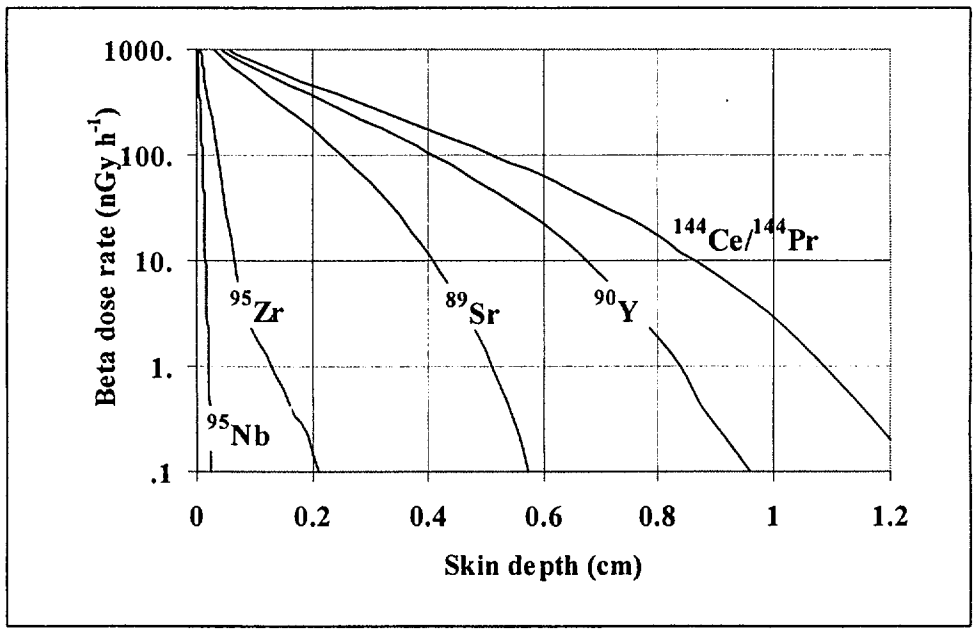

Figure 7. *Dose rate in water from a 1 Bq point isotropic beta source on the air-water boundary, averaged over 1 cm^2 circular area at different skin depths (Pöllänen 1997).*

Acute ulceration (skin wound) is the primary lesion resulting from irradiation with radioactive particles. The skin surface dose and the energy of the emissions from the particle determine the depth and size of the ulcer. The full lesion usually develops within 2 weeks of irradiation. A small pale and circular area with a slight blue tinge, surrounded by a halo of erythema, can be detected prior to the development of the ulcer. The estimated threshold dose for acute ulceration is ~75 Gy, measured over an area of 1.1 mm^2 at skin depth of 16 μm. This corresponds to a dose of ~1 Gy averaged over an area of 1 cm^2 at depth of 100 - 150 μm. A dose below 220 Gy (at depth of 16 μm over 1.1 mm^2) may lead to an ulcer that is likely to last for less than 1 week. A larger area erythema will also occur. Acute epithelial necrosis may be produced because of irradiation caused by low-energy beta particles. The dose from a point source to produce a 50 percent incidence of acute epidermal necrosis or acute ulceration varies from approximately 5 Gy to approximately 10 Gy, averaged over 1 cm^2 at a depth of 70 μm (NCRP 1999). This is to be compared e.g. with the effect from homogeneous X-ray irradiation, in which case a skin entrance dose of 5 Gy would only cause transient erythema.

The principal stochastic risk associated with irradiation of the skin is basal cell and squamuos cell skin cancers. The risk for radiation-induced skin cancer does not increase by very non-uniform radiation, i.e., radioactive particles do not cause more skin cancers per unit average dose compared with that caused by uniformly distributed doses in the skin.

5.2 Dosimetric quantities and skin dose limits

The fundamental dosimetric quantity in radiological protection is the absorbed dose, which is the energy absorbed per unit mass (unit Gy). The absorbed dose may be defined at a specified point but usually it is used to mean the average dose over a tissue or organ. The use of the average dose as an indicator of the probability of subsequent stochastic effects is a reasonable approximation over a limited range of dose. The average absorbed dose is not directly relevant to deterministic effects since the dose-response relationship is not linear.

The probability of stochastic effects depends on the absorbed dose as well as on the type and energy of radiation causing the dose. The absorbed dose averaged over a tissue or organ and weighted for the quality of the radiation, the equivalent dose (unit Sv), is of interest in radiological protection. The relationship between the equivalent dose and the probability of stochastic effects also depends on the organ or tissue irradiated. It is useful to indicate

the combination of different doses to several different tissues in a way that is likely to correlate well with the total of the stochastic effects. The effective dose is the sum of weighted equivalent doses in all tissues and organs of the body.

The equivalent dose and effective dose provide a basis for estimating the probability of stochastic effects only for absorbed doses well below the thresholds for deterministic effects. The ICRP recommendations for effective dose limits are sufficient to ensure the avoidance of deterministic effects in all body tissues and organs except the lens of the eye and the skin (ICRP 1991). The skin is not adequately protected by a limit of effective dose because it may be subject to localised exposure. Separate limits are needed.

In the case of stochastic effects, the equivalent dose can be averaged over the whole area of the skin. The stochastic effects are expected to arise in the basal cell layer. Some deterministic effects also arise in the basal cell layer, others in the deeper layer of the dermis. The ICRP (1990) recommends that the annual limit for occupational exposure is 500 mSv for the skin (150 mSv for the lens of the eye), averaged over any 1 cm^2, regardless of the area exposed. The nominal depth is 7 mg cm^{-2}. This limit is intended to protect the skin against deterministic effects. The limit for the public is reduced by an arbitrary reduction factor of 10 because the total period of exposure may be nearly twice as long as for occupational exposure, and because the exposed individuals may show a wider range of sensitivity than a more limited population of workers. The recommended annual limit for the public is 50 mSv for the skin (15 mSv for the lens of the eye), averaged over any 1 cm^2 area of the skin and regardless of the area exposed.

The NCRP (1989) recommendation on an occupational radiation exposure limit for a hot particle on the skin is intended to prevent acute deep ulceration of the skin, and is based on the time integral of the beta particles emitted from a radioactive particle. The NCRP recommends that exposure to the skin must be limited to 10^{10} beta particles emitted from the surface of a radioactive particle. This limit is obtained primarily from beta particle emissions from irradiated fuel particles, and refers to about 5 Gy averaged over 1 cm^2 at depth 70 μm in tissue (Baum and Kaurin 1991). Recently, the NCRP (1999) recommended that "the dose to skin at a depth of 70 μm from hot particles on skin (including ear), hair or clothing be limited to no more than 0.5 Gy averaged over the most highly exposed 10 cm^2 of skin". The NCRP skin dose limits are higher than

those of the ICRP by a factor of 10 (Charles *et al.* 2000). Thus, there is disparity between the skin dose limits applied in USA and Europe.

5.3 Method of skin dose calculation

Determination of a skin dose caused by a radioactive particle deposited on the skin represents a complex problem. Although the geometrical arrangement appears to be simple, several problems arise in the dose calculation. The dose gradient is very sharp due to the short range of beta particles in tissue (Fig. 7). The energy spectrum of beta particles is continuous in contrast to gammas. Beta particles of varying energy interact with the surrounding materials, i.e. air, skin, and the particle matrix itself, in such a manner that analytical dose calculations may not be feasible.

The dose caused by a radioactive particle deposited on the skin depends primarily on the manner in which photons and beta particles interact with skin. Alpha particles are neglected in the dose calculations owing to their short range (up to ~50 μm in the skin). The dose to the basal cell layer of the epidermis is determined mainly by beta radiation; photons usually play a negligible role. This difference is smaller for large nuclear fuel particles because of the significant self-absorption of betas.

Several methods have been developed to calculate skin doses (see Pöllänen 1997). Loevinger (1956) proposed an analytical empirical function that can be used for estimating the point-source beta dose distribution in tissue. Later, the parameters of the empirical equation were revised and other point source dose distribution functions have been developed. The dose distribution in tissue around a point source of a beta emitting radionuclide, often referred to as 'point kernel', is also determined by numerically solving the transport equation or using a simplified form of the equation. The more accurate dose distribution data of betas and photons are generated using Monte Carlo calculations. Precalculated dose distributions are utilized in some methods.

Although there are many different methods of calculating skin doses produced by beta particles and photons, most of them are appropriate only for some predetermined purposes. For example, Monte Carlo methods, which are appropriate for detailed dose analyses in specified situations, are not necessarily suitable in routine dose calculations. Analytic representations of point source dose distributions may be useful only for certain nuclides; their validity for other nuclides is questionable. In addition, they can be used only

for point sources, not necessarily for three-dimensional particles. Extensive tabulations, such as those presented by Cross *et al.* (1992) and Rohloff and Heinzelmann (1996), can be used for dose estimation but their applicability for routine dose estimation is limited.

Skin doses are often calculated by assuming the skin is uniformly contaminated by beta active nuclides, not by individual particles. Moreover, the calculations are often based on the assumption that the particles are surrounded by an infinite homogeneous medium (water). Because of diminished backscattering in the air-tissue interface, the skin doses are then overestimated up to about 35 % (Cross *et al.* 1992). The dimensions of the particles are also frequently neglected. Especially for low energy beta emitters, the doses are overestimated if the effect of self-shielding is omitted. Gamma rays are often neglected, which may lead to underestimation of doses in certain cases.

A new model (PSS, Point Source and Self-absorption) has been developed to calculate doses caused by radioactive particles deposited on the skin (publication IV, Pöllänen 1997). The model, calculates the beta and photon dose rate to the skin at definite depths and averaged over a circular area of 1 cm^2. The source particle is assumed spherical and homogeneous. Neither protective clothes nor air gaps are assumed. The model uses point-source dose conversion factors that are analytically corrected for the self-shielding of beta particles. In the following, the doses are calculated for the basal cell layer of the skin (nominal depth 70 μm, circular target area) although any depth and any target area is possible provided appropriate point-source conversion factors are available.

The PSS model was compared to VARSKIN Mod 2 (Durham 1992) in publication IV. Skin doses, calculated with the PSS and VARSKIN Mod 2, were compared for spherical uranium dioxide particles of different sizes and unit activity by assuming the particles are deposited on the skin. The differences between the calculated doses are generally below two; the results were nearly equal deep (in terms of range of beta particles) in the skin. Both models show that the self-absorption of beta particles must be taken into account in skin dose calculations.

5.4 Skin doses from nuclear fuel particles

Radiation doses caused by uranium fuel fragments with composition of long-lived nuclides similar to nuclear fuel and deposited on the skin were estimated in publication II. Skin doses were calculated for particles of different sizes originating from the Chernobyl reactor by assuming the particles are composed of long-lived nuclides of some low-volatile elements. However, radioactive decay and dependency on the amount of nuclides in the particles as a function of fuel burnup and reactor type were neglected in the calculations. In addition, short-lived nuclides and some important low-volatile elements were not considered at all. Pöllänen (1997) considered these deficiencies for U-type particles and in publication VI for Ru-type particles generated in the fuel fragmentation of the Chernobyl accident. A summary of the results is presented in the following.

The nuclides of non-volatile elements incorporated in the calculations were selected based on their radiological importance (Table IV). The nuclide composition of low-volatile elements in reactor fuel as a function of fuel burnup and decay time was computed using the ORIGEN2 and OTUS codes. Activities were calculated separately for U-type and Ru-type particles (Figure 8, Table V).

The elements considered are alkaline earths Sr, Ba; refractory oxides Zr, Nb; noble metals Ru, Rh, Tc, Mo, Pd; rare earths + others Y, La, Ce, Pr, Nd, Pm, Sm, Eu, Np, Pu, U (classification from WASH-1400, 1975). Their release fraction in fuel meltdown and vaporisation processes is below 20 % (WASH-1400, 1975). Since the gaseous species and volatile elements in the nuclear fuel particles observed in the environment were strongly depleted or totally missing, they were omitted in the calculations. This assumption may underestimate the doses. The criteria for the selection of the nuclides presented in Table IV were as follows: a) half-life is more than a few hours (some daughter nuclides may have shorter half-life), b) the amount in the nuclear fuel is sufficiently large, and c) beta energies are high enough to produce a notable dose on the skin.

Table IV. *Nuclides considered in the dose calculations. The maximum energy of the beta particles, E_{max}, refers to the most probable decay branch. CF_β is the beta dose rate from a point source of 1 Bq at the air-water boundary averaged over 1 cm^2 at the basal cell layer of the skin (Cross et al. 1992). The values denoted by * are calculated using SADDE Mod2 and VARSKIN Mod2 (Durham 1992). CF_γ refers to the gamma dose rate from a point source of 1 Bq averaged over 1 cm^2 at the basal cell layer of the skin (Rohloff and Heinzelmann 1996).*

Nuclide	$t_{1/2}$	E_{max} (MeV)	Probability per decay	CF_β (μGy h^{-1} Bq^{-1})	CF_γ (μGy h^{-1} Bq^{-1})
^{89}Sr	50.6 d	1.49	0.999	1.67	1.17×10^{-6}
^{90}Sr	28.6 y	0.546	1.00	1.38	-
^{90}Y	64.1 h	2.28	0.999	1.76	1.80×10^{-6}
^{91}Sr	9.5 h	1.10	0.339	1.57 *	1.01×10^{-2}
^{91}Y	58.5 d	1.54	0.997	1.67	3.60×10^{-5}
^{92}Y	3.54 h	3.63	0.857	1.76 *	3.33×10^{-3}
^{93}Y	10.1 h	2.89	0.902	1.73 *	1.32×10^{-3}
^{95}Zr	64.0 h	0.366	0.554	1.06	1.30×10^{-2}
^{95}Nb	35.1 d	0.160	0.999	0.23	1.30×10^{-2}
^{97}Zr	16.9 h	1.91	0.860	1.70 *	2.77×10^{-3}
^{97}Nb	72.1 min	1.28	0.983	1.58 *	1.31×10^{-2}
^{99}Mo	66.0 h	1.21	0.827	1.54	3.49×10^{-3}
^{103}Ru	39.4 d	0.226	0.900	0.568	1.25×10^{-2}
^{105}Ru	4.44 h	1.19	0.499	1.63 *	1.67×10^{-2}
^{105}Rh	35.4 h	0.567	0.750	1.17	2.80×10^{-3}
^{106}Ru	368 d	0.0394	1.00	-	-
^{106}Rh	30 s	3.54	0.787	1.85	4.53×10^{-3}
^{109}Pd	13.5 h	1.03	0.999	1.55 *	4.11×10^{-3}
^{140}Ba	12.8 d	0.991	0.370	1.46	1.00×10^{-2}
^{140}La	40.2 h	1.35	0.445	1.64	2.61×10^{-2}
^{141}La	3.94 h	2.43	0.970	1.73 *	3.58×10^{-4}
^{141}Ce	32.5 d	0.435	0.705	1.54	3.12×10^{-3}
^{142}Pr	19.1 h	2.16	0.963	1.69 *	4.32×10^{-4}
^{143}Ce	33.0 h	1.10	0.480	1.48 *	9.78×10^{-3}
^{143}Pr	13.6 d	0.935	1.00	1.52	1.57×10^{-10}
^{144}Ce	284.3 d	0.318	0.772	0.815	1.77×10^{-3}
^{144}Pr	17.3 min	3.00	0.977	1.82	3.15×10^{-4}
^{145}Pr	5.98 h	1.81	0.970	1.62 *	2.20×10^{-4}
^{147}Nd	11.0 d	0.805	0.811	1.31 *	8.08×10^{-3}
^{147}Pm	2.62 y	0.225	0.999	0.535	3.54×10^{-7}
^{148}Pm	5.37 d	2.46	0.555	1.60 *	7.48×10^{-3}
^{149}Pm	53.1 h	1.07	0.962	1.54 *	3.53×10^{-4}
^{151}Pm	28.4 h	0.843	0.427	1.65 *	9.60×10^{-3}
^{153}Sm	46.7 h	0.702	0.441	1.43	7.77×10^{-3}
^{156}Eu	15.2d	0.487	0.320	1.36	1.29×10^{-2}
^{237}U	6.75 d	0.238	0.531	0.632 *	1.62×10^{-2}
^{238}Np	2.12 d	1.25	0.450	0.770 *	1.23×10^{-2}
^{239}Np	2.36 d	0.436	0.520	1.09 *	1.51×10^{-2}

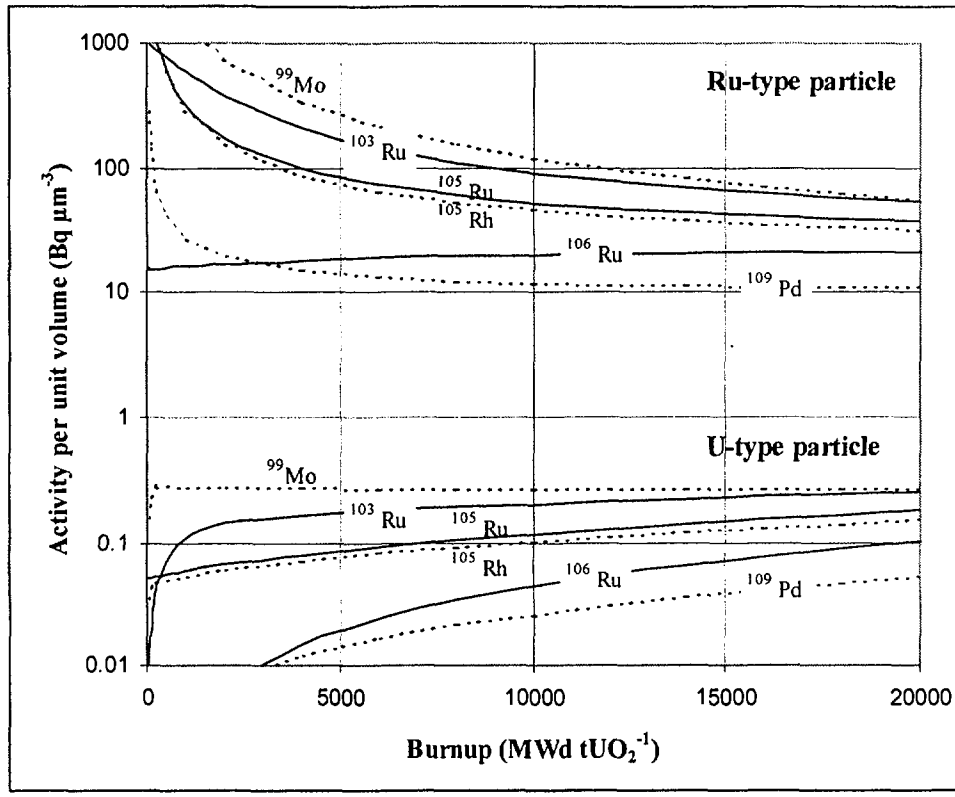

Figure 8. *Calculated activity of ^{99}Mo, ^{103}Ru, ^{105}Ru, ^{105}Rh, ^{106}Ru and ^{109}Pd per unit volume of an Ru-type particle and a U-type particle as a function of fuel burnup (Chernobyl reactor assumed). The activity of ^{106}Rh is not presented because of its short half-life. In practice, its activity is equal to the activity of ^{106}Ru.*

In general, the activity of most of the nuclides presented in Table IV per unit volume in a U-type particle is of the order of 0.05 - 0.3 Bq μm^{-3} (a complete set of activities is presented in Pöllänen, 1997; see also Fig. 3) whereas in the case of an Ru-type particle the activities of the nuclides of noble metals are higher by a factor of 100 - 1000. This is due to the fact that Ru-type particles are composed almost entirely of fission products whereas the U-type particles are composed mainly of bulk uranium dioxide. This is also the reason for the different behaviour of activities per unit volume as a function of fuel burnup (Fig. 8).

Table V. *Total activity of nuclear fuel particles as a function of equivalent volume diameter, d_p, for the decay times of 1 d and 10 d. The particles are assumed to originate from RBMK fuel irradiated to average burnup. The density of the particles is assumed to be 10500 kg m^{-3}. For U-type particles, the total activity, A_{tot}, is the sum of the activities of the nuclides presented in Table III, whereas only nuclides of noble metals Ru, Rh, Tc, Mo and Pd are taken into account for Ru-type particles (publication VI).*

	Decay time 1 d		Decay time 10 d	
	U-type	Ru-type	U-type	Ru-type
d_p (μm)	A_{tot} (Bq)	A_{tot} (Bq)	A_{tot} (Bq)	A_{tot} (Bq)
1	3.0	130	1.3	57
2	24	1000	10	460
3	80	3500	35	1520
4	190	8000	83	3600
5	370	16000	160	7100
6	640	28000	280	12000
7	1000	43000	440	20000
8	1500	65000	660	29000
9	2200	94000	940	42000
10	3000	130000	1300	57000
15	9900	430000	4400	200000
20	24000	1000000	10000	460000

In addition to particle type, size is the most relevant quantity with respect to dose (Table VI) since for homogeneous particles the activity is directly proportional to particle mass, which is consequently proportional to the cube of the diameter (Table V). The composition and burnup and decay time of the fuel (= time of deposition) from which the particles have originated have a notable influence on the dose rates (Figs. 9 and 10).

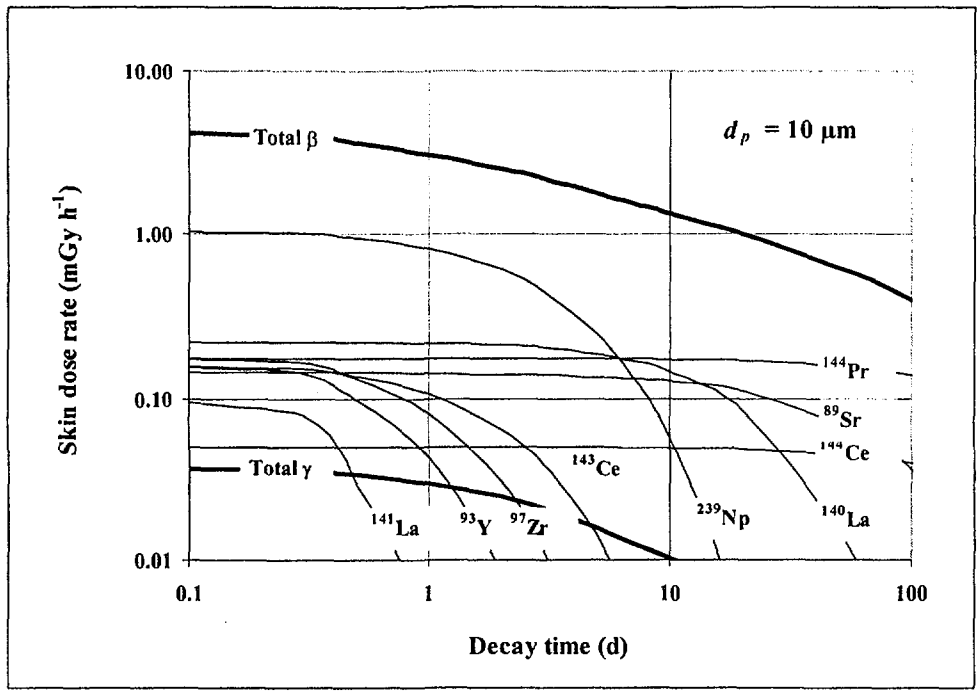

Figure 9. *Beta and gamma (total y) dose rates to the basal cell layer as a function of time, caused by a d_p = 10 μm U-type nuclear fuel particle deposited on the skin. The particle is assumed to originate from RBMK fuel irradiated to average burnup. All nuclides in Table IV are considered in the curves 'Total β' and 'Total γ', whereas other curves are for the beta dose rate of individual nuclides (not all nuclides are shown).*

The burnup of the fuel has a notable influence on the dose rates, although the effect for U-type is far less dramatic than for Ru-type particles (Fig. 10). Contrary to Ru-type particles, the more irradiated the fuel the more active the U-type particles.

Table VI. *Beta dose rate to the basal cell layer of the skin, caused by U-type and Ru-type particles deposited on the skin, as a function of particle diameter, d_p, for two decay times. The particles are assumed to originate from RBMK fuel irradiated to average burnup. The dose rates are averaged over 1 cm^2 at a skin depth of 70 μm. For U-type particles, all the nuclides presented in Table IV are taken into account, whereas only the nuclides of noble metals Ru, Rh, Tc, Mo and Pd are taken into account for Ru-type particles.*

	Beta dose rate at decay time 1 d		Beta dose rate at decay time 10 d	
d_p (μm)	U-type (mGy h^{-1})	Ru-type (mGy h^{-1})	U-type (mGy h^{-1})	Ru-type (mGy h^{-1})
1	0.0036	0.15	0.0016	0.049
2	0.028	1.2	0.012	0.38
3	0.093	3.8	0.040	1.2
4	0.22	8.8	0.094	2.9
5	0.41	17	0.18	5.4
6	0.70	29	0.31	9.1
7	1.1	45	0.48	14
8	1.6	66	0.70	21
9	2.2	93	0.99	29
10	3.0	130	1.3	39
15	9.4	390	4.2	120
20	21	890	9.4	270

Short-lived nuclides, such as ^{239}Np, are of primary importance within a few days from the end of the chain reaction (Fig. 9); their contribution is negligible later. The proportion of gamma rays emitted from nuclear fuel particles deposited on the skin is negligible; the dose caused by beta particles is 100 times larger than the dose caused by gamma rays. Reactors with high specific power may generate particles that have much higher activity per unit volume than particles produced by reactors with low specific power. A U-type particle originating for example from a PWR reactor may produce twice as large a skin dose than one of the same size originating from a RBMK reactor (Fig. 11).

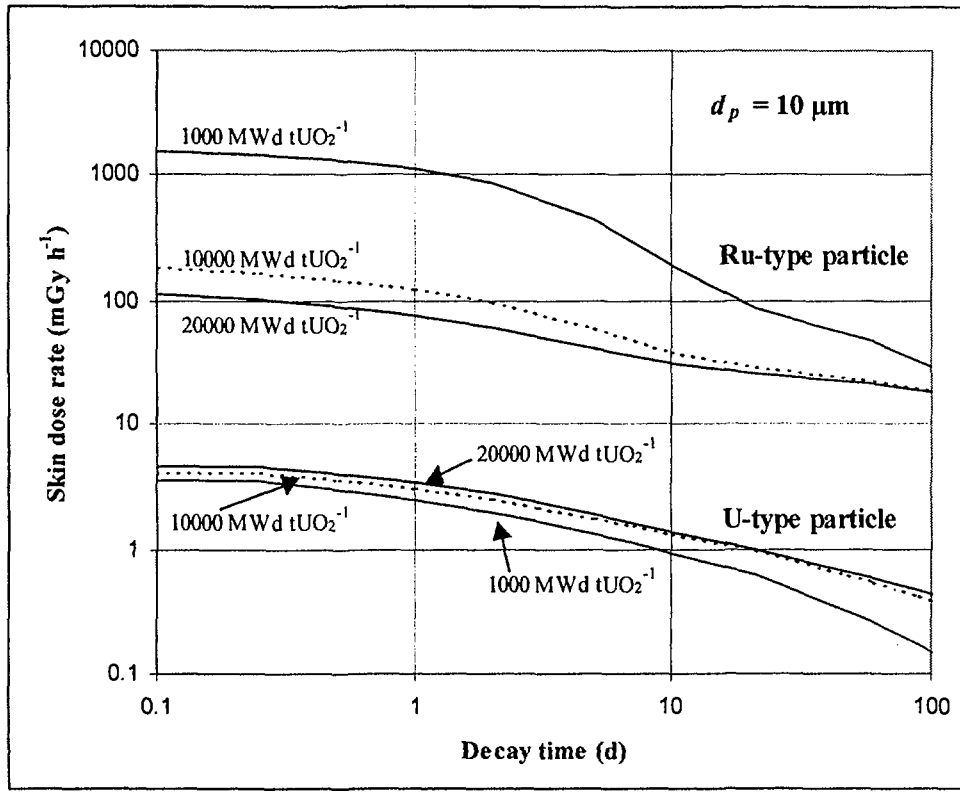

Figure 10. *Beta dose rate to the basal cell layer (averaged over 1 cm^2 at a nominal depth of 70 μm) as a function of decay time caused by U-type and Ru-type particles of 10 μm in equivalent volume diameter deposited on the skin. A Chernobyl type RBMK reactor is assumed in the calculations. The centremost curves refer to fuel of average burnup (10000 MWd tUO_2^{-1}) from which the particles are assumed to have originated. The upper and lower curves are for the particles emitted from low-burnup fuel (1000 MWd tUO_2^{-1}) and high-burnup fuel (20000 MWd tUO_2^{-1}).*

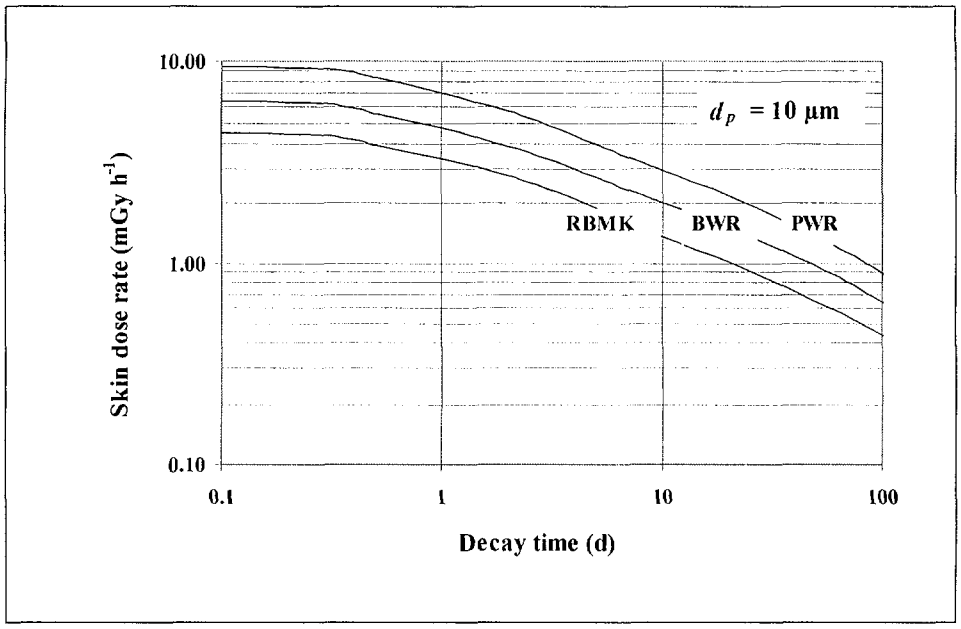

Figure 11. *Beta dose rates to the basal cell layer as a function of time, caused by a d_p = 10 µm U-type nuclear fuel particle deposited on the skin. The particles are assumed to originate from RBMK, BWR and PWR fuel.*

5.5 Skin doses from selected nuclear fuel particles released in the Chernobyl accident

The results of the calculations presented above are for hypothetical particles, i.e. particle characteristics, from which the skin doses are calculated, are derived from the properties of the nuclear fuel. Here skin doses are estimated for some U-type nuclear fuel particles detected in various European countries after the Chernobyl accident by assuming the particles are deposited on the skin (results are from Pöllänen 1997). Similar calculations are presented in publication VI for Ru-type particles detected in Poland.

For calculating the particle properties, the primary assumption is that nuclides of the same element behave similarly in a fuel fragmentation process. This makes it possible to estimate the amount of short-lived nuclides in the particle from the measured amount of long-lived nuclides. The activities of the nuclides that belong to other elements are included by assuming negligible fractionation between different non-volatile elements.

The calculations are performed as follows: the activity ratios of observed nuclides of the same element, such as $^{141}Ce/^{144}Ce$, are used first in estimating the burnup of the fuel from which the particle originated (see appendix H in Pöllänen 1997). The equivalent volume diameter of the particles is then estimated from the sum of the burnup-dependent activities of ^{95}Zr, ^{141}Ce and ^{144}Ce per unit volume. This size is then used to estimate the proportions of nuclides presented in Table IV, which are for some reason not detected. Usually, the reason is that the activity analyses were performed too late to detect short-lived nuclides.

The activities are computed by assuming a decay time of 1 d. If several activity ratios, e.g. $^{141}Ce/^{144}Ce$ and $^{103}Ru/^{106}Ru$, give different burnups, their average value is used. The fractionation of detected elements is taken into account in the computation. For example, the nuclides of ^{103}Ru and ^{106}Ru are enriched by a factor of about 5 in the particle detected by Rytömaa *et al.* (1986) (appendix H, Table H1 in Pöllänen 1997). This enrichment factor is then taken into account in estimating the proportions of the short-lived nuclides of Ru and Rh. If volatile nuclides, such as ^{131}I or ^{137}Cs, not mentioned in Table IV are observed in the particles, they are taken into account in the dose calculation. The other important nuclides of these elements are taken into account by assuming the same fractionation as for the observed elements.

The reported total activities of the particles are typically by a factor of 2 - 4 smaller than those obtained by calculations because of the presence of short-lived nuclides, mainly ^{239}Np (Table VII). The differences in the dose rates are approximately the same. The U-type nuclear fuel particles detected in north-western Europe after the Chernobyl accident and potentially deposited on the skin do not produce such a beta dose that the ICRP annual dose limit of 50 mGy at skin depth of 70 μm would be exceeded within 1 h. This is not the case for Ru particles (publication VI). However, nuclear fuel particles near the Chernobyl nuclear power plant were active enough to produce severe skin damage in a short time, provided the particles would have been deposited on the skin.

Table VII. *The total activity of some U-type nuclear fuel particles detected in Europe after the Chernobyl accident and the beta dose rate that they may cause on the skin by assuming a decay time of 1 d (Pöllänen 1997). One particle is selected from each author and the particle code is that used by the original authors.* A_{det} *is the total activity of nuclides detected in the particles and* $\dot{D}_{det}$ *is the respective beta dose rate to the basal cell layer of the skin averaged over 1* cm^2*. If daughter nuclides, such as* ^{95}Nb, ^{106}Rh, ^{140}La *and* ^{144}Pr*, are not reported by original authors they are included in the computation by assuming equilibrium with their parents.* A_{all} *is the calculated total activity of nuclides presented in Table IV including detected volatile nuclides and* $\dot{D}_{all}$ *is the respective basal cell beta dose rate averaged over 1* cm^2*.*

Reference and location	Code	A_{det} (Bq)	A_{all} (Bq)	$\dot{D}_{det}$ (mGy h^{-1})	$\dot{D}_{all}$ (mGy h^{-1})
Rytömaa *et al.* 1986 Finland, Uusikaupunki	F2	430	1200	0.39	1.2
Saari *et al.* 1989 Finland, Uusikaupunki	U37(2)	620	2500	0.46	2.6
Devell 1987 Sweden, Studsvik	HP-9	5400	7400	4.5	7.3
Robertson 1986 Sweden, Älvkarleby	HP-3	3000	4500	2.4	4.6
Van der Wijk *et al.* 1987 Ukraine, Kiev	GHP1	1900	7400	1.4	7.2
Broda 1987 Poland, Mikolajki	M4	1900	7200	1.4	7.0
Balashazy *et al.* 1988 Hungary, Budapest	No 1	680	1700	0.68	1.8
Khitrov *et al.* 1994 Ukraine, Vil'cha	-	110000	450000	43	250
Salbu *et al.* 1994 Ukraine, near Chernobyl	No 1	2700000	29000000	1700	8800

6 SUMMARY OF THE RESULTS AND DISCUSSION

In the present thesis, nuclear fuel particles are investigated from the point of view of health hazards, the main focus being on their characterisation, their transport and dispersion in the atmosphere and the estimation of possible skin doses. The basic statement is that the release of nuclear fuel particles into the environment cannot be considered unique to severe accidents only (publication I, Pöllänen 1997). They were frequently identified in the environment after past nuclear accidents, especially in the Chernobyl accident, and in incidents from a number of other sources (Pöllänen 1997). Their possible release in future nuclear incidents cannot be totally dismissed.

The main results can be summarised as follows:

- Nuclear fuel particles should not be considered as 'becquerels' distributed homogeneously either in the environment or in a sample. Routinely used analysis procedures designed for bulk samples are not necessarily appropriate for nuclear fuel particles. Routine bulk analysis methods may lead to meaningless or even erroneous results. (Publications VII and VIII)
- The identification, isolation, and analysis of individual particles enables results to be obtained that are otherwise inaccessible owing to the interference of non-relevant bulk particles in the sample. Several complementary analysis techniques are needed to characterise particle properties thoroughly. The order in which different analysis techniques are used should be carefully thought through especially in the case when destructive analysis methods will be applied. (Publications VII and VIII)
- The characteristics of radioactive particles reflect the properties of the source material, which allows the performance of forensic analyses. Although complicated physical-chemical phenomena during the release may affect particle characteristics, it is possible to calculate the properties of individual particles in certain cases. These calculations are needed for the complete evaluation of the threats to health caused by nuclear fuel particles. (Publications VII and VIII)
- In a severe nuclear accident, large (aerodynamic diameter more than 20 μm) and highly active particles (activity even hundreds of kBq's) may be

transported hundreds of kilometres in the air before deposition. Effective release heights are then several hundreds of meters. (Publications II, III and V)

- The transport of particulate materials differs to that of gaseous species. Air parcel trajectories are not necessarily sufficient to identify the areas that may receive radioactive materials. Thus, in operational use particle trajectory or dispersion model calculations are needed. (Publications II, III and V)
- Realistic atmospheric conditions and the effects of turbulent dispersion must be taken into account in calculating the transport of radioactive particles should a nuclear incident occur. Simplified transport range calculations are adequate only in limited cases. (Publications II, III and V)
- In the Chernobyl accident, the effective release height may have been considerably higher than reported previously (up to 2 km) or particles may have been lifted up to higher altitudes in deep convective cells. (Publication V, Valkama and Pöllänen 1996)
- The composition of the particles may have an essential influence on skin doses. The presence of short-lived nuclides in particles emitted from low burnup fuel in particular contributes notably to skin beta dose rates. The contribution of gamma rays is often negligible. The self-absorption of beta particles in the nuclear fuel particle itself must be taken into account in dose calculations. (Publications IV and VI, Pöllänen 1997)
- The specific activity of the Ru-type particles found in the environment after the Chernobyl accident may be by a factor of about 100 higher than those composed mainly (in terms of mass) of bulk U. Ru-type particles are almost entirely composed of fission products. In a severe nuclear accident, reactors operating with high specific power may generate fuel particles that consequently may have high specific activity. (Publication VI, Pöllänen 1997)
- Contrary to particles composed mainly of bulk U, the specific activity of the Ru-type particles emitted from low burnup fuel may be considerable higher than that emitted from high burnup fuel. Thus, health threats are not necessarily the greatest for particles originating from high burnup fuel. (Publication VI, Pöllänen 1997)
- Even individual nuclear fuel particles, released uncontrolled into the environment in a severe nuclear accident, may represent an acute health hazard. When deposited on the body they may produce a high but much localised dose to the skin. Compared to the ICRP annual occupational dose limit for the public (50 mSv averaged over 1 cm^2 at a depth of 70 μm and intended to protect skin against deterministic effects) they may produce a

basal cell beta dose that exceeds this limit in a short time. This dose may be exceeded in 1 h provided that an Ru-type particle larger than 8 μm in diameter is deposited onto the skin (RBMK fuel assumed) whereas for U-type particles the dose refers to the diameter of about 30 μm. (Publication VI, Pöllänen 1997)

In order to assess the significance of the radioactive material that may be released into the environment with respect to radiation hazards, it is crucial to take into account the possibility that the material may be in the form of highly active particles. An awareness of this possibility is a prerequisite for taking appropriate countermeasures in a nuclear incident. As regards preparedness, the existence of a radiological hazard due to the presence of highly active particulate materials in a release plume must be realised and taken into account in contingency plans.

The possible release of nuclear fuel particles in the environment represents a technical, analytical, and even philosophical challenge for radiation protection. Their identification and detection in the environment necessitates properly designed environmental radiation monitoring and sampling systems that take the particulate nature of the releases into account. Traditional laboratory practices are designed for bulk sample activity analysis rather than for the analysis of the individual particles that have to be taken into account in estimating the relevance of the analysis results. Finally, the interpretation of the hazard, i.e. the possibility of receiving nuclear fuel particles deposited onto skin, which subsequently may produce high local doses, is far from clear with respect to radiological protection.

The Radiation and Nuclear Safety Authority (STUK 2001) has published a guide for the protective actions of members of the public and generic intervention levels to be applied in a state of a radiation emergency. This guide acts as a design basis for other authorities for weighting between different intervention operations. The principle is to prevent acute severe deterministic effects and to keep late stochastic effects as low as reasonably achievable. The practical question evokes whether the threat of nuclear fuel particles should be separately evaluated in the guide.

In a state of an acute radiation emergency, the recommended intervention actions such as sheltering and evacuation are based on the measurement of the external dose rate. Basic protective actions against hot particles are presumably appropriate in almost all practical situations. However, the

problem that highly active particles may be present in the air although the external dose rate is below the recommended operative action level (for example, the recommended external dose rate limit for sheltering is 100 μSv h^{-1}) is not only theoretical. The management of this situation requires special knowledge and equipment that are not necessarily available to the staff operating in field conditions. The possibility that highly active particles may serve as an additional health threat must be evaluated case by case based on expert judgement by the authorities familiar with radiation protection issues.

ACKNOWLEDGEMENTS

My warmest thanks to Harri Toivonen PhD, who introduced me to the fascinating field of atmospheric radioactive particles and whose attitude, enthusiasm and support created an encouraging atmosphere for preparing the scientific research. His contribution as a co-author of the original publications of the present thesis is greatly appreciated.

I am also grateful to Ms Tarja Ilander for her technical assistance in preparing some of the original publications. Her expertise, skill, and endurance in programming the OTUS, TROP, and PSS computer codes are highly acknowledged.

I thank Mr. Ilkka Valkama, Dr. Tuomas Valmari, Mr. Mikael Moring, Mr. Juhani Lahtinen, Ms. Wendla Paile, Dr. Raimo Mustonen, and Professor Sisko Salomaa for reviewing the thesis with expertise and constructive comments and criticism.

The contribution of the specialists that participated in the preparation of the original publications is highly appreciated. The preparation of the original papers would not have been possible without their efficient and fruitful cooperation.

March 2002 Roy Pöllänen

REFERENCES

Arvela H, Markkanen M, Lemmelä H. Mobile survey of environmental gamma radiation and fall-out levels in Finland after the Chernobyl accident. Radiation Protection Dosimetry 1990; 32: 177-184.

Balásházy I, Fehér I, Szabadyné-Szende G, Lörinc M, Zombori P, Pogány L. Examination of hot particles collected in Budapest following the Chernobyl accident. Radiation Protection Dosimetry 1988; 22, 263-267.

Barabanova A, Osanov D P. The dependence of skin lesions on the depth-dose distribution from β-irradiation of people in the Chernobyl nuclear power plant accident. International Journal of Radiation Biology 1990; 57: 775-782.

Bartnicki J, Salbu B, Saltbones J, Foss A, Lind O C. Gravitational settling of particles in dispersion model simulations using the Chernobyl accident as a test case. DNMI report No. 131, 2001.

Baum J W, Kaurin D G. Reassessment of data used in setting exposure limits for hot particles. Radiation Protection Dosimetry 1991; 39, 49-54.

Broda R. Gamma spectroscopy analysis of hot particles from the Chernobyl fallout. Acta Physica Polonica 1987; B18: 935-950.

Broda R, Kubica B, Szeglowski Z, Zuber K. Alpha emitters in Chernobyl hot particles. Radiochimica Acta 1989; 48: 89-96.

Bunzl K. Detection of radioactive hot particles in environmental samples by repeated sample mixing. Applied Radiation and Isotopes 1998; 49: 1625 - 1631.

Charles M W, Burkhart W R, Darley P J, Hopewell J W, Mill A J. Effects of hot particles on the skin: The considerations of a EULEP/EURADOS task group. Radiation Protection Dosimetry 2000; 92:161-168.

COMARE 1999. Committee on Medical Aspects of Radiation in the Environment (COMARE). Sixth report. A reconsideration of the possible

health implications of the radioactive particles found in the general environment around the Dounreay Nuclear Establishment in the light of the work undertaken since 1995 to locate their source. National Radiological Protection Board, 1999.

Croff A C. ORIGEN2: a versatile computer code for calculating the nuclide compositions and characteristics of nuclear materials. Nuclear Technology 1983; 54: 335-352.

Cross W G, Freedman N O, Wong P Y. Beta ray dose distributions from skin contamination. Radiation Protection Dosimetry 1992; 40: 149-168.

Devell L. Nuclide composition of Chernobyl hot particles. In: Von Philipsborn H and Steinhäusler F (eds.). Hot particles from the Chernobyl fallout. Proceedings of an International Workshop held in Theuern 28/29 October 1987. Schriftenreihe des Bergbau- und Industriemuseums Ostbauern Theuern, 1988; BAND 16: 23-34.

Durham J S. VARSKIN MOD2 and SADDE MOD2: Computer codes for assessing skin dose from skin contamination. Richland, WA: Battelle Pacific Northwest Laboratories; NUREG/CR-5873 (PNL-7913), 1992.

Garland J A, Nicholson K W. A review of methods for sampling large airborne particles and associated radioactivity. Journal of Aerosol Science 1991; 22: 479-499.

Hofmann W, Crawford-Brown D J, Martonen T B. The radiological significance of beta emitting hot particles released from the Chernobyl nuclear power plant. Radiation Protection Dosimetry 1988; 22: 149-157.

Hyder M L, Lussie W G, Witmer F E. Explosion in the Tomsk-7 reprocessing plant on April 6, 1993. Nuclear Safety 1996; 37: 222-234.

IAEA 1991. The international Chernobyl project. Report by an International Advisory Committee, IAEA, Vienna, 1991. Part D, 107-201.

ICRP 1990. 1990 Recommendations of the International Commission on Radiological Protection. ICRP Publication 60. Pergamon Press, Oxford.

ICRP 1991. The biological basis for dose limitation in the skin. ICRP Publication 59. Pergamon Press, Oxford, 1991.

Jantunen M, Reponen A, Kauranen P, Vartiainen M. Chernobyl fallout in Southern and Central Finland. Health Physics 1991; 60: 427-434.

Jaracz P, Piasecki E, Mirowski S, Wilhelmi Z. Analysis of gamma-radioactivity of "hot particles" released after the Chernobyl accident, II. An interpretation. Journal of Radioanalytical and Nuclear Chemistry 1990; 141: 243-259.

Jambers W, De Bock L, Van Grieken R. Recent advances in the analysis of individual environmental particles. Analyst 1995; 120: 681-692.

Khitrov L M, Cherkezyan V O, Rumyantsev O V. Hot particles after the Chernobyl accident. Geochemistry International 1994; 31: 46-55.

Kerekes A, Falk R, Suomela J. Analysis of hot particles collected in Sweden after the Chernobyl accident. Statens Strålskyddinstitut, SSI-rapport 91-02, 1991.

Kolb W. Radionuclide concentration in ground level air from 1984 to mid 1986 in North Germany and North Norway; influence of the Chernobyl accident. Physikalisch-Technische Bundesanstalt, 1986, PTB-Ra-18, 53-56.

Kritidis P, Catsaros N, Probonas M. Hot particles in Greece after the Chernobyl accident, estimations on inhalation probability. In: Von Philipsborn H and Steinhäusler F (eds.). Hot particles from the Chernobyl fallout. Proceedings of an International Workshop held in Theuern 28/29 October 1987. Schriftenreihe des Bergbau- und Industriemuseums Ostbauern Theuern, 1988; BAND 16: 115-120.

Kutkov V A, Arefieva Z S, Muraviev Yu B, Komaritskaya O I. Unique form of airborne radioactivity: nuclear fuel "hot particles" of the Chernobyl accident. Extended synopses of International Symposium on Environmental Impact of Radioactive Releases, IAEA-SM-339/57P, 1995; 625-630.

Lindner G, Wilhelm Ch, Kaminski S, Schell B, Wunderer M, Wahl U. Inhalation of nonvolatile radionuclides after the Chernobyl accident - a retrospective approach. Proceedings of Eight International Congress of the

International Radiation Protection Association, May 17-22, 1992, Montreal, Canada, 261-264.

Loevinger, R. The dosimetry of beta sources in tissue: the point source dose function. Radiol. 1956; 66: 55-62.

Lujanas V, Mastauskas A, Lujaniene G, Spirkauskaite N. Development of radiation in Lithuania. Journal of Environmental Radioactivity 1994; 23: 249-263.

Luokkanen S, Kulmala M, Raunemaa T. Chernobyl fallout in Finland: hot areas. J. Aerosol Science. 1988; 19: 1363-1366.

Mandjukov I G, Mandjukova B V, Alexiev A, Andreev Ts. High activity hot particles in Kozloduy nuclear power plant - status of the investigations. Radiation Protection Dosimetry 1994; 54: 133-138.

Mattsson R, Hatakka J. Hot particle in inhalate air after the Chernobyl accident. Finnish Association for Aerosol Research, Report Series in Aerosol Science 1986; 2: 28-30 (in Finnish).

Mietelski J W, Was B. Plutonium from Chernobyl in Poland. Applied Radiation and Isotopes 1995; 46: 1203-1211.

Moring M, Ikäheimonen T K, Pöllänen R, Ilus E, Klemola S, Juhanoja J, Eriksson M. Uranium and plutonium containing particles in a sea sediment sample from Thule, Greenland. Journal of Radioanalytical and Nuclear Chemistry 2001; 248: 623-627.

Osuch S, Dabrowska M, Jaracz P, Kaczanowski J, Le Van Khoi, Mirowski S, Piasecki E, Szeflinska G, Szeflinski Z, Tropilo J, Wilhelmi Z, Jastrzebski J, Pienkowski L. Isotopic composition of high-activity particles released in the Chernobyl accident. Health Physics 1989; 57: 707-716.

NCRP 1989. Limit for exposure to "hot particles" on the skin: recommendations of the National Council on Radiation Protection and Measurements. NCRP report No. 106, 1989.

NCRP 1999. Biological effects and exposure limits for "hot particles". Recommendations of the National Council on Radiation Protection and Measurements. NCRP report No. 130, 1999.

Paatero J, Hatakka J. Measurements of long-lived radioactivity in the air and precipitation in Finland 1991-1994. Finnish Meteorological Institute, Publications on Air Quality, Helsinki 1997.

Pavlotskaya F I., Goryachenkova T A, Yemel'yanov V V, Kazinskaya I Ye, Barsukova K V, Myasoyedov B F. Modes of occurrence of plutonium in hot particles. Geochemistry International 1994; 31: 62-69.

Perkins R W, Robertson D E, Thomas C W, Young J A. Comparison of nuclear accident and nuclear test debris. Proceedings in International Symposium on Environmental Contamination Following a Major Nuclear Accident, Vienna, Austria, 16 - 20 Oct. 1989. IAEA-SM-306/125; 1989: 111-139.

Petryaev E P, Sokolik G A, Ovsyannikova S V, Leynova S L, Ivanova T G. Forms of occurrence and migration of radionuclides from the Chernobyl NPP accident in typical landscapes of Byelorussia. Proceedings of the Seminar on Comparative Assessment of the Environmental Impact of Radionuclides Released during Three Major Nuclear Accidents: Kyshtym, Windscale, Chernobyl. Luxembourg, 1-5 October 1990, 185-210.

Piasecki E, Jaracz P, Mirowski S. Analysis of gamma-radioactivity in "hot particles" released after the Chernobyl accident, I. Calculations of fission products in hot particles (a detective approach). Journal of Radioanalytical and Nuclear Chemistry 1990; 141: 221-242.

Pöllänen R, Salonoja M, Toivonen H, Valkama I. Uranium fuel particles in a RBMK accident: Particle characteristics and atmospheric transport. Proceedings in the fifth Finnish national aerosol symposium. June 1-3, 1993. Report Series in Aerosol Science N:o 23, 278 - 283, 1993.

Pöllänen R, Toivonen H, Lahtinen J, Ilander T. Transport of large particles released in a nuclear accident. STUK-A125, 1995.

Pöllänen R, Toivonen H, Lahtinen J, Ilander T. OTUS - Reactor inventory management system based on ORIGEN2. STUK-A126, 1995.

Pöllänen R, Kansanaho A, Toivonen H. Detection and analysis of radioactive particles using autoradiography. STUK-YTO-TR99, 1996.

Pöllänen R. Nuclear fuel particles and radiological hazard. Licentiate thesis, University of Helsinki, 1997.

Robertson D E. Letter to the National Institute of Radiation Protection, Stockholm, Sweden, November 1986.

Rohloff F, Heinzelmann M. Calculation of dose rates for skin contamination by beta radiation. Radiation Protection Dosimetry 1986; 14: 279-287.

Rytömaa T, Toivonen H, Servomaa K, Sinkko K, Kaituri M. Uranium aerosols in Chernobyl fall-out, Finnish Centre for Radiation and Nuclear Safety, internal report, Helsinki, 1986.

Romero 2001. IAEA coordinated research programme (CRP). Radiochemical, chemical and physical characterisation of radioactive particles in the environment. Preliminary version of the report of the research coordination meeting 7-11 May 2001, IAEA, Vienna.

Saari H, Luokkanen S, Kulmala M, Lehtinen S, Raunemaa T. Isolation and characterization of hot particles from Chernobyl fallout in Southwestern Finland. Health Physics 1989; 57, 975-984.

Salbu B. Source-related characteristics of radioactive particles: a review. Radiation Protection Dosimetry 2000; 92:49-54.

Salbu B, Krekling T, Oughton D H, Østby G, Kashparov V A, Brand T L, Day J P. Hot particles in accidental releases from Chernobyl and Windscale nuclear installations. Analyst 1994; 119: 125-130.

Sandalls F J, Segal M G, Victorova N. Hot particles from Chernobyl: a review. Journal of Environmental Radioactivity 1993; 18, 5-22.

Sinkko K, Aaltonen H, Mustonen R, Taipale T K, Juutilainen J. Airborne radioactivity in Finland after the Chernobyl accident in 1986, supplement 1 to annual report STUK-A55. STUK-A56, Finnish Centre for Radiation and Nuclear Safety, Helsinki 1987.

STUK - Radiation and Nuclear Safety Authority. Protective actions in a radiation emergency (in Finnish). Guide VAL 1.1, 2001.

Tcherkezian (Cherkezyan) V, Shkinev V, Khitrov L, Kolesov G. Experimental approach to Chernobyl hot particles. J. Environmental Radioactivity 1994; 22: 127-139.

Toivonen H, Servomaa K, Rytömaa T. Aerosols from Chernobyl: particle characteristics and health implications. In: Von Philipsborn H and Steinhäusler F (eds.). Hot Particles from the Chernobyl Fallout. Proceedings of an International Workshop held in Theuern 28/29 October 1987. Schriftenreihe des Bergbau- und Industriemuseums Ostbauern Theuern, 1988; BAND 16: 97-105.

Vajda N. Radioactive particles in the environment, occurrence, characterisation, appropriate analytical techniques. Preliminary version of a review prepared for the International Atomic Energy Agency, 2001.

Valkama I, Salonoja M. Operational long-range dispersion and dose model for radioactive releases, Finnish Meteorological Institute 1993 (in Finnish).

Valkama I, Salonoja M, Toivonen H, Lahtinen J, Pöllänen R. Transport of radioactive gases and particles in the Chernobyl accident: comparison of environmental measurements and dispersion calculations. International symposium on environmental impact of radioactive releases, Vienna, Austria, 8-12 May 1995, IAEA-SM-339/69.

Valkama I, Pöllänen R. Transport of radioactive materials in convective clouds. Proceedings of the Fourteenth International Conference on Nucleation and Atmospheric Aerosols 1996, 411 - 414.

Valkama I, Ilvonen M. The Finnish operational emergency model framework. In: Kujala E, Laihia K, Nieminen K (eds.). Proceedings of the NBC 2000 Symposium on Nuclear, Biological and Chemical Threats in the 21st century, 13-15.6.2000, Espoo, Finland. University of Jyväskylä, Department of Chemistry, Research report no. 75: 703-704.

Van der Hoven I. Deposition of particles and gases. In: Slade D (ed.) Meteorology and Atomic Energy 1968: 202-208. USAEC Report TID-24190, U.S. Atomic Energy Commission, NTIS.

Van der Wijk A, de Meijer R J, Jansen J F W, Boom G. Core fragments and ruthenium particles in the Chernobyl fallout. In: Von Philipsborn H and Steinhäusler F (eds.). Hot Particles from the Chernobyl Fallout. Proceedings of an International Workshop held in Theuern 28/29 October 1987. Schriftenreihe des Bergbau- und Industriemuseums Ostbauern Theuern, 1988; BAND 16: 53-61.

Viktorova N V, Garger E K. Biological monitoring of the deposition and transport of radioactive aerosol particles in the Chernobyl NPP zone of influence. Proceedings of the Seminar on Comparative Assessment of the Environmental Impact of Radionuclides Released during Three Major Nuclear Accidents: Kyshtym, Windscale, Chernobyl. Luxembourg, 1-5 October 1990, 223-236.

Wahl U, Lindner G, Recknagel E. Radioaktive Partikel im Tschernobyl-Fallout. In: Köhnlein W, Traut H, Fischer N. (eds.). Die Wirkung niedriger Strahlendosen - biologische und medizinische Aspekte. Springer, Berlin-Heidelberg, 1989, 165-176.

WASH-1400. Reactor safety study. An assessment of accident risks in U.S. commercial nuclear power plants. United States Nuclear Regulatory Commission, NUREG-75/014, 1975.

Zeissler C, Wight S A, Lindstrom R M. Detection and characterisation of radioactive particles. Applied Radiation and Isotopes 1998; 49: 1091-1097.

Errata:

Publication II

Second sentence in the text of Fig. 3 should be: Figures (a), (b) and (c) represent effective release heights 100, 500 and 2000 m, respectively.

Reference [12]: The correct volume of Health Physics is 57.

Publication III

The text of Table 1: Uranium dioxide fuel mass is 219 000 kg.

Table 2: Half -life of ^{144}Ce is 284.3 d.

Discussion: The activity of single ruthenium particles found in Poland was even more than 100 kBq (Schubert and Behrend 1987).

Reference [19]: The year of publication is 1988.

Publication VII

Table 2: Half -life of ^{137}Cs is 30 y.

The second sentence of the text of Fig. 3 should be: The 'α particles' show the presence of alpha-active materials.

I

TOIVONEN H, PÖLLÄNEN R, LEPPÄNEN A, KLEMOLA S, LAHTINEN J, SERVOMAA K, SAVOLAINEN A L, VALKAMA I.
A nuclear incident at a power plant in Sosnovyy Bor, Russia.
Health Physics 1992; 63: 571 - 573.

A NUCLEAR INCIDENT AT A POWER PLANT IN SOSNOVYY BOR, RUSSIA

H. Toivonen,* R. Pöllänen,* A. Leppänen,* S. Klemola,* J. Lahtinen,* K. Servomaa,* A. L. Savolainen,† and I. Valkama†

Abstract—**Several radionuclides were identified in the surface air in Finland following a nuclear incident in Sosnovyy Bor on 24 March 1992. In addition to gases, the release contained small uranium fuel particles. The radionuclide concentrations were of the same order of magnitude as the concentrations detected in Northern Finland in 1987 after the nuclear explosion in Novaya Zemlya (1 mBq m^{-3}) but five orders of magnitude smaller than the concentrations during the Chernobyl accident in 1986. The radiological consequences in Finland were insignificant. However, studies show that even a minor release, across the sea and more than 100 km away, can be detected and important information, including the time of the incident and the composition of the release and the burn-up of the damaged fuel, can be revealed by the most accurate radioactivity measurements.**

Health Phys. 63(5):571–573; 1992

Key words: emissions, atmospheric; air sampling; accidents, reactor; radioactivity, airborne

INTRODUCTION

UNIT 3 of the RBMK nuclear power plant in Sosnovyy Bor, near St. Petersburg, Russia, was operating at the nominal power level of 1,000 MW_e until 24 March 1992. At 02:37 local time (23:37 Universal Time Coordinated, UTC, 23 March 1992), one of the 1,700 fuel channels broke down. Small amounts of noble gases, iodine, and other radionuclides were released and transported atmospherically toward the southern coast of Finland (Fig. 1).

The continuous air sampling program of the Finnish Centre for Radiation and Nuclear Safety (STUK) has revealed iodine in the Finnish air space about five times per year during the last 10 y. Artificial radioactivity is usually found during winter and early spring in connection with light winds and stable dispersion conditions.

* Finnish Centre for Radiation and Nuclear Safety, P.O. Box 268, SF-00101 Helsinki, Finland; † Finnish Meteorological Institute, P.O. Box 503, SF-00101 Helsinki, Finland.

(*Manuscript received* 16 *May* 1992; *accepted* 17 *June* 1992)
0017-9078/92/$3.00/0

SAMPLING AND RESULTS

One of the air sampling stations, located in Imatra in Eastern Finland, detected ^{131}I in the air just before the incident in Sosnovyy Bor (Table 1). A minor release obviously occurred before the sudden damage to the fuel channel.

The highest concentrations were measured along the East coast of the Gulf of Finland, in Loviisa and Kotka (Table 2), 12–20 h after the incident occurred. Later, the same nuclides were identified in Helsinki, Nurmijärvi, and Imatra (Fig. 1), but the concentrations were about 100 times smaller (Toivonen et al. 1992).

The radiation doses in Finland were negligible. The integrated ^{131}I concentration in Loviisa air was 70 Bq s m^{-3}. Assuming an inhalation rate of 1 m^3 h^{-1} for an adult (i.e., an intake of 20 mBq), this causes a thyroid dose of 5 nGy. During the Chernobyl fallout, the integrated concentration in Nurmijärvi was 1.7×10^7 Bq s m^{-3}, 200,000 times greater than after the 1992 incident in Sosnovyy Bor (Sinkko et al. 1987).

The air filters were analyzed in autoradiography (exposure time, 3 d). Four particles were found in a filter through which 895 m^3 of air had passed. One of the particles was isolated and studied in gamma spectrometry. The particle contained isotopes of cerium and zirconium (0.1 Bq). The data from the Chernobyl fallout showed that these nuclides were always attached to a uranium matrix. According to earlier studies, the measured activities of ^{141}Ce and ^{95}Zr suggest that the size of the isolated fuel particle was about 1 μm (Toivonen et al. 1987).

The activity ratio of the isotopes ^{133}I and ^{131}I is useful in estimating the age of the released material. The observed ratio of 2.66 (Table 3) is outside the range possible for the iodine isotopes in equilibrium in the reactor core; after a stable neutron flux of about 2 wk,

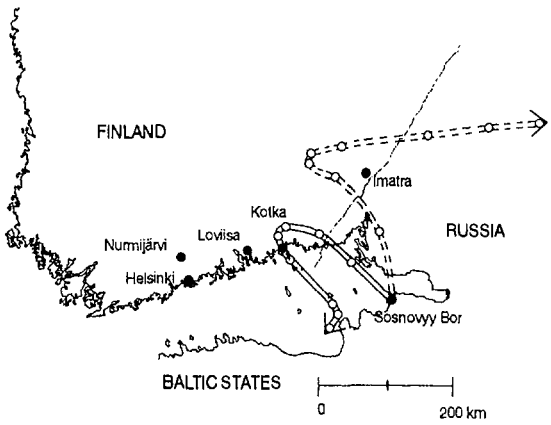

Fig. 1. Surface air parcel trajectory (solid line) and 925 hPa air parcel trajectory, about 500 m above ground (dashed line) from Sosnovyy Bor on 24 March 1992 at 00 UTC. The length of the trajectories is 48 h. The time between the markings (O–O) is 6 h. On 24 March there was an extensive low-pressure area reaching from Southern and Central Europe up to the Baltic States and southern-most Finland. A ridge of high pressure was extending from Central Scandinavia to the central part of Finland. Due to this ridge there was a weak southeastern air flow (0–3 ms^{-1}) over Sosnovyy Bor area toward the Finnish coast. The thermal and kinematic plume rise of gases was probably insignificant. Due to the light winds and the air being slightly warmer than the sea, there seems to have existed a shallow, stable layer over the sea during the morning hours. The plume probably stayed in this layer near the ground. Three-dimensional cross sections of the trajectories showed very limited vertical mixing in the surface layer over the Gulf of Finland. The air masses from Sosnovyy Bor reached the Finnish coast in about 10–12 h.

Table 1. Airborne ^{131}I in Imatra between 1 January 1992 and 23 March 1992. During the period of 19 March to 23 March, southern wind prevailed in Southeastern Finland. Some iodine was most likely released from Sosnovyy Bor before the incident on March 24.

Period	Concentration ($\mu Bq\ m^{-3}$)
13.1–16.1	1.7
6.2–10.2	1.3
19.3–23.3	6

the activity ratio is 2.3 for fresh fuel and 1.93 for fuel near its exhaust burn-up (Anttila 1986).

CONCLUSIONS

The measured activity ratios of the radionuclides, together with nuclide inventory calculations as a function of the fuel burn-up, allow several conclusions to be made concerning the incident. The following reasoning is based on data gathered regarding the emissions in Sosnovyy Bor.

(1) The radioactive substances definitely came from the Sosnovyy Bor area and the incident occurred early in the morning local time on 24 March 1992. This is known due to the presence of short-lived radionuclides and meteorological evidence.

(2) The damage occurred in a fuel element that was near its exhaust burn-up because low activity ratios of ^{141}Ce:^{144}Ce (1.07 ± 0.04) and ^{103}Ru:^{106}Ru (2.04 ± 0.15) were found.

(3) The neutron flux had not been stable in the damaged fuel channel during the last few days or weeks before the incident occurred. This was concluded from the high ^{133}I:^{131}I activity ratio.

(4) Dispersion and concentration calculations show that the ^{131}I concentrations observed in Finland are explained by a release of 10^{10} Bq—100 million times less than the release from the Chernobyl accident.

(5) The release contained not only noble gases and iodine, but other radioactive substances that were dispersed as an aerosol containing small fuel particles.

Table 2. Radionuclide concentrations in Kotka. A high-volume air sampler was used (150 $m^3\ h^{-1}$), and the filters were analyzed several times using low background gamma spectrometers.

Sampling period	(a) 14:25–20:15
(UTC)	(b) 20:15–05:56
Reference time	(a) 17:20, 24 March
(UTC)	(b) 01:01, 25 March

Nuclide	Concentration ($\mu Bq\ m^{-3}$) (a)	(b)
^{95}Zr	840	4
^{95}Nb	1,150	18
^{97}Zr	880	
^{99}Mo	1,900	
^{99m}Tc[a]		
^{103}Ru	1,430	20
^{106}Ru	630	32
(^{105}Rh)	1,200	
^{127}Sb	65	
(^{129m}Te)	470	
(^{132}Te)	1,000	48
^{131}I	830	61
^{132}I[a]		
^{133}I	1,320	73
^{134}Cs	260	19
^{136}Cs	66	
^{137}Cs	380	28
^{140}Ba	1,600	20
^{140}La[a]		
^{141}Ce	820	4
^{143}Ce	660	
^{144}Ce	750	
(^{237}U)	300	
(^{238}Np)	300	
^{239}Np	10,000	

[a] Identified.
( ) = Low accuracy.

Table 3. ^{133}I:^{131}I concentration ratios at the reference time and at the incident time. The only source of error in the estimation of the activity ratios is the accuracy of the gamma spectrometric analysis; standard error propagation formula was used. The error estimate of the average ratio is weighted by the square of the individual measurement errors.

Sample	Reference time (UTC)	Iodine concentration ratio at the reference time	Iodine concentration ratio at the incident time, 23.3 at 23:37 UTC
Loviisa I	24.3 at 11:10	1.88 ± 0.12	2.64 ± 0.17
Loviisa II	24.3 at 22:15	1.37 ± 0.08	2.69 ± 0.16
Kotka I	24.3 at 17:20	1.59 ± 0.07	2.69 ± 0.11
Kotka II	25.3 at 01:01	1.20 ± 0.15	2.54 ± 0.31
Helsinki	24.3 at 23:56	1.04 ± 0.27	2.14 ± 0.54
		Average:	2.66 ± 0.08

REFERENCES

Anttila, M. Activity inventory of the fuel in an RBMK type reactor. Helsinki, Finland: Technical Research Centre of Finland; Tsherno-2/86; 1986 (in Finnish).

Sinkko, K.; Aaltonen, H.; Mustonen, R.; Taipale, T. K.; Juutilainen, J. Airborne radioactivity in Finland after the Chernobyl accident in 1986. Helsinki, Finland: Finnish Centre for Radiation and Nuclear Safety; STUK-A56; 1987.

Toivonen, H.; Klemola, S.; Lahtinen, J.; Leppänen, A.; Pöllänen, R.; Kansanaho, A.; Savolainen, A. L.; Sarkanen, A.; Valkama, I.; Jäntti, M. Radioactive release from Sosnovyy Bor, St. Petersburg, in March 1992. Helsinki, Finland: Finnish Centre for Radiation and Nuclear Safety; STUK-A104; 1992.

Toivonen, H.; Servomaa, K.; Rytömaa, T. Aerosols from Chernobyl: Particle characteristics and health implications. In: von Philibsborn, H.; Steinhäusler, F, eds. Hot particles from the Chernobyl fallout, proceedings of an International Workshop, Theuern, Finland, October 1987. 5th Radiometric Seminar Theuern. Theuern, Germany: Schriftenreihe des Bergbau—und Industriemuseums, Ostbayern Theuern, Band 16; 1988: 97–105.

■ ■

II

PÖLLÄNEN R, TOIVONEN H.
Skin doses from large uranium fuel particles - application to the Chernobyl accident.
Radiation Protection Dosimetry 1994; 54: 127 - 132.

Radiation Protection Dosimetry
Vol. 54, No. 2, pp. 127–132 (1994)
Nuclear Technology Publishing

SKIN DOSES FROM LARGE URANIUM FUEL PARTICLES: APPLICATION TO THE CHERNOBYL ACCIDENT

R. Pöllänen and H. Toivonen
Finnish Centre for Radiation and Nuclear Safety
PO Box 14, FIN-00881 Helsinki, Finland

Received July 17 1993, In Final Revised Form January 4 1994, Accepted January 12 1994

Abstract — Radiation dose to the skin caused by large nuclear fuel particles is calculated as a function of the particle size. The size range considered is 6–40 μm (aerodynamic diameter 20–140 μm). Air–tissue surface effects and self-absorption of the particles are taken into account in the dose estimation. The nuclide composition of the particles is estimated from the inventory of the Chernobyl reactor. When deposited on the skin the uranium fuel particle of size 40 μm can cause a dose of 1.6 $Gy.cm^{-2}$ to the basal cell layer in one day. The transport range calculations show that these particles may remain airborne tens of kilometres away from the power plant.

INTRODUCTION

In a nuclear accident the reactor core may be seriously damaged due to energetic events, e.g. strong reactivity transients, steam explosions or hydrogen explosions. These events can break down the containment surrounding the core and large amounts of radioactive substances, either gases or particles, can be released to the atmosphere. The gases are mainly krypton and xenon and compounds of iodine whereas the particles usually contain several radionuclides.

Small particles (aerodynamic diameter d_a less than a few micrometres) are mainly formed from the gaseous species by nucleation and condensation. Generally, their nuclide composition deviates from the nuclide composition of the fuel. Nuclear fuel particles formed by mechanical fragmentation are usually large ($d_a \geq 100$ μm). Smaller particles down to a few micrometres, are also formed mechanically in energetic events, as happened in the Chernobyl accident in 1986. Such particles were also released in the Sosnovyy Bor incident (1992)[1].

The tiny fuel fragments contain the same non-volatile radionuclides as the fuel, on average. Noble gases and gaseous forms of iodine are missing. Caesium, tellurium and sometimes ruthenium are often depleted or missing. The activity of non-volatile nuclides in a fuel particle can be estimated from the radionuclide inventory of the core.

Particle transport from the site of the accident depends strongly on weather conditions. If a large amount of heat is released to the environment, the radioactive plume can rise rapidly several hundreds or even thousands of metres above the ground. Particles less than a few micrometres in size can stay in the atmosphere days or sometimes years provided that they are initially transported to the upper parts of the atmosphere.

The large particles leave the main aerosol stream mainly by sedimentation. Therefore, the behaviour and the radiological consequences of the large particles are not described properly by assuming that the 'particle plume' is mixed in the same way as the gaseous plume (Figure 1). Deterministic particle trajectory calculations are needed. For each transport distance x there exists, in principle, one maximum particle size d_{max} that can be calculated in a straightforward way. If the mean upward wind speed is small relative to the particle settling velocity and atmospheric turbulence is negligible during the transport only a few particles larger than d_{max} remain airborne at distances greater than x.

Consequence analyses of severe accidents are often performed in a way that does not take properly into account the particle nature of the release. The properties of the particles have an important role in the possible radiological hazard that the radioactive substances may cause. Tissue, in contact with the uranium fuel fragments, can receive a very large and highly non-uniform radiation dose. Even a local ulceration may develop if

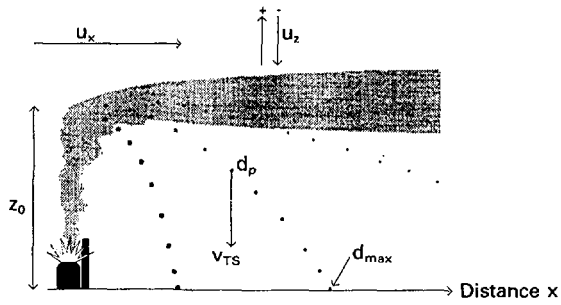

Figure 1. Schematic presentation of plume transport for particles of various sizes. v_{TS} settling velocity, z_0 effective release height, u_x wind velocity, u_z vertical velocity (upward or downward) of the air.

a single 'hot particle' is deposited on the skin. NCRP estimates[2] that an acute skin damage (deep ulceration) is not expected if the total beta emission is below 10^{10}.

Calculations of the dose to the skin from radioactive particles in contact with the skin are often performed for infinite homogeneous media assuming point source geometry[3]. The doses are then overestimated due to the backscattering from non-existing tissue above the skin. Self-shielding of the particle is another phenomenon that is often omitted in the dose assessment. The reduction of the skin dose is significant if the particles contain nuclides of low beta energy. The present paper gives an analytical method to cope with the self-shielding.

ACTIVITY OF NUCLEAR FUEL PARTICLES

Activity of a nuclear fuel particle as a function of particle size can be calculated from the radionuclide inventory of the reactor core. Let the total activity of isotope N be A_N in a reactor fuel. The average concentration of nuclide N in the fuel is

$$C_N = A_N/m_{fuel} \quad (1)$$

where m_{fuel} is the total mass of the fuel. The activity of nuclide N in a single particle p is then

$$A_{p,N} = m_p C_N = A_N \frac{\pi \rho_p d_p^3}{6 m_{fuel}} \quad (2)$$

where m_p is the mass and d_p the diameter of a spherical particle of density ρ_p.

The radionuclide inventory and the beta activity of single fuel particles are given in Table 1 for the RBMK reactor. These nuclides, having half-lives in excess of a few weeks, were detected in the nuclear fuel particles that spread over Europe after the Chernobyl accident. Highly volatile nuclides, e.g. ^{131}I and ^{137}Cs, are not included in Table 1 because they do not necessarily remain in the fragmented nuclear fuel. Iodine and caesium are mainly incorporated into small particles of varying composition. Ruthenium, however, was often detected in the fuel fragments but sometimes it was completely or partially missing.

Mainly due to continuous refueling, the RBMK reactor core contains fuel elements with different burnup. The activity concentrations calculated in this study refer to the core-averaged burnup of about 10 MW.d per kilogram of fuel. Especially for long-lived nuclides, the concentration can be remarkably larger in case of fuel elements with discharge burnup.

SKIN DOSES

Acute skin damage can be caused by a large nuclear fuel particle. The threshold dose for ulceration, caused by a particle of diameter less than 1 mm, is estimated to be 75 Gy over an area of 1.1 mm^2 at a depth of 16 μm[9]. This represents a skin dose of about 1 Gy calculated over an area of 1 cm^2 at a depth of 100–150 μm. The NCRP limit of 10^{10} total beta emissions[2], intended to prevent acute deep ulceration, may lead to a higher skin dose of about 5 Gy[9].

In the present paper the skin dose is averaged over an area of 1 cm^2 at three different depths: 0.07 mm (directional dose equivalent H′(0.07) for basal cells), 0.4 mm (average depth related to the production of late deterministic effects such as dermal atrophy[10]) and 3 mm (depth of the lens of the eye). The dose conversion factors for a point source used in this study are given in Table 2[11]. They apply to the tissue–air boundary. The dose estimates have to be corrected for the attenuation of beta particles in three-dimensional sources. A simple method is given below.

The effect of self-shielding has been investigated in the case of macroscopic (millimetres in size) and variable density sources[12,13]. The self-shielding is important, especially at low beta energies. Compared with the millimetre sized objects, the particles considered in this study are small ($d_p < 40$ μm) but their density is high ($\rho_p = 10.5$ g.cm^{-3}). Thus, the self-shielding may be important, at least for the largest particles.

The activity of the various nuclides is usually determined using gamma spectrometry. The self-absorption of the gamma radiation is negligible in a fuel particle. However, the real beta activity $A_{p,N}$ appears to have been reduced to $A_{p,N} \times SAF$, where SAF is the self-absorption factor, i.e. the fraction of the original beta flux that reaches the surface of the particle. Assuming that the particle is spherical and homogeneous[14]

$$SAF = \frac{1}{r_p} \int_0^{r_p} \int_0^{\pi} \frac{r^2 \, dr \sin(\theta) \, d\theta}{s^2} \exp(-\mu_\rho s) \quad (3)$$

$$s = (r^2 + r_p^2 - 2 r r_p \cos(\theta))^{\frac{1}{2}}, \quad (4)$$

where $r_p = d_p/2$ is the radius of the particle. μ_ρ/ρ_p is the mass attenuation coefficient. It is a function of the maximum beta energy E_{max} (MeV)[15]

$$\mu_\rho/\rho_p = A \, E_{max}^{-B} \ (m^2.kg^{-1}) \quad (5)$$

Coefficients A and B are related to the effective atomic number of the absorber. Assuming that the particles are pure UO_2 we can set A = 2.3 and B = 1.4[16].

Equation 3 is solved numerically in Reference 14. An analytical solution was found.

$$SAF = 2 (\mu_\rho d_p)^{-1} - 2 (\mu_\rho d_p)^{-2} [1 - \exp(-\mu_\rho d_p)]. \quad (6)$$

When $\mu_\rho d_p \ll 1$, the approximation

$$SAF = 1 - \frac{\mu_\rho d_p}{3} \quad (7)$$

can be used.

Figure 2 shows the self-absorption factor for selected

Table 1. Activity (Bq) of uranium fuel particles originating from a RBMK reactor as a function of particle size (physical diameter d_p and aerodynamic diameter d_a). Chernobyl inventory is used in this study[4–7]. The inventory of daughter nuclides is assumed to be the same as the inventory of the parent nuclides. The inventory of ^{91}Y is estimated on the basis of the activity ratio of $^{91}Y/^{89}Sr = 1.26$[4,8]. Uranium dioxide fuel mass is 192,000 kg.

Nuclide	Inventory (Bq)	d_a: 20 μm d_p: 6.2 μm	30 μm 9.3 μm	40 μm 12.2 μm	50 μm 15.3 μm	100 μm 28.9 μm	140 μm 39.4 μm
^{89}Sr	2.3×10^{18}	16	53	120	240	1600	4000
^{90}Sr	2.0×10^{17}	1.4	4.6	10	21	140	350
^{90}Y	2.0×10^{17}	1.4	4.6	10	21	140	350
^{91}Y	2.9×10^{18}	20	67	150	300	2000	5100
^{95}Zr	5.0×10^{18}	34	120	260	510	3500	8800
^{95}Nb	5.0×10^{18}	34	120	260	510	3500	8800
^{103}Ru	4.9×10^{18}	33	110	250	500	3400	8600
^{106}Ru	2.0×10^{18}	14	46	100	210	1400	3500
^{106}Rh	2.0×10^{18}	14	46	100	210	1400	3500
^{140}Ba	5.3×10^{18}	36	120	280	540	3700	9300
^{140}La	5.3×10^{18}	36	120	280	540	3700	9300
^{141}Ce	5.6×10^{18}	38	130	290	570	3900	9800
^{144}Ce	3.2×10^{18}	22	74	170	330	2200	5600
^{144}Pr	3.2×10^{18}	22	74	170	330	2200	5600
Total	4.7×10^{19}	320	1100	2400	4800	33000	82000

Table 2. Dose rate ($\mu Gy.h^{-1}$) from beta particles in water from a 1 Bq point source on air–water boundary, averaged over 1 cm^2 at depth h (Monte Carlo calculation)[11]. $t_{\frac{1}{2}}$ is the half-life of the nuclides and X_{90} is the distance (mm) at which 90% of the beta energy is absorbed.

Nuclide	$t_{\frac{1}{2}}$	X_{90} (mm)	h = 0.07 mm	h = 0.4 mm	h = 3 mm
^{89}Sr	50.6 d	3.03	1.67	0.887	0.0546
^{90}Sr	28.6 a	0.787	1.38	0.335	—
^{90}Y	64.1 h	5.17	1.76	1.05	0.2
^{91}Y	58.5 d	3.24	1.67	0.897	0.0637
^{95}Zr	64.0 d	0.461	1.06	0.0857	—
^{95}Nb	35.1 d	0.094	0.230	—	—
^{103}Ru	39.3 d	0.267	0.568	0.028	—
^{106}Ru	368.2 d	0.008	—	—	—
^{106}Rh	29.9 s	7.92	1.85	1.17	0.326
^{140}Ba	12.8 d	1.65	1.46	0.490	0.0007
^{140}La	40.2 h	2.97	1.64	0.845	0.0385
^{141}Ce	32.5 d	0.605	1.54	0.169	—
^{144}Ce	384.3 d	0.277	0.815	0.0287	—
^{144}Pr	17.3 min	6.71	1.82	1.13	0.285

maximum beta energies as a function of particle size. Nuclide specific values are given in Table 3. In the case of nuclides with several beta decay branches and, consequently, several maximum beta energies, the total SAF is calculated as a sum of SAFs of each branch weighted by the branching probability.

Beta absorption, even in relatively small particles, is important for beta emitters of low energy like ^{95}Zr, ^{95}Nb, ^{103}Ru, ^{106}Ru and ^{144}Ce. The flux from the high energy beta emitters (^{90}Y, ^{106}Rh and ^{144}Pr) is attenuated less than 10% even in the largest particle considered in this study.

Total beta dose rate in three different depths of the skin as a function of particle size is presented in Table 4. The dose rate is given with and without SAF. Self-absorption is not very significant in small particles. For the largest particles the dose rate in the basal cell layer of the skin is reduced to two thirds. Self-absorption does not alter dose rates significantly at a depth of 3 mm.

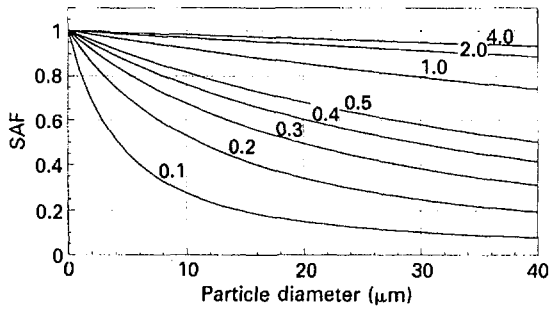

Figure 2. Self-absorption of beta particles in uranium fuel. SAF is defined in Equation 3. Maximum beta energy (MeV) is marked above each curve. ρ_p = 10.5 g.cm^{-3}.

Nuclides ^{140}La, ^{144}Pr, ^{140}Ba, ^{141}Ce and ^{91}Y cause about two thirds of the skin dose rate to the basal cells. The dose at a depth of 3 mm is caused mainly by high energy beta emitters ^{144}Pr and ^{106}Rh.

ICRP recommends that the annual equivalent dose limits for occupational workers are 150 mSv for the lens of the eye and 500 mSv for the skin, averaged over any 1 cm^2, regardless of the area exposed[10]. For the public the limits are 15 mSv and 50 mSv, respectively. The skin dose limits provide sufficient protection against the deterministic effects in the basal cell layer at a nominal depth of 7 mg.cm^{-2},

The dose rate in the basal layer of the skin for a d_p = 40 μm particle is about 70 mGy.h^{-1} averaged over 1 cm^2. When a particle of this size is deposited on the skin the total beta dose in 24 h is approximately 1.6 Gy. Particles larger than 25 μm (physical diameter) can cause a skin dose of 500 mGy averaged over 1 cm^2 in one day. Correspondingly, particles larger than 10 μm can cause a dose of 50 mGy. At a depth of 3 mm, relevant to the eye lens dose, a particle of physical diameter about 20 μm will in 24 h deliver a dose averaged over an area of 1 cm^2 of 15 mGy.

ATMOSPHERIC TRANSPORT OF PARTICLES OF DIFFERENT SIZES

In case of a possible nuclear accident it is essential

Table 3. Self-absorption factor SAF for various nuclides as a function of particle size. Particle density is assumed to be 10.5 g.cm^{-3}. The maximum beta energy E_{max} refers to the most probable decay branch.

Nuclide	E_{max} (MeV)	d_a: d_p:	20 μm 6.2 μm	30 μm 9.3 μm	40 μm 12.2 μm	50 μm 15.3 μm	100 μm 28.9 μm	140 μm 39.4 μm
^{89}Sr	1.49		0.972	0.959	0.946	0.933	0.879	0.841
^{90}Sr	0.546		0.893	0.846	0.805	0.765	0.622	0.539
^{90}Y	2.28		0.984	0.977	0.970	0.962	0.931	0.907
^{91}Y	1.54		0.973	0.960	0.948	0.935	0.883	0.846
^{95}Zr	0.366		0.833	0.765	0.709	0.656	0.487	0.402
^{95}Nb	0.160		0.574	0.462	0.388	0.330	0.196	0.148
^{103}Ru	0.226		0.690	0.591	0.519	0.458	0.299	0.235
^{106}Ru	0.0394		0.134	0.092	0.071	0.057	0.030	0.022
^{106}Rh	3.54		0.991	0.986	0.982	0.977	0.957	0.942
^{140}Ba	0.991		0.919	0.885	0.855	0.826	0.716	0.649
^{140}La	1.35		0.971	0.956	0.943	0.929	0.871	0.830
^{141}Ce	0.435		0.870	0.815	0.768	0.723	0.568	0.483
^{144}Ce	0.318		0.768	0.680	0.613	0.553	0.381	0.304
^{144}Pr	3.00		0.989	0.983	0.978	0.973	0.949	0.932

to be prepared for hot particle release. Estimation of the transport range is needed. Particle transport depends strongly on weather conditions and particle properties, e.g. horizontal wind speed u_x, vertical velocity u_z of the air, maximum effective release height z_0 and density ρ_p of the particles. Provided that u_z and u_x are constant during transport, the expected maximum particle size d_{max} that can enter the target area is[17]

$$d_{max} = k \left(\frac{z_0 u_x \pm u_z x}{\rho_p x} \right)^{\frac{1}{2}} \quad (8)$$

where x is distance between source and target area, and the '±' sign represents the upward and downward velocity of air (see Figure 1). Constant $k = (18\,\eta/g)^{\frac{1}{2}} \approx 5.8 \times 10^{-3}$ (kg.s)$^{\frac{1}{2}}$.m^{-1} for dry air at STP conditions.

Figure 3 shows the effects of the release height on the range of particles in air. Even rather large particles ($d_p \geq 10$ μm) can be transported several hundreds of kilometres if the effective release height is thousands of metres. Relatively minor vertical air flows have a significant influence on the transport of the particles of size $d_p \leq 20$ μm. Deterministic transport range calculations are appropriate for large particles because the air turbulence has less significance.

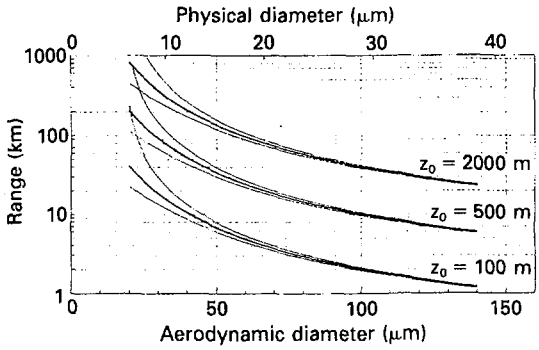

Figure 3. Maximum transport distance of aerosol particles for three different effective release heights z_0. The horizontal wind speed u_x is 5 m.s^{-1}. The centremost curve of each set was calculated assuming no vertical movements of air masses. Equation 8 with constant $u_z = \pm 1$ cm.s^{-1} was used to produce the other curves (redrawn from Reference 17). $\rho_p = 10.5$ g.cm^{-3}.

The weather conditions and particle properties vary greatly. Transformation to the new conditions can be done approximately as follows: transport range x is directly proportional to u_x and z_0 and inversely proportional to ρ_p. Compared to a 'reference case', e.g. to one of the curves presented in Figure 3, the transport range under the new conditions is $x_{new} = x_{ref}\,(u_{x,new}/u_{x,ref})\,(z_{o,new}/z_{0,ref})\,(\rho_{p,ref}/\rho_{p,new})$, where x_{ref} is the transport range in the reference case. For example, let $u_{x,new} = 3$ m.s^{-1}, $z_{0,new} = 400$ m, $\rho_{p,new} = 8$ g.cm^{-3} and $x_{ref} = 2$ km for $d_p = 28.9$ μm ($d_a = 100$ μm). The new transport range is then 3.15 times the range in the reference case, i.e. 6.3 km.

Transport calculations of the nuclear fuel fragments must be connected to the prevailing weather conditions. In operational use, particle trajectory calculations, similar to air parcel calculations, are needed. Simple transport range estimation, i.e. Equation 8, is adequate provided that vertical air flows are small compared with the gravitational settling velocity of the particles.

Table 5. Transport range (km) of $d_p = 40$ μm ($d_a = 140$ μm) particle at different effective release heights and wind velocities.

Release height (m)	Wind velocity (m.s^{-1})				
	1.0	3.0	5.0	7.0	10.0
100	0.23	0.69	1.1	1.6	2.3
300	0.69	2.1	3.4	4.8	6.9
500	1.1	3.4	5.7	8.0	11
1000	2.3	6.9	11	16	23
2000	4.6	14	23	32	46
3000	6.9	21	34	48	69

Table 4. Beta dose rate (mGy.h^{-1}) for the skin averaged over 1 cm^2 at depth h from a virtual point source (no self-shielding) and from particles of different sizes (self-shielding included) consisting of RBMK fuel (Table 1). SAF = self-absorption factor (see text).

d_a (μm)	d_p (μm)	h = 0.07 mm		h = 0.4 mm		h = 3 mm	
		Point source	SAF included	Point source	SAF included	Point source	SAF included
20	6.2	0.38	0.34	0.13	0.13	0.015	0.014
30	9.3	1.3	1.1	0.45	0.42	0.049	0.048
40	12.2	2.9	2.4	1.0	0.94	0.11	0.11
50	15.3	5.7	4.6	2.0	1.8	0.22	0.21
100	28.9	38	28	14	11	1.5	1.4
140	39.4	97	64	34	28	3.7	3.4

DISCUSSION

Detailed particle activity calculations have to be performed using the specific activity of the fuel elements with different burnup. Accidentally released fuel fragments originating from nuclear reactors that are operating in a very high burnup regime (for example some nuclear submarines), can be much more radioactive than the particles described in this study. The skin doses are then considerably higher.

Table 1 shows that the beta activity of a RBMK fuel particle with a diameter of $d_p = 40$ μm is slightly less than 10^5 Bq, i.e. the NCRP limit of 10^{10} beta emissions may be exceeded in approximately one day. The transport range of these particles at different release heights and wind velocities is given in Table 5. The risk that the NCRP limit is exceeded in one day exists within distances up to tens of kilometres from the plant. In the Chernobyl accident this distance is estimated to be 40 km[17].

Ruthenium particles that were found after the Chernobyl accident are of special radiological importance. The activities of single ruthenium particles found in Poland were up to 100 kBq[18]. The size of a typical carrier-free 10 kBq ^{103}Ru (and 2.8 kBq ^{106}Ru) particle is estimated to be $d_p \approx 4.5$ μm[19]. Thus, a Ru particle of size $d_p \approx 9$ μm has an activity of the order of 100 kBq. These particles are a potential health hazard, and they can be transported hundreds of kilometres away from the plant.

REFERENCES

1. Toivonen, H., Pöllänen, R., Leppänen, A., Klemola, S., Lahtinen, J., Servomaa, K., Savolainen, A. L. and Valkama, I. *A Nuclear Incident at a Power Plant in Sosnovyy Bor, Russia.* Health Phys. **63**, 571–573 (1992).
2. National Council on Radiation Protection and Measurements. *Limit for Exposure to 'Hot Particles' on the Skin.* NCRP Report No 106 (Bethesda, MD: NCRP Publications) (1989).
3. Traub, R. J., Reece, W. R., Scherpelz, R. I. and Sigalla, L. A. *Dose Calculations for Contamination of the Skin Using the Computer Code VARSKIN.* NUREG/CR-4418 (Pacific North-west Laboratory, Richland, WA) (1987).
4. Khan, S. A. *The Chernobyl Source Term: A Critical Review.* Nucl. Saf. **31**(3), (1990).
5. International Nuclear Safety Advisory Group. *Summary Report on the Post-Accident Review Meeting on the Chernobyl Accident.* IAEA Safety Series 75-INSAG-1 (1986).
6. International Nuclear Safety Advisory Group. *Radionuclides Source Terms from Severe Accidents to Nuclear Power Plants with Light Water Reactors.* IAEA Safety Series 75-INSAG-2 (1987).
7. USSR State Committee on the Utilization of Atomic Energy (Comp.). *The Accident at the Chernobyl Nuclear Power Plant and its Consequences.* Parts 1 and 2. Presented at experts meeting, Vienna, 25–29 Aug. (1986).
8. Goldman, M., Catlin, R. J. and Anspangh, L. *Health and Environmental Consequences of the Chernobyl Nuclear Power Plant Accident.* Report DOE/ER-0332 (1987).
9. International Commission on Radiological Protection. *The Biological Basis for Dose Limitation in the Skin.* ICRP Publication 59. Ann. ICRP **22**(2) (Oxford: Pergamon Press) (1991).
10. International Commission on Radiological Protection. *1990 Recommendations of the International Commission on Radiological Protection.* ICRP Publication 60. Ann. ICRP **21**(1–3) (Oxford: Pergamon Press) (1990).
11. Cross, W. G., Freedman, N. O. and Wong, P. Y. *Beta Ray Dose Distributions from Skin Contamination.* Radiat. Prot. Dosim. **40**(3), 149–168 (1992).
12. Durham, J. S. *Hot Particle Dose Calculations Using the Computer Code VARSKIN Mod 2.* Radiat. Prot. Dosim. **39**(1–3), 75–78 (1991).
13. Durham, J. S., Reece, W. D. and Merwin, S. E. *Modelling Three-Dimensional Beta Sources for Skin Dose Calculations Using VARSKIN Mod 2.* Radiat. Prot. Dosim. **37**(2), 89–94 (1991).
14. Tsoulfanidis, N. *Hot Particles Self-Absorption Factor.* Health Phys. **60**, 841–842 (1991).
15. Thontadarya, S. R. *Effect of Geometry on Mass Attenuation Coefficient of β-particles.* Int. J. Appl. Radiat. Isot. **35**(10), 981–982 (1984).
16. Nathu Ram, Sundara Rao, I. S. and Mehta, M. K. *Mass Absorption Coefficients and Range of Beta Particles in Be, Al, Cu, Ag and Pb.* Pramāna **18**(2), 121–126 (1982).
17. Pöllänen, R. and Toivonen, H. *Transport of Large Uranium Fuel Particles Released from a Nuclear Power Plant in a Severe Accident.* J. Radiol. Prot. **14**, 55–65 (1994).
18. Osuch, S., Dąbrowska, M., Jaracz, P., Kaczanowski, J., Le Van Khoi, Mirowski, S., Piasecki, E., Szeflińska, G., Szefliński, Z., Tropiło, J., Wilhelmi, Z., Jastrzębski, J. and Pieńkowski, L. *Isotopic Composition of High-Activity Particles Released in the Chernobyl Accident.* Health Phys. **57**, 707–716 (1989).
19. Devell, L. *Nuclide Composition of Chernobyl Hot Particles.* In: Hot Particles from the Chernobyl Fallout. Eds. H. Von Philipsborn and F. Steinhäusler. Proc. Int. Workshop, Theuern 28/29 October 1987. Schriftenreihe des Bergbau- und Industriemuseums Ostbauern Theuern, BAND 16, 23–24 (1987).

III

PÖLLÄNEN R, TOIVONEN H.
Transport of large uranium fuel particles released from a nuclear power plant in a severe accident.
Journal of Radiological Protection 1994; 14: 55 - 65.

Reprinted with permission from the publisher.

J. Radiol. Prot. 1994 Vol. 14 No 1 55–65 Printed in the UK

Transport of large uranium fuel particles released from a nuclear power plant in a severe accident

Roy Pöllänen and Harri Toivonen
Finnish Centre for Radiation and Nuclear Safety, P.O. Box 268, SF-00101 Helsinki, Finland

Received 18 February 1993, accepted for publication 10 November 1993

Abstract. Large amounts of radioactive particles can be released in a severe nuclear accident. The particles that may cause a serious health risk via inhalation or deposition on the skin can be transported hundreds of kilometres via air flows. In the present study the transport range of uranium fuel particles of sizes between $d_a = 20–140$ μm is estimated in simplified meteorological conditions. The analysis is applied to the particle transport in the Chernobyl accident. The results of the calculations are supported by the environmental findings of the particles. The wind speed and the initial plume rise have a crucial influence on the transport distance. A simple ballistic analysis is not adequate if the vertical air flow varies greatly during transport. In such weather conditions the analysis must be connected with three-dimensional trajectory calculations.

1. Introduction

Radioactive material released from a nuclear power plant during a severe accident can rise to several hundreds of metres or even up to a few kilometres. Radioactive particles are then transported hundreds, or sometimes thousands, of kilometres within the plume. Large particles settle down rather quickly but small particles can stay in the atmosphere for days or sometimes weeks.

Particles larger than 100 μm in diameter are mainly produced by mechanical fragmentation. However, in the extreme conditions of a nuclear reactor core, the sudden release of energy in a power excursion or explosion may be so large that small particles down to less than a few micrometres in diameter are produced mechanically [1]. This was the case in Chernobyl in 1986 [2].

Particles can be formed through nucleation and condensation from the vaporised reactor fuel, but the size of these particles is generally smaller than 1 μm. They consist mainly of volatile substances, e.g. caesium, iodine and ruthenium, whereas the overall radionuclide composition of the fuel particles is close to the radionuclide inventory of the core. The Chernobyl accident dispersed uranium fuel particles with activity up to tens of kBqs all over Europe [3].

It is usually assumed in consequence analyses of severe nuclear accidents that particles within a release plume have a predetermined dry deposition velocity defined as

$$v_{dep} = J_0/C_0 \qquad (1)$$

where J_0 is the particle flux to the ground and C_0 is the undisturbed concentration above the ground. Deposition velocity is the effective velocity of particle migration to a surface.

The dry deposition velocity of particles depends on particle properties (size), surface characteristics (roughness) and atmospheric conditions. Van der Hoven [4] suggests that when the gravitational settling velocity of the particles is greater than 1 m s^{-1} (aerodynamic diameter $d_a > 200$ μm), the particles fall so fast that turbulent dispersion is no longer important. Small particles ($d_a < 1$ μm) are deposited as a result of turbulent diffusion and Brownian motion. When $d_a > 10$ μm the gravitational settling is important [5]. The particles considered in this study ($d_a = 20–140$ μm), known later as large particles, have a settling velocity

0952-4746/94/010055+11 $19.50

greater than 0.01 m s^{-1} which is the value often used for dry deposition (e.g. in [6]). Particles of this size are deposited mainly due to sedimentation or turbulent dispersion.

In radiation protection and emergency preparedness the large nuclear fuel particles pose different problems to those of the small radioactive particles or gaseous fission products. The problems are clearly seen in operational air concentration measurements. The average nuclide concentration (Bq m^{-3}) is not meaningful if all the activity comes from a few particles. Moreover, the radiologial risks connected with these highly radioactive particles are not the same as those in a homogeneous exposure. The large particles can also be transported to areas other than those areas where the gases or small particles are transported in a complex three-dimensional wind field. These differences are discussed briefly below.

The monitoring networks, which are employed in several countries and designed to detect environmental radioactivity, measure average activity concentration (Bq m^{-3}) in air or the concentration integral of the radionuclides. Single particles are not registered. Afterwards, however, the existence of large radioactive particles can be verified in autoradiography.

A similar situation is met in a typical consequence analysis when statistical models, e.g. Gaussian type models like 'tilted plume model' or 'drift deposition model' [5], are used. The predictions of these models are of statistical nature. In the case where average activity concentration is low, but the activity comes from a few large particles, the interpretation of calculated results can be misleading. One may ask what does the calculated average concentration (Bq m^{-3}) mean if the activity is in large particles whose number concentration is low (for example less than 10^{-3} m^{-3}) or, in the extreme situation, only in one particle. For example, after the Sosnovyy Bor incident in 1992 we found four particles in a filter through which 900 m^3 of air had passed. Most of the activity was in these small uranium fuel particles [7].

The dose conversion factors (Sv Bq^{-1}) for inhalation are defined for small particles (AMAD = 1 μm). This may be relevant for caesium and iodine, but not for the fragments of the uranium fuel. The results of the analyses are usually interpreted as an averaged value for the quantity considered, e.g. the effective dose. The overall activity concentraton in air may be below the level of countermeasures. However, there is a risk that a severe local injury may be caused by a single 'hot particle' deposited on the skin or in the upper airways.

Large particles are not distributed within the plume in the same way as gaseous fission products or small particles. Soon after the release the large particles leave the main aerosol stream mainly by sedimentation. In weather types, where wind conditions (wind speed and wind direction) differ significantly at different heights, the large particles and gaseous species or small particles are transported separately (figure 1). It is even possible that in some areas the fall-out contains mainly large fuel particles, not gaseous fission products or small particles.

For sheltering purposes it is crucial to find out the maximum transport range of particles that can cause an acute health risk, i.e. the areas of particle deposition must be recognised beforehand. This is a field that needs further studies.

In this paper the transport range of uranium fuel particles is studied using simple ballistic analyses with predetermined particles sizes, wind velocity and effective release height. The effect of macroscopic vertical air flows and dispersion due to atmospheric turbulence is estimated using the concept of effective vertical velocity. In the case of the macroscopic air flows the results are applied to large particle transport in the Chernobyl accident.

2. Gravitational settling

The theory of gravitational settling is presented in the textbooks of aerosol physics, e.g. in reference [8]. A brief summary is given below. Definitions of the variables and the constants are given in table 1.

The air flow around a freely falling particle is characterised by the Reynolds number

$$Re_p = \frac{\rho_{air} v_{TS} d_p}{\eta}. \qquad (2)$$

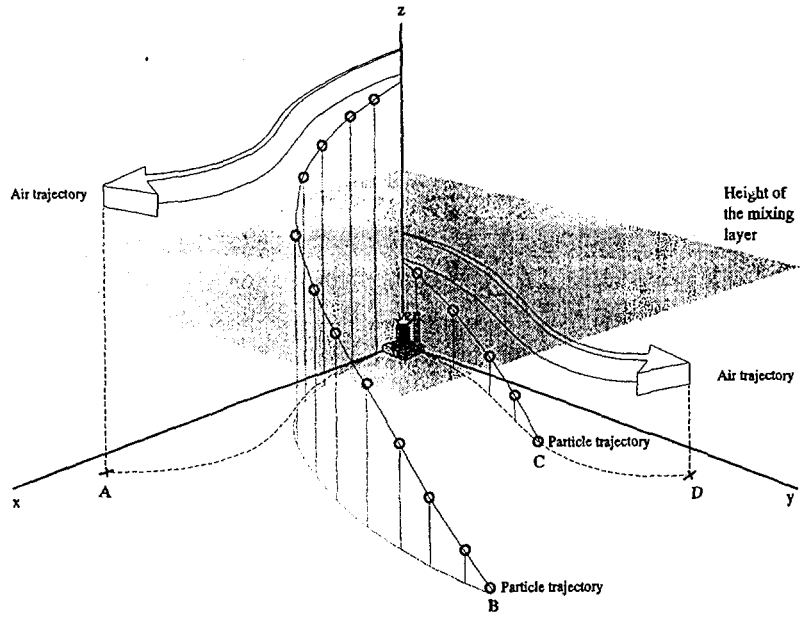

Figure 1. Hypothetical air and particle trajectories below and above some mixing height (in *x, y, z* coordinate system). A trajectory is a path along which an air parcel or a particle moves in the atmosphere. Wind conditions (direction and speed) differ in both air layers and, consequently, the trajectories of the air parcels are not in the same directions. Particles originally above the mixing height behave initially according to the conditions of the upper layer. When they reach the mixing layer they move according to the conditions prevailing there. Fall-out of particles may vary in different regions: (A) little or no fall-out, (B) mainly large particles, (C) large and small particles, (D) small particles.

In the Stokes regime, when $Re_p < 1.0$, the terminal settling velocity is

$$v_{TS} = \frac{\rho_p d_p^2 g C}{18\eta}. \tag{3}$$

When $0.05 < Re_p < 4$ equations

$$C_D Re_p^2 = \frac{4\rho_{air}\rho_p d_p^3 g}{3\eta^2} \tag{4}$$

and

$$v_{TS} = \frac{\eta}{\rho_{air} d_p}\left(\frac{C_D Re_p^2}{24} - 2.33\times 10^{-4}(C_D Re_p^2)^2 + 2.0154\times 10^{-6}(C_D Re_p^2)^3 - 6.9105\times 10^{-9}(C_D Re_p^2)^4\right). \tag{5}$$

can be used for the settling velocity.

It is often convenient to use particle aerodynamic diameter, d_a, instead of the Stokes diameter, d_p, i.e. the analysis is made for unit density spheres that have the same settling velocity as the particles considered. The two diameters are coupled in the Stokes regime by

$$d_a = d_p(\rho_p/\rho_a)^{1/2}. \tag{6}$$

Beyond the Stokes regime equation (6) is not valid. Generally, the relationship between d_p and d_a is defined with the aid of the equal settling velocities of the particles.

The settling velocity of a uranium fuel particle and its Reynolds number are presented in figure 2 as a function of particle diameter. Serious errors in transport range calculation are made [9] if sedimentation velocity presented in equation (3) is used beyond its application regime.

Table 1. Nomenclature.

Symbol	Definition	Value
u_x	Wind velocity (m s^{-1})	Variable
u_z	Effective vertical velocity (m s^{-1})	Variable
$u_{z,l}$	Effective large scale vertical velocity (m s^{-1}) of an air parcel	Variable
$u_{z,t}$	Effective vertical dispersion velocity (m s^{-1}) of the plume	Variable
x	Distance (m) between the nuclear power plant and the target area, x-coordinate	Variable
z	z-coordinate	Variable
y	y-coordinate	Variable
z_0	Height of the release (m)	Variable
x_i, z_i	Distances in x and z direction from the effective release point (m)	Variable
t, t_x, t_z	Time (s)	Variable
Δt	Time step (s)	Variable
d_p	Particle Stokes diameter (m)	Variable
d_a	Particle aerodynamic diameter (m)	Variable
d_{max}	Stokes diameter (m) of the largest particle that can travel distance x	Variable
ρ_p	Particle density, UO_2 (kg m^{-3})	10 500
ρ_u	Unit density (kg m^{-3})	1000
ρ_{air}	Air density (kg m^{-3})	1.205
η	Air dynamic viscosity (kg s^{-1} m^{-1})	1.81×10^{-5}
g	Acceleration of gravity (m s^{-2})	9.81
C	Slip correction factor	1
v_{TS}	Terminal settling velocity (m s^{-1})	Variable
v_{dep}	Deposition velocity (m s^{-1})	Variable
σ_z	Vertical dispersion parameter (m)	Variable
J_0	Particle flux (either mass, number or activity) to the ground	Variable
C_0	Undisturbed particle concentration above the ground (mass, number or activity)	Variable

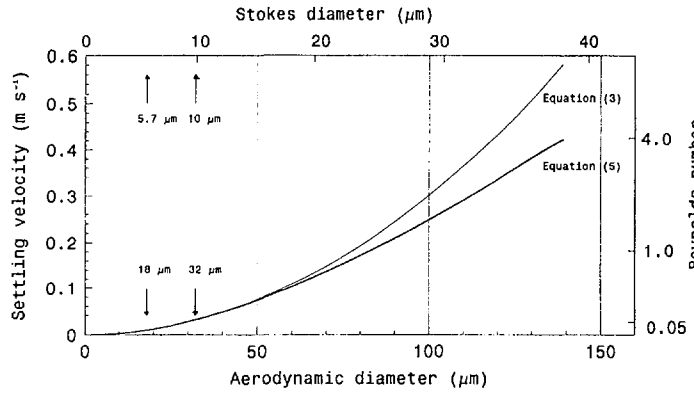

Figure 2. Settling velocity as a function of particle size. Stokes diameter, d_p, is calculated for uranium fuel particles with density of $\rho_p = 10.5$ g cm^{-3}. The upper curve represents Stokes sedimentation velocity (equation (3)) whereas the lower curve is 'the real velocity' calculated by equation (5). The Reynolds number refers to the unit density particles with aerodynamic diameter, d_a. The Reynolds number must be multiplied by d_p/d_a if it is connected to the Stokes diameter. Uranium dioxide particles of sizes $d_a = 18$ μm ($d_p = 5.7$ μm) and $d_a = 32$ μm ($d_p = 10$ μm) have sedimentation velocities of 0.01 m s^{-1} and 0.03 m s^{-1}, respectively (cf figure 3).

3. Turbulent dispersion

Turbulent dispersion is described in references [4] and [5]. Some qualitative points are discussed here regarding large particle transport.

Turbulent dispersion is basically a highly non-linear phenomenon and thus, unlike the gravitational settling, only statistical properties of the turbulent flows can be predicted. Caused by the eddy motion of air, turbulent dispersion depends strongly on prevailing weather conditions. The role of sedimentation and turbulent dispersion in the transport of the large particles is different. Sedimentation moves particles out of the gaseous plume, whereas turbulent dispersion spreads both the gaseous plume and the 'particle plume'.

The transport range of large particles depends on the vertical turbulence of air (either small scale or large scale turbulence). In the present deterministic analysis the concept of effective vertical velocity, u_z, is introduced.

In the case of large scale vertical movements of air (synoptic scale turbulence) the effective large scale vertical velocity of air, $u_{z,l}$, can be calculated from the wind fields. It is simply the upward or downward velocity of air during particle transport or during a small interval considered.

However, in the case of microscale and mesoscale turbulence the effective vertical velocity is chosen in a different way. Pasquill classification (or other classifications) [5] together with Briggs formulas (or others) [5] of plume width give a possibility to use 'semi-deterministic' ways to calculate the transport range of the large particles. In this study the choice is made using an expansion velocity of the (gaseous) plume, i.e. the concept of an effective vertical dispersion velocity of the plume, $u_{z,t}$, is introduced (see section 4.3).

In practice, there is no need to distinguish between the components of the effective vertical velocity. The effective vertical velocity, u_z, is the sum of the large scale and small scale vertical velocities

$$u_z = u_{z,l} + u_{z,t}. \tag{7}$$

In the following calculations the vertical velocities $u_{z,l}$ and $u_{z,t}$ are treated separately (either $u_{z,l}$ or $u_{z,t}$ is chosen, they are not used at the same time).

Although the instantaneous vertical velocities in turbulent air can be high, the net spread of the plume (and the corresponding effective expansion velocity) is substantially smaller than would be expected from these instantaneous velocities. Particles are assumed to be dispersed by turbulence in the same way as particles that have no inertia. In reality the plume of monodisperse large particles is spread less than the plume consisting only of small particles and gases, i.e. the behaviour is more deterministic than we assume.

4. Transport range of large uranium fuel particles

The transport range of the large particles can be calculated in a deterministic way provided that the statistical phenomena (turbulence) do not dominate sedimentation, i.e. the deposition velocity shall not be much greater than the settling velocity. At least in stable atmospheric conditions this is true for large particles.

The particle transport range depends strongly on plume rise, particle properties and meteorological conditions. Plume rise can be evaluated, in principle, from the heat energy content of the plume and its initial momentum [5]. In practice during an accident the rise is evaluated by measurements.

In the following analysis three simplified cases are considered. First, a ballistic range calculation is performed assuming that no vertical air flows exist during the aerosol transport. Second, the outcome of a constant effective vertical velocity is analysed. Third, an effort is made to take into account the more complex vertical air flows during particle transport. A simple example is given.

4.1. No vertical air flow

During a severe nuclear accident the release plume rises according to the initial momentum of the plume and the thermal energy available. The particles within the plume reach a height z_0. The deposition on the ground occurs after a

period of

$$t_z = z_0 / v_{TS}, \tag{8}$$

provided that the terminal settling velocity, v_{TS}, is constant (relative to the ground) during the settling for the particle size considered.

If the horizontal wind velocity, u_x, is constant, the travelling time of the particle over a distance, x, between the release point and the target area is simply

$$t_x = x / u_x. \tag{9}$$

The expected maximum particle size, d_{max}, on the target area is estimated from $t_z = t_x$ and using equation (3). The result is

$$d_{max} = \left(\frac{18 \eta z_0 u_x}{\rho_p g C x} \right)^{1/2}. \tag{10}$$

If the particles are large enough (d_a greater than about 50 μm, see figure 2), equation (5) instead of equation (3) must be used and the calculations have to be done numerically (see later).

Equation (10) is valid if vertical air flows are insignificant during aerosol transport. Also the particle size, the wind speed and the wind direction must be approximately constant during the travelling time. The air viscosity, η, is practically constant and the slip correction factor, C, is negligible for large particles. The nearly constant terms can be taken out of the square root giving

$$d_{max} = k \left(\frac{z_0 u_x}{\rho_p x} \right)^{1/2}, \tag{11}$$

where constant $k = (18\eta / gC)^{1/2} \approx 5.8 \times 10^{-3}$ kg$^{1/2}$ s$^{1/2}$ m^{-1} for dry air at STP conditions.

4.2. Constant vertical velocity

In a real transport situation vertical air flows always exist. During the travelling time, the particles move up or down faster or slower depending on the direction of the effective vertical velocity, $u_z = u_{z,1}$. The net settling velocity is changed to $v_{TS} + u_z$, where u_z is negative for upward air flows and positive for downward air flows. The maximum particle size can now be written as

$$d_{max} = k \left(\frac{z_0 u_x - u_z x}{\rho_p x} \right)^{1/2}. \tag{12}$$

Figure 3 shows the transport range of the particles that rise initially to different heights. The variability of the range may be large in the case of aerodynamic diameter less than about 50 μm. These particles can be transported hundreds of kilometres if the plume rises 500 m above the ground. In these conditions the long

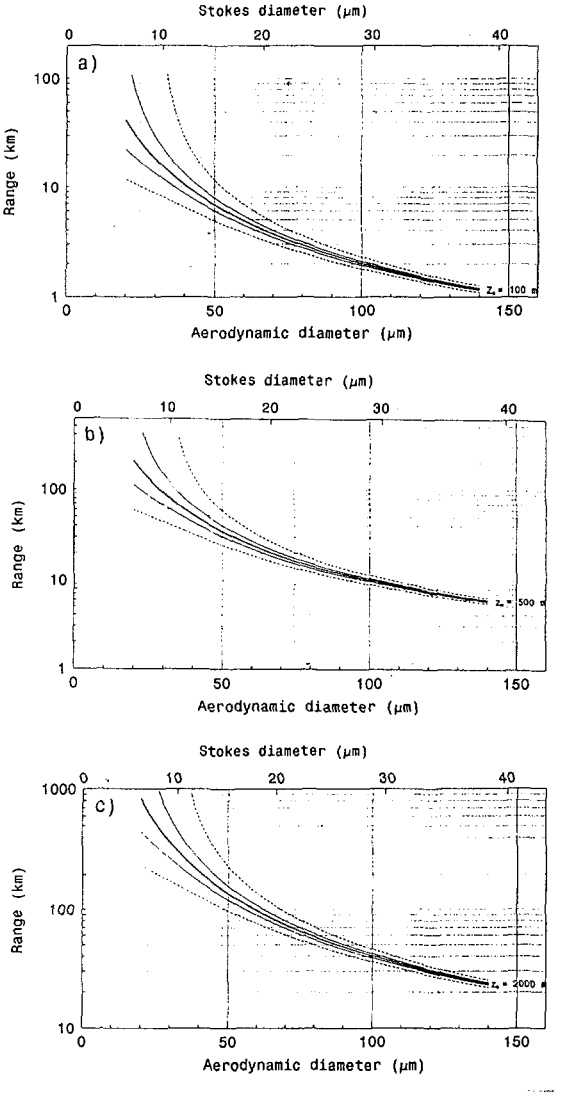

Figure 3. Maximum transport distance for particles of $d_a = 20$–140 μm. Figures (*a*), (*b*) and (*c*) represent effective release heights 100, 500 and 200 m, respectively. The wind velocity is 5 m s^{-1}. In the centremost thick curve of each set, no vertical movements of air masses exist. In the thin curves of each release height, equation (12) with constant $u_z = \pm 0.01$ m s^{-1} (solid line) or $u_z = \pm 0.03$ m s^{-1} (dashed line) were used.

range transport of the larger particles is possible provided that the effective upward wind velocity is substantially higher than 0.01 m s^{-1}.

For emergency preparedness a simple transformation equation for other situations is needed because weather conditions and particle properties, i.e. wind velocity, u_x, effective release height, z_0 and particle density, ρ_p, can vary greatly. Transport range, x, is directly proportional to u_x and z_0 and inversely proportional to ρ_p. By selecting one of the curves in figure 3(*a*)–(*c*) as a 'reference curve', the transport range in new conditions, x_{new}, can be calculated using an approximate equation

$$x_{new} = x_{ref} \frac{u_{x,new}}{u_{x,ref}} \frac{z_{0,new}}{z_{0,ref}} \frac{\rho_{p,ref}}{\rho_{p,new}} \qquad (13)$$

where the subscript 'ref' refers to the reference case and the subscript 'new' to the new conditions.

4.3. Complex vertical air flow

Generally the maximum particle size cannot be explicitly solved as in equation (12), because the effective vertical velocity depends strongly on the meteorological situation. Moreover, the horizontal wind velocity and the wind direction may change drastically during particle transport. The aim of the following rough calculations is to obtain an estimate for the magnitude of the variability of the maximum distance that the particles can travel in a complex atmospheric environment.

The influence on particle transport by the vertical movements of the air may be analysed using parametric equations derived for certain classified weather conditions. Parametric expressions are easy to use in calculations. Here the effective vertical velocity, $u_z = u_{z,t}$, is assumed to be of the same order of magnitude as the change in the vertical dispersion of the plume as a function of time. It should be noted that the vertical velocity is only an analytical function of the distance x, not height z.

Let us assume that the weather is neutral (Pasquill class D). Instead of class D it is also possible to use stable weather classes. For the neutral case the vertical dispersion parameter is [5]

$$\sigma_z(x) = 0.06x(1 + 0.0015x)^{-1/2}. \qquad (14)$$

The parameter, σ_z, and the horizontal distance, x, are expressed in metres. σ_z is the standard deviation of the Gaussian distribution that describes the vertical dispersion of the plume. Equation (14) holds in open lands at short distances of 0.1–10 km. However, an extrapolation up to 100 km is sometimes used.

In the present analysis the vertical expansion rate of the plume is assumed to be proportional to the change of σ_z per unit time. In this case the effective vertical dispersion velocity, $u_{z,t}$, is estimated from the time derivative of equation (14) combined with equation (9)

$$u_z(x) = u_{z,t}(x) = \frac{d\sigma_z(u_x t)}{dt}$$

$$= \frac{\sigma_z(x)u_x}{x} - 0.208\frac{\sigma_z^3(x)u_x}{x^2}. \qquad (15)$$

Wind velocity and wind direction are assumed to be constant during transport. The interpretation of u_z is obvious: it is the spreading velocity of the plume (the spread of one standard deviation) due to turbulence in neutral atmospheric conditions. Equation (15) allows us to calculate an estimate for the dispersion of the maximum transport distance as a function of the particle size assuming that the direction of u_z is either upwards or downwards. Even in this very simple case the maximum particle size has to be solved numerically (see later).

The results of the transport range calculations are shown in figure 4. The 'uncertainty band' is generally broadened compared with figure 3. The reason is that the effective vertical velocity is now larger, particularly at short distances. For example, at distances of 0.5 and 5 km the effective vertical velocity is 0.18 m s^{-1} and 0.058 m s^{-1}, respectively.

4.4. A numerical approach

The initial coordinates (x–z coordinate system) of the particle are (x_i, z_i). The real sedimentation velocity of the particle is $v_{TS} + u_z$, where u_z is either positive (downward velocity), negative (upward velocity) or zero. Depending on application u_z is either $u_{z,l}$ or $u_{z,t}$. At time, t, the

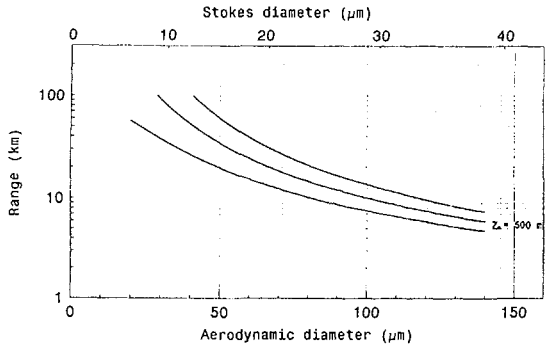

Figure 4. Maximum transport distance for particles $d_a = 20$–140 μm. The effective release height is 500 m and the wind speed is 5 m s^{-1}. The centremost curve represents no vertical movements of the air masses (same curve as in figure 3(*b*) in the middle). The upper and lower curves are calculated using equation (15) with upward (upper curve) and downward velocity (lower curve), u_z. The 'uncertainty band' refers to both directions of the coordinate axes. For example, a particle with $d_a = 100$ μm can be transported 7.5–14 km away from the plant. On the other hand, if the distance between the release point and the target area is 10 km, the particles of sizes $d_a = 80$–120 μm can reach the target area.

particle is at a point (x_{i+1}, z_{i+1}), where

$$\begin{aligned} x_{i+1} &= x_i + (u_x)_i \Delta t, \qquad i = 0, 1, 2, \ldots \\ z_{i+1} &= z_i - [(v_{TS} + (u_z)_i] \Delta t, \qquad i = 0, 1, 2, \ldots \end{aligned} \tag{16}$$

It is assumed that the wind conditions do not change markedly during a short time interval Δt. After every step a new location (x_{i+1}, z_{i+1}) is calculated until $z_{i+1} \leq 0$. Equations (16) are easily implemented in a small computer program.

5. Large particle transport in the Chernobyl accident

The numerical approach presented above is applied to the particle transport of the earliest phase of the Chernobyl accident, i.e. in the atmospheric conditions that were prevailing during the initial plume transport towards the Nordic countries. Weather and transport conditions are well described in many reports, e.g. in references [10] and [11].

The initial release from the plant rose to a few kilometres although the main release rose less than 1 km. On the basis of the weather data of the European Centre for Medium Range Forecasts (ECMWF) the Swedish Meteorological and Hydrological Institute (SMHI) calculated three-dimensional air parcel trajectories originating from Chernobyl at 00 UTC on 26 April 1986 [11]. The coordinates, including the height (in units of hPa) of the trajectory points were given on every sixth hour. The trajectories show that the released material was transported towards the southern parts of Scandinavia. The lower part of the plume ($z_0 < 750$ m) was transported towards Sweden and the higher parts towards Finland.

The particle transport range is estimated from the coordinate data of SMHI calculations with ECMWF data. The transport of the particles is assumed to take place in two separate air layers and wind conditions. Horizontal and vertical velocities of the wind in both air layers are assumed to be those that were prevailing along the $z_0 = 1500$ m trajectory (air layer above height 750 m) and along the $z_0 = 750$ m trajectory (air layer below height 750 m).

According to the three-dimensional trajectories, the vertical velocities of the air were mainly downwards (descending air) during the first day. Thereafter the vertical velocities were facing upwards (ascending air). During the transport the wind speed in the lower air layer was about 7 m s^{-1}. In the upper layer the wind speed was slightly higher. A stepwise approximation is applied to the consecutive data points, i.e. numerical calculations according to equations (16) are done assuming that the wind conditions were constant between each trajectory point (6 h).

Table 2 shows the results of the transport range calculations in two cases. In the first case no vertical velocity of air is assumed. In the second case the vertical velocity of air is assumed to be constant between the data points. Only sedimentation is taken into account. The effect of turbulence is not studied. The large scale vertical movement of the air has a significant effect on the behaviour of the small particles. The transport range of the large particles is not significantly affected by the variation of the vertical wind velocity.

Table 2. Transport range and total beta activity of particles originated from the Chernobyl accident. In case (a) vertical velocity, u_z, of the air is assumed to be zero during the transport whereas in case (b) u_z is constant between data points (see text). Effective release height $z_0 = 2000$ m. The total beta activity is estimated from the radionuclide inventory of the core. Radionuclides ^{89}Sr, ^{90}Sr, ^{90}Y, ^{91}Y, ^{95}Zr, ^{95}Nb, ^{103}Ru, ^{106}Ru, ^{106}Rh, ^{140}Ba, ^{140}La, ^{141}Ce, ^{144}Ce and ^{144}Pr are included in the estimation of the total beta activity.

d_a (μm)	d_p (μm)	(a) Range (km)	(b) Range (km)	Total β-activity (Bq)
20	6.2	1200	1000	360
30	9.3	640	460	1200
40	12.2	360	320	2700
50	15.3	230	210	5400
100	28.9	74	72	36000
140	39.4	43	42	91000

Uranium fuel particles were found in north-eastern Poland, 500–650 km from Chernobyl. The activities of the non-volatile nuclides ^{95}Zr and ^{141}Ce were typically 200–300 Bq [12]. The particle size can be estimated from the reactor nuclide inventory. The above mentioned activities represent particle diameter of $d_p = 10$ μm. The calculated transport range of these particles is about 400–550 km (table 2).

The diameters of the hot particles found in south-western parts of Finland were between $d_p = 2$–7 μm (about 1500 km from Chernobyl) [13–14]. The mean geometric diameter was 3.8 μm corresponding to the aerodynamic diameter of 10 μm [13]. The particles found in Sweden were slightly larger ($d_p = 2.7$–12.3 μm) but the distance from Chernobyl is smaller [15].

The findings above are close to the results predicted by the calculations. The difference has obvious explanations. The settling velocity depends linearly on the particle density which may have been smaller than assumed (10.5 g cm^{-3}). Thus, the transport range can be somewhat longer than the values presented in table 2. In addition, the effective release height could have been substantially above 2000 m. Also the air flow was certainly more complicated than the pattern assumed in the present study.

The uranium fuel particles can cause high local doses when deposited on the skin. NCRP [16] estimates that below the total emission of 10^{10} beta particles no acute skin damage is to be expected. This threshold value represents a dose of about 5 Gy calculated to the skin of area 1 cm^2 at a depth of 7 mg cm^{-2}. The limit of NCRP is exceeded in 1 day if a uranium fuel particle with beta activity of about 100 kBq is deposited on the skin. Table 2 shows that the risk of this exposure may have existed within 40 km from the Chernobyl plant.

6. Discussion

The methods presented in this study together with information from wind fields can be used in two ways: (1) If the effective release height of the plume is known, it is possible to estimate the maximum size of the particles that can travel to the target area. This information is highly important in identifying the areas that may receive a fall-out containing hot particles. (2) If nuclear fuel particles of certain size are found on the target area, it is possible to obtain an estimate for the true effective release height of the plume. This knowledge is useful in the dispersion studies of the plume in general.

Air parcel trajectories are useful for estimating the transport of gaseous pollutants. During the nuclear incident in Sosnovyy Bor in 1992 we used trajectory analysis successfully in predicting the route of the plume [7,17]. Air parcel trajectories may be modified in such a way that they can be applied to particle trajectories. An additional downward velocity that represents particle settling must be added to the vertical wind component. In addition, contrary to air trajectories, particle trajectories must be stopped when they intersect the Earth's surface.

Before particle trajectory calculations can be performed the size of the particles and their density must be known. Moreover, the effective release height of the particles must be estimated. In operational use the above mentioned quantities are, of course, very uncertain and the transport ranges of the particles are only suggestive.

Only three-dimensional trajectory analysis can take into account the real meteorological

conditions and identify the areas where large particles might be deposited (see figure 1). However, the results of the present study are useful in the case of an accident provided that the net vertical movements of air and the variation of the wind speed during the transport are small. The existence of large and highly radioactive particles in a release plume may lead to an operational re-identification of the fall-out areas.

Acknowledgments

We thank Mr Juhani Lahtinen, Finnish Centre for Radiation and Nuclear Safety, for stimulating suggestions during the work. We are also much obliged to Mr Ilkka Valkama, Finnish Meteorological Institute, for valuable meteorological remarks.

Résumé

Un accident nucléaire grave peut relâcher de grandes quantités de particules radioactives. Via l'écoulement de l'air, les particules qui peuvent produire des risques sanitaires sérieux, par inhalation ou dépôt sur la peau, peuvent franchir des centaines de kilomètres. Cette étude fait l'estimation des distances de transport des particules d'uranium venant du combustible, de tailles 20 $\mu m \leq d_s \leq 140$ μm, dans des conditions météorologiques simplifiées. On applique l'analyse au transport de particules lors de l'accident de Chernobyl. La distribution dans l'environnement de ces particules valident les résultats des calculs. La vitesse du vent, le panache initial, ont une influence cruciale sur les distances de transport. Une analyse balistique simple ne convient pas si l'écoulement vertical de l'air varie dans de grandes proportions durant le transport. Dans de telles conditions climatiques, il faut lier l'analyse à des calculs de trajectoires, en trois dimensions.

Zusammenfassung

Große Mengen radioaktiver Partikel können bei einem schweren Unfall in einem kernkraftwerk freigesetzt werden. Die Partikel, die ein ernsthaftes Gesundheitsrisiko durch Einatmen bzw. Ablagerung auf der Haut verursachen, können über hunderte von Kilometern über Luftströme transportiert werden. In der vorleigenden Studie werden Uran-Partikel mit einer Größe zwischen $d_a = 20$–140 μm bei vereinfachten meteorologischen Bedingungen untersucht. Die Analyse wird auf den Transport der Partikel beim Unfall in Tschernobyl angewandt. Die Ergebnisse der Berechnungen werden erhärtet durch die Umweltbefunde der Partikel. Die Windgeschwindigkeit und der ursprüngliche Aufstieg der Wolke können einen entscheidenden Einfluß auf die Transportstrecke haben. Eine einfache ballistische Analyse reicht nicht aus, wenn der vertikale Luftstrom während des Transport stark schwankt. Bei diesen Wetterbedingungen muß die Analyse mit einer dreidimensionalen Berechnung der Flugbahnen gekoppelt werden.

References

[1] Powers D A, Kress T S and Jankowski M W 1987 The Chernobyl source term *Nucl. Safety* **28** 10–28

[2] US Nuclear Regulatory Commission 1987 *Report on the Accident at the Chernobyl Nuclear Power Station* NUREG-1250, rev 1 (Washington, DC: US Government Printing Office)

[3] Sandalls F J, Segal M G and Victorova N 1993 Hot particles from Chernobyl: A review *J. Environ. Radioact.* **18** 5–22

[4] Slade D (ed.) 1968 Deposition of particles and gases *Meteorology and Atomic Energy* USAEC Report TID-24190 (Oak Ridge: Atomic Energy Commission, Technical Information Centre)

[5] Hanna S R, Briggs G A and Hosker Jr. R P 1982 Gaussian plume model for continuous sources *Atmospheric Diffusion* ed. J S Smith (Springfield: Technical Information Center U.S. Department of Energy)

[6] Nordlund G, Partanen J P, Rossi J, Savolainen I and Valkama I 1985 Radiation doses due to long-range transport of airborne radionuclides released by a reactor accident—effects of changing dispersion conditions during transport *Health Phys.* **49** 1239–49

[7] Toivonen H, Pöllänen R, Leppänen A, Klemola S, Lahtinen J, Servomaa K, Savolainen A L and Valkama I 1992 A nuclear incident at a power plant in Sosnovyy Bor, Russia *Health Phys.* **63** 571–3

[8] Hinds W C 1982 Uniform particle motion *Aerosol Technology* (New York: John Wiley) pp 38–68

[9] Barla M C and Bayülken A R 1991 On the importance of the atmospheric parameters in the fission products distribution of a severe reactor accident *Nucl. Safety* **32** 544–50

[10] Savolainen A L, Hopeakoski T, Kilpinen J, Kukkonen P, Kulmala A and Valkama I 1986 *Dispersion of Radioactive Releases Following the Chernobyl Power Plant Accident* Interim report No. 1986:2 (Helsinki: Finnish Meteorological Institute)

[11] Persson C, Rodhe H and De Geer L-E 1986 Tjernobylolyckan, en meteorologisk analys av hur radioaktivitet spreds till Sverige *SMHI meteorologi* Nr 24 (SMHIs tryckeri Norrköping: Sveriges meteorologiska och hydrologiska institut) (In Swedish)

[12] Osuch S *et al* 1989 Isotopic composition of high-activity particles released in the Chernobyl accident *Health Phys.* **39** 707–16

[13] Saari H, Luokkanen S, Kulmala M, Lehtinen S and Raunemaa T 1989 Isolation and characterization of hot particles from Chernobyl fallout in Southwestern Finland *Health Phys.* **57** 975–84

[14] Rytömaa T, Toivonen H, Servomaa K, Sinkko K and Kaituri M 1986 *Uranium Aerosols in Chernobyl Fall-out* Internal Report 1986 (Helsinki: Finnish Centre for Radiation and Nuclear Safety)

[15] Devell L 1987 *Evaluation and Interpretation of Chernobyl Hot Particle Analysis* Technical Note NP-87/59 (Nyköping: Studsvik Energiteknik AB)

[16] National Council on Radiation Protection and Measurements 1989 *Limit For Exposure to "Hot Particles" on the Skin* NCRP Report 106 (Bethesda: NCRP)

[17] Toivonen H, Pöllänen R, Leppänen A, Klemola S and Lahtinen J 1992 Release from the nuclear power plant in Sosnovyy Bor in March 1992 *Radiochim. Acta* **57** 169–72

IV

PÖLLÄNEN R, TOIVONEN H.
Skin dose calculations for uranium fuel particles below 500 μm in diameter.
Health Physics 1995; 68: 401 - 405.

SKIN DOSE CALCULATIONS FOR URANIUM FUEL PARTICLES BELOW 500 μm IN DIAMETER

Roy Pöllänen and Harri Toivonen*

Abstract—**Two different methods for skin dose calculations, VARSKIN Mod 2 and PSS are compared for a spherical uranium fuel particle (diameter 1–500 μm) deposited on the skin. Nuclide specific beta dose rate at different skin depths for a particle of unit activity is determined as a function of particle size. Both methods show that the effects of self-shielding must be included in the dose calculations for low and medium energy beta emitters. Skin dose rate is drastically overestimated when point source approximation is used. For high energy beta emitters (e.g., ^{90}Y, ^{106}Rh, and ^{144}Pr) the volume source can be approximated as a point source. The difference in doses is then below 20% for particles up to 100 μm in diameter. The models give equal results deep in the skin (in terms of range of the beta particles). The reason is that the correction due to the diminished backscattering in air-tissue interface is insignificant at large distances. For three-dimensional sources the backscattering correction should be introduced in the VARSKIN Mod 2.**

Health Phys. 68(3):401–405; 1995

Key words: uranium; beta particles; dose, skin; dose assessment

INTRODUCTION

RADIOACTIVE PARTICLES deposited on the skin can cause large local doses. Estimation of the skin doses caused by beta particles is a complex problem. The beta particles of varying energy interact in a complicated way with the surrounding material, i.e.,the particle itself, air, protective clothing, and tissue. Several methods to calculate skin doses have been developed. The dose estimates are performed using analytical empirical approximations (e.g., Loevinger 1956; Chabot et al. 1988), Monte Carlo calculations (e.g., Cross et al. 1992; Faw 1992) or semi-empirical equations like the point kernel method in VARSKIN (Traub et al. 1987).

Calculations are often based on the assumption that the particles are surrounded by an infinite homogeneous medium. Skin doses are then overestimated up to about 35% (Cross et al. 1992) due to enhanced backscattering from tissue that does not exist above the skin. Also, dimensions of the particles are often neglected. For low energy beta emitters in particular, the doses are greatly overestimated if the effect of self-shielding is omitted.

The present paper aims at comparing the results of dose calculations that are performed using two different methods. VARSKIN Mod 2 (Durham 1992) is developed in Pacific Northwest Laboratory and the PSS model (Point Source and Self-absorption) in the Finnish Centre for Radiation and Nuclear Safety (Pöllänen and Toivonen 1994). Comparison between these methods is valuable because their basis of calculation is different and they are not well validated for a three-dimensional source.

The skin doses are often calculated assuming that the skin is uniformly contaminated by beta active nuclides. Recently, however, there has been much interest and need to calculate doses caused by hot particles. For simplicity, the present analysis is limited to spherical particles deposited on the skin.

The activity A_p of non-volatile nuclides in a nuclear fuel particle can be estimated from the radionuclide inventory of the core (Pöllänen and Toivonen 1994). For homogeneous particles $A_p \propto d_p^3$ (d_p is diameter of the spherical particle). Particle size is thus the most dominant quantity in dose estimates. To study backscattering and self-shielding effects it is useful to present the results for unit activity as a function of the particle size, i.e., the dose rate (Gy h^{-1}) is calculated from a 1 Bq source at skin depth h averaged over 1 cm^2.

MODELS

VARSKIN Mod 2

VARSKIN Mod 1 (Traub et al. 1987) is a widely used semi-empirical code when assessing the radiological risks connected to the radionuclide contamination on the skin. Skin dose rate from beta emitters in a hot particle is calculated by integrating numerically the Berger point kernel (Berger 1971). Deficiencies of the code are corrected in the new version, VARSKIN Mod 2 (Durham et al. 1991a; Durham 1992).

VARSKIN Mod 2 calculates doses from uniform skin contamination and from single or multiple hot particles. The code has options for three-dimensional sources, protective clothing, and air gaps. Additional features include methods to model volume-averaged

* Finnish Centre for Radiation and Nuclear Safety, P.O. Box 14, FIN-00881 Helsinki, Finland.

(*Manuscript received* 26 *May* 1994; *revised manuscript received* 23 *August* 1994, *accepted* 6 *October* 1994)

0017-9078/95/$3.00/0

doses and gamma doses. The code can calculate doses and dose rates at various skin depths, either averaged over the target area or radially from the center of the exposure area.

In modeling a three-dimensional source, attenuation due to source material and attenuation due to particle geometry ($1/r^2$) are included. Attenuation within the source is treated by calculating the path length of beta particles which is then modified by the ratio of the densities of the source particle and water. For one and two-dimensional sources on air-tissue interface, the scaled absorbed dose distributions are corrected for diminished backscattering.

For three-dimensional sources the backscattering correction is omitted. According to the code manual (Durham 1991b) "the greatest contribution to skin dose is from the portion of the source that is nearest to the skin." Due to the high density of the source particles "the backscatter component is probably underestimated from the portion of the source that is nearest to the skin. This underestimate is compensated . . . by the overestimate of backscatter from the portions of the source that are farthest from the skin." The validity of these statements is discussed later.

PSS-model

A skin dose model, now known as PSS, was recently developed (Pöllänen and Toivonen 1994). PSS is based on point source dose conversion factors (Cross et al. 1992) and on self-absorption correction within the spherical source particle. The model is intended to calculate the beta dose rate to the skin using conversion factors defined for different skin depths and circular target areas.

PSS is a simple semianalytical tool for quick hand calculations. The PSS model was developed to apply point source dose conversion factors for volume sources. These factors are modified by analytical means to account for the self-shielding and geometry effects (see later) that have an influence on skin doses. Calculations

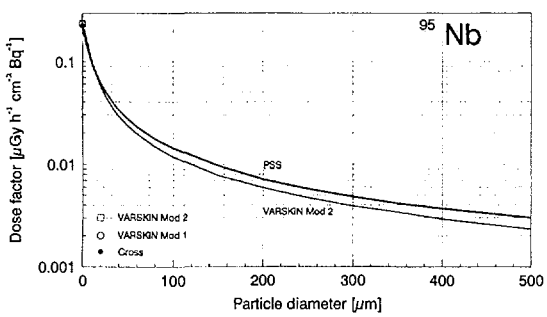

Fig. 1. Dose factor (μGy h^{-1} cm^{-2} Bq^{-1}) as a function of particle size for ^{95}Nb at skin depth of 70 μm calculated by PSS (thick line) and VARSKIN Mod 2 (thin line). Dose conversion factors used in PSS, VARSKIN Mod 1, and VARSKIN Mod 2 for a point source are marked in the vertical axis (see Table 1). They are practically equal (see Fig. 2).

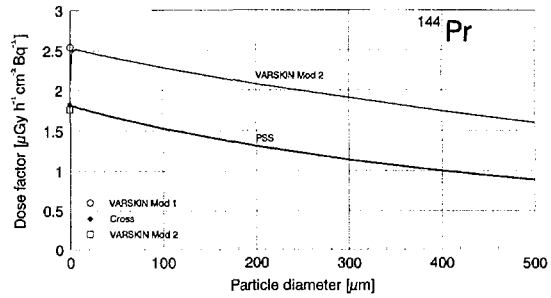

Fig. 2. Dose factor (μGy h^{-1} cm^{-2} Bq^{-1}) as a function of particle size for ^{144}Pr at skin depth of 70 μm calculated by PSS (thick line) and VARSKIN Mod 2 (thin line). Point source dose conversion factor used in PSS is labeled as a dot in the vertical axis. Circle and square refer to VARSKIN Mod 1 and VARSKIN Mod 2, respectively.

have been so far performed for the skin depths of 0.07, 0.4, and 3 mm averaged over the target area of 1 cm^2 (ICRP 1991). In principle, any depth and any target area is possible provided that dose conversion factors for a point source are available.

Nuclide specific skin dose rate (Gy cm^{-2} h^{-1}), averaged over 1 cm^2 at a skin depth h, is written formally as

$$\dot{D}_N = A(N, d_p)CF(N, h)SAF(N, d_p, \mu_\rho/\rho_p), \quad (1)$$

where

$A(N, d_p)$ = the activity of nuclide N (Bq) in a spherical particle of diameter d_p;

$CF(N, h)$ = the dose conversion factor (Gy cm^{-2} h^{-1} Bq^{-1}) of nuclide N for a point source on air-tissue interface at depth h; and

$SAF(N, d_p, \mu_\rho/\rho_p)$ = the self-absorption factor of nuclide N in a homogeneous spherical particle (diameter d_p and mass attenuation coefficient μ_ρ/ρ_p).

When a particle contains m beta emitters the total skin dose rate is

$$\dot{D} = \sum_{N=1}^{m} \dot{D}_N. \quad (2)$$

The self-absorption factor (SAF) is the fraction of the original beta flux (i.e., flux without attenuation) that reaches the surface of the particle (Tsoulfanidis 1991). The mass attenuation coefficient [m^2 kg^{-1}] is a function of the maximum beta energy E_{max} (MeV) (Nathu Ram et al. 1982)

$$\mu_\rho/\rho_p = aE_{max}^{-b}. \quad (3)$$

Coefficients a and b are related to the effective atomic number of the particle. Assuming that the parti-

Table 1. Dose conversion factors for a point source at different skin depths h. Maximum beta energy $E_{\beta,max}$ refers to the most probable decay branch. X_{90} is the distance in water at which 90% of the beta energy is absorbed. Point source conversion factor refers to the dose rate (μGy h^{-1}) in water from a 1 Bq point source averaged over 1 cm^2 at skin depth of h. Air-water boundary is assumed by Cross and VARSKIN Mod 2 (one- and two-dimensional sources). Water-water boundary is assumed by VARSKIN Mod 1. In case of a three-dimensional source VARSKIN Mod 2 uses dose conversion factors that are close to those in VARSKIN Mod 1.

			Point source conversion factors at depth h								
			h = 0.07 mm			h = 0.4 mm			h = 3 mm		
Nuclide	$E_{\beta,max}$ (MeV)	X_{90} (mm)	Cross	VARS1	VARS2	Cross	VARS1	VARS2	Cross	VARS1	VARS2
^{89}Sr	1.49	3.03	1.67	2.35	1.62	0.887	1.11	0.888	0.0546	0.0485	0.0532
^{90}Sr	0.546	0.787	1.38	1.83	1.42	0.335	0.357	0.356	—	—	—
^{90}Y	2.28	5.17	1.76	2.48	1.73	1.05	1.38	1.02	0.2	0.220	0.213
^{91}Y	1.54	3.24	1.67	2.37	1.62	0.897	1.15	0.896	0.0637	0.0643	0.0629
^{95}Zr	0.366	0.461	1.06	1.31	1.08	0.0857	0.0758	0.0698	—	—	—
^{95}Nb	0.160	0.094	0.230	0.234	0.210	—	—	—	—	—	—
^{103}Ru	0.226	0.267	0.568	0.575	0.664	0.028	0.0049	—	—	—	—
^{106}Ru	0.0394	0.008	—	—	—	—	—	—	—	—	—
^{106}Rh	3.54	7.92	1.85	2.55	1.75	1.17	1.51	1.06	0.326	0.351	0.324
^{140}Ba	0.991	1.65	1.46	1.97	1.42	0.490	0.584	0.499	0.0007	—	—
^{140}La	1.35	2.97	1.64	2.36	1.54	0.845	1.07	0.790	0.0385	0.0390	0.0317
^{141}Ce	0.435	0.605	1.54	1.51	1.55	0.169	0.174	0.165	—	—	—
^{144}Ce	0.318	0.277	0.815	0.877	0.860	0.0287	0.0109	0.0108	—	—	—
^{144}Pr	3.00	6.71	1.82	2.54	1.76	1.13	1.47	1.06	0.285	0.311	0.291

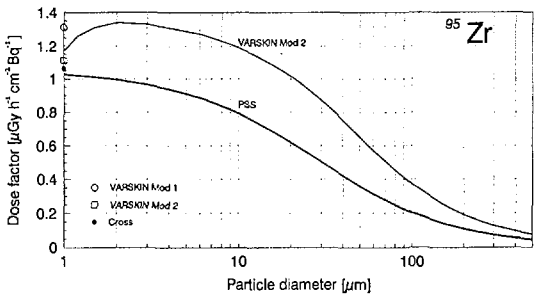

Fig. 3. Dose factor (μGy h^{-1} cm^{-2} Bq^{-1}) as a function of particle size for ^{95}Zr at skin depth of 70 μm calculated by PSS (thick line) and VARSKIN Mod 2 (thin line). The dose conversion factors for a point source are given at the vertical axis (see Fig. 2).

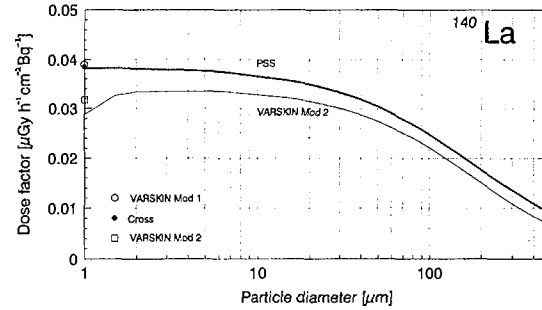

Fig. 4. Dose factor (μGy h^{-1} cm^{-2} Bq^{-1}) as a function of particle size for ^{140}La at skin depth of 3 mm calculated by PSS (thick line) and VARSKIN Mod 2 (thin line). The dose conversion factors for a point source are given at the vertical axis (see Fig. 2).

cles are pure uranium dioxide, we can set a = 2.3 and b = 1.4 (Nathu Ram et al. 1982). For a spherical particle the self-absorption factor has an analytical expression (Pöllänen and Toivonen 1994).

$$SAF = 2(\mu_\rho d_\rho)^{-1} - 2(\mu_\rho d_\rho)^{-2}(1 - e^{-\mu_\rho d_\rho}). \quad (4)$$

For nuclides with several decay branches and, consequently, several maximum beta energies, the total SAF is calculated as the sum of SAF's of each branch i weighted by the branching probability β_i

$$SAF\,(N, d_\rho, \mu_\rho/\rho_\rho) = \sum_{i=1}^{n} \beta_i SAF_i[N, d_\rho, (\mu_\rho/\rho_\rho)_i], \quad (5)$$

where n is the total number of branches of nuclide N.

CALCULATIONS

Skin doses are compared from the point of view of self-shielding and beta scattering effects in air-tissue interface. They are often very important effects and their treatment in VARSKIN Mod 2 and PSS differ. Other phenomena, like different geometry treatment, are considered here only qualitatively.

The calculations are made for a spherical particle deposited on the skin. The effect of protective clothes or air gaps is not analyzed. Nuclide specific beta dose rate per unit activity is estimated at different skin depths as a function of particle size. Skin depths considered are 0.07 mm [directional dose equivalent H' (0.07) for basal cells], 0.4 mm (average depth in estimating the production of long-lived deterministic damage), and 3 mm (depth of the lens of the eye).

The target area is fixed to 1 cm^2 (ICRP 1991). The dose estimates are calculated for uranium dioxide particles of diameter d_p = 1–500 μm and density of ρ_p = 10.5 g cm^{-3}. VARSKIN Mod 2 does not calculate doses for three-dimensional particles smaller than 1 μm. PSS can treat directly only spherical particles. However, an effective diameter can be calculated from the volume of the particle. Geometrical shape is of secondary importance in dose calculations of small particles. Furthermore, often only the volume of the particle can be estimated from the activity measurements; the detailed geometry remains unknown.

Nuclides ^{89}Sr, ^{90}Sr, ^{90}Y, ^{91}Y, ^{95}Zr, ^{95}Nb, ^{103}Ru, ^{106}Ru, ^{106}Rh, ^{140}Ba, ^{140}La, ^{141}Ce, ^{144}Ce, and ^{144}Pr are considered in the present calculations. These nuclides were detected in nuclear fuel particles that dispersed over Europe after the Chernobyl accident in 1986 (e.g., Philipsborn and Steinhäusler 1988). Nuclide specific information and point source conversion factors at different skin depths are given in Table 1. Nuclides that have X_{90} distance (see Table 1) smaller than 0.4–0.5 mm are referred to here as low energy beta emitters. High energy beta emitters are henceforth those whose X_{90} distance is larger than 3 mm. Medium energy nuclides are those with X_{90} distance between above mentioned limits.

Self-absorption

The effect of self-shielding as a function of particle size and beta energy is investigated in terms of the self-absorbtion factor (SAF) by Pöllänen and Toivonen (1994). Beta absorption is found to be important for low energy beta emitters even in relatively small particles (e.g., SAF = 0.8 for ^{95}Zr in 8 μm fuel particles). For high energy beta emitters, or if the target is located deep in the skin (in terms of X_{90} distance), the effect is less stressed.

Dose rate per unit activity as a function of particle diameter for ^{95}Nb is given in Fig. 1. ^{95}Nb emits beta particles of very low energy. The results of VARSKIN Mod 2 and PSS are practically equal. The curve calculated by PSS describes the behavior of self-absorption, i.e., $\dot{D}/A$ in eqn (1) scaled by the point source dose conversion factor CF.

In case of low energy beta emitters the point source approximation can be used only for particles smaller than a few μm. For larger particles the effect of self-shielding must be evaluated. For low energy beta emitters in large three-dimensional particles (>100 μm) the self-shielding may reduce doses by a factor of more than ten when compared to point source calculations.

Dose rate per unit activity for ^{144}Pr is given in Fig. 2. ^{144}Pr emits beta particles of very high energy. The relative behavior of the dose factor as a function of particle size predicted by VARSKIN Mod 2 and PSS is very similar. This is true for all high energy beta emitters and all skin depths considered. However, VARSKIN Mod 2 often gives higher doses than PSS mainly due to greater point source conversion factors.

Backscattering in air-tissue interface

Dose conversion factors for a point source used in the PSS (Cross et al. 1992) include the effect of diminished backscattering in air-tissue interface. The backscattering correction, neglected in VARSKIN Mod 1, is included in VARSKIN Mod 2 for one and two-dimensional sources (see Table 1). For three-dimensional sources it is excluded. Therefore, these dose conversion factors are often close to the VARSKIN Mod 1 conversion factors.

According to the VARSKIN Mod 2 manual (Durham 1992) backscattering is treated rather as a scattering from the source material, not from the nonexistent tissue outside the body. This is a good approximation only when the range of the beta particles is much less than the dimensions of the source. This is not necessarily true for hot particles below sizes of 500 μm, as shown in the present analysis.

The need for the backscattering correction for a three dimensional source is justified in the light of the results presented in Fig. 3. For ^{95}Zr at a skin depth of 0.07 mm VARSKIN Mod 2 predicts higher dose rates for particles up to 15 μm in diameter than for an ideal point source. The dose factor curve behaves similarly for every nuclide and skin depth. (Due to the linear scaling of the x-axis it is poorly seen in Figs. 1 and 2.) A more detailed analysis of VARSKIN Mod 2 results, whether they describe a true physical phenomenon or a calculational shortcoming, is beyond the scope of the present paper.

If backscattering is an insignificant phenomenon having no influence on the dose rates, i.e., X_{90} distance in water is about equal to the skin depth considered, VARSKIN Mod 2 and PSS give approximately equal results for large particles. Except for ^{144}Ce at skin depth of 0.4 mm VARSKIN Mod 2 and PSS use nearly equal point source dose conversion factors (for ^{144}Ce PSS predicts six times higher doses than VARSKIN Mod 2).

An example where backscattering plays no significant role in dose estimation is given in Fig. 4 for ^{140}La at skin depth of 3 mm (see also Fig. 1). Dose factors calculated by PSS are in this case slightly higher than the predictions of VARSKIN Mod 2. This is mostly due to differences in the dose conversion factors of the point source.

CONCLUSIONS

VARSKIN Mod 2 and PSS show that the beta dose rate to the skin is overestimated if point source approximation is used for volume sources. The larger the particle, the larger the difference. The effect of self-shielding is clearly seen for low energy beta emitters like ^{95}Nb. For high energy beta emitters self-shielding is much less important.

Generally the dose factor curves behave similarly in both models. The difference between the calculated dose factors is below two (except for ^{144}Ce at skin depth of 0.4 mm). In cases of negligible air-tissue interface effects, the models predict almost identical doses at all depths.

Although the methods of calculation are different both models seem to give approximately equal results in the particle size range considered provided that backscattering effects are implemented in VARSKIN Mod 2. Deviations are then mostly due to the differences of point source conversion factors.

Some of the differences between the results obtained with VARSKIN Mod 2 and PSS may also come from the different source particle geometry treatment in the models. In VARSKIN Mod 2 the influence of the source particle geometry is considered as an $1/r^2$ attenuation within the source and surrounding air. In PSS the attenuation within the source is inherently considered in the self-absorption factor. However, most of the source particle surface is not in contact with the skin. The distance between this non-contact surface of the particle and the skin surface evokes a question as to whether the point source conversion factors used in PSS may be applied to large three dimensional particles.

Preliminary calculations show that the geometry correction has no importance for particles below 100 μm in diameter. For 500 μm particles the doses from high energy beta emitters may be reduced up to 30% compared to present PSS calculations. The doses from low energy beta emitters do not change significantly.

REFERENCES

Berger, M. J. Distribution of absorbed dose around point sources of electrons and beta particles in water and other media. J. Nucl. Med. 12(Suppl. 5):5–23; 1971.

Chabot, G. E.; Skrable, K. W.; French, C. S. When hot particles are not on the skin. Radiat. Protect. Mgmt. 5:31–42; 1988.

Cross, W. G.; Freedman, N. O.; Wong, P. Y. Beta ray dose distributions from skin contamination. Radiat. Protect. Dosim. 40:149–168; 1992.

Durham, J. S.; Reece, W. D.; Merwin, S. E. Modelling three-dimensional beta sources for skin dose calculations using VARSKIN Mod 2. Radiat. Protect. Dosim. 37:89–94; 1991a.

Durham, J. S. Hot particle dose calculations using the computer code VARSKIN Mod 2. Radiat. Protect. Dosim. 39:75–78; 1992b.

Durham, J. S. VARSKIN MOD2; SADDE MOD2: Computer codes for assessing skin dose from skin contamination. Richland, WA: Battelle Pacific Northwest Laboratories; NUREG/CR-5873 (PNL-7913); 1992.

Faw, R. E. Absorbed doses to skin from radionuclide sources on the body surface. Health Phys. 63:443–448; 1992.

International Commission on Radiological Protection. 1990 recommendations of the International Commission on Radiological Protection. Oxford: Pergamon Press; ICRP Publication No. 60; Ann. ICRP 21(1–3);1991.

Loevinger, R. The dosimetry of beta sources in tissue: The point source dose function. Radiology 66:55–62; 1956.

Nathu Ram; Sundara Rao, I. S.; Mehta, M. K. Mass absorption coefficients and range of beta particles in Be, Al, Cu, Ag and Pb. Pramāna 18:121–126; 1982.

von Philipsborn, H.; Steinhäusler, F, eds. Hot particles from the Chernobyl fallout, proceedings of an International Workshop, Theuern, October 1987. 5th Radiometric Seminar Theuern. Theuern, Germany: Schriftenreihe des Bergbau- und Industriemuseums, Ostbayern Theuern, Band 16; 1988.

Pöllänen, R.; Toivonen, H. Skin doses from large uranium fuel particles—application to the Chernobyl accident. Radiat. Protect. Dosim. 50:127–132; 1994.

Traub, R. J.; Reece, W. R.; Scherpelz, R. I.; Sigalla, L. A. Dose calculations for contamination of the skin using the computer code VARSKIN. Hanford, WA: Battelle Pacific Northwest Laboratories; NUREG/CR-4418 (PNL-5610: 1987.

Tsoulfanidis, N. Hot particles self-absorption factor. Health Phys. 60:841–842; 1991.

■■

V

PÖLLÄNEN R, VALKAMA I, TOIVONEN H.
Transport of radioactive particles from the Chernobyl accident.
Atmospheric Environment 1997; 31: 3575 - 3590.

Pergamon

PII: S1352-2310(97)00156-8

Atmospheric Environment Vol. 31, No. 21, pp. 3575–3590, 1997

1352-2310/97 $17.00 + 0.00

TRANSPORT OF RADIOACTIVE PARTICLES FROM THE CHERNOBYL ACCIDENT

ROY PÖLLÄNEN,* ILKKA VALKAMA† and HARRI TOIVONEN*

*Finnish Centre for Radiation and Nuclear Safety (STUK), P.O. Box 14, 00881 Helsinki, Finland; and †Finnish Meteorological Institute (FMI), P.O. Box 503, 00101 Helsinki, Finland

(*First received* 10 *May* 1996 *and in final form* 27 *March* 1997. *Published August* 1997)

Abstract—After the Chernobyl accident large and highly radioactive particles were found in several European countries. Particles > 20 μm in aerodynamic diameter were transported hundreds of kilometres from the plant, and they were sufficiently active (> 100 kBq) to cause acute health hazards. Here, a particle trajectory model is used to identify the areas of large particle fallout. Effective release height of the particles and atmospheric phenomena related to their transport are investigated by comparing particle findings with locations given by trajectory calculations. The calculations showed that in the Chernobyl accident either the maximum effective release height must have been considerably higher than previously reported (> 2000 m) or convective warm air currents may have lifted radioactive material upwards during transport. Large particles have been transported to other areas than small particles and gaseous species. The particulate nature of the release plume must be taken into account in dispersion and transport analyses. Air parcel trajectories alone are not necessarily sufficient for identifying the fallout area of radioactive material.

Key word index: Chernobyl accident, radioactive particles, long-range transport, particle transport.

INTRODUCTION

Radioactive particles were found in many European countries after the accident (25 April, 1986; 21:23 hours UTC) and subsequent release from the Chernobyl nuclear power plant Unit IV in Ukraine. The total mass of radioactive particulate material released during 25 April–5 May, 1986 was 6000–8000 kg (Sandalls *et al.*, 1993). Most of the released radioactive material was in particulate form (Khitrov *et al.*, 1994), whereas noble gases and most of iodine were in gaseous form. The total mass of released inactive materials (steam, carbon, structural materials) was probably much larger. Although these materials may have influenced the behaviour of radioactive particles they have no radiological importance.

Release of radioactive particles cannot be considered unique to the Chernobyl accident only. For example, radioactive particles were found in the Windscale (Sellafield, U.K.) region following a fire in the core of Pile 1 (Sandalls *et al.*, 1993; Salbu *et al.*, 1994). More recently, particles were found after the incident in Sosnovyy Bor, Russia (Toivonen *et al.*, 1992). Their presence was also shown in the 1993 Tomsk accident in Russia (Tcherkezian *et al.*, 1995). Some particulate emission is also possible during the normal operation of nuclear power plants (UNSCEAR, 1993). Radioactive particles are often treated as a scientific curiosity (Sandalls *et al.*, 1993). However, sometimes their activities may be so high that even a single particle may cause a severe health hazard.

Health effects depend on the number of released particles and their properties. Particle size and activity are the dominant quantities affecting radiological hazards. Risk estimates are usually performed for inhalable beta-emitting particles smaller than a few micrometres in size (Burkart, 1988; Hofmann *et al.*, 1988; Kritidis *et al.*, 1988; Lange *et al.*, 1988; Likhtariov *et al.*, 1995; Lindner *et al.*, 1992; Vapirev and Grozev, 1993), whereas the effects of large particles are neglected. For example, occupational dose limits may be exceeded in a relatively short time if a large and highly radioactive particle is deposited on the skin (Pöllänen and Toivonen, 1994a).

Here, a particle is considered large if its aerodynamic diameter, d_a, is > 20 μm (Pöllänen and Toivonen, 1994b). The terminal settling velocity is then > 1 cm s^{-1}. Gravitational settling and turbulent dispersion are the main dry-deposition mechanisms whereas small particles with aerodynamic diameters < 1 μm are deposited mainly as a result of turbulent mixing and Brownian diffusion.

Long-range transport of large particles depends on weather conditions, particle properties and effective

release height (Pöllänen and Toivonen, 1994b). Wind speed and, especially, wind direction determine the areas that may receive highly radioactive particles. Sedimentation velocity depends on particle size, shape and density. Effective release height in addition to sedimentation velocity and vertical air flows determine the time difference between release and deposition on the ground. During this time the particles are transported by the wind to a distance determined by the wind velocity. In the Chernobyl accident most of the particulate material was deposited within 20 km of the plant, but about one-third was transported even thousands of kilometres (Powers *et al.*, 1987).

The particulate nature of the release plume must be taken into account in radiation protection and emergency preparedness (Pöllänen and Toivonen, 1994b). Large particles may be transported to different areas than small particles and gaseous species (Pöllänen *et al.*, 1993; Valkama *et al.*, 1995), which is supported by environmental findings in Finland (Arvela *et al.*, 1990; Jantunen *et al.*, 1991) and Poland (Mietelski and Waś, 1995) after the Chernobyl accident. In addition, the present dispersion models are not necessarily adequate tools for describing the radiological hazards caused by highly radioactive particles. The calculated average concentration in air ($Bq\,m^{-3}$) may be meaningless if radioactive materials are only in large particles with low number concentration.

Dispersion of airborne material during the Chernobyl accident has been widely studied, using different approaches (e.g. Albergel *et al.*, 1988; ApSimon *et al.*, 1987; Gudiksen *et al.*, 1989; Langner *et al.*, 1995; Persson *et al.*, 1987; Puhakka *et al.*, 1990; Savolainen *et al.*, 1986; Smith and Clark, 1986; Wheeler, 1988). Eulerian-, Gaussian- or Lagrangian-type dispersion models have been used for the calculation of nuclide-specific concentration and fallout; however, transport and deposition of large particles have generally been neglected in these studies. Trajectory models are often used for timing and localization purposes; here a particle trajectory model is used to identify the areas of large-particle fallout.

To evaluate the risks associated with radioactive particles, the following information is needed: activity, size, nuclide-specific and chemical compositions of the particles, the doses that these particles may cause when inhaled or deposited on the skin and their frequency of occurrence in air, ground and water. In practice, the particle properties as well as information about their abundance result from measurements, although during the early phases of release they must be estimated. In general, the full risk related to particulate emissions in the Chernobyl accident has not been evaluated. The focus of our study is on particle transport and dry deposition. Some results regarding transport during the first day of the Chernobyl release have been reported by Valkama *et al.* (1995). A more detailed analysis for the whole 10-day release period is presented here.

RADIOACTIVE PARTICLES IN EUROPE AFTER THE CHERNOBYL ACCIDENT

Radioactive particles from Chernobyl were found in at least 15 European countries (Fig. 1). The particles were found in air filters or were collected from different surfaces (ground, leaves, moss, needles, clothing, etc.). The method and the time of collection and the location of sampling have a crucial effect on the detectable characteristics of the particles. The most prominent feature of the particle findings was the extreme clustering and sparsity of the sampling. Particles were systematically collected in only a few locations, not over wide areas, and only a few hundred radioactive particles are reported in the literature.

Using GM tubes and beta counters, many teams have isolated single particles attached to surfaces. The detection threshold in terms of activity may be large, e.g. 50 Bq by Osuch *et al.* (1989) and 50–100 Bq by Mandjoukov *et al.* (1992). Sampling is typically performed several weeks or even years after deposition. Impactors have also been used for sampling but, unfortunately, at locations a long distance from Chernobyl (Fig. 1) and too late to detect large particles.

The properties of particles that can be detected depend on the method of analysis. Alpha-, beta- and gamma-ray spectrometers are widely used for nuclide identification. The total beta (and alpha) activities of single particles are sometimes analysed with autoradiography or other emulsion techniques. Visual identification is performed with (electron) microscopes, whereas elemental composition is studied using X-ray analysis, activation analysis or chemical procedures. The procedure of particle sampling, preparation and analysis is so tedious that in most cases particles have been analysed several months after sample collection which excludes detection of short-lived nuclides.

Large-scale fallout is spatially heterogeneous, i.e. territorial distribution of nuclides such as ^{95}Zr, ^{141}Ce, ^{144}Ce, ^{134}Cs and ^{137}Cs varies widely (Arvela *et al.*, 1990; Jantunen *et al.*, 1991; Mietelski and Waś, 1995). The nonvolatile elements Ce and Zr are a sign of fuel particle emissions. Smaller inhomogeneities with elevated amounts of radioactive materials were also identified (Luokkanen *et al.*, 1988); these "hot spots" were a few kilometres in diameter. In Lithuania a small number of hot spots (several tens of square metres in area) were found on the ground (Lujanas *et al.*, 1994). Near the Chernobyl power plant, hot spot areas with marked occurrence of radioactive particles were detected (IAEA, 1991). In Poland spots as small as 30 cm in diameter were identified (Broda, 1987).

Small particles are usually composed of volatile species such as iodine and caesium. Most large particles, often referred to as "hot particles", have compositions similar to those of nuclear fuel; however, they are often depleted in volatile elements. The varying activity ratios of nonvolatile elements refer

Fig. 1. Location of sites where radioactive particles have been found and reported. Numbers refer to references in the Appendix, Table A1. Impactors are used for sampling in circled sites. The exact location of particle findings around Chernobyl is not accurate.

to fuel with different burnups. Typical activity of uranium fuel particles found in Finland was 100 Bq (Saari *et al.*, 1989; Rytömaa *et al.*, 1986) and in Poland 1000 Bq (Osuch *et al.*, 1989); near the plant activity may be > 1 MBq (Salbu *et al.*, 1994). Large fuel particles have been identified as a major contributor to the total activity deposited within 60 km of the plant. Of the particles identified within 10 km, $> 95\%$ are attributed to fuel and $< 3\%$ to condensed particles (Salbu *et al.*, 1994).

Nearly monoelemental ruthenium/rhodium particles, which are often identified as "white inclusions" (Schubert *et al.*, 1987), are also found. Some of the Ru particles were $> 10\ \mu m$ in diameter. The most active Ru particle found in Sweden was 49 kBq (Kerekes *et al.*, 1991), in Poland 308 kBq (Broda, 1987) and in Greece 43 kBq (Kritidis *et al.*, 1988). The territorial distribution of the Ru particles found in Poland differs from that of U particles, suggesting that either these particle types were not released simultaneously or their transport properties in the atmosphere were different (Osuch *et al.*, 1989). Demchuk *et al.* (1990) reported that, near the plant, the proportion of Ru particles was 5–10%. The abundance ratio of U particles to Ru particles was 7:1 up to 50 km from the Chernobyl Power Plant (Likhtariov *et al.*, 1995). In Poland it was 4:3 (Osuch *et al.*, 1989) or 1:1 (Broda, 1987). In Greece too, the ratio was 4:3 (Kritidis *et al.*,

1988). However, different detection limits may have affected these numbers.

Most particles found at a large distance ($\gtrsim 500$ km) from the plant were < 1 μm in diameter although coarse particles up to tens of micrometres were also found; inactive material was sometimes present in these particles. Near the plant particles up to hundreds of micrometres in diameter were found (e.g. Cuddihy *et al.*, 1989; Salbu *et al.*, 1994; Krivokhatsky *et al.*, 1991). Particle size must be known if transport range calculations are to be compared with environmental findings; unfortunately, the sizes are documented in only a few cases. Here an effort is made to estimate the sizes of the particles for which no size estimation is given in the original papers (Appendix).

PARTICLE TRANSPORT CALCULATION

Comparison between the trajectories of large particles and environmental findings is not possible for estimating the time of particle arrival because air monitoring networks do not necessarily register single radioactive particles. Moreover, particles were typically collected several weeks after the accident. Particle trajectories are, however, very suitable for localization purposes.

In the Chernobyl accident the effective release height of the particles was very uncertain and changed considerably during the release. The only possibility, therefore, is to calculate the maximum transport distance of the particles and to identify the areas that may have received fallout containing hot particles. On the other hand, environmental findings of large particles enable to estimate the effective release height. This may help us to understand the processes that have an influence on particle transport.

A simple method for estimating the transport range of particles of different sizes is presented by Pöllänen and Toivonen (1994b). A computer program, known as TROP (Transport Range Of Particles), was developed for transport range calculations (Pöllänen *et al.*, 1995). Here, the transport range, x, is defined as the horizontal distance between the release site and the point of deposition. It is equal to the length of the rectilinear particle trajectory. In the Stokes regime, when airflow around a freely falling particle is laminar, the transport range has an analytical expression (Pöllänen *et al.*, 1995)

$$x = \frac{18\,\eta\, z_0\, u_x}{\rho_p\, d_p^2\, g} \tag{1}$$

provided that horizontal wind velocity, u_x, is constant and vertical wind velocity is zero during transport. z_0 is the effective release height, ρ_p the density of a spherical particle of diameter d_p, g the acceleration of gravity and η the viscosity of air. Although the length of curvilinear trajectories is often close to the transport range, the true point of deposition in certain weather types cannot be calculated directly using equation (1). Three-dimensional trajectory calculations utilizing actual weather conditions are then needed.

Trajectory calculations are performed using the TRAjectory, Dispersion and dOSe model known as TRADOS (Valkama and Salonoja, 1993). TRADOS can be used either for risk assessment and population dose estimation or for real-time calculations in a nuclear accident. The model has two separate submodels: a Lagrangian trajectory model and a Gaussian dispersion and radiological dose model. The trajectory module produces dispersion meteorology data for the dose module, and can be used (as in the present analysis) separately from the dispersion and dose model.

TRADOS can utilize data from the Nordic High Resolution Limited Area Model (HIRLAM) or from the European Center for Medium Range Forecasts (ECMWF). Weather parameters are stored routinely four times a day in a database. Before storage, all data are converted from HIRLAM model levels to constant pressure levels. The database contains 47 parameters for seven pressure levels from the surface of the ground up to 100 hPa (~ 15 km). The parameters include horizontal wind components, vertical wind component, air temperature, relative humidity, geopotential height, surface pressure and cumulative precipitation for large-scale rain and convective rain. The areal coverage of the TRADOS model is 3800 km $\times$ 4800 km and extends from Iceland to the Ural mountains and from Italy to Novaja Zemlya. The spatial resolution of the model is 55 km. Since the HIRLAM weather model was not operational in 1986, a special database, covering the period of April 25–May 10 1986, was obtained from the Danish Meteorological Institute and is used here. The same weather data have previously been used by the Swedish Meteorological Institute (Langner *et al.*, 1995).

In TRADOS, the transport of gaseous material is described by a set of three-dimensional numerical trajectories (Eerola, 1990). The method is similar to that adopted by Haageson *et al.* (1987), Reap (1972) and Reiff *et al.* (1986). One important advantage of this approach is that the method is rather insensitive to vertical coordinate system and geographic projection. The iterative method is also very stable and allows rather long time steps, typically 0.5–1.0 h, in contrast to other well-established schemes that use time steps of a few tens of minutes (e.g. Martin *et al.*, 1987). Numerical trajectories are usually insensitive to horizontal advection scheme errors (Maryon and Heasman, 1990).

TRADOS can compute several sets of trajectories in a single run. Inside one set, the time between subsequent trajectories and the spatial coordinates of the origin or the elevation where the trajectories are initiated can be changed. Trajectories can be computed either backwards or forwards in time. Elevation

batches are useful in accidents when the initial plume rise is not known. The accuracy of a single trajectory can be estimated by creating a relative uncertainty envelope described by four trajectories around the main trajectory (limited cluster analysis). The initiation point of each envelope trajectory is then displaced 30–50 km from the release site. In general, the expected mean relative errors in numerical forecast trajectories are usually in the range of 250–350 km per 36 h (Stunder, 1996). In anticyclonic conditions, such as those prevailing in the Chernobyl area in April–May 1986, the trajectories are usually more accurate.

Normally, the trajectory models compute air parcel trajectories, i.e. paths of massless particles. As shown earlier (Pöllänen *et al.*, 1993; Pöllänen and Toivonen, 1994b; Valkama *et al.*, 1995), they are not sufficient for estimating particle transport. Large particles do not passively follow the air currents. Because of significant sedimentation velocity the particles settle to lower air layers, where they are subject to different wind conditions. A particle model was implemented in the trajectory module of TRADOS by adding sedimentation velocity, v_{TS}, of the particle to the vertical velocity of an air parcel. In the Stokes regime, when the airflow around the falling particle is laminar, the equation

$$v_{TS} = \frac{\rho_p g d_p^2}{18\eta} \tag{2}$$

is used for the sedimentation velocity (Hinds, 1982).

Transport analyses are performed for spherical particles of unit density, ρ_a, which have the same settling velocity as the "physical" particle. The aerodynamic diameter, d_a, is expressed by (Hinds, 1982)

$$d_a = d_p \left(\frac{\rho_p}{\chi \rho_a} \right)^{1/2}. \tag{3}$$

The aerodynamic diameter $d_a \approx 3.2 \times d_p$ if the density of the particles is 10,500 kg m^{-3} (nominal density of the uranium fuel) and dynamic shape factor, χ, is 1 (sphere). In an $x - y$ coordinate system, particle trajectories often resemble paths of air parcels but close to the centre of cyclones or large frontal systems the routes may differ. This behaviour was also observed in the Chernobyl accident (Valkama *et al.*, 1995).

Unlike air parcel trajectories the trajectories of large particles terminate when they hit the ground. However, the point of deposition cannot be determined accurately because of atmospheric turbulence. In the boundary layer the particles may be subject to vertical dispersion which may notably affect the travel distances. Van der Hoven (Hanna *et al.*, 1982) suggests that when $v_{TS} > 1$ m s^{-1} (particle radius $\gtrsim 100$ μm) the particles are falling through turbulence so fast that diffusion is no longer important. Small particles are assumed to disperse by turbulence in the same way as particles having no inertia. Between these limits the role of turbulence is not clear.

Even if settling velocity is a small fraction of vertical turbulent velocities it does not follow that "ballistic" distance becomes irrelevant in determining particle ranges in air. Small scale eddies produce a quasi-random walk which may move particles upwards or downwards. Although these velocities are higher than sedimentation velocity they are more or less instantaneous. Because of large sedimentation velocity and because sedimentation does not only occur in the lowest air layer, it is probable that number concentration of large particles is not homogeneous, i.e. particles are not well mixed in the boundary layer. It takes a high-resolution random-walk transport model to accurately simulate the small-scale dispersion patterns. Since it was not available, small-scale atmospheric turbulence is not taken into account in estimating the travel distances of large particles.

PARTICLE TRANSPORT FROM THE CHERNOBYL ACCIDENT

The source term as well as the atmospheric conditions varied considerably during the release. About one-quarter of the total radioactive material was released during the early stages of the accident (IAEA, 1986). The emissions later decreased, reaching a minimum on 2 May 1986 but then increased again until 6 May 1986, when the release practically ceased. The initial explosion lifted radioactive materials to an altitude > 1000 m. After the explosion period, the initial plume never exceeded an altitude of 400 m (Persson *et al.*, 1987). In the ATMES report (Klug *et al.*, 1992), 1500 m was used for the plume centre-of-mass height during the first 6 h. The height was later assumed to be 600 m (26 and 27 April) and 300 m (up to 6 May).

Weather conditions and the dispersion of (gaseous) materials during the release are well documented (see e.g. Savolainen *et al.*, 1986; Persson *et al.*, 1987; Smith and Clark, 1986; Puhakka *et al.*, 1988). At the time of the accident, a high-pressure centre with strong inversion at about 400–500 m was dominant over the release site. Below this layer a rather weak airflow was evident towards Central Europe. Above the inversion strong southeasterly winds prevailed. Particulate and gaseous materials were then transported towards Poland and the Nordic countries.

The environmental findings and TRADOS calculations are compared by calculating the maximum travel distance of the particles of different sizes originating from different release heights. This information is valuable for dispersion estimations in general but also for emergency preparedness purposes. The initial release stage (the first 12 h) is considered separately from the later period.

Particles released at the initial stage of the accident

Radioactive materials emitted in the initial stage of the Chernobyl accident were segmented into two main air layers (e.g. Persson *et al.*, 1987; Savolainen

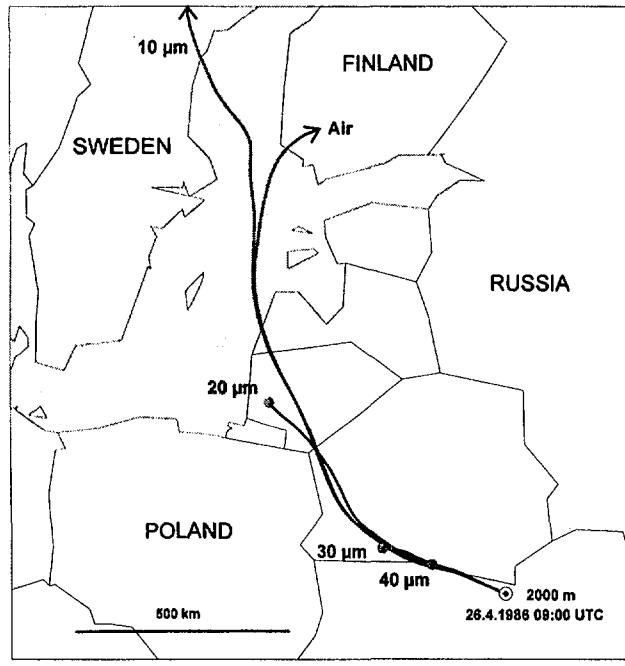

Fig. 2. Route of an air parcel and particles with aerodynamic diameters between 10 and 40 μm originating from Chernobyl on 26 April 1986 at 09:00 hours UTC at an effective release height of 2000 m. The air parcel and the 10 μm particle trajectories do not enter the ground whereas the other particle trajectories are terminated.

Table 1. Length of the particle trajectories as a function of particle size (aerodynamic and equivalent volume diameter) for different effective release heights. Lengths are calculated for the trajectories originating from Chernobyl on 25 April 1986 at 21:00, 22:00, ..., 26 April at 08:00 hours UTC (time interval between trajectories is 1 h). Lower and upper limits refer to the minimum and maximum lengths of these trajectories

Particle size			Trajectory length (km) for release heights 500–3000 m					
d_a (μm)	d_p (μm)	v_{TS} (m s^{-1})	500 m	1000 m	1500 m	2000 m	2500 m	3000 m
20	6.2	0.012	90–150	250–410	570–780	810–1000	1200–1600	1400–1800
30	9.3	0.027	64–83	140–200	250–320	400–480	530–640	650–800
40	12	0.047	42–51	94–120	160–210	220–280	290–370	350–470
50	15	0.073	29–36	67–81	110–140	150–200	190–250	240–310
60	19	0.10	23–29	47–60	81–99	110–140	150–190	180–230
70	22	0.14	17–22	38–44	63–75	88–110	110–140	140–170

et al., 1986; Valkama *et al.*, 1995). Gaseous materials and small particles at altitudes 400–1200 m were transported towards Sweden whereas Finland received radioactive material that was transported at higher altitudes. However, the particulate nature of the release altered this dichotomy. Large radioactive particles that were originally in the upper air layer were sedimented to the lower air layer where they were transported according to prevailing conditions (Fig. 2). The fallout pattern of ^{137}Cs in the central Sweden (Persson *et al.*, 1987) and the occurrence of hot particles in central Norway (Salbu, 1989) may be partly explained by this phenomenon. Note that although radioactive particles found in Scandinavia were usually considerably smaller than 20 μm in aerodynamic diameter they may have been attached to larger pieces of inactive material (Broda, 1987; Salbu, 1989). Trajectories of these agglomerates may diverge from those of "pure" radioactive particles. Even small changes in the sedimentation velocity may cause deviations in the route of particles.

Particle trajectory analysis utilizing three-dimensional wind fields takes varying meteorological conditions into account. The lengths of the particle trajectories originating from Chernobyl at different release heights have been calculated for particles of different sizes (Table 1). The trajectories are from the period when radioactive materials were transported

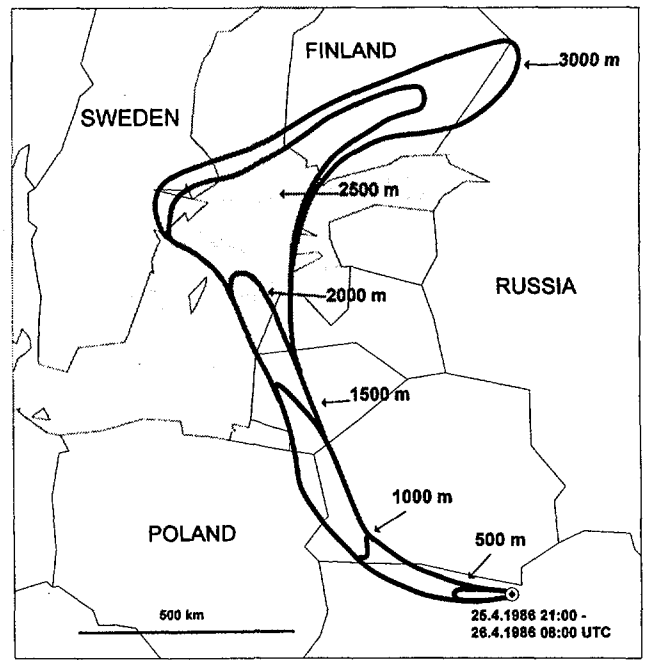

Fig. 3. Deposition area of particles 20 μm in aerodynamic diameter originating from different release heights (500–3000 m) from 25 April at 21:00 hours to 26 April, 1986 at 08:00 hours UTC (see Table 1). The boundaries are drawn by connecting the end points (points of deposition) of particle trajectories; the sides are projected vertically to the x–y plane. Note that particle emission was not constant during the first 12 h after the explosion. The deposition area thus refers only to the effects of varying atmospheric conditions and effective release heights.

to Sweden and Finland, i.e. within 12 h from the beginning of the release. Note that the ranges presented in Table 1 are close to those obtained by manual calculations (Pöllänen and Toivonen, 1994b).

Trajectories of particles 20 μm in aerodynamic diameter, originating at altitudes of 500–3000 m within 12 h from the beginning of the accident, were terminated when they hit the ground. The end points (and sides) of trajectories form a closed area when they are connected (Fig. 3). According to the trajectory calculations, the particle deposition area is narrow up to about 1000 km from the plant. At longer distances the deposition area widens as a result of wind shear between the lower and higher parts of the plume.

Turbulent dispersion in the mixing layer is not taken into account when the outer limits of the deposition areas are estimated. The question arises if it is possible that large particles could stay airborne considerably larger distances than predicted by simple "ballistic trajectories"? In southeastern Sweden, 1000-1200 km from Chernobyl, particles up to 37 μm in aerodynamic diameter were found (Appendix). Length of their calculated trajectories is $\lesssim$400 km (Table 1) provided that the effective release height is 2000 m (in the Chernobyl accident this height is often considered to be the upper limit). Since vertical dispersion is much less in the free atmosphere than in the mixing layer, this particle must have been airborne in the mixing layer an additional 600 km; in terms of time, more than one day with sedimentation velocity of 0.04 m s^{-1}. This appears to be questionable. However, it is possible that either the effective release height must have been $>$ 2000 m or convective cells with rising currents of warm air, developing during the day of April 26 in Belarus and the Baltic states, lifted the particles to higher altitudes. Deep convection may considerably shift and broaden the deposition pattern of particles (Valkama and Pöllänen, 1996). Synoptic weather observations on 26 April 1986 support the assumption of convective updraft (see Persson *et al.*, 1987; Bonelli *et al.*, 1991).

In northeastern Poland, 500-700 km from Chernobyl, particles up to $\sim$60 μm in aerodynamic diameter were found (appendix). Their sedimentation velocity is so large (up to $\sim$0.1 m s^{-1}) that turbulent dispersion alone, rapid transport in a prefrontal low-level jet, warm frontal conveyer belt (Puhakka *et al.*, 1990) or even effective release height of 3000 m cannot explain these findings. Convective uplift in cumulus clouds is a possible explanation. However, these particles could not have been released before the early morning hours (local time) of 26 April because they

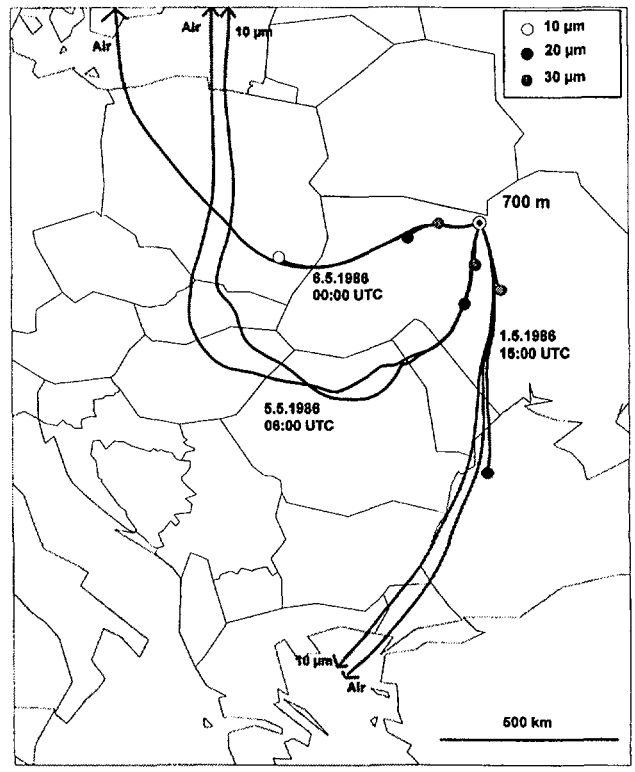

Fig. 4. Route of air parcels and particles with aerodynamic diameters between 10 and 30 μm originating from Chernobyl on 1 May at 15:00 hours, 5 May at 06:00 hours and 6 May 1986 at 00:00 hours UTC. Release height is 700 m. The trajectories for a particle 10 μm in diameter do not necessarily hit the ground due to large-scale vertical flows. The trajectories for particles 20 and 30 μm in aerodynamic diameter are terminated.

remained airborne < 9 h (initial height < 3000 m). The deposition map presented in Fig. 3 is consistent with ^{144}Ce findings from Poland (Mietelski and Was, 1995).

Particles released during 10 *days*

Radioactive materials from Chernobyl were transported throughout Europe during the 10-day release period. After 26 April, the proportion of large particles in the release plume was much smaller than during the initial stages of the accident. Particles > 20 μm in aerodynamic diameter, however, were found in Hungary, Romania, Bulgaria and Greece (appendix). Trajectory analyses show that these countries were affected during the later periods of the accident (Fig. 4).

The outer limit of the deposition area of $d_a = 20$ μm particles is calculated for the total 10-day release period (including the first day) by assuming that the effective release height was 400 and 700 m, respectively (Fig. 5). Large-scale convective vertical flows in early May widen the deposition area to the south and southwest. Again, particle findings can be explained by assuming that vertical flows in cumulus clouds lifted the particles upwards. An effective release height of even 700 m, which is higher than the value of 400 m reported by Persson *et al.* (1987), does not explain the findings.

HOT PARTICLES ON THE SKIN

Particles > 10 μm in aerodynamic diameter are not of inhalable size (Hinds, 1982). They may be deposited in the upper airways, in nasal passages or the mouth. On the skin they may cause large, highly nonuniform doses. ICRP (1990) recommends that the annual equivalent dose limit for the public is 50 mSv, averaged over any 1 cm^2, regardless of the area exposed. This limit provides sufficient protection against deterministic effects in the basal cell layer at a nominal depth of 7 mg cm^{-2} (i.e. 70 μm below the skin surface).

Pöllänen and Toivonen (1994a) estimated that a uranium fuel particle > 10 μm in physical diameter can cause a dose of 50 mGy (mSv) averaged over 1 cm^2 in one day. The time for exceeding this dose is calculated for other particle sizes (Table 2), using the PSS model presented by Pöllänen and

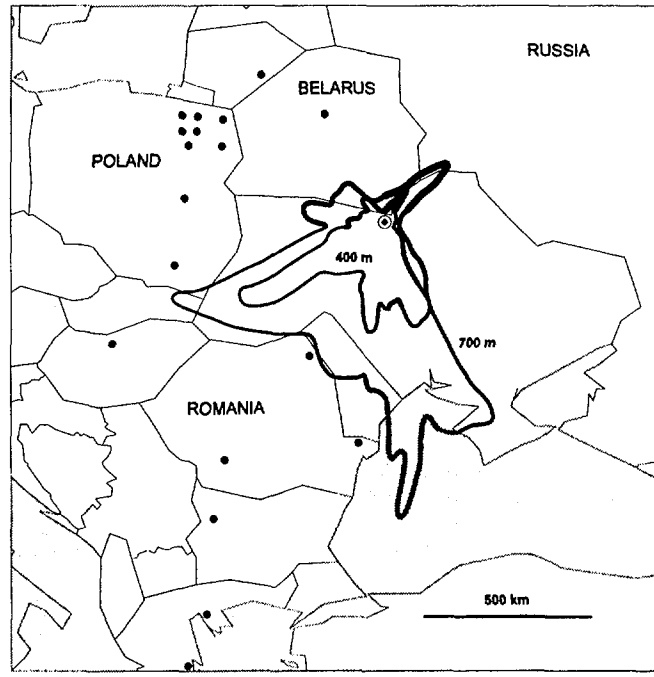

Fig. 5. Deposition area of particles 20 μm in aerodynamic diameter originating from release heights of 400 and 700 m during the 10-day total release period (25 April at 21:00 hours to 5 May 1986 at 24:00 hours UTC). The boundaries are drawn by connecting the end points of particle trajectories. The trajectories are calculated at 1 h intervals (totally 244 points for both release heights). The actual density of the end points varies depending on atmospheric conditions throughout the release period. The bold line represents areas with several trajectory end points. The deposition area refers only to the atmospheric conditions during the release. Line thickness thus does not necessarily represent the amount of particles (particles/m^2) deposited on the ground. Note that turbulent dispersion may also broaden the deposition area. Those sites (outside the deposition area) where particles > 20 μm in aerodynamic diameter are detected are marked as black spots.

Table 2. Activity, beta dose rate of the skin and time needed to receive a skin dose of 50 mSv from ruthenium or uranium fuel particles as a function of particle size (aerodynamic and equivalent volume diameter). The beta dose rate for the skin is averaged over 1 cm^2 at skin depth of 70 μm. The total activity of Ru particles is calculated from the volumetric activity of 100 Bq μm^{-3} (^{103}Ru + ^{106}Ru, activity ratio 5:1). Short-lived nuclides are not taken into account. The activities and dose rates for U particles are taken from Pöllänen and Toivonen (1994). Density of the particles is 10,500 kg m^{-3}

Particle size		Ru particle (A_{vol} = 100 Bq μm^{-3})			U particle		
d_a (μm)	d_p (μm)	A_{Ru} (Bq)	$\dot{D}$ (mGy cm^{-2} h^{-1})	$t_{50\,mSv}$	A_{tot} (Bq)	$\dot{D}$ (mGy cm^{-2} h^{-1})	t_{50mSv} (h)
20	6.2	12,000	7.7	6.5 h	320	0.34	150
30	9.3	42,000	24	2.1 h	1100	1.1	45
40	12	97,000	52	57 min	2400	2.4	21
50	15	190,000	97	31 min	4800	4.6	11
60	19	330,000	160	19 min	8500	7.9	6.3
70	22	530,000	240	12 min	14,000	12	4.1

Toivonen (1995). Note that large U particles, > 1 MBq in activity and hundreds of micrometres in aerodynamic diameter, were found near the plant (Salbu *et al.*, 1994).

The specific activity of Ru particles may be hundred times higher than the specific activity of U particles. The skin dose caused by a Ru particle may be very large (Table 2). Although the release cloud contained much less Ru than U particles, their small size in addition to high activity is a potential health hazard even at hundreds of kilometres from the damaged plant. The largest Ru particle found in Poland, 500 km

from Chernobyl, was > 50 μm in aerodynamic diameter (appendix) and its activity was 0.3 MBq (^{103}Ru + ^{106}Ru) (Broda, 1987).

CONCLUSIONS

Estimation of the effective release height of radioactive substances is based on comparison of the maximum sizes of the particles found in the environment and their estimated travel distance in air. The present study shows that the TRADOS model is very useful in estimating the transport and dispersion of radioactive particles. In general, environmental findings of radioactive particles from the Chernobyl accident and the results of the transport calculations are consistent. The maximum effective release height, however, must either have been considerably higher than previously reported or particles may have been lifted up to higher altitudes in deep convective cells.

Although a full risk estimation of the Chernobyl particles is beyond the scope of this paper, the following conclusions can be made:

1. The particulate nature of the release plume must be taken into account in the dispersion and transport analyses.
2. Large particles are transported to other areas than small particles and gaseous species owing to sedimentation and different wind conditions during transport.
3. Air parcel trajectories alone are not sufficient to identify the fallout areas of radioactive material.
4. Convective updraft in cumulus clouds should be included in the transport modelling of radioactive materials.
5. Highly radioactive particles (> 100 kBq) may be transported hundreds of kilometres from the plant. A dose of 50 mSv cm^{-2} may be exceeded in a short time provided that such particles are deposited on the skin.
6. To estimate the risks related to hot particles, new methods of evaluating particle source term, transport, deposition and health effects must be developed.

Traditionally, the deposition of particulate substances are taken into account via deposition velocity. The effects of large particles are sometimes modelled using higher deposition velocities (Rossi and Vuori, 1988). A maximum difference by a factor of two is then attained in early health effects as well as long-term collective doses if different particle-size categorizations are used. This type of (statistical) approach, however, is not necessarily adequate for estimating the transport and health effects of single particles. "Radioactivity" is dispersed in these models, not individual particles. To estimate the risks that large particles may cause, the size distribution and number of particles released in each size class should be available. Such information can rarely be obtained, particularly during the early stages of an accident. To understand the radiological hazard, however, the simulations must be performed separately for each size class.

Acknowledgements—The authors thank the Danish Meteorological Institute for processing the HIRLAM database. Ms. Tarja Ilander is kindly acknowledged for her technical assistance.

REFERENCES

Akopova, A. B., Magradze, N. V., Moiseenko, A. A., Chalabian, T. S., Viktorova, N. V. and Garger, E. K. (1991) Autoradiographic investigation of radionuclide alpha-activity in soil and plant samples from Chernobyl zone. *Nuclear Tracks Radiation Measurement* **19**, 733–738.

Albergel, A., Martin, D., Strauss, B. and Gros, J.-M. (1988) The Chernobyl Accident: modelling of dispersion over Europe of the radioactive plume and comparison with air activity measurements. *Atmospheric Environment* **22**, 2431–2444.

ApSimon, H. M., Wilson, J. J. N., Guirguis, S. and Stott, P. A. (1987) Assessment of the Chernobyl release in the immediate aftermath of the accident. *Nuclear Energy* **26**, 295–301.

Arvela, H., Markkanen, M. and Lemmelä, H. (1990) Mobile survey of environmental gamma radiation and fall-out levels in Finland after the Chernobyl accident. *Radiation Protection Dosimetry* **32**, 177–184.

Balásházy, I., Fehér, I., Szabadyné-Szende, G., Lörinc, M., Zombori, P. and Pogány, L. (1988) Examination of hot particles collected in Budapest following the Chernobyl accident. *Radiation Protection Dosimetry* **22**, 263–267.

Behrens, H. (1988) Hot particles found in the area of Munich. In Hot Particles from the Chernobyl Fallout, eds. H. Von Philipsborn and F. Steinhäusler, *Proceedings of an International Workshop held in Theuern 28/29 October 1987*. Schriftenreihe des Bergbau- und Industriemuseums Ostbauern Theuern, BAND 16, pp. 35–38.

Bonelli, P., Calori, G. and Finzi, G. (1991). The influence of deep convection phenomena on trajectories computed by long-range transport models. In *Proceedings of the 19th International Technical Meeting on Air Pollution Modelling and its Applications*, CCMS/NATO, Crete, pp. 273–279.

Broda, R. (1987) Gamma spectroscopy analysis of hot particles from the Chernobyl fallout. *Acta Physica Polonica* **B18**, 935–950.

Broda, R., Kubica, B., Szeglowski, Z. and Zuber, K. (1989) Alpha emitters in Chernobyl hot particles. *Radiochimica Acta* **48**, 89–96.

Broda, R., Mietelski, J. W. and Sieniawski, J. (1992) Radioactive ^{125}Sb and ^{60}Co in "ruthenium" hot particles from Chernobyl fallout. *Journal of Radioanalytical Nuclear Chemistry, Letters* **166**, 173–180.

Burakov, B. E., Anderson, E. B., Galkin, B. Ya., Pazukhin, E. M. and Shabalev, S. I. (1994) Study of Chernobyl "hot" particles and fuel containing masses: implications for reconstructing the initial phase of the accident. *Radiochimica Acta* **65**, 199–202.

Burkart, W. (1988) Dose and health implications from particulate radioactivity (hot particles) in the environment. In Hot Particles from the Chernobyl Fallout. eds. H. Von Philipsborn and F. Steinhäusler, *Proceedings of an International Workshop held in Theuern*, 28–29 October 1987. Schriftenreihe des Bergbau- und Industriemuseums Ostbauern Theuern, Band 16, pp. 121–129.

Cuddihy, R. G., Finch, G. L., Newton, G. J., Hahn, F. F., Mewhinney, J. A., Rothenberg, S. J. and Powers, D. A. (1989) Characteristics of radioactive particles released from the Chernobyl nuclear reactor. *Environmental Science and Technology* **23**, 89–95.

Demchuk, V. V., Voytsekhovich, O. V., Kashparov, V. A., Viktorova, N. V. and Laptev, G. V. (1990) Analysis of Chernobyl fuel particles and their migration characteristics in water and soil. *Proceedings of Seminar on Comparative Assessment of the Environmental Impact of Radionuclides Released during Three Major Nuclear Accidents: Kyshtym, Windscale, Chernobyl.* Luxembourg, 1–5 October 1990, pp. 493–514.

Devell, L. (1988) Nuclide composition of Chernobyl hot particles. In Hot Particles from the Chernobyl fallout, eds. H. Von Philipsborn and F. Steinhäusler, *Proceedings of an International Workshop held in Theuern*, 28–29 October 1987. Schriftenreihe des Bergbau- und Industriemuseums Ostbauern Theuern, Band 16, pp. 23–34.

Dovlete, C. (1990) Hot particles identified in deposition samples in Romania during 1988–1990. *Proceedings of the International Symposium on Post-Chernobyl Environmental Radioactivity Studies in East European Countries*, Kazimierz, Poland, 17–19 September 1990, pp. 49–51.

Eerola, K. (1990) Experimentation with a three-dimensional trajectory model. Meteorological Publications No. 15, Finnish Meteorological Institute.

Georgi, B., Helmeke, H.-J., Hietel, B. and Tschiersch, J. (1988) In Hot Particles from the Chernobyl Fallout, eds. H. Von Philipsborn and F. Steinhäusler, *Proceedings of an International Workshop held in Theuern*, 28–29 October 1987. Schriftenreihe des Bergbau- und Industriemuseums Ostbauern Theuern, BAND 16, pp. 39–52.

Gudiksen, P. H., Harvey, T. F. and Lange, R. (1989) Chernobyl source term, atmospheric dispersion, and dose estimation. *Health Physics* **57**, 697–706.

Haagenson, P. L., Kuo Y.-H. and Skumanich, M. (1987) Tracer verification of trajectory models. *Journal of Climate and Applied Meteorology* **26**, 410–426.

Hanna, S. R., Briggs, G. A. and Hosker, Jr. R. P. (1982) *Handbook on Atmospheric Diffusion.* Technical Information Center, U.S. Department of Energy, DOE/TIC-11223, pp. 67–68.

Hinds, W. C. (1982) *Aerosol Technology.* Wiley, New York, pp. 38–68 and 211–232.

Hofmann, W., Crawford-Brown, D. J. and Martonen, T. B. (1988) The radiological significance of beta emitting hot particles released from the Chernobyl nuclear power plant. *Radiation Protection Dosimetry* **22**, 149–157.

Horn, H.-G., Bonka, H. and Maqua, M. (1987) Measured particle bound activity size-distribution, deposition velocity, and activity concentration in rainwater after the Chernobyl accident. *Journal of Aerosol Science* **18**, 681–684.

IAEA (1986) USSR State Committee on the Utilization of Atomic Energy. The accident at the Chernobyl nuclear power plant and its Consequences. IAEA Expert Meeting in Vienna, 25–29 August 1986.

IAEA (1991) The international Chernobyl project. Report by an International Advisory Committee, IAEA, Vienna, 1991. Part D, pp. 107–201.

ICRP (1990) 1990 *Recommendations of the International Commission on Radiological Protection.* ICRP Publication 60. Pergamon Press, Oxford.

Jantunen, M., Reponen, A., Kauranen, P. and Vartiainen, M. (1991) Chernobyl fallout in Southern and Central Finland. *Health Physics* **60**, 427–434.

Jaracz, P., Piasecki, E., Mirowski, S. and Wilhelmi, Z. (1990) Analysis of gamma-radioactivity of "hot particles" released after the Chernobyl accident, II. An interpretation. *Journal of Radioanalytical Nuclear Chemistry* **141**, 243–259.

Jost, D. T., Gäggeler, H. W., Baltensperger, U., Zinder, B. and Haller, P. (1986) Chernobyl fallout in size-fractionated aerosol. *Nature* **324**, 22–23.

Kauppinen, E. I., Hillamo, R. E., Aaltonen, S. H. and Sinkko, K. T. S. (1986) Radioactivity size distributions of ambient aerosols in Helsinki, Finland, during May 1986 after the Chernobyl accident: preliminary report. *Environmental Science and Technology* **20**, 1257–1259.

Keck, G. and Cabaj, A. (1988) Hot particles in the Chernobyl fallout and in the fallout from nuclear weapon tests: a comparison. In Hot Particles from the Chernobyl Fallout, eds. H. Von Philipsborn and F. Steinhäusler, *Proceedings of an International Workshop held in Theuern*, 28–29 October 1987. Schriftenreihe des Bergbau- und Industriemuseums Ostbauern Theuern, Band 16, pp. 85–95.

Kerekes, A., Falk, R. and Suomela, J. (1991) Analysis of hot particles collected in Sweden after the Chernobyl accident. Statens Strålskyddinstitut, SSI-rapport 91–02.

Khitrov, L. M., Cherkezyan, V. O. and Rumyantsev, O. V. (1994) Hot particles after the Chernobyl accident. *Geochemistry International* **31**, 46–55.

Klug, W., Graziani, G., Grippa, G., Pierce, D. and Tassone, C. (1992) Evaluation of long range atmospheric transport models using environmental radioactivity data from the Chernobyl accident, The ATMES Report.

Kolb, W. (1986) Radionuclide concentration in ground level air from 1984 to mid 1986 in North Germany and North Norway; influence of the Chernobyl accident. Physikalisch-Technische Bundesanstalt, PTB-Ra-18, pp. 53–56.

Kritidis, P., Catsaros, N. and Probonas, M. (1988) Hot particles in Greece after the Chernobyl accident, estimations on inhalation probability. In Hot Particles from the Chernobyl Fallout, eds. H. Von Philipsborn and F. Steinhäusler, *Proceedings of an International Workshop held in Theuern*, 28–29 October 1987. Schriftenreihe des Bergbau- und Industriemuseums Ostbauern Theuern, Band 16, pp. 115–120.

Krivokhatsky, A. S., Dubasov, Yu. V., Smirnova, E. A., Skovorodkin, N. V., Savonenkov, V. G., Alexandrov, B. M. and Lebedev, E. L. (1991) Actinides in the near release from the Chenobyl NPP accident. *Journal of Radioanalytical Nuclear Chemistry Articles* **147**, 141–151.

Kuriny, V. D., Ivanov, Yu.A., Kashparov, V. A., Loshchilov, N. A., Protsak, V. P., Yudin, E. B., Zhurba, M. A. and Parshakov, A. E. (1993) Particle-associated Chernobyl fall-out in the local and intermediate zones. *Annals of Nuclear Energy* **20**, 415–420.

Kutkov, V. A., Arefieva, Z. S., Muraviev, Yu. B. and Komaritskaya, O. I. (1995) Unique form of airborne radioactivity: nuclear fuel "hot particles" of the Chernobyl accident. Extended synopses of International Symposium on Environmental Impact of Radioactive Releases, IAEA-SM-339/57P.

Lancsarics, Gy., Fehér, I., Sági, L. and Pálfalvi, J. (1988) Transuranium elements in the hot particles emitted during the Chernobyl accident. *Radiation Protection Dosimetry* **22**, 111–113.

Lange, R., Dickerson, M. H. and Gudiksen, P. H. (1988) Dose estimates from the Chernobyl accident. *Nuclear Technology* **82**, 311–323.

Langner, J., Persson, C. and Robertson, L. (1995) The Chernobyl accident: a case study of dispersion of ^{137}Cs using high resolution meteorological data. In *Dispersion Prognoses and Consequences in the Environment*, ed. U. Tveten, Final Report from the NKS, Project BER-1.

Likhtariov, I. A., Repin, V. S., Bondarenko, O. A. and Nechaev S. Ju. (1995) Radiological effects after inhalation of highly radioactive fuel particles produced by the Chernobyl accident. *Radiation Protection Dosimetry* **59**, 247–254.

Lindner, G., Wilhelm, Ch., Kaminski, S., Schell, B., Wunderer, M. and Wahl, U. (1992) Inhalation of non-volatile radionuclides after the Chernobyl accident—a retrospective approach. *Proceedings of 8th International Congress of the International Radiation Protection Association*, May 17–22, 1992, Montreal, Canada, pp. 261–264.

Lujanas, V., Mastauskas, A., Lujaniene, G. and Spirkauskaite, N. (1994) Development of radiation in Lithaunia. *Journal of Environmental Radioactivity* **23**, 249–263.

Luokkanen, S., Kulmala, M. and Raunemaa, T. (1988) Chernobyl fallout in Finland: hot areas. *Journal of Aerosol Science* **19**, 1363–1366.

Lyul, A. YU. and Kolesov, G. M. (1994) Elemental composition and uranium isotope ratios in hot particles from the Chernobyl accident. *Journal of Radioanalytical Nuclear Chemistry, Articles* **181**, 25–32.

Mandjoukov, I. G., Burin, K., Mandjoukova, B., Vapirev, E. I. and Tsacheva, Ts. (1992) Spectrometry and visualization of 'standard' hot particles from the Chernobyl accident. *Radiation Protection Dosimetry* **40**, 235–244.

Martin, D., Mithieux, C. and Strauss, B. (1987) On the use of the synoptic vertical wind component in a transport trajectory model. *Atmospheric Environment* **21**, 45–52.

Maryon, R. H. and Heasman, C. C. (1990) The accuracy of plume trajectories forecast using the U.K. Meteorological Office operational forecasting models and their sensitivity to calculation schemes. *Atmospheric Environment* **22**, 259–272.

Mattsson, R. and Hatakka, J. (1986) Hot particle in inhalate air after the Chernobyl accident. Finnish Association for Aerosol Research, *Report Sewies in Aerosol Science* **2**, 28–30 (in Finnish).

Mietelski, J. W. and Wąs, B. (1995) Plutonium from Chernobyl in Poland. *Applications of Radiation Isotopes* **46**, 1203–1211.

Misaelides, P., Sikalidis, C., Tsitouridou, R., Alexiades, C. (1987) Distribution of fission products in dust samples from the region of Thessalonici, Greece, after the Chernobyl nuclear accident. *Environmental Pollution* **47**, 1–8.

Osuch, S., Dąbrowska, M., Jaracz, P., Kaczanowski, J., Le Van Khoi, Mirowski, S., Piasecki, E., Szefliński, G., Szefliński, Z., Tropiło, J., Wilhelmi, Z., Jastrzębski, J. and Pieńkowski, L. (1989) Isotopic composition of high-activity particles released in the Chernobyl accident. *Health Physics* **57**, 707–716.

Paatero, J., Mattsson, R. and Hatakka, J. (1994) *Measurements of Airborne Radioactivity in Finland, 1983–1990, and Applications to Air Quality Studies.* Finnish Meteorological Institute, Publications on Air Quality, Helsinki.

Pavlotskaya, F. I., Goryachenkova, T. A., Yemel'yanov, V. V., Kazinskaya, I. Ye., Barsukova, K. V. and Myasoyedov, B. F. (1994) Modes of occurrence of plutonium in hot particles (translated from *Geokhimiya* 7 (1993) 972–979), *Geochemistry International* **31**, 62–69.

Perkins, R. W., Robertson, D. E., Thomas, C. W. and Young, J. A. (1989) Comparison of nuclear accident and nuclear test debris. *Proceedings in International Symposium on Environmental Contamination Following a Major Nuclear Accident*, Vienna, Austria, 16–20 Oct. 1989, IAEA-SM-306/125, pp. 111–139.

Persson, C., Rodhe, H. and De Geer, L.-E. (1987) The Chernobyl accident—a meteorological analysis of how radionuclides reached and were deposited in Sweden, *Ambio* **16**, 20–31.

Piasecki, E., Jaracz, P. and Mirowski, S. (1990) Analysis of gamma-radioactivity in "hot particles" released after the Chernobyl accident, I. Calculations of fission products in hot particles (a detective approach). *Journal of Radioanalytical Nuclear Chemistry* **141**, 221–242.

Powers, D. A., Kress, T. S. and Jankowski, M. W. (1987) The Chernobyl source term. *Nuclear Safety* **28**, 10–28.

Puhakka, T., Jylhä, K., Saarikivi, P., Koistinen, J. and Koivukoski, J. (1990) Meteorological factors influencing the radioactive deposition in Finland after the Chernobyl accident. *Journal of Applied Meteorology* **29**, 813–829.

Pöllänen, R., Salonoja, M., Toivonen, H. and Valkama, I. (1993) Uranium fuel particles in a RBMK accident: particle characteristics and atmospheric dispersion. *Proceedings of the 5th Finnish National Aerosol Symposium*, 1–3 June 1993. Report Series in Aerosol Sciences **23**, 278–283.

Pöllänen, R. and Toivonen, H. (1994a) Skin doses from large uranium fuel particles: application to the Chernobyl accident. *Radiation Protection Dosimetry* **54**, 127–132.

Pöllänen, R. and Toivonen, H. (1994b) Transport of large uranium fuel particles released from a nuclear power plant in a severe accident. *Journal of Radiological Protection* **14**, 55–65.

Pöllänen, R. and Toivonen, H. (1995) Skin dose calculations for uranium fuel particles below 500 μm in diameter. *Health Physics* **68**, 401–405.

Pöllänen, R., Toivonen, H., Lahtinen, J. and Ilander, T. (1995) Transport of large particles released in a nuclear accident. STUK-A125. Finnish Centre for Radiation and Nuclear Safety, Helsinki.

Pöllänen, R. and Toivonen, H. (1996) Size estimation of radioactive particles released in the Chernobyl accident. In eds. M. Kulmala and P. E. Wagner, *Proceedings of the 14th International Conference on Nucleation and Atmospheric Aerosols* 1996, pp. 670–673.

Pöllänen, R., Kansanaho, A. and Toivonen, H. (1996) Detection and analysis of radioactive particles using autoradiography. STUK-YTO-TR99. Finnish Centre for Radiation and Nuclear Safety, Helsinki.

Reap, R. M. (1972) An operational three-dimensional trajectory model. *Journal of Applied Meteorology* **11**, 1193–1202.

Reiff, J., Forbes, G. S., Spieksma, F. Th. M. and Reynders, J. J. (1986) African dust reaching Northwestern Europe: A case study to verify trajectory calculations. *Journal of Climate and Applied Meteorology* **25**, 1543–1567.

Reineking, A., Becker, K. H., Porstendörfer, J. and Wicke, A. (1987) Air activity concentrations and particle size distributions of the Chernobyl aerosol. *Radiation Protection Dosimetry* **19**, 159–163.

Robertson, D. E. (1986) Letter to the National Institute of Radiation Protection, Stockholm, Sweden, November 1986.

Rossi, J. and Vuori, S. (1988) Effect of particle size on atmospheric dispersion and radiation doses. Technical Report ROSA-10/88

Rudhard, J., Schell, B. and Lindner, G. (1992) Size distribution of hot particles in the Chernobyl accident. *Proceedings of International Symposium on Radioecology*: Chemical Speciation—Hot Particle, Znojmo, Czech Republic, 12–16 October 1992.

Rulík, P., Bučina, I. and Malátová, I. (1989) Aerosol particle size distribution in dependence on the type of radionuclide after the Chernobyl accident and in the NPP Effluents. *Proceedings of the XVth Regional Congress of IRPA*, Visby, Gotland, Sweden, 10–14 September, 1989, pp. 102–107.

Rytömaa, T., Toivonen, H., Servomaa, K., Sinkko, K. and Kaituri, M. (1986) Uranium aerosols in Chernobyl fallout, Finnish Centre for Radiation and Nuclear Safety, Internal Report, Helsinki.

Saari, H., Luokkanen, S., Kulmala, M., Lehtinen, S. and Raunemaa, T. (1989) Isolation and characterization of hot particles from Chernobyl fallout in Southwestern Finland. *Health Physics* **57**, 975–984.

Salbu, B. (1989) Radionuclides associated with colloids and particles in the Chernobyl accident. *Proceedings of the Joint OECD (NEA)/CEC Workshop on Recent Advances in Reactor Accident Consequences Assessments*, Rome, 1988, CSNI Report 145, Rome, Vol. 1, pp. 53–67.

Salbu, B., Krekling, T., Oughton, D. H., Østby, G., Kashparov, V. A., Brand, T. L. and Day, J. P. (1994) Hot particles in accidental releases from Chernobyl and Windscale nuclear installations. *Analyst* **119**, 125–130.

Sandalls, F. J., Segal, M. G. and Victorova, N. (1993) Hot particles from Chernobyl: a review. *Journal of Environmental Radioactivity* **18**, 5–22.

Savolainen, A. L., Hopeakoski, T., Kilpinen, J., Kukkonen, P., Kulmala, A. and Valkama, I. (1986) Dispersion of radioactive releases following the Chernobyl nuclear power plant accident, Finnish Meteorological Institute, Interim report No.1986/2, ISSN 0782–6079.

Schubert, P. and Behrend, U. (1987) Investigations of radioactive particles from the Chernobyl fall-out. *Radiochimica Acta* **41**, 149–155.

Sinkko, K., Aaltonen, H., Mustonen, R., Taipale, T. K. and Juutilainen, J. (1987) Airborne radioactivity in Finland after the Chernobyl accident in 1986, Suppl. 1 to Annual Report STUK-A55, STUK-A56.

Sisefsky, J. (1961) Debris from tests of nuclear weapons. *Science* **133**, 735–740.

Smith, F. B. and Clark, M. J. (1986) Radionuclide deposition from the Chernobyl cloud. *Nature* **322**, 690–691.

Stunder, B. J. B. (1996) An assessment of the quality of forecast trajectories. *Journal of Applied Meteorology* **35**, 1319–1331.

Tcherkezian (Cherkezyan), V., Shkinev, V., Khitrov, L. and Kolesov, G. (1994) Experimental approach to Chernobyl hot particles. *Journal of Environmental Radioactivity* **22**, 127–139.

Tcherkezian, V., Galushkin, B., Goryachenkova, T., Kashkarov, L., Lïul, A., Roschina, I. and Rumiantsev, O. (1995) Forms of contamination of the environment by radionuclides after the Tomsk accident (Russia 1993). *Journal of Environmental Radioactivity* **27**, 133–139.

Toivonen, H., Pöllänen, R., Leppänen, A., Klemola, S., Lahtinen, J., Servomaa, K., Savolainen, A. L. and Valkama, I. (1992) A nuclear incident at a power plant in Sosnovyy Bor, Russia, *Health Physics* **63**, 571–573.

Valkama, I. and Salonoja, M. (1993) Operational long-range dispersion and dose model for radioactive releases, Finnish Meteorological Institute, Helsinki (in Finnish).

Valkama, I., Salonoja, M., Toivonen, H., Lahtinen, J. and Pöllänen, R. (1995) Transport of radioactive gases and particles from the Chernobyl accident: comparison of environmental measurements and dispersion calculations. *Proceedings of an International Symposium on Environmental Impact of Radioactive Releases*, Vienna 8–12 May 1995, IAEA-SM-339/69, pp. 57–68.

Valkama, I. and Pöllänen, R. (1996) Transport of radioactive materials in convective clouds. In eds. M. Kulmala and P. E. Wagner. *Proceedings of the Fourteenth International Conference on Nucleation and Atmospheric Aerosols* 1996, pp. 411–414.

Vapirev, E. I., Kamenova, Ts., Mandjoukov, I. G. and Mandjoukova, B. (1990) Visualization, identification and spectrometry of a hot particle. *Radiation Protection Dosimetry* **30**, 121–124.

Vapirev, E. I. and Grozev, P. A. (1993) Assessments of the risk for the Bulgarian population due to standard UO_2 hot particles released during the Chernobyl accident. *Radiation Protection Dosimetry* **46**, 273–279.

Vapirev, E. I., Tsacheva, Ts., Bourin, K. I., Hristova, A. V., Kamenova, Ts. and Gourev, V. (1994) Nuclear spectroscopy and electron microprobe study of a Ba hot particle originating from the Chernobyl accident. *Radiation Protection Dosimetry* **55**, 143–147.

Wahl, U., Lindner, G. and Recknagel, E. (1989) Radioaktive Partikel im Tschernobyl-Fallout. In *Die Wirkung niedriger Strahlendosen—Biologische und Medizinische Aspekte*, ed. W. Köhnlein, H. Traut and N. Fischer. Springer, Berlin-Heidelberg, pp. 165–176.

van der Wijk, A., de Meijer, R. J., Jansen, J. F. W. and Boom, G. (1988) Core fragments and ruthenium particles in the Chernobyl fallout. In Hot Particles from the Chernobyl Fallout, eds. H. Von Philipsborn and F. Steinhäusler, Proceedings of an International Workshop held in Theuern 28/29 October 1987. Schriftenreihe des Bergbau- und Industriemuseums Ostbauern Theuern, BAND 16, pp. 53–61.

Wheeler, D. A. (1988) Atmospheric dispersal and deposition of radioactive material from Chernobyl. *Atmospheric Environment* **22**, 853–863.

Winkelmann, I., Endrulat, H.-J., Fouasnon, S., Gesewsky, P., Haubelt, R., Klopfer, P., Köhler, H., Kohl, R., Kucheida, D., Müller, M.-K., Schmidt, H., Vogl, K., Weimer, S., Wildermuth, H., Winkler, S., Wirth, E. and Wolff, S. (1986) Ergebnisse von Radioaktivitätsmessungen nach dem Reaktorunfall in Tschernobyl, ISH-HEFT 99, pp. 34–38.

UNSCEAR (1993). United Nations Committee on the effects of Atomic Radiation. Sources and effects of ionizing radiation. 1993 Report to the general assembly, with scientific annexes. New York, United Nations, 1993. Annex B, Table 33, pp. 165–169.

APPENDIX: SIZE ESTIMATION OF RADIOACTIVE PARTICLES FOUND AFTER THE CHERNOBYL ACCIDENT

After the Chernobyl accident large numbers of hot particles were detected in different samples, but only a small number were further analysed. Moreover, reports dealt mainly with activity of the particles and less frequently with particle size. Here, we attempt to estimate the size of these particles. The method employed in the size estimation as well as the aerodynamic diameter of the particles are presented here (Table A1); only the maximum sizes of the particles at each site are estimated.

The particle sizes were obtained directly using cascade impactors (see Fig. 1), electron microscopes and sometimes optical microscopes. Emulsion techniques and detailed nuclide-specific activities were used for the indirect size estimation. The impactor and microscope data as well as the estimations of particle sizes done by the original authors are preferred in Table A1. If no size estimation is given in the references, the estimation is performed using the methods given in the present study.

The impactors fractionate airborne particles into different size classes. The particles are collected onto impactor plates with different cutoff aerodynamic diameters, but individual particles are not registered. The impactor data in Table A1 refer to the largest detected aerodynamic diameter. The aerodynamic diameter can be calculated by measuring the sedimentation velocity of single particles (Kerekes *et al.*, 1991). Particle density can be estimated provided that the diameter and shape are known.

Although particle identification in electron microscopy can be tedious, the method is very useful for estimating the size and shape of individual particles. The elemental composition of the particles is usually measured at the same time with X-ray analysis. Autoradiography is often used to separate particles from the bulk material of the sample. The total beta activity of individual particles can then be estimated from the size of the black spot on the autoradiography film (Sisefsky, 1961; Pöllänen *et al.*, 1996). Particle size can be estimated from total activity using reactor core inventory data.

Size estimation from nuclide-specific activities is based on the assumption that the non-volatile elements remain attached to the particles, i.e. the nuclide ratios of these elements are not changed during the fuel fractionation processes (e.g. Piasecki *et al.*, 1990; Jaracz *et al.*, 1990). The equivalent volume diameter, d_p (μm), is calculated from the known activity per unit volume, A_{vol} (Bq μm^{-3}), of a nuclide or a sum of nuclides

$$d_p = \left(\frac{6}{\pi}\frac{A_{meas}}{A_{vol}}\right)^{1/3}, \qquad \text{(A1)}$$

where A_{meas} is the measured activity of the nuclide or sum of nuclides. In our study, size is estimated separately both for ruthenium particles and for uranium fuel particles. The

Table A1. Activity (A) and aerodynamic diameter (d_a) of the most active (i.e. largest) particles found in different locations after the Chernobyl accident

No.	Reference	Location	Number		A (Bq)		d_a (μm)	
			U	Ru	U	Ru	U	Ru
1	Rytömaa *et al.* (1986)	Uusikaupunki	8	1	120	200	23	5.1
		Soviet train carriage	4	1	15,000	29,000	110	27
2	Mattsson *et al.* (1986)[a]	Helsinki			$> 200^{tot}$		> 16	
		Nurmijärvi			$> 200^{tot}$		> 16	
3	Sinkko *et al.* (1987)	Nurmijärvi	8	2	$18^{Ce\text{-}144}$	$9^{Ru\text{-}106}$	18	3.3
4	Kauppinen *et al.* (1986)[b]	Helsinki					> 16	
5	Saari *et al.* (1989)[c]	Uusikaupunki	20	1	320	130	15*	4.4
		Lohja	1	—	45	—	8*	—
6	Paatero *et al.* (1994)	Helsinki	1	—	140	—	24	—
		Nurmijärvi	1	—	—	—	—	—
7	Devell (1988)	Nyköping	6	6	750	31,000	41	27
8	Kerekes *et al.* (1991)[c]	Stockholm	9	9	$110^{Ce\text{-}144}$	49,000	33	37*
		Gotland	5	5	$67^{Ce\text{-}144}$	5300	28	15
		Gävle	—	13	—	9800	—	7.8*
9	Robertson (1986)	Gävle	1	—	380	—	33	—
	Perkins *et al.* (1989)[c]	Älvkarleby	2	—	450	—	35	—
		Stockholm	3	1	380	7400	33	17
		Nyköping	6	—	420	—	34	—
		Gusum	7	—	250	—	29	—
		Västervik	9	1	340	9300	32	18
		Oskarshamn	4	—	440	—	34	—
		Öland	2	1	160	—	24	—
10	Salbu (1989)	Kjeller	—	1	—	$65^{Ru\text{-}106}$	—	6.3
11	Lujanas *et al.* (1994)[d]	Vilnius					22[d]	
12	Schubert *et al.* (1987)	Masurian Lakes	1	8	—	170,000	—	45*
13	Osuch *et al.* (1989)[a]	Mikołajki	9	51	4000^{tot}	200,000	44	51
		Warsaw	10	11				
		Lomża	12	7				
		Białystok	82	12				
		Suwałki	1	7				
14	Broda (1987), Broda *et al.* (1989, 1992)[a]	Mikołajki andKraków	28	37	2000^{tot}	308,000	35	58
15	Van der Wijk *et al.* (1988)	Poland	1	3	36	90,000	15	39
		Kiev	1	—	950	—	45	—
		Minsk	1	—	420	—	34	—
16	Georgi *et al.* (1988)[b]	Neuherberg, Vienna, Helgoland, Hannover					≲16	
17	Kolb (1986)	Brunswick	12 (total)		15^{tot}		6.9	
18	Reineking *et al.* (1987)	Göttingen	3	—	3.1	—	5	—
19	Wahl *et al.* (1988)	Konstanz	10	5	41	270	16	5.6
20	Behrens (1988)	Neuherberg	1	3	—	3100	—	13

21	Winkelmann *et al.* (1987)[b]	Neuherberg					≲10	
22	Horn *et al.* (1987)[b]	Aachen					≲10	
23	Burkart *et al.* (1988)	Würenlingen	1	1	40	360	15	6.2
		Baar	3	2	35	79	15	4.0
		—	—	—	—	3000^{Ru-103}	—	13
24	Jost *et al.* (1986)[b]	Spiez, Zürich					≲7	
25	Rulik *et al.* (1989)[b]	Moravský-Krumlov,Ostrava, Prague					≲7	
26	Keck *et al.* (1988)	Vienna	2	—	66	—	18	—
27	Balashazy *et al.* (1988) Lansarics *et al.* (1988)	Budapest	12	3	230	570	33*	7.2
28	Dovlete (1990)	Iaci	3	—	59^{Ce-144}	—	33	—
		Tulcea	1	—	57^{Ce-144}	—	26	—
		Craiova	1	—	110^{Ce-144}	—	27	—
29	Mandjoukov *et al.* (1992), Vapirev *et al.* (1990, 1994)[a]	Sofia	110	20	410	—	42*	—
30	Kritidis *et al.* (1988)[a]	Athens, Thessaloniki	18	6	240	43,000	28	30
31	Misaelides *et al.* (1987)	Thessaloniki	—	1	—	1500	—	9.8
32	Cuddihy *et al.* (1989)	Shipping crate	10 (total)				> 50*	
33	Pavlotskayaet *al.* (1994)	30 km zone	7 (total)		$16,000^{Ce-144}$		170	
34	Tcherkezianet *al.* (1994)	30 km zone	10 (total)		9900^{Ce-144}		150	
35	Salbu *et al.* (1994)	30 km zone	10 (total)		$950,000^{Ce-144}$		680	
36	Khitrov *et al.* (1994)	Vil'cha	1 (total)		$16,000^{Ce-144}$		170	
		Kiev	1 (total)		$660,000^{Ru-106}$		140	
37	Lyul *et al.* (1994)	Near plant	10 (total)		$40,000^{Ce-144}$		240	
38	Rudhard *et al.* (1994)	Near plant	—		—		100*	
39	Kutkov *et al.* (1995)	Plant staff	—		—		12 (AMAD)	
40	Demchuk *et al.* (1990)	Near plant	—		—		45 (mean)	
41	IAEA (1991)	Polesskoe	1 (total)		70^{Ce-144}		28	
42	Burakov *et al.* (1994)	< 12 km from plant	3 (total)		—		> 200*	
43	Akopova *et al.* (1991)[d]	30 km zone	56 (total)		—		< 200[d]	
44	Kuriny *et al.* (1993)[e]	< 10 km from plant	1200 (total)		—		20–400[e]	
45	Krivokhatsky *et al.* (1991)	0.5–12 km from the plant	—		—		> 1 mm	

Only those studies are mentioned in which either single particles were detected and further analysed or particle sizes were directly measured. Numbers before the references refer to the numbers in the map presented in Fig. 1. The number of analysed particles, their activities and aerodynamic diameters are given for both uranium fuel particles (U) and ruthenium particles (Ru). Sometimes particles cannot be categorized into U and Ru classes in which case only the total number of analysed particles is given. Particle sizes ("physical" diameter) given in the references (microscopes or other means) are preferred (conversion into aerodynamic diameter is performed here) and are denoted as *. If the sizes are not given in the original study, aerodynamic diameters are calculated using methods given in the present paper (from equivalent volume diameter of the particles; see text). The activity of U particles refers to the sum of activities of ^{95}Zr, ^{141}Ce and ^{144}Ce. The activity of Ru particles is the sum of ^{103}Ru and ^{106}Ru. Sometimes the references give only total activity of particles or the activities of the long-lived nuclides ^{106}Ru and ^{144}Ce.

[a] Detailed activities of individual particles are given for only a few particles or not at all.

[b] Impactor measurement; aerodynamic diameter (maximum size) of particles are given as such.

[c] Particle sizes (SEM) do not necessarily match calculated sizes.

[d] Particle size is determined using emulsion techniques (d_p is presented).

[e] Chernobyl hot particles data base was created consisting γ-spectrometric data of 1200 particles with characteristic sizes 20-400 μm (not d_a) and activities more than 37 Bq (1987). Particles reported in Ref. no. 35 and 40 are in this data base.

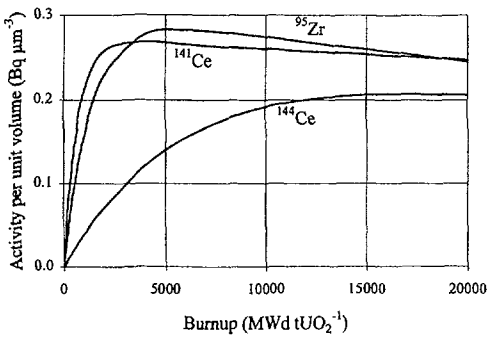

Fig. A1. Activity per unit volume (Bq μm^{-3}) for ^{95}Zr, ^{141}Ce and ^{144}Ce in uranium fuel as a function of fuel burnup (MWd per ton of uranium dioxide fuel). The burnup of 10,000 MWd per tonne of fuel refers to average burnup.

aerodynamic diameters presented in Table A1 are calculated using Equation (3). The shape of the U particles was often irregular. Moreover, the density of the particles may be smaller than 10,500 kg m^{-3} which is the value used here. If the dynamic shape factor is 1.36 (Hinds, 1982) and density 8300 kg m^{-3} (Saari *et al.*, 1989; Krivokhatsky *et al.*, 1991), the aerodynamic diameter is $2.47 \times d_p$, which gives smaller values (by a factor of 0.76) than those in Table A1.

In addition to volatility, the activity concentration of nuclides in a particle depends on fuel burnup, although this dependency is sometimes weak (Fig. A1). The hot particles are here assumed to originate from the fuel of average burnup. Inactive agglomerated and condensed material may be present in the particles. Broda *et al.* (1989) reported particle sizes of 20–600 μm and Robertson (1986) of up to 21 μm. The equivalent volume calculated from particle activity alone thus represents the lower limit rather than a true estimate of the particle size.

Ruthenium particles

The activity of Ru particles in addition to direct size measurements was published by Kerekes *et al.* (1991), Schubert *et al.* (1987) and Salbu (1989). The activity of ^{103}Ru per unit volume was about 50 Bq μm^{-3} for particles collected by Kerekes *et al.* (1991) but slightly higher for particles collected by Schubert *et al.* (1987). Salbu (1989) determined that a Ru particle 2 μm in diameter showed a ^{106}Ru activity of 65 Bq on 12 December 1988 (activity ratio ^{103}Ru:^{106}Ru is about 5:1 for fuel of average burnup with zero decay time). Kerekes *et al.* (1991) measured the aerodynamic diameters of Ru particles, and calculated that their density was 10,500 kg m^{-3}, which is the value used here. Using hand calculations, Devell (1988) estimated that the total Ru activity ($^{106}Ru + ^{103}Ru$) per unit volume was 250 Bq μm^{-3} with a particle density of 12,200 kg m^{-3}. Vapirev *et al.* (1994) mentioned a value of 200 Bq μm^{-3} whereas Likhtariov *et al.* (1995) reported 10 Bq μm^{-3}, which is much lower than other estimates. In the present study the total activity per unit volume is calculated from

$$A_{vol} = 100 \text{ Bq } \mu m^{-3}. \quad \text{(A2)}$$

The activity ratio ^{103}Ru:^{106}Ru was very high for some particles. Broda *et al.* (1989) reported a value of 12.3 (for a particle of 308 kBq total activity) and Kritidis *et al.* (1988) 37.9 (for a particle of 42.8 kBq total activity). These values are typical for fuel of low burnup. Activity per unit volume of these particles may be higher than 100 Bq μm^{-3}.

Uranium fuel particles

The isotopic composition of U particles generally reflects the core inventory (Osuch *et al.*, 1989). The frequently observed nuclides, ^{95}Zr, ^{141}Ce and ^{144}Ce, are appropriate for estimating the size of U particles (Pöllänen and Toivonen, 1996). The sum of their activities in the unit volume of fuel irradiated to average burnup can be calculated from their average inventory in the RBMK reactor core. Pöllänen and Toivonen (1994a) used a value of 0.75 Bq μm^{-3} in their skin dose estimations. In the present study

$$A_{vol} = 0.7 \text{ Bq } \mu m^{-3} \quad \text{(A3)}$$

for fuel particles for which size estimation was not done in the references. This number is consistent with the data presented by Piasecki *et al.* (1990). Saari *et al.* (1989) calculated the volumes of the uranium fuel particles directly from SEM pictures. They found a linear activity-to-size dependency that gave higher values for the volumetric activity.

Sometimes only the long-lived nuclide, ^{144}Ce, is reported. Rudhard *et al.* (1992) and Bálasházy *et al.* (1988) estimated the activity per unit volume from the core inventory and calculated the particle size. They used values of 0.18 and 0.12 Bq μm^{-3} for ^{144}Ce; Saari *et al.* (1989) gave higher values. Devell (1988) and Rytömaa *et al.* (1986) estimated 0.3 Bq μm^{-3} for ^{141}Ce (activity ratio ^{144}Ce:$^{141}Ce \approx 0.7$ for fuel of average burnup; see Fig. A1). Here the following value is used for ^{144}Ce:

$$A_{vol} = 0.2 \text{ Bq } \mu m^{-3}. \quad \text{(A4)}$$

Sometimes only total activity is reported (e.g. Mattsson *et al.*, 1986). The concept of "total" activity may be misleading, because it sometimes includes only detected nuclides (this depends very much on the gamma-ray analysis date) or those that are typical of the reactor fuel. Nevertheless, the total activity can give us a rough estimate of particle size.

According to the Bulgarian findings (Vapirev *et al.*, 1994) the total activity per unit volume for uranium fuel particles was 1–1.5 Bq μm^{-3} (refers only to detected nuclides). Saari *et al.* (1989) reported considerably higher values, whereas Likhtariov *et al.* (1995) gave lower figures (0.4 Bq μm^{-3}). The estimate by Pöllänen and Toivonen (1994a) is 2.6 Bq μm^{-3} for non-volatile nuclides in the particles. In our study the total activity per unit volume is assumed to be

$$A_{vol} = 3 \text{ Bq } \mu m^{-3}. \quad \text{(A5)}$$

Equations (A3)–(A5) may give somewhat different sizes for a particle of known nuclide-specific activity if they are applied each in turn to the same particle. In practice, these differences are insignificant.

VI

PÖLLÄNEN R.
Highly radioactive ruthenium particles released from the Chernobyl accident: particle characteristics and radiological hazard.
Radiation Protection Dosimetry 1997; 71: 23 - 32.

Radiation Protection Dosimetry
Vol. 71, No. 1, pp. 23–32 (1997)
Nuclear Technology Publishing

HIGHLY RADIOACTIVE RUTHENIUM PARTICLES RELEASED FROM THE CHERNOBYL ACCIDENT: PARTICLE CHARACTERISTICS AND RADIOLOGICAL HAZARD

R. Pöllänen
Finnish Centre for Radiation and Nuclear Safety
PO Box 14
FIN-00881 Helsinki, Finland

Received October 31 1996, Amended December 11 1996, Accepted December 16 1996

Abstract — After the Chernobyl accident highly radioactive Ru particles, more than 100 kBq in activity and more than 10 μm in diameter, were found hundreds of kilometres away from the plant. Since particle sampling and analyses have not necessarily been adequate, an approach based on inventory calculations is used for estimating their radiological hazard. Elemental composition of the particles suggests that short-lived nuclides may essentially contribute to the risks, although usually only ^{103}Ru and ^{106}Ru were detected. Because large Ru particles are not of inhalable size, skin doses are calculated for various particle compositions, sizes and decay times. Calculations support the assumption that Ru particles are metallic precipitates. The composition may have a notable impact on skin doses which are not necessary the largest for particles originating from fuel of high burnup. Even an individual particle may be a severe radiological hazard. A dose of 50 mGy.cm^{-2} for the basal cell layer may be exceeded in one hour provided that an Ru particle larger than 8 μm in diameter is deposited on the skin.

INTRODUCTION

Radioactive particles are often considered as a unique form of 'radioactivity' and a curiosity from the point of view of analyses of the consequences of nuclear accidents. Indeed, radioactive particulate substances released into the atmosphere are of special radiological importance. Far from being a curiosity, however, they represent a challenging problem in the field of nuclear safety[1], as shown in this paper.

Highly radioactive particles (hot particles) present a potential health hazard, even far from the damaged plant[2–4]. Their radiological risks differ from those in a uniform exposure. Even if their number concentration in air is low it is possible that some persons are 'lucky' enough to receive a hot particle deposited, for example, on the skin. Consequently, only a few cells in a tissue may be exposed at levels that may cause severe health damage. Since activity of a particle may be hundreds of kilobecquerels, the dose in its immediate vicinity may be very high.

Radioactive particles were detected in many European countries after the Chernobyl accident, and were typically collected and analysed weeks or even years afterwards, thereby precluding the detection of short-lived nuclides; in addition, particles were usually analysed with gamma ray spectrometers only. Although inactive materials, nuclides with low gamma yield or pure beta emitters as well as those with low activity were not generally detected, they may have exerted an essential influence on the possible radiological hazard.

Risk estimations have been performed for inhalable hot particles[5–8]; however, some of the particles found after the Chernobyl accident were so large that they could not be inhaled. When instead deposited on the skin, they may be sufficiently active to produce, within a short time[2], a dose exceeding the ICRP annual equivalent dose limit of 50 mSv for the public[9], intended to protect the basal cell layer against deterministic effects. Here beta skin doses are estimated for Ru-rich particles of different sizes and elemental and nuclide compositions. Particle properties are assumed to be similar to those found after the Chernobyl accident. If necessary, they are supplemented by characteristics calculated from nuclide- and element-specific inventories of the nuclear fuel.

RUTHENIUM PARTICLES IN THE CHERNOBYL ACCIDENT

'Hot' particles observed after the Chernobyl accident have been classified into multi-elemental fuel fragments and mono-elemental (or bi-elemental) particles[1]. Excluding noble bases, fragments of uranium dioxide fuel contain radioactive species typical of reactor fuel and are also depleted in volatile elements. Measurements performed by a gamma ray spectrometer revealed that some particles contained only a few radionuclides, typically ^{103}Ru and ^{106}Ru/^{106}Rh. They are often referred to as mono-elemental particles, although elemental analyses showed that these particles contained other elements also. Since mono-elemental Ru particles were not detected after nuclear weapon tests and after previous nuclear accidents, their release was a unique feature of the Chernobyl accident.

Formation and release

The formation mechanisms of highly radioactive Ru particles are still unclear, partly owing to the sparsity of sampling and incompleteness of analyses of single particles (misinterpretations have been made[10] as activity analyses alone are not sufficient to solve the problem of particle formation) and partly owing to complicated physical and chemical phenomena occurring during the accident. The following processes are suggested[1]:

(1) Mechanical emission of liquid particles from the molten fuel, followed by solidification of the droplets.
(2) Liquid droplets formed by homogeneous nucleation of a vapour, followed by solidification of the droplets.
(3) Condensation of water steam onto existing water-soluble particles, followed by evaporation of water from the aqueous liquid droplet.
(4) Mechanical emission of solid particles present in the fuel.

Several authors identified the Ru particles as metallic precipitates (white inclusions) which is supported by their similar elemental composition and shape. Broda *et al*[11], however, reopened the question of particle formation owing to the unlikely purity of the particles, the presence of elements that had not been detected in precipitates (Fe, Ni, Co, Sb) and the incompatible activity ratios of the isotopes ^{103}Ru and ^{106}Ru. Broda *et al* suggested that Ru particles were formed outside the fuel rods rather than being present in the fuel as white inclusions fragmented by the explosion.

The chemical form may greatly affect the release behaviour of semivolatile Ru. A strongly oxidising atmosphere may lead to oxidation of Ru into more volatile forms[12]. One the basis of ^{103}Ru:^{106}Ru distribution, Osuch *et al*[13] concluded that characteristics of Ru particles represent local properties of irradiated fuel and that the 'particles have not been formed in a process of condensation of mixed Ru vapours'. Kashparov *et al*[14] came to a different conclusion using similar data. They stated that particles might have been formed from a mixture of volatile RuO_4. Schubert and Behrend[15], however, showed that the oxygen content of Ru particles was below a few per cent (only surface oxidation). Kashparov *et al*[14] suggested that spherical Ru particles detected in Western Europe 'could have been present in the nuclear fuel at the moment of the accident', whereas large and irregularly shaped Ru particles deposited near the plant 'were formed at the rate of ruthenium oxidation during the accident and its subsequent condensation on the particles of materials of iron group elements'.

The release of Ru particles may also depend on the burnup of the reactor fuel[16], in which fission product precipitates accumulate at the grain boundaries of the fuel. The higher the burnup, the more the fuel is fractured and, consequently, the higher the grain boundary release may be. This is supported by the fact that only a few particles originating from low burnup fuel were observed.

The complex behaviour of Ru is supported by environmental findings. The deposition patterns of Ru in Finland[17] and Poland[18] showed that the Chernobyl fallout was a combination of patterns from the explosion and burning phases of the accident.

Transport and deposition

In general, radionuclide fallout from Chernobyl was spatially inhomogeneous, the territorial distribution of various nuclides as well as number concentration of particles deposited on the ground varying greatly. 'Hot spot' areas with marked occurrence of radioactive particles were found in several European countries. Pöllänen *et al*[2] used a trajectory model to identify the areas of radioactive particle fallout. Environmental findings of large particles were compared with locations given by trajectory calculations, in which it was concluded that the particulate nature of the release plume must be taken into account in estimations of the radiological risks.

The prominent feature of the Chernobyl accident was that large, highly radioactive particles were transported far from the damaged plant in a manner different from small particles and gases[2]. Moreover, the abundance of Ru particles compared with U particles was dependent on the detection site, suggesting that they were either transported or released differently[13]. Radiological consequences are determined by the characteristics of radioactive particles; particle transport is dominated by size and atmospheric conditions, and health effects by nuclide composition and activity.

Characteristics of particles detected in the environment

Radioactive particles cannot always be considered as 'becquerels' dispersed in air, per unit volume of air or in per unit mass of the sample[4]. Nevertheless, current routinely used air monitoring techniques do not necessarily identify single radioactive particles. Tedious procedures are needed for particle localisation and isolation as well as for analyses of activity, size and elemental composition; usually only some of these properties were reported.

Activities were reported for individual Ru particles identified in Finland[19,20], Sweden[21–23], Norway[24], Poland[11,13,15,25,26], Germany[27,28], Switzerland[29], Hungary[30], Bulgaria[31] and Greece[7,32]. Ru particles were also apparently detected in Lithuania[33], Belarus[34] and Ukraine[35,36] but the activities were not published. The total activity of particles (^{103}Ru + ^{106}Ru) detected in Finland, Germany, Switzerland and Hungary was less than 1 kBq, whereas in Bulgaria up to a few kBq were

recorded; in Sweden and Greece up to a few tens of kBq, and up to hundreds of kBq in Poland. Gamma ray measurements performed within a few weeks of the accident show almost pure Ru/Rh particles. Minor amounts of nuclides, such as ^{99}Mo and ^{131}I, were also detected. Measurements performed later revealed the presence of long-lived ^{60}Co and ^{125}Sb[11,22,26]. The non-volatile species, ^{95}Zr, ^{95}Nb, ^{141}Ce and ^{144}Ce, were also sometimes detected.

The elemental composition was estimated qualitatively by Rytömaa *et al*[19], Kerekes *et al*[22] and Salbu[24] and quantitatively by Schubert and Behrend[15], using electron microscopes and X ray analysis (Table 1). Particles were mainly composed of the elements Ru, Rh, Mo, Pd and Tc but small amounts of Fe and Ni were also present. U was detected in one particle[19]. Ru particles were sometimes attached to a large inactive particle[23–25]; these carriers may influence particle transport.

Particle sizes were detected using SEM[15,22,24], which in addition to activity analysis, make it possible to estimate the activities of various nuclides per unit volume of the particle (Bq.μm^{-3}). These volumetric activities enable the sizes of particles to be estimated using gamma ray analysis only. Kerekes *et al*[22] estimated that the activity of ^{103}Ru per unit volume is 50 Bq.μm^{-3}. The results of Schubert and Behrend[15] give equal or higher values. Likhtariov *et al*[5] reported a value of 10 Bq.μm^{-3}, which is considerably lower than the values obtained in other estimates.

Ru particles were often round edged and spherical in shape. Kerekes *et al.*[22] calculated the density of the particles from their aerodynamic diameter, in which the average value (two particles) was 10.5 g.cm^{-3}. Bramman *et al*[37] reported that metallic inclusions are typically 5–10 μm, but rarely exceed 20 μm in diameter; carrier-free Ru particles found in Western Europe were within these limits[2]. Kashparov *et al*[14] reported that, in addition to small (<10 μm) spherical particles, irregularly shaped large (20–250 μm) Ru particles were detected near the plant. Khitrov *et al*[38] found a particle (presumably an Ru particle) with activity of 660 kBq (^{106}Ru) and mass 0.5 μg. The diameter of this particle is 45 μm, assuming that the density is 10.5 g.cm^{-3} (the same result is achieved using the activity ratio ^{103}Ru:^{106}Ru = 5 and the volumetric activity 100 Bq.μm^{-3}, see later text).

ESTIMATION OF PARTICLE ACTIVITY

The activity, composition and size of Ru particles as well as their abundance in various media (air, food, ground etc.) must be known in order to estimate their potential health effects and risks. Unfortunately, at the time of the Chernobyl accident particle sampling and detection were not necessarily representative and the analytical methods were not necessarily adequate for estimating all relevant properties of the particles. Gamma spectrometric analyses alone do not give sufficient information on the elemental composition. Thus, dose calculations cannot be fully performed using the information gathered merely from particles detected in the environment. Since the characteristics of irradiated nuclear fuel and the behaviour of Ru and other elements within it essentially influence the properties of Ru particles, an approach based on inventory calculations is used.

The presence of radioactive material in a particle determines the radiological risks. In addition to gamma spectrometric analyses, the elemental composition of Ru particles found in the environment suggests that additional radionuclides must be also taken into account in the dose estimations. The isotopes ^{103}Ru and ^{106}Ru with varying activity ratios were detected in all particles that were analysed within about one year of the accident. The short-lived isotopes ^{105}Ru, ^{105}Rh and ^{109}Pd may also contribute to the short-term risk; however, they were not detected because the activity analyses were performed too late. Measurements done within one month of the accident showed the presence of ^{99}Mo[21,23]. The low-volatile isotopes ^{131}I and ^{137}Cs as well as ^{60}Co and ^{125}Sb were frequently observed, but their activities were low. The beta-emitting nuclides considered in the following calculations are presented in Table 2; nuclides with half-life less than a few hours or with low (specific) activity are neglected.

Inventory calculations

The amount of (radioactive) materials in a reactor core, known as the 'inventory', is calculated using the ORIGEN2[41] computer code. The code computes numerically the time-dependent concentrations of a large number of nuclides and elements that are generated or depleted simultaneously through neutron-induced transmutation, radioactive decay and nuclear fission. Since the inventory depends on the design and operational history of the reactor and different physical processes (mainly nuclear fission and decay) occurring during operation, a set of ORIGEN2 calculations for the Chernobyl reactor (fuel mass 219 tUO_2, constant specific power 14.6 MW.tUO_2^{-1}, fuel enrichment 1.8%, reactor model CANDUSEU) was performed as a function of fuel burnup and decay time. Fuel outages were neglected in the calculations, i.e. the detailed operational history of Chernobyl nuclear power plant Unit IV was not used. Results of the ORIGEN2 calculations, i.e. concentrations of nuclides and elements in reactor fuel, are stored in a database that is used in estimating the characteristics of irradiated fuel and particles. A database management system was developed to reprocess the data[42].

The activity concentration of radionuclides (Figure 1) and mass concentration of elements (Figure 2) in the RBMK reactor fuel are of special concern in estimating the amount of radioactive materials in an Ru particle. Note that the activity concentration of short-lived

nuclides, especially, is determined mainly by the prevailing fission power level before the reactor shutdown/accident. Since the specific power used in the present calculations is assumed to be constant during irradiation (detailed operational history is not used), the concentrations calculated here are more indicative than the true estimates of the amount of materials present in the Chernobyl reactor fuel.

Activity ratios can be used for estimating the properties of the material from which the nuclides were released. Fractionation of non-chemical origin can be studied using the activity ratios for pairs of isotopes of the same element. Activity ratio ^{103}Ru:^{106}Ru (Figure 3), for example, is used in estimating fuel burnup[19,20].

Activity per unit volume

Since the formation mechanisms and composition of Ru particles are ambiguous, detailed activities are calculated separately for particles composed of pure Ru (not RuO_4) and for particles containing those elements identified in metallic precipitates. For reasons of convenience both types of particles are assumed to have a density of 10500 $kg.m^{-3}$ which is the value obtained by Kerekes *et al*[22] (density of pure Ru is 12200 $kg.m^{-3}$). The activities are calculated for a unit volume of the material considered[43]. For homogeneous and spherical particles of different sizes the activity of nuclide N can be calculated from the equation

Table 1. Characteristics of analysed Ru particles detected in Finland, Sweden, Norway and Poland. Findings are presented in which activity analysis and size or elemental composition analyses were performed, or in which particles were analysed using a gamma ray spectrometer within one month of the Chernobyl accident. $A_{^{103}Ru}$ and $A_{^{106}Ru}$ are the activities of ^{103}Ru and ^{106}Ru, d_p is the equivalent volume diameter of the particle, $A_{vol,^{103}Ru}$ is activity of ^{103}Ru per unit volume.

Ref.	Location and time of activity analysis	Code	$A_{^{103}Ru}$ (Bq)	$A_{^{106}Ru}$ (Bq)	d_p (μm)	$A_{vol,^{103}Ru}$ (Bq.μm^{-3})	Elemental composition	Remarks
(19)	Soviet train carriage. (summer 1986)	S1	23,000	6400	—	—	Contains U	Site of deposition unknown.
(21)	Stockholm, Gävle.	HP-1	10,000	2800	—	—	—	^{51}Cr: 1.7 kBq, ^{99}Mo: 4 kBq, ^{131}I: 90Bq, ^{132}Te: 22 Bq.
	(beginning of May 1986)	HP-2	6900	1800	—	—	—	^{131}I: 100 Bq, ^{132}Te: 70 Bq.
		HP-6	24,300	7100	—	—	—	—
(22)	Stockholm, Gävle. (one year after the accident)	Haga1	17,400	4350	9.0	46	Mo, Tc, Ru[a]	^{125}Sb: 3.8 Bq, ^{60}Co: 1.7 Bq, ^{137}Cs: 0.4 Bq.
		Guan1	39,300	9830	11.5	49	Ru, Tc, Mo[a]	^{125}Sb: 26 Bq, ^{60}Co: 7 Bq, ^{144}Ce: 57 Bq.
		Guan2	31,800	9430	10.7	50	Ru[a]	^{125}Sb: 15 Bq, ^{60}Co: 3.1 Bq.
		Haga9	3600	830	3.9[b]	120[b]	Ru, Tc, Mo[a]	^{125}Sb: 1.3 Bq, ^{60}Co: 0.1 Bq.
		Gävle3	7900	1800	2.4[b]	1100[b]	Ru, Rh[a]	
(23)	Stockholm,	HP-4	7080	370	—	—	—	^{99}Mo: 3200 Bq. Minor amounts of ^{95}Zr/Nb, ^{131}I.
	Västervik. (17–20 May 1986)	HP-30	7550	1800	—	—	—	^{99}Mo: 330 Bq, ^{131}I: 50 Bq. Minor amounts of ^{95}Zr/Nb, ^{134}Cs, ^{134}Cs, ^{140}Ba, ^{141}Ce and ^{144}Ce.
(24)	Central Norway. (12 May 1988)	—	—	65	2	—	Ru, Mo, Tc	Spherical particle, agglomerated to a large and irregularly shaped inactive particle.
(15)	Masurian Lakes region	HS1	139,000	28,000	14	97	Ru, Tc, Mo, Fe, Rh, Ni, Pd	Metallic particles, only surface oxidation. Elements mentioned beside compose
	(autumn 1986)	HS2	4990	1050	—	—	—	92.3–98.3 weight % of total mass of the particles.
		HS3	28,100	4960	7–10[c]	160–54[c]	—	Gamma ray spectroscopic investigations revealed that ^{60}Co and ^{137}Cs were also present in the particles.
		HS4	23,200	4540	9–10[c]	61–44[c]	—	
		HS5	13,000	2790	6–7[c]	110–72[c]	Mo, Ru, Fe, Tc, Ni, Rh, Pd	
		HS7	34,400	5450	6[c]	300[c]	Ru, Tc, Rh, Mo, Pd, Fe, Ni	
		HS8	41,700	8730	—	—		
		HS9	32,100	7270	6[c]	280[c]	Ru, Rh, Pd, Ni, Fe, Mo	

[a]Other metals such as Fe and Ni was observed in most cases.
[b]Uncertain size estimation.
[c]Sizes are estimated in this study from SEM pictures.

Table 2. Nuclides considered in the present study. $t_{1/2}$ is the half-life. The maximum energy of the beta particles, E_{max}, refers to the most probable decay branch. The distance in water at which 90% of the beta energy is absorbed is denoted as X_{90}. D is the beta dose rate from a 1 Bq point source at the air-water boundary[39] averaged over 1 cm² at the basal cell layer of the skin (nominal depth 70 μm). Values denoted by * are calculated here using SADDE Mod2 and VARSKIN Mod2[40].

Nuclide	$t_{1/2}$	E_{max} (MeV)	X_{90} (mm)	$\dot{D}$ (μGy.h^{-1}.Bq^{-1})
^{99}Mo	66.0 h	1.21	2.23	1.54
^{103}Ru	39.4 d	0.226	0.267	0.568
^{105}Ru	4.44 h	1.19	2.08*	1.63*
^{105}Rh	35.4 h	0.567	0.731*	1.17
^{106}Ru	368 d	0.0394	0.00764	–
^{106}Rh	30 s	3.54	7.92	1.85
^{109}Pd	13.5 h	1.03	1.78*	1.55*

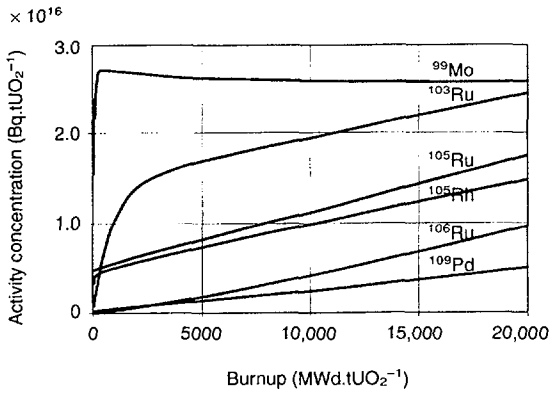

Figure 1. Activity concentration (Bq per tonne of UO_2 fuel) of ^{99}Mo, ^{103}Ru, ^{105}Ru, ^{105}Rh, ^{106}Ru and ^{109}Pd in RBMK fuel as a function of fuel burnup.

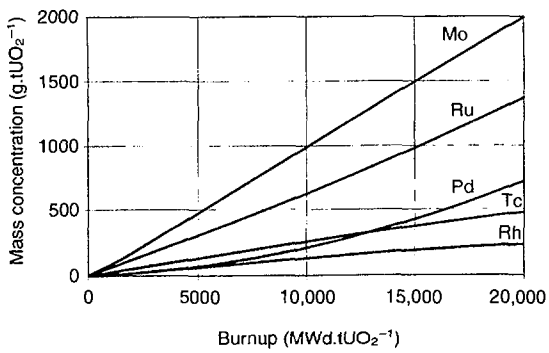

Figure 2. Mass concentration (g per tonne of UO_2 fuel) of Mo, Ru, Pd, Tc and Rh in RBMK fuel as a function of fuel burnup.

$$A_N(d_p) = \frac{\pi}{6} d_p^3 A_{vol,N} \quad (1)$$

where d_p (μm) is the equivalent volume diameter and $A_{vol,N}$ (Bq.μm^{-3}) the activity per unit volume.

Particles composed of pure Ru

Here it is assumed that, at the time of particle formation, the particle is composed of different isotopes of Ru (stable isotopes included); other elements are not present. After the formation, the nuclides ^{105}Rh and ^{106}Rh are generated through decay of their parent nuclides ^{105}Ru and ^{106}Ru.

Hofmann *et al*[6] calculated radiation doses and the lung cancer risk from a Ru particle of 1 μm diameter, composed entirely of ^{103}Ru (300 Bq). The activity per unit volume for such a particle is 570 Bq.μm^{-3}, whereas Devell[21] estimated 200 Bq.μm^{-3}. The volumetric activity of ^{103}Ru obtained in the present study is between these values, provided that fuel burnup is larger than 5000 MWd.tUO$_2^{-1}$ (Figure 4). In general, the calculated activities per unit volume are higher by a factor of about 2–4 than in the Ru particles found after the Chernobyl accident (Table 1). Other materials (short-lived nuclides, stable materials or those with low specific activity) must be present in the Chernobyl particles.

Particles composed of elements identified in precipitates

The elemental composition of Ru particles from Chernobyl has been published quantitatively by Schubert and Behrend[15]. For particles HS1, HS5, HS7 and HS9 (see Table 1 and original paper) the mass concentration ratios Ru:Mo and Ru:Pd were larger by a factor of two or more than those presented in Figure 3, i.e. Mo and Pd were depleted with respect to Ru. The ratio Ru:Rh was similar to that of the fuel. Kerekes *et al*[22] found that Ru was a dominant element of the particles. Two particles were almost entirely composed of Ru,

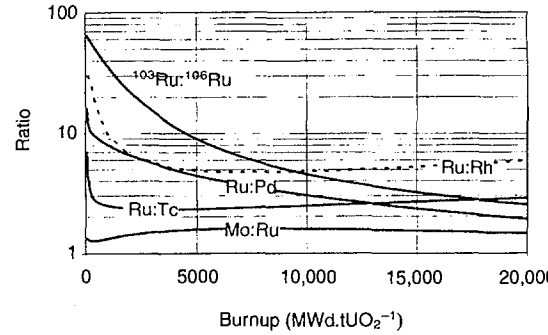

Figure 3. Activity ratio of the nuclides ^{103}Ru:^{106}Ru and mass concentration ratios of the elements Ru, Rh, Mo, Tc and Pd in RBMK fuel as a function of fuel burnup.

whereas one particle contained mainly Mo and Tc. In general, however, the studies showed that the proportions of different elements varied greatly.

The composition of metallic precipitates depends on the temperature and oxygen potential of the fuel[44]. Here, 'Ru' particles are assumed to be homogeneous and composed of the elements Ru, Rh, Mo, Pd and Tc with the same relative amounts as are formed during irradiation[45]; Fe and Ni are not considered in the calculations. The calculated activities per unit volume as a function of fuel burnup are shown in Figure 5, in which the volumetric activity of ^{103}Ru is now similar to that observed in Chernobyl particles (Table 1). Note that Pöllänen *et al*[2] used 100 Bq.μm^{-3} (^{103}Ru + ^{106}Ru) in their estimation of Ru particle size.

The most active Ru particles detected in Poland (308 kBq)[25] and Greece (43 kBq)[7] showed high ^{103}Ru:^{106}Ru activity ratios (12.3 and 37.9, respectively), and had probably originated from low burnup fuel (4000 and 1000 MWd.tUO$_2^{-1}$, respectively, see Figure 3).

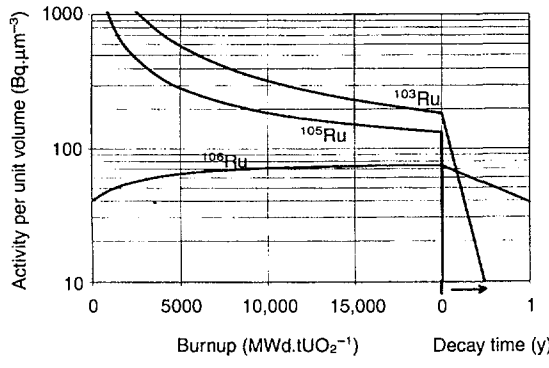

Figure 4. Activity of ^{103}Ru, ^{105}Ru and ^{106}Ru per unit volume of pure Ru as a function of fuel burnup. As an example, activities per unit volume as a function of decay time are presented for pure Ru originating from fuel irradiated to a burnup of 20,000 MWd.tUO$_2^{-1}$ (refers to average burnup of exhausted fuel).

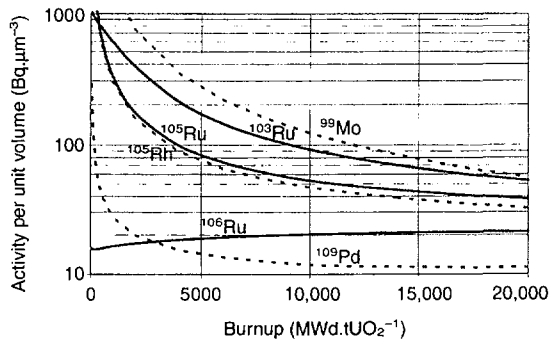

Figure 5. Activities of ^{99}Mo, ^{103}Ru, ^{105}Ru, ^{105}Rh, ^{106}Ru and ^{109}Pd per unit volume of a metallic precipitate, composed entirely of Ru, Rh, Tc, Mo and Pd, as a function of fuel burnup.

They may be smaller than previously estimated[2] owing to the large volumetric activity.

RUTHENIUM PARTICLES DEPOSITED ON THE SKIN

In a severe nuclear accident the radiological hazard caused by Ru particles refers to their high specific activity; relatively small but very active particles may be transported hundreds of kilometres in the air before deposition. The largest Ru particles, however, are not of inhalable size, and when deposited on the skin, they are able to produce high non-uniform beta doses in a short time. In the present study skin doses are calculated for Ru particles of two different compositions taking into account the effects of fuel burnup, decay time and particle size. Individual particles are considered here, not skin contamination (Bq.cm^{-2}).

Skin dose model

Skin beta doses are calculated using a semi-analytical PSS model[46] based on point source dose conversion factors[39] corrected by self-shielding of beta particles in a homogeneous and spherical particle. In the present study, the doses are calculated for the basal cell layer of the skin (nominal depth 70 μm, circular target area) although any depth and any target area is possible provided that appropriate point source conversion factors are available.

Let an Ru particle contain m beta emitters that, in turn, may have n decay branches with branching probability β_i. The total skin beta dose rate (Gy.h^{-1}) averaged over 1 cm^2 at skin depth h, can be formally written as

$$\dot{D} = \sum_{N=1}^{m} A_N(d_p)\, CF_N(h) \sum_{i=1}^{n} \beta_{N,i}\, SAF_{N,i}(d_p,(\mu_\rho/\rho_p)_i) \qquad (2)$$

where

$A_N(d_p)$ = the activity of nuclide N in a particle of diameter d_p,

$CF_N(h)$ = the point source conversion factor for nuclide N at skin depth h,

$SAF_{N,i}(d_p,(\mu_\rho/\rho_p)_i)$ = the self-absorption factor of nuclide N (branch i) in a particle of diameter d_p and mass attenuation coefficient μ_ρ/ρ_p.

The self-absorption factor is a fraction of the initial beta flux that reaches the surface of the particle. The mass attenuation coefficient is a function of the maximum beta energy of each branch and effective atomic number of the particle. Beta absorption is especially important for low energy beta emitters (Figure 6); if particle diameter is smaller than a few μm the point source conversion factors can be applied without correction for self-shielding.

Beta dose to the skin

The beta dose caused by a homogeneous, spherical, radioactive particle deposited on the skin is mainly determined by particle size, since $A_N \propto d_p^3$; particle composition may also contribute (Figure 7). Ru particles originating from low burnup fuel may produce as much as 10 times higher skin doses than those originating from high burnup fuel. The short-lived nuclides ^{105}Ru and ^{109}Pd affect skin doses mainly within 1 d of the reactor shutdown (^{105}Rh within a few days). ^{99}Mo has a notable impact for decay times less than one week, especially in precipitates originating from low-burnup fuel (see also Figure 5). When the decay time is several weeks the beta dose rate caused by a pure Ru particle is about three times larger than that produced by a metallic precipitate, because the activities per unit volume of ^{103}Ru and ^{106}Ru in pure Ru are three times higher than those in Ru precipitates (Figures 4 and 5).

The significance of various compositions and the effects of short-lived nuclides are demonstrated for four Ru particles found in Poland by Schubert and Behrend[15] (see Table 1 and original paper). The activities and beta doses are calculated by assuming that the decay time is 1 d (Table 3). Burnup of the fuel from which particles had originated is estimated using the activity ratio ^{103}Ru:^{106}Ru (see Figure 3). Burnup-dependent specific activity, calculated for each nuclide in a specified element (e.g. activity of ^{99}Mo in mass unit of Mo), multiplied by mass of the element considered (see Table 2 in original paper) gives the activity of short-lived nuclides. Without their contribution, skin dose rates are underestimated by a factor of 1.5–2.5.

To avoid deterministic effects on the basal cell layer of the skin (nominal depth 70 μm) ICRP recommends that the annual equivalent dose limit for the public is 50 mSv, averaged over any 1 cm^2 and regardless of the area exposed[9]. Highly radioactive Ru particles detected in northeastern Poland, 500–650 km from Chernobyl, were from the explosion phase of the accident. Particles were deposited on the ground within about two days. Table 3 shows that in Poland there was a risk that the ICRP annual skin dose limit for the public may be exceeded in even a few tens of minutes.

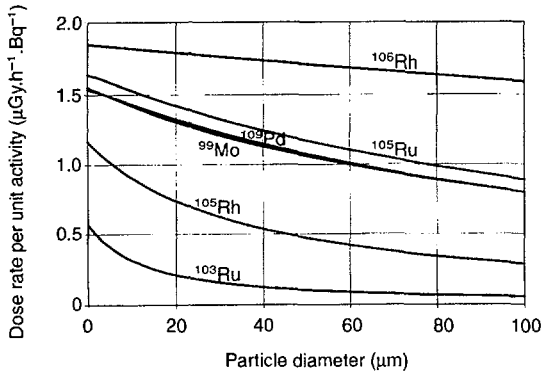

Figure 6. Basal cell dose rate (nominal depth 70 μm, averaged over 1 cm^2) per unit activity for different nuclides as a function of Ru particle diameter. The density of the particle is 10,500 kg.m^{-3} and effective atomic number 44. The nuclide-specific dose rates for a point source (for a particle of 0 μm in diameter) are those presented in Table 2.

The activity ratio ^{103}Ru:^{106}Ru of Ru particles found in Europe was generally between 4 and 5, i.e. they had originated from fuel irradiated at near average burnup. Pöllänen *et al*[2] calculated the skin dose rates for Ru particles of different sizes by taking into account only the long-lived ^{103}Ru and ^{106}Ru. Dose rates may be considerably higher if short-lived nuclides in an Ru precipitate are considered (Table 4). The activities and dose rates in Table 4 refer to decay times of 1 d and 10 d. Particles of different sizes are assumed to preserve the proportions of Ru, Rh, Mo, Pd and Tc and to reflect the properties of fuel irradiated to average burnup (Figure 5, burnup 10000 MWd.tUO$_2^{-1}$). At a decay time of 1 d a large part of the total dose rate is generated by short-lived nuclides, of which ^{99}Mo is responsible for about 50%; at a decay time of 10 d their contribution is negligible.

Particles in Table 4 are assumed to be deposited on the skin 1 d and 10 d after their formation and release. For emergency preparedness purposes it is useful to estimate the particle residence time needed to receive a certain skin dose. For example, Ru precipitates larger than 8 μm in diameter (decay time 1 d) may deliver a dose of 50 mSv to the basal cell layer of the skin in less than one hour. The activities of ^{103}Ru and ^{106}Ru would then be 24,000 Bq and 5400 Bq, respectively. In Sweden, more than 1000 km from Chernobyl, Ru particles with

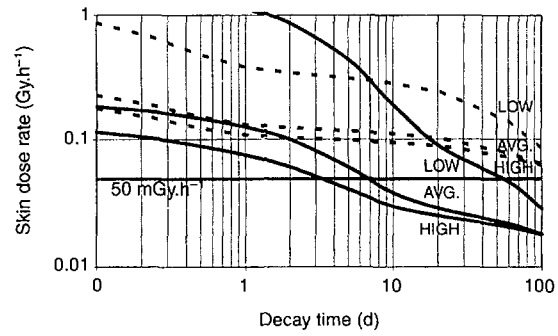

Figure 7. The beta dose rate to the basal cell layer (averaged over 1 cm^2 at a nominal depth of 70 μm) as a function of decay time caused by an Ru particle 10 μm in diameter deposited on the skin. Two sets of the curves represent pure Ru particles (dashed line) and particles similar in composition to metallic precipitates (solid line). The centremost curve of each set refers to fuel of the average burnup (10,000 MWd.tUO$_2^{-1}$,'AVG.') from which the particles are assumed to have originated. The upper and lower curves are for the particles emitted from low burnup fuel (1000 MWd.tUO$_2^{-1}$; 'LOW') and high burnup fuel (20,000 MWd.tUO$_2^{-1}$; 'HIGH'), respectively. The horizontal line represents a dose rate of 50 mGy.h^{-1}.

higher activities were found[21,22]. In Finland, about 1500 km from Chernobyl, Ru particles of this size were not detected (perhaps due to sparse sampling). Uranium fuel particles of equal size were, however, found[19,20].

CONCLUSIONS

Although Ru particles were detected only after the Chernobyl accident there is a possibility that they might also be released in severe nuclear accidents in other types of nuclear reactor. Highly radioactive Ru particles are of special radiological importance, since they may produce acute health damage that must be taken into account in radiation protection and emergency preparedness. The current time-consuming, tedious and sometimes inadequate procedures of particle sampling, isolation and analyses, however, do not necessarily allow us to make prompt on-line dose estimations. Doses can be estimated without knowledge of particle size by assuming a certain elemental composition (e.g. either a pure Ru particle or metallic precipitate) and by performing gamma ray analysis of long-lived ^{103}Ru and ^{106}Ru. Particle size and the proportion of nuclides that are not (or cannot be) detected can then be calculated. In the present study it is shown that:

(1) Inventory calculations are necessary for estimating the properties of nuclear fuel particles and their radiological risks.
(2) The activities per unit volume of Ru particles, composed almost entirely of fission products, are higher than those of particles composed mainly of bulk U or other low activity materials.
(3) The volumetric activities of Ru particles emitted from low burnup fuel may be considerably higher than those emitted from high burnup fuel. Thus, radiological risks are not necessarily the greatest for particles originating from high burnup fuel.

Table 3. Calculated activities of the short-lived nuclides ^{99}Mo, ^{105}Ru, ^{105}Rh and ^{109}Pd (decay time 1 d) in four Polish particles[15] of known elemental composition (see Table 1). The last two columns indicate the beta dose rate to the basal cell layer (nominal depth 70 μm, averaged over 1 cm^2) if particles had been deposited on the skin. Only ^{103}Ru and ^{106}Ru/^{106}Rh are taken into account in the column on the left whereas the column on the right also contains short-lived nuclides. The density of the particles is assumed to be 10500 kg.m^{-3}.

Particle code	Activity (Bq)						Skin dose rate (mGy.h^{-1})	
	^{103}Ru	^{106}Ru	^{99}Mo	^{105}Ru	^{105}Rh	^{109}Pd	^{103}Ru+^{106}Ru	All
HS1	137,000	27,900	32,000	1900	68,000	2100	86	190
HS5	12,800	2790	7800	180	3700	90	10	25
HS7	33,800	5440	2000	430	8200	110	23	35
HS9	31,500	7260	6.9	440	11,000	180	25	37

Table 4. Activities and the beta dose rate to the basal cell layer of the skin as a function of Ru particle diameter for two decay times. The time required to receive a skin dose of 50 mSv is denoted as t_{50mSv} (radioactive decay is taken into account). Doses are averaged over 1 cm^2 at a skin depth of 70 μm. Relatively low activity nuclides (such as ^{105}Ru and ^{109}Pd) are not shown in the table, although they are taken into account in the calculation of dose rate and residence time.

d_p (μm)	Time of deposition on the skin 1 d						Time of deposition on the skin 10 d				
	$A_{^{99}Mo}$ (Bq)	$A_{^{103}Ru}$ (Bq)	$A_{^{105}Rh}$ (Bq)	$A_{^{106}Ru}$ (Bq)	$\dot{D}$ (mGy.h^{-1})	t_{50mSv}	$A_{^{99}Mo}$ (Bq)	$A_{^{103}Ru}$ (Bq)	$A_{^{106}Ru}$ (Bq)	$\dot{D}$ (mGy.h^{-1})	t_{50mSv}
1	50	48	18	11	0.15	1200 h	5.2	41	10	0.049	1500 h
2	400	380	140	85	1.2	47 h	42	330	83	0.38	150 h
3	1400	1300	480	280	3.8	13 h	140	1100	280	1.2	42 h
4	3200	3000	1100	680	8.8	5.7 h	330	2600	660	2.9	18 h
5	6300	6000	2200	1300	17	3.0 h	650	5100	1300	5.4	9.3 h
6	11,000	10,000	3900	2300	29	1.8 h	1100	8800	2200	9.1	5.6 h
7	17,000	16,000	6100	3600	45	1.1 h	1800	14,000	3600	14	3.6 h
8	26,000	24,000	9100	5400	66	45 min	2700	21,000	5300	21	2.4 h
9	37,000	35,000	13,000	7700	93	32 min	3800	30,000	7600	29	1.7 h
10	50,000	48,000	18,000	11,000	130	24 min	5200	41,000	10,000	39	1.3 h
15	170,000	160,000	60,000	36,000	390	7.6 min	18,000	140,000	35,000	120	25 min
20	400,000	380,000	140,000	84,000	890	3.4 min	42,000	330,000	83,000	270	11 min

(4) Inventory calculations support the assumption that highly radioactive Ru particles observed in Western Europe after the Chernobyl accident were metallic precipitates.

(5) The composition of particles has an essential influence on the radiological hazard. The presence of short-lived nuclides in particles emitted from low burnup fuel in particular contributes notably to skin dose rates.

(6) Even an individual particle may be a radiological hazard. A dose of 50 mSv for the basal cell layer (nominal depth of 70 μm, averaged over 1 cm^2) may be exceeded in one hour provided that an Ru particle larger than 8 μm in diameter is deposited on the skin. In the Chernobyl accident particles of this size were transported more than 1000 km from the plant.

REFERENCES

1. Sandalls, F. J., Segal, M. G. and Victorova, N. *Hot Particles from Chernobyl: A Review.* J Environ. Radioact. **18**, 5–22 (1993).
2. Pöllänen, R., Valkama, I. and Toivonen, H. *Transport of Radioactive Particles from the Chernobyl Accident.* Submitted for publication.
3. Pöllänen, R. and Toivonen, H. *Skin Doses from Large Uranium Fuel Particles: Application to the Chernobyl Accident.* Radiat. Prot. Dosim. **54**, 127–132 (1994).
4. Pöllänen, R. and Toivonen, H. *Transport of Large Uranium Fuel Particles Released from a Nuclear Power Plant in a Severe Accident.* J. Radiol. Prot. **14**, 55–65 (1994).
5. Likhtariov, I. A., Repin, V. S., Bondarenko, O. A. and Nechaev, S. Ju. *Radiological Effects after Inhalation of Highly Radioactive Fuel Particles Produced by the Chernobyl Accident.* Radiat. Prot. Dosim. **59**, 247–254 (1995).
6. Hofmann, W., Crawford-Brown, D. J. and Martonen. T. B. *The Radiological Significance of Beta Emitting Hot Particles Released from the Chernobyl Nuclear Power Plant.* Radiat. Prot. Dosim. **22**, 149–157 (1988).
7. Kritidis, P., Catsaros, N. and Probonas, M. *Hot Particles in Greece after the Chernobyl Accident, Estimations on Inhalation Probability.* In: Hot Particles from the Chernobyl Fallout. Eds H. Von Philipsborn and F. Steinhäusler. Proc. Int. Workshop, Theuern, 28/29 October 1987. Schriftenreihe des Bergbau- und Industriemuseums Ostbauern Theuern, BAND **16**, 115–120 (1988).
8. Lindner, G., Wilhelm, Ch., Kaminski, S., Schell, B., Wunderer, M. and Wahl, U. *Inhalation of Nonvolatile Radionuclides after the Chernobyl Accident — a Retrospective Approach.* In: Proc. Eight Int. Congress of the International Radiation Protection Association, 17–22 May 1992, Montreal, Canada, pp. 261–264 (1992).
9. International Commission on Radiological Protection. *1990 Recommendations of the International Commission on Radiological Protection.* ICRP Publication 60. Ann. ICRP **21**(1–3) (Oxford: Pergamon Press) (1990).
10. Powers, D. A., Kress, T. S. and Jankowski, M. W. *The Chernobyl Source Term.* Nucl. Safety **28**, 19–20 (1987).
11. Broda, R., Mietelski, J. W. and Sieniawski. J. *Radioactive ^{125}Sb and ^{60}Co in "Ruthenium" Hot Particles from Chernobyl Fallout.* J. Radioanal. Nucl. Chem. Lett. **166**, 173–180 (1992).
12. Ronneau, C., Cara, J. and Rimski-Korsakov, A. *Oxidation-Enhanced Emission of Ruthenium from Nuclear Fuel.* J. Environ. Radioact. **26**, 63–70 (1995).
13. Osuch, S., Dąbrowska, M., Jaracz, P., Kaczanowski, J., Le Van Khoi, Mirowski, S., Piasecki, E., Szeflińska, G., Szefliński, Z., Tropiło, J., Wilhelmi, Z., Jastrzębski, J. and Pieńkowski, L. *Isotopic Composition of High-Activity Particles Released in the Chernobyl Accident.* Health Phys. **57**, 707–716 (1989).
14. Kashparov, V. A., Ivanov, Y. A., Zvarisch, S. I., Protsak, V. P., Khomutinin, Y. V., Kurepin, A. D. and Pazukhin, E. M. *Formation of Hot Particles During the Chernobyl Nuclear Power Plant Accident.* Nucl. Technol. **114**, 246–253 (1996).
15. Schubert, P. and Behrend, U. *Investigations of Radioactive Particles from the Chernobyl Fall-out.* Radiochim. Acta **41**, 149–155 (1987).
16. Jaracz, P., Piasecki, E., Mirowski, S. and Wilhelmi, Z. *Analysis of Gamma-Radioactivity of "Hot Particles" Released after the Chernobyl Accident, II. An Interpretation.* J. Radioanal. Nucl. Chem. **141**, 243–259 (1990).
17. Arvela, H., Markkanen, M. and Lemmelä, H. *Mobile Survey of Environmental Gamma Radiation and Fall-out Levels in Finland after the Chernobyl Accident.* Radiat. Prot. Dosim. **32**, 177–184 (1990).
18. Mietelski, J. W. and Wąs, B. *Plutonium from Chernobyl in Poland.* In: Proc. Int. Symp. on Pu in the Environment, Ottawa, 6–8 July 1994 (1994).
19. Rytömaa, T., Toivonen, H., Servomaa, K., Sinkko, K. and Kaituri, M. *Uranium Aerosols in Chernobyl Fall-out.* Finnish Centre for Radiation and Nuclear Safety, Helsinki, internal report (1986).
20. Saari, H., Luokkanen, S, Kulmala, M., Lehtinen, S. and Raunemaa, T. *Isolation and Characterization of Hot Particles from Chernobyl Fallout in Southwestern Finland.* Health Phys. **57**, 975–984 (1989).
21. Devell, L. *Nuclide Composition of Chernobyl Hot Particles.* In: Hot Particles from the Chernobyl Fallout. Eds H. Von Philipsborn and F. Steinhäusler. Proc. Int. Workshop, Theuern 28/29 October 1987. Schriftenreihe des Bergbau- und Industriemuseums Ostbauern Theuern, BAND **16**, 23–34 (1988).
22. Kerekes, A., Falk, R. and Suomela, J. *Analysis of Hot Particles Collected in Sweden after the Chernobyl Accident.* Statens strålskyddsinstitut, SSI-rapport 91-02 (1991).

23. Robertson, D. E. Letter to the National Institute of Radiation Protection, Stockholm, Sweden, (November 1986).
24. Salbu, B. *Radionuclides Associated with Colloids and Particles in the Chernobyl Accident.* In: Proc. Joint OECD (NEA)/CEC Workshop on Recent Advances in Reactor Accident Consequences Assessments, Rome, 1988. CSNI Report 145, Vol. **1**, pp. 53–67 (1989).
25. Broda, R. *Gamma Spectroscopy Analysis of Hot Particles from the Chernobyl Fallout.* Acta Phys. Pol. **B18**, 935–950 (1987).
26. van der Wijk, A., de Meijer, R. J., Jansen, J. F. W. and Boom, G. *Core Fragments and Ruthenium Particles in the Chernobyl Fallout.* In: Hot Particles from the Chernobyl Fallout. Eds H. Von Philipsborn and F. Steinhäusler, Proc. Int. Workshop, Theuern, 28/29 October 1987. Schriftenreihe des Bergbau- und Industriemuseums Ostbauern Theuern, BAND **16**, 53–61 (1988).
27. Behrens, H. *Hot Particles Found in the Area of Munich.* In: Hot Particles from the Chernobyl Fallout. Eds H. Von Philipsborn and F. Steinhäusler. Proc. Int. Workshop, Theuern, 28/29 October 1987. Schriftenreihe des Bergbau- und Industriemuseums Ostbauern Theuern, BAND **16**, 35–38 (1988).
28. Wahl, U. Lindner, G. and Recknagel, E. *Radioaktive Partikel im Tschernobyl-Fallout.* In: Die Wirkung niedriger Strahlendosen — biologische und medizinische Aspekte. Eds W. Köhnlein, H. Traut and N. Fischer (Berlin-Heidelberg: Springer) pp. 165–176 (1989).
29. Burkart, W. *Dose and Health Implications from Particulate Radioactivity (Hot Particles) in the Environment.* In: Hot Particles from the Chernobyl Fallout. Eds H. Von Philipsborn and F. Steinhäusler. Proc. Int. Workshop, Theuern, 28/29 October 1987. Schriftenreihe des Bergbau- und Industriemuseums Ostbauern Theuern, BAND **16**, 121–129 (1988).
30. Balásházy, I., Fehér, I., Szabadyné-Szende, G., Lörinc, M., Zombori, P. and Pogány, L. *Examination of Hot Particles Collected in Budapest following the Chernobyl Accident.* Radiat. Prot. Dosim. **22**, 263–267 (1988).
31. Antonov, A., Belokonski, I. Bonchev, T., Bosevski, V., Gorinov, I., Hristova, A., Kamenova, T., Kostadinov, K., Mavrudiev, V., Mandzhukova, B., Mandzhukov, I., Minev, L., Radev, S., Semova, T., Tsankov, L., Uzunov, P., Vapirev, E. and Yanev, Y. *Studies on Micro-uniformity of the Radioactive Contaminations, Hot Particles and Homogeneous Radioactivity.* In: Hot Particles from the Chernobyl Fallout. Eds H. Von Philipsborn and F. Steinhäusler. Proc. Int. Workshop, Theuern, 28/29 October 1987. Schriftenreihe des Bergbau- und Industriemuseums Ostbauern Theuern, BAND **16**, 131–140 (1988).
32. Misaelides, P., Sikalidis, C., Tsitouridou, R. and Alexiades, C. *Distribution of Fission Products in Dust Samples from the Region of Thessalonici, Greece, after the Chernobyl Nuclear Accident.* Environ. Pollut. **47**, 1–8 (1987).
33. Lujanas, V., Mastauskas, A., Lujaniene, G. and Spirkauskaite, N. *Development of Radiation in Lithaunia.* J. Environ. Radioact. **23**, 249–263 (1994).
34. Petryaev, E. P., Sokolik, G. A., Ovsyannikova, S. V., Leynova, S. L. and Ivanova, T. G. *Forms of Occurrence and Migration of Radionuclides from the Chernobyl NPP Accident in Typical Landscapes of Byelorussia.* In: Proc. Seminar on Comparative Assessment of the Environmental Impact of Radionuclides Released during Three Major Nuclear Accidents: Kyshtym, Windscale, Chernobyl. Luxembourg, 1–5 October 1990, pp. 185–209 (1990).
35. Demchuk, V. V., Voytsekhovich, O. V., Kashparov, V. A., Viktorova, N. V. and Laptev, G. V. *Analysis of Chernobyl Fuel Particles and Their Migration Characteristics in Water and Soil.* In: Proc. Seminar on Comparative Assessment of the Environmental Impact of Radionuclides Released during Three Major Nuclear Accidents: Kyshtym, Windscale, Chernobyl. Luxembourg, 1–5 October 1990, pp. 493–514 (1990).
36. Jaracz, P., Mirowski, S., Piasecki, E. and Wilhelmi, Z. *New Data on Hot Particles from the Chernobyl Accident (Measurements and Comparative Studies).* In: Proc. Int. Symp. on Radioecology: Chemical Speciation – Hot Particle, Znojmo, Czech Republic, 12–16 Oct. 1992 (1992).
37. Bramman, J. I., Sharpe, R. M., Thom, D. and Yates, G. *Metallic Fission-Product Inclusions in Irradiated Oxide Fuels. J. Nucl. Mat.* **25**, 201–215 (1968).
38. Khitrov, L. M., Cherkezyan, V. O. and Rumyantsev, O. V. *Hot Particles after the Chernobyl Accident.* Geochem. Int. **31**, 46–55 (1994).
39. Cross, W. G., Freedman, N. O. and Wong, P. Y. *Beta Ray Dose Distributions from Skin Contamination.* Radiat. Prot. Dosim. **40**(3), 149–168 (1992).
40. Durham, J. S. *VARSKIN MOD2 and SADDE MOD2: Computer Codes for Assessing Skin Dose from Skin Contamination* (Richland, WA: Battelle Pacific Northwest Laboratories) NUREG/CR-5873 (PNL-7913) (1992).
41. Croff, A. C. *ORIGEN2: A Versatile Computer Code for Calculating the Nuclide Compositions and Characteristics of Nuclear Materials.* Nucl. Technol. **54**, 335–352 (1983).
42. Pöllänen, R., Toivonen, H., Lahtinen, J. and Ilander, T. *OTUS — Reactor Inventory Management System Based on ORIGEN2.* Finnish Centre for Radiation and Nuclear Safety, STUK-A126 (1995).
43. Pöllänen, R. and Toivonen, H. *Size Estimation of Radioactive Particles Released in the Chernobyl Accident.* In: Proc. Fourteenth Int. Conf. on Nucleation and Atmospheric Aerosols, pp. 670–673 (1996).
44. D'Annucci, F., Sari, C. and Schumacher, G. *Migration of Metallic Fission Products in Reactor Oxide Fuels.* Nucl. Technol. **35**, 80–86 (1977).
45. Jenkins, I. L. and Brown, P. E. *Characterization of Dissolution Residues — Fuel Element Cladding and Fission Product Insolubles.* Radiochim. Acta **36**, 25–30 (1984).
46. Pöllänen, R. and Toivonen, H. *Skin Dose Calculations for Uranium Fuel Particles Below 500 μm in Diameter.* Health Phys. **68**, 401–405 (1995).

VII

PÖLLÄNEN R, IKÄHEIMONEN T K, KLEMOLA S, JUHANOJA J.
Identification and analysis of a radioactive particle in a marine sediment sample.
Journal of Environmental Radioactivity 1999; 45: 149-160.

ELSEVIER

Journal of
Environmental Radioactivity 45 (1999) 149–160

JOURNAL OF
ENVIRONMENTAL
RADIOACTIVITY

Identification and analysis of a radioactive particle in a marine sediment sample

R. Pöllänen[a,*], T.K. Ikäheimonen[a], S. Klemola[a], J. Juhanoja[b]

[a]*STUK - Radiation and Nuclear Safety Authority, P.O. Box 14, 00881 Helsinki, Finland*
[b]*University of Helsinki, Institute of Biotechnology, P.O. Box 56, 00014 Helsinki, Finland*

Received 20 April 1997; received in revised form 15 July 1998; accepted 2 September 1998

Abstract

A radioactive particle was identified in a marine sediment sample. Characteristics of the particle were determined using various methods. Particle isolation and preliminary activity estimation were performed using gamma-ray spectrometry and autoradiography. Long-lived radionuclides were detected in the particle using alpha-, beta- and gamma-ray analyses. Particle size and elemental composition were determined using SEM. Elemental composition, nuclide composition and structure suggest that the particle may have originated from the Chernobyl accident. The present study shows that routinely used laboratory methods/procedures in environmental radiation detection are not necessarily appropriate for analyses of individual particles as they are (too much) focused on radiation monitoring and not on characterization of radioactive materials.

1. Introduction

The Chernobyl accident in April 1986 indicated that radioactive releases cannot be considered only as 'Becquerels' dispersed in air or other substances. Despite the fact that most of the released radioactive materials were in particulate form (Khitrov et al., 1994), the monitoring systems (procedures) in various European countries are designed to detect environmental radioactivity, not individual particles. The possibility that radioactive releases may be in particulate form must be considered in radiation protection and emergency preparedness, because even an individual highly radioactive particle may constitute a severe health hazard (Pöllänen & Toivonen, 1994; Pöllänen et al., 1997). This implies accurate knowledge of the particle characteristics.

*Corresponding author.

0265-931X/99/$ - see front matter
PII: S0265-931X(98)00099-X

In the present study a comprehensive analysis is performed for a radioactive 'hot' particle detected in a sediment sample. Since particle characteristics reflect properties of the material from which the particle originated, they can be used for estimating location of the release site, time of the release and possible formation and transport mechanisms of the particle. This information allows estimation of the significance of various physical and chemical processes that occurred during the particle formation and release and, in general, the role of particles for estimating their radiological risks in a nuclear accident.

2. Sampling and preliminary analysis

The Radiation and Nuclear Safety Authority (STUK) monitors radionuclides in the Baltic Sea on a regular basis by means of a permanent annual programme. The samples of seawater, bottom sediment, fish and other biota are collected at 20 locations. The sample considered here was collected on 22 May 1995, using a 'Gemini' sediment sampler (Ilus, 1996) at Station BY-15 (Ikäheimonen et al., 1997), which is located in the Gotland Deep (57°19.01'N, 20°01.96'E, depth 236 m).

The sediment sample was sectioned in 5 cm slices, dried and homogenized. Gamma-ray analysis of the uppermost 5 cm slice was performed according to standard procedures (Rantavaara et al., 1994). Low detection limits were obtained by using extended counting time (3900 min) and an efficient HPGe detector. Long-lived radionuclides, such as ^{125}Sb, ^{60}Co and ^{154}Eu, were observed in the sample (Table 1). These nuclides were detected in 'hot' particles released in the Chernobyl accident (e.g. Broda et al., 1992; Jaracz et al., 1995; Kuriny et al., 1993), thus suggesting that the activity concentration in the sample is inhomogeneous. This was verified by dividing the sample into two subsamples and analysing them separately. Am in addition to Eu were identified in only one of the samples; thus, radioactive material must be in only one to several particles. We attempted to isolate and analyse the characteristics of the(se) particle(s).

Table 1
Concentrations of artificial gamma-emitting nuclides in sediment sample IT020/96 (mass 14.4 g; Ikäheimonen et al., 1999). The uncertainty refers to statistical and calibration errors. The results are calculated to the sampling date (22 May 1995)

Nuclide	$t_{1/2}$ (a)	Activity (Bq kg^{-1} dry weight)	Uncertainty (%)
^{60}Co	5.3	1.8	12
^{125}Sb	2.8	14	8
^{134}Cs	2.1	5	7
^{137}Cs	30	218	3
^{154}Eu	8.6	5.0	10

3. Methods of analyses and results

3.1. Particle isolation

Isolation of radioactive particles was performed using autoradiography in which emulsion-coated autoradiography film was placed on the sediment sample which was distributed homogeneously on filter paper. Exposure for 30 days in a lightproof cassette revealed the presence of one large black spot (visual diameter a few mm) and small number of hardly visible spots; thus, 'radioactivity' was incorporated in small particles rather than being homogeneously distributed in the sample. The particle producing the largest spot was isolated from the sample, using consecutive autoradiograms, and was finally fixed on adhesive tape.

In addition to localization purposes, autoradiography can also be used for quantitative analyses (Pöllänen et al., 1996). The particle on the adhesive tape was placed in such an exposure geometry that beta dose rate coefficients for a water–water boundary (Cross et al., 1992) could be used. The detected size of the black spot compared with the calculated ('theoretical') value enabled estimation of the particle activity by a factor of 2–3 (Pöllänen et al., 1996). It was discovered that the nuclides present in Table 1 cannot produce the large black spot observed; thus, high-energy pure beta emitters, such as $^{90}Sr/^{90}Y$, must have been present in the particle, with an activity of the order of 1 Bq.

3.2. Gamma-ray analysis of the particle

The activities of gamma-emitting nuclides of the isolated particle were determined using a high-resolution Ge detector with relative efficiency of 40%. The spectra were analysed using the GAMMA computer code developed at STUK which accounts for the loss of counts due to true coincidence summing (Sinkko & Aaltonen, 1985). Because of ideal point-source geometry and low background, additional radionuclides were identified (Table 2). The nuclides ^{134}Cs, ^{137}Cs and ^{125}Sb were distributed in the sediment sample, whereas ^{241}Am and ^{154}Eu were in the particle only. ^{154}Eu is an activation product that is produced during normal operation of nuclear power plants (Jaracz et al., 1995; Kuriny et al., 1993).

Uncertainties in Tables 1 and 2 refer only to statistical and calibration (for homogeneously distributed sample) errors. Direct comparison of the results presented in Tables 1 and 2 is not possible, however, because the exact location of the particle in the sediment sample is not known (values presented in Table 1 are calculated by assuming a homogeneous sample). For reasons of geometry, the concentrations presented in Table 1 may deviate by a factor of about 2 for those nuclides identified only in the particle.

3.3. SEM microanalysis

Electron micrographs of the particle on the adhesive tape were taken with a scanning electron microscope (SEM; Zeiss DSM 962) using either secondary electrons or

Table 2
Activities of the gamma-emitting nuclides in the particle at the time of analysis. The activities (except ^{241}Am) are also back-calculated to the time of the Chernobyl accident (Chernobyl particle assumed). A total volume of 650 μm^3 was used for estimating activities per unit volume

Nuclide	$t_{1/2}$ (a)	Activity (October 1996) (Bq)	Uncertainty (%)	Activity (26 April 1986) (Bq)	Activity per unit volume (26 April 1986) (Bq μm^{-3})
^{60}Co	5.3	0.008	18	0.031	4.8×10^{-5}
^{125}Sb	2.8	0.014	23	0.200	3.1×10^{-4}
^{134}Cs	2.1	< 0.005	—	< 0.15	—
^{137}Cs	3.0	0.104	4	0.133	2.0×10^{-4}
^{144}Ce	0.78	0.015	40	140	0.22
^{154}Eu	8.6	0.045	7	0.105	1.6×10^{-4}
^{155}Eu	4.9	0.034	11	0.150	2.3×10^{-4}
^{241}Am	433	0.10	11	—	—

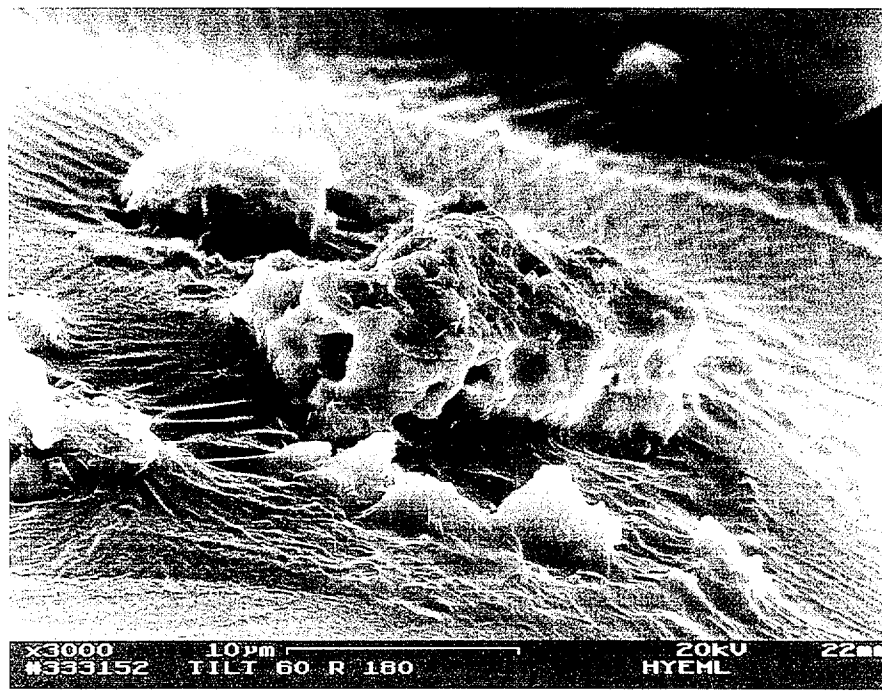

Fig. 1. Secondary electron image of the hot particle (tilted 60°). The irregularly shaped particle, surrounded by inactive sediment particles, is located in the middle. The background of the figure corresponds to the surface of the adhesive tape and glue. Scale bar = 10 µm.

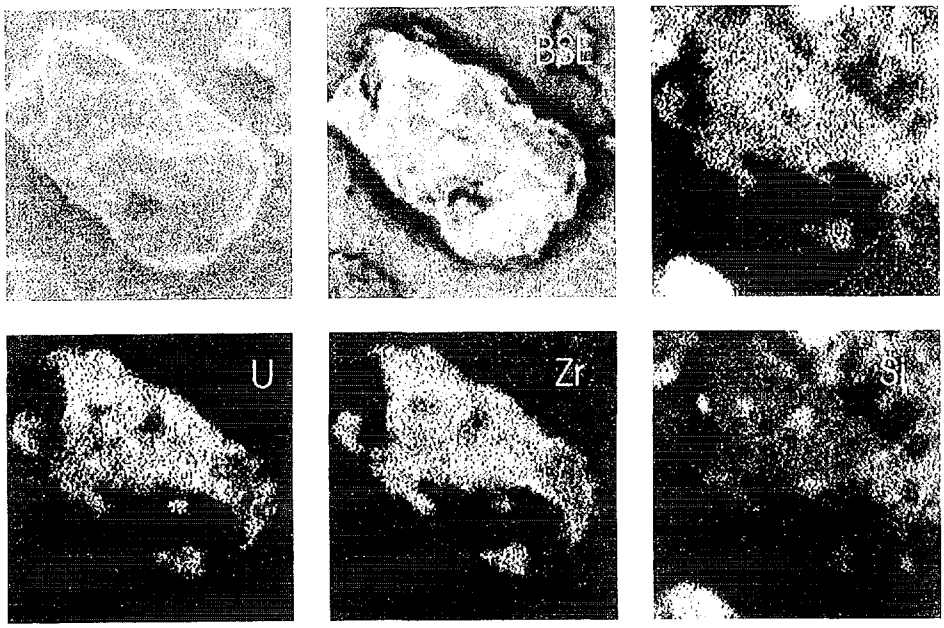

Fig. 2. Secondary electron (SE) and backscattered electron (BSE) images of the particle (no tilt) and X-ray maps for Al (K-line), U (M-line), Zr (L-line) and Si (K-line). Width of the images is 20 μm. Acceleration voltage was 10 keV.

backscattered electrons (Figs. 1 and 2). Micrographs were taken at various tilt angles to estimate particle volume. Since particle shape was irregular the volume could not be determined accurately but was estimated to be 550–750 μm^3 by assuming that the particle was nonporous.

X-ray spectra and X-ray maps were measured with the energy-dispersive spectrometer (Link ISIS). The Si(Li)-detector is equipped with a thin window that allows detection of light elements. Quantitative X-ray analysis showed that the particle contained mainly U (40–50 wt%), Zr (30–40 wt%) and O and minor amounts of Al, Si and Fe (usually <1 wt%). The particle has probably been in a molten state, because the U and Zr were evenly distributed in the particle and no granular structure, such as that detected by Salbu et al. (1994) and Toivonen et al. (1988), was observed. Particles with similar composition were found after the Chernobyl accident (e.g. Burakov et al., 1994; Perkins et al., 1989; Mandjoukov et al., 1992).

3.4. Beta spectrometry

Total beta activity of the particle located on the adhesive tape was measured using a proportional counter (Berthold LB770). Since the beta counter was not calibrated for point-source detection, test measurements were performed for estimating detector efficiency using a ^{90}Sr standard. The lower limit of total beta activity of the particle

was estimated to be 4.5 Bq which is one order of magnitude larger than the sum of activities presented in Table 2. Pure high-energy beta emitters, such as ^{90}Sr, must therefore have been present in the particle. By assuming equilibrium between ^{90}Y and ^{90}Sr the activity obtained for ^{90}Sr was 2.1 Bq, which is somewhat higher than that predicted by autoradiography.

A liquid scintillation counter (Wallac Quantulus 1220) was used for nuclide identification, i.e. to verify the presence of ^{90}Sr. The particle on the adhesive tape was placed in a counting bottle containing Hisafe Optiscint scintillation liquid. Despite the fact that the tape and self-absorption of beta particles in the radioactive particle itself may somewhat modify the shape of the beta spectrum, ^{90}Sr was clearly identified. Since the scintillation counter was not calibrated for point-source detection, only an estimate of ^{90}Sr activity could be obtained. The estimated activity was 2.2 Bq which was almost the same value as that obtained using the proportional counter. The activity, back-calculated to 26 April 1986, was 2.7 Bq; the activity per unit volume was 0.004 Bq μm^{-3}, assuming the volume to be 650 μm^3.

The Quantulus 1220 can be operated in a mode that allows separation of beta pulses from alpha pulses. An additional spectrum was measured using this pulse-shape analysis mode (Fig. 3). Alpha-active materials were identified in the particle (although the activities cannot be calculated from this measurement). This observation was expected because U was detected in SEM microprobe analysis. It is also compatible with the fact that transuranic elements were detected in nuclear fuel particles released from the Chernobyl accident.

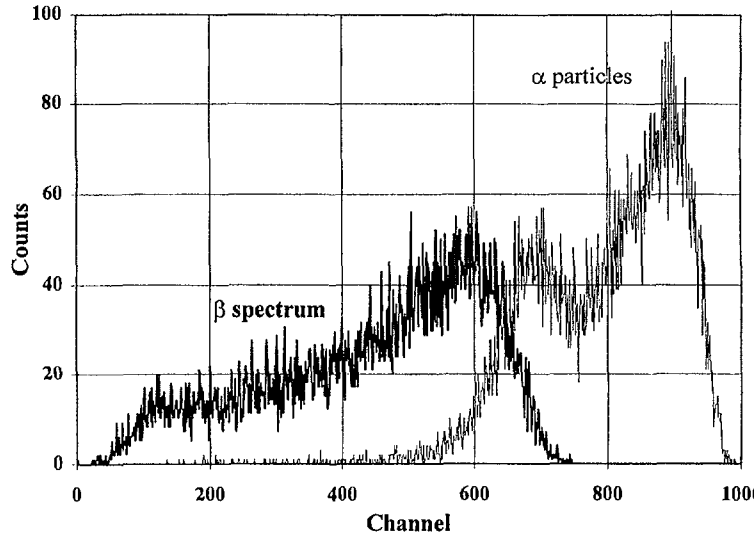

Fig. 3. Beta spectrum (mainly ^{90}Sr/^{90}Y) of the particle measured by liquid scintillation counter. They show the presence of alpha-active materials. Beta-particle distortions prevent its use in activity determination.

3.5. Alpha spectrometry

The alpha spectrum of the entire particle on the adhesive tape was measured first (Canberra PIPS). The spectrum could not be used for nuclide identification due to the presence of alpha particle self-absorption in the radioactive particle itself (Fig. 4); however, an estimate for the lower limit of total alpha activity could be obtained; the value was 0.06–0.1 Bq. Since the energy of alpha particles was below 5.6 MeV no alpha emitters with higher energies, such as ^{243}Cm and ^{244}Cm, were present in the particle.

So far, only nondestructive methods were used in the present particle analysis. To obtain quantitative nuclide-specific results the particle must be digested and dispersed homogeneously onto a metallic plate as a massless sample. The particle was wet-ashed using strong hydrochloric and nitric acids. Before ashing, the liquid tracers ^{242}Pu and ^{243}Am were added to the solution. After ashing the transuranic elements were coprecipitated with hydroxides. The Pu, Am + Cm and U fractions were separated with an ion-exchange method (Taipale & Tuomainen, 1985). They were electrodeposited on stainless-steel discs and measured with an alpha spectrometer (Fig. 4 and Table 3). Short-lived alpha-active nuclides, such as ^{242}Cm, were not observed, while isotopes of U were below the detection limit.

The sum of the activities presented in Table 3 (about 0.05 Bq) is smaller than the estimated total activity and may be due to incomplete digestion of Pu and Am in wet ashing (tracer nuclides were in liquid form). The activity of ^{241}Am determined by

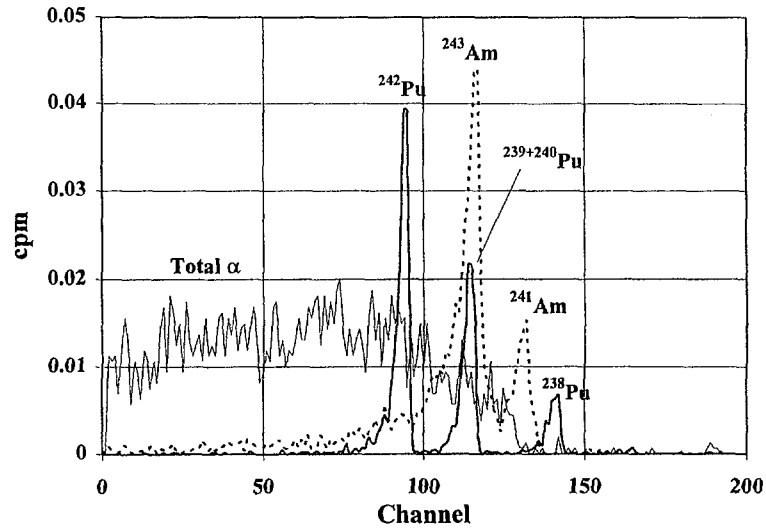

Fig. 4. Alpha spectrum measured from the three-dimensional particle (total α thin solid line) and alpha spectra from Pu fraction (thick solid line) and Am fraction (dashed line). Nuclides ^{242}Pu and ^{243}Am were used as tracer nuclides. The correction of recovery for Pu and Am peaks is not accounted for the number of counts.

Table 3
Alpha-active nuclides detected in the particle (October 1996). The sum of the activities is given for ^{239}Pu and ^{240}Pu. The uncertainty refers to statistical error; the methodological error related to the use of tracer nuclides is < 5%. A total volume of 650 μm^3 was used for estimating activities per unit volume

Nuclide	$t_{1/2}$ (a)	Activity (Bq)	Uncertainty (%)	Activity per unit volume (Bq μm^{-3})
^{238}Pu	87.7	0.007	10	1.1×10^{-5}
^{239}Pu	24100			
		0.026	5	4.0×10^{-5}
^{240}Pu	6570			
^{241}Am	433	0.011	6	—

radiochemical analyses differed by a factor of about 10 from that obtained with a gamma-ray spectrometer. This discrepancy can be explained by assuming incomplete dissolution of Am.

4. Discussion

In environmental radiation monitoring, laboratory procedures are designed and focused mainly on the detection of radiation, not necessarily on the characterization of radioactive materials as evidenced by the fact that activity concentrations are traditionally reported (see Table 1). As shown here, however, radionuclides cannot necessarily be considered as 'becquerels' dispersed homogeneously in the sample. The results, averaged over a mass unit, are not meaningful if radioactive material is located in only one particle. The same problem was discovered in air monitoring when activity in a filter was demonstrated in only a small number of particles (Pöllänen & Toivonen, 1994).

The presence of radioactive material in a sample is usually determined with a gamma-ray spectrometer, and less frequently with alpha and beta measurements; however, gamma-ray analyses only are not adequate for identifying radioactive particles. Autoradiography can be used for particle identification, isolation and preliminary activity analysis, but several methods are needed to characterize particle properties completely. The problem is that laboratory procedures are usually tailored for homogeneously distributed samples, not for point sources. In practice, we noted the importance of cross-checking of the results between various methods.

The presence of radioactive particles in environmental samples evokes the question of possible radiological risks that they may cause; however, risk estimation is not possible without detailed knowledge of particle characteristics. Elemental composition (the particle contained Zr, U and transuranic elements), nuclide composition (mainly nonvolatile, long-lived nuclides) and structure (the particle was irregular and

has probably been in the molten state) suggest that the particle considered here is a nuclear fuel particle that probably originated from the Chernobyl accident. Although several different experimental methods are used for particle analysis, they are not necessarily sufficient for risk estimation at the time of particle deposition due to the presence of relatively short-lived nuclides (Pöllänen, 1997). Calculations of reactor fuel inventory, applied for micrometre-sized objects, are then needed (Pöllänen et al., 1995).

Inventory calculations for the Chernobyl reactor were performed with the ORIGEN2 computer code to estimate activity ratios and activities per unit volume as a function of fuel burnup (Pöllänen & Toivonen, 1996). Due to the differences in cross-sections in data libraries used by ORIGEN2, the calculated activity concentrations of ^{154}Eu and ^{155}Eu differ considerably from those obtained by Jaracz et al. (1995). The concentrations were re-evaluated by Anttila (1996) using the CASMO-4 code. Observed activity ratios and activities per unit volume of the particle, compared with those of reactor fuel obtained by calculations make it possible to estimate fuel burnup and relative depletion/enrichment of various elements (the particle was assumed to be a Chernobyl particle).

Activity ratios $^{239+240}Pu/^{238}Pu$ and $^{155}Eu/^{154}Eu$ refer to burnups of 10000 MWd tUO_2^{-1} and 13000 MWd tUO_2^{-1}, respectively (Fig. 5). Calculated activities per unit volume of fuel, however, cannot be compared with those presented in Tables 2

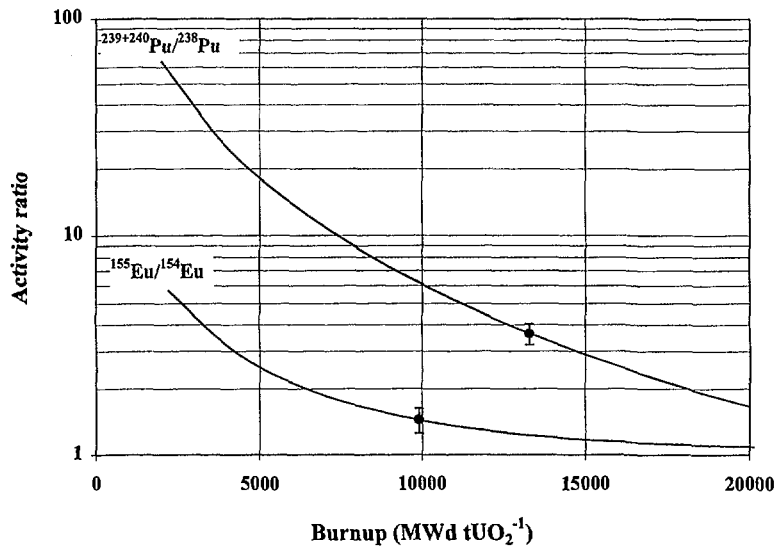

Fig. 5. Calculated activity ratios $^{239+240}Pu/^{238}Pu$ and $^{155}Eu/^{154}Eu$ for the Chernobyl fuel as a function of fuel burnup (10000 MWd tUO_2^{-1} refers to average burnup). The Pu ratio was calculated using ORIGEN2 and OTUS software (Pöllänen et al., 1995) and the Eu ratio using CASMO-4 (Anttila, 1996). The values observed for the particle are substituted in the curves. Error bars refer to uncertainties in activity measurements.

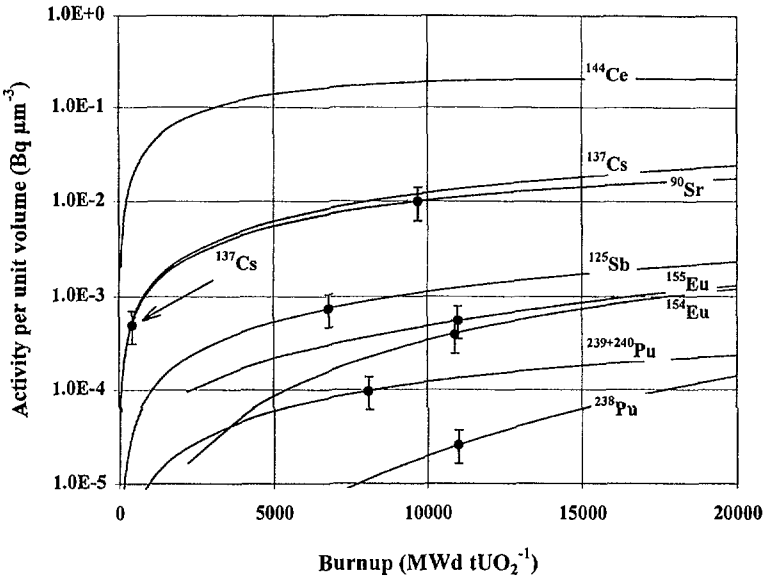

Fig. 6. Calculated activities per unit volume for the Chernobyl fuel as a function of fuel burnup. Volumetric activities were calculated using ORIGEN2 and OTUS software (Pöllänen and Toivonen, 1996) and in the case of Eu using CASMO-4 (Anttila, 1996). Measured activities per unit volume of the particle, corrected to the proportion of Zr, are substituted for the curves (not ^{144}Ce). Error bars refer to uncertainties in estimating particle volume and composition (UO_2 particle with metallic Zr was assumed). Note that the (unknown) proportions of nuclides ^{242}Cm and ^{244}Cm in the particle are not considered in the estimation of Pu activities per unit volume.

and 3 without accounting for the proportion of elements (mainly Zr) that were not present in the Chernobyl reactor fuel. Corrected activities per unit volume of the particle, substituted in the calculated curves, show that ^{90}Sr, ^{125}Sb, ^{154}Eu, ^{155}Eu, ^{238}Pu and $^{239+240}$Pu appear to be present in approximately the same proportion as in the fuel, whereas ^{137}Cs was strongly depleted (Fig. 6). The value obtained for ^{144}Ce was slightly higher than that predicted by the calculations (for a wide range of burnups). This may be due to experimental errors, since ^{144}Ce was just above the detection limit in gamma-ray analysis.

The amount of short-lived nuclides in the particle can be estimated by assuming that their proportions remained unchanged during particle formation (or that they were depleted by a known factor). For example, the activities of ^{141}Ce and ^{143}Ce, back-calculated from ^{144}Ce to the time of the Chernobyl accident, were estimated to be 200 Bq (burnup 10 000 MWd tUO_2^{-1}); the activities of ^{89}Sr and ^{91}Sr, back-calculated from ^{90}Sr, were estimated to be 50 Bq.

The particle considered here was collected in the Gotland Deep, about 1000 km from Chernobyl. Is it possible that the particle originated from the Chernobyl accident? The equivalent volume diameter of the particle was 10.2–11.3 µm, which resulted in an aerodynamic diameter of 27–30 µm by assuming that the dynamic

shape factor is 1.5 (Hinds, 1982) and density 10 500 kg m^{-3}. Radioactive particles of this size were observed on the southeastern coast of Sweden, near Gotland, after the Chernobyl accident (Pöllänen et al., 1997).

5. Conclusions

(1) Routinely used laboratory procedures are not necessarily appropriate for particle analyses.
(2) Inadequate results may be obtained if 'radioactivity' is assumed to be homogeneously distributed in a sample. The presence of radioactive particulate materials must be verified if their existence in the sample is suspected.
(3) Several complementary (experimental and calculative) methods are needed for complete characterization of radioactive particles.
(4) The characteristics of the particle analysed here refer to a nuclear fuel particle probably originating from the Chernobyl accident.

References

Anttila, M. (1996). Personal communications.

Broda, R., Mietelski, J. W., & Sieniawski, J. (1992). Radioactive ^{125}Sb and ^{60}Co in "ruthenium" hot particles from Chernobyl fallout. *Journal of Radioanalytical Nuclear Chemistry Letters, 166*, 173–180.

Burakov, B. E., Anderson, E. B., Galkin, B. Ya., Pazukhin, E. M., & Shabalev, S. I. (1994). Study of Chernobyl "hot" particles and fuel containing masses: Implications for reconstructing the initial phase of the accident. *Radiochimica Acta, 65*, 199–202.

Cross, W. G., Freedman, N. O., & Wong, P. Y. (1992). Beta ray dose distributions from skin contamination. *Radiation Protection Dosimetry, 40*(3), 149–168.

Hinds, W. C. (1982). *Aerosol technology*. Properties, behavior, and measurement of airborne particles. New York: Wiley.

Ikäheimonen, T. K., Ilus, E., & Klemola, S. (1999). Monitoring of radionuclides in the Baltic Sea in 1995. Finnish Centre for Radiation and Nuclear Safety, STUK-A Report Series (to be published).

Ilus, E. (1996). Evaluation of sediment sampling devices and methods used in the NKS/EKO-1 project. NKS/EKO-1 (96) (TR-1, pp. 1–54). Risø, Denmark, 1996.

Jaracz, P., Mirowski, S., Trziska, A., Isajenko, K., Jagielak, J., Kempisty, T. & Józefowicz, E. T. (1995). Calculations and measurements of ^{154}Eu and ^{155}Eu in 'fuel-like' hot particles from Chernobyl fallout. *Journal of Environmental Radioactivity, 26*, 83–97.

Khitrov, L. M., Cherkezyan, V. O., & Rumyantsev, O. V. (1994). Hot particles after the Chernobyl accident. *Geochemistry International, 31*, 46–55.

Kuriny, V. D., Ivanov, Yu. A., Kashparov, V. A., Loshchilov, N. A., Protsak, V. P., Yudin, E. B., Zhurba, M. A. & Parshakov, A. E. (1993). Particle associated Chernobyl fall-out in the local and intermediate zones. *Annals of Nuclear Energy, 20*(6), 415–420.

Mandjoukov, I. G., Burin, K., Mandjoukova, B., Vapirev, E. I. & Tsacheva Ts. (1992). Spectrometry and visualization of 'standard' hot particles from the Chernobyl accident. *Radiation Protection Dosimetry. 40*, 235–244.

Perkins, R. W., Robertson, D. E., Thomas, C. W., & Young, J. A. (1989). Comparison of nuclear accident and nuclear test debris. *Proceedings of the International Symposium on Environmental Contamination Following a Major Nuclear Accident* (pp. 111–139). Vienna, Austria, 16–20 October 1989, IAEA-SM-306/125.

Pöllänen, R. (1997). Highly radioactive ruthenium particles released from the Chernobyl accident: particle characteristics and radiological hazard. *Radiation Protection Dosimetry, 71*(1), 23–32.

Pöllänen, R., Kansanaho, A., & Toivonen, H. (1996). Detection and analysis of radioactive particles using autoradiography. Report on Task FIN A847 of the Finnish Support Programme to IAEA Safeguards, Finnish Centre for Radiation and Nuclear Safety, STUK-YTO-TR99.

Pöllänen, R., & Toivonen, H. (1994). Transport of large uranium fuel particles released from a nuclear power plant in a severe accident. *Journal of Radiological Protection, 14*, 55–65.

Pöllänen, R., & Toivonen, H. (1996). Size estimation of radioactive particles released in the Chernobyl accident. *Proceedings of the Fourteenth International Conference on Nucleation and Atmospheric Aerosols* (pp. 670–673).

Pöllänen, R., Toivonen, H., Lahtinen, J., & Ilander, T. (1995). OTUS – Reactor inventory management system based on ORIGEN2. Finnish Centre for Radiation and Nuclear Safety, STUK-A126.

Pöllänen, R., Valkama, I., & Toivonen, H. (1997). Transport of radioactive particles from the Chernobyl accident. *Atmospheric Environment, 31*, 3575–3590.

Rantavaara, A., Klemola, S., Saxén, R., Ikäheimonen, T. K., & Moring, M. (1994). Radionuclide analysis of environmental field trial samples at STUK. Report on Task FIN A847 of the Finnish Support Programme to IAEA Safeguards. Finnish Centre for Radiation and Nuclear Safety, STUK-YTO-TR 75.

Salbu, B., Krekling,T., Oughton, D. H., Østby, G., Kashparov, V. A., Brand, T. L., & Day, J. P. (1994). Hot particles in accidental releases from Chernobyl and Windscale nuclear installations. *Analyst, 119*, 125–130.

Sinkko, K., & Aaltonen, H. (1985). Calculation of the true coincidence summing correction for different sample geometries in gamma-ray spectroscopy. Finnish Centre for Radiation and Nuclear Safety, STUK-B-VALO 40.

Taipale, T. K., & Tuomainen, K. (1985). Radiochemical determination of plutonium and americium from seawater, sediment and biota samples. Finnish Centre for Radiation and Nuclear Safety, STUK-B-VALO 26.

Toivonen, H., Servomaa, K., & Rytömaa, T. (1988). Aerosols from Chernobyl: Particle characteristics and health implications. In: H. Von Philipsborn, & F. Steinhäusler (Eds.), Hot particles from the Chernobyl fallout. *Proceedings of an International Workshop* (BAND 16, 97–105), Theuern, 28/29 October 1987. Schriftenreihe des Bergbau- und Industriemuseums Ostbauern Theuern.

VIII

PÖLLÄNEN R, KLEMOLA S, IKÄHEIMONEN T K, RISSANEN K, JUHANOJA J, PAAVOLAINEN S, LIKONEN J. Analysis of radioactive particles from the Kola Bay area. *Analyst 2001; 126: 724-730.*

THE ANALYST

An international journal
of analytical and
bioanalytical science

REPRINT

With the
Compliments of the Author

www.rsc.org/analyst

RS•C
ROYAL SOCIETY OF CHEMISTRY

FULL PAPER
THE ANALYST
www.rsc.org/analyst

Analysis of radioactive particles from the Kola Bay area

R. Pöllänen,*[a] S. Klemola,[a] T. K. Ikäheimonen,[a] K. Rissanen,[a] J. Juhanoja,[b] S. Paavolainen[c] and J. Likonen[d]

[a] *STUK - Radiation and Nuclear Safety Authority, P.O. Box 14, 00881 Helsinki, Finland. E-mail: roy.pollanen@stuk.fi*
[b] *University of Helsinki, Institute of Biotechnology, P.O. Box 56, 00014 Helsinki, Finland*
[c] *Defence Forces Research Institute of Technology, P.O. Box 5, 34111 Lakiala, Finland*
[d] *VTT Chemical Technology, P.O. Box 1404, 02044 VTT, Finland*

Received 1st February 2001, Accepted 1st March 2001
First published as an Advance Article on the web 26th March 2001

Two types of radioactive particle were identified in marine sediment and lichen samples collected from the Kola Bay, NW Russia. The particles were identified by means of gamma-ray spectrometry and autoradiography, separated and subjected to various analysis techniques. Several complementary techniques are needed to characterise particle properties thoroughly. ^{137}Cs was present in the sediment matrix in large (≈ 100 μm) greenish particles that were most probably pieces of paint. Although their element composition was heterogeneous, ^{137}Cs was found to be evenly distributed. ^{60}Co in the lichen matrix was present in small (≈ 1 μm) particles. No U or transuranium elements were detected in either type of particle.

Introduction

Environmental samples were collected in the Kola Bay area, NW Russia, within the framework of a joint research programme carried out in the Russian Arctic Seas between the Radiation and Nuclear Safety Authority (STUK) and the Murmansk Marine Biological Institute. The studies were focused on radioactive contamination at the site of several potential sources. The naval shipyards and military nuclear bases located in Severomorsk and Polarnyy have facilities for nuclear fuel storage and radioactive waste (Fig. 1). Storage vessels are also located around the city of Murmansk. The Atomflot civilian nuclear icebreaker base has a liquid-waste purification plant.

Samples of sediment, algae and lichen, as well as benthic samples, were collected during the expedition in the Kola Bay in 1995.[1] Preliminary laboratory analyses revealed that the radioactive materials were not homogeneously distributed in some of the sediment and lichen samples. An effort was made to identify the presence of radioactive particles and to separate them from the bulk samples. A number of laboratory analysis techniques were tested in order to determine the characteristics of the radioactive particles.

Aim of investigation

A number of papers dealing with radioactive contamination in the northwest arctic of Russia have been recently published.[1–5] In these studies the possible particulate nature of the radioactive contamination are often disregarded in estimating the total amount of contamination or the possible radiological impact of the discharges. However, 'For areas affected by radioactive particulate contamination, sampling may not be representative, leaching prior to analysis may be partial and the contaminated inventory underestimated. Consequently large errors in impact assessments may arise'.[6] Despite the extensive sampling no information on the general levels of radioactive contamination are presented here; these results will be published later. The main objective is to acquire experience about the feasibility of different techniques in analysing the properties of individual radioactive particles. Some of the analytical methods used here are not commonly used in particle analysis and the present paper could give new ideas for other investigators to analyse environmental samples in an alternative way.

The reason for analysing the properties of individual radioactive particles is to produce data that cannot be obtained

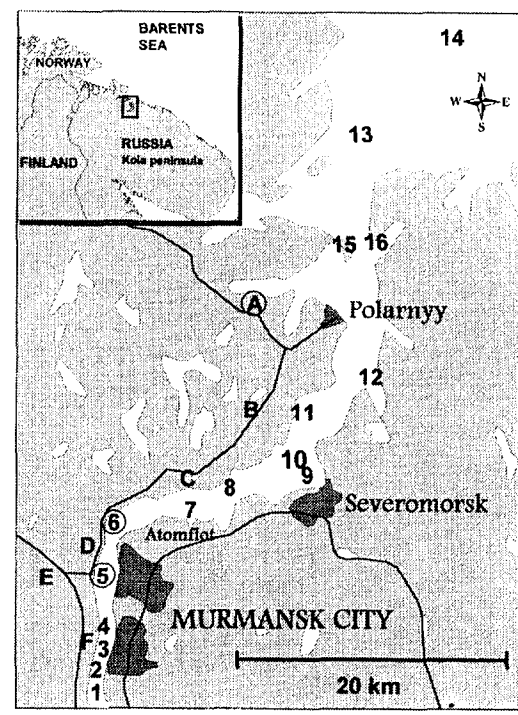

Fig. 1 Location of the sampling sites. The numbers (1–16) refer to the sediment samples and the letters (A–F) to the lichen samples. Radioactive particles isolated and analysed in the present study were from circled locations 5 (sampling depth 47 m), 6 (depth 72 m) and A.

DOI: 10.1039/b101099i

by analysing bulk samples only. In bulk sample analyses the information derived from non-relevant background particles may mask the information originating from relevant particles. According to Zeissler *et al.*[7] the characterisation of microscopic radioactive particles 'contributes to the understanding of difficulties encountered in environmental sample characterisation by bulk methods and provides insights into bioavailability and waste remediation issues'.

The origin of radioactive particles in an environmental sample may vary greatly. In some cases it might be possible to identify the source from which the particles originated and to characterise the phenomena that have occurred during particle formation and release. This information may be valuable for example in contamination cases, in radiation monitoring or in a number of safeguard applications. Prerequisite for unambigious source identification is detailed knowledge of the characteristics of all relevant sources. This information was not available in the present study and, thus, unambiguous source identification was not possible.

Sample collection and pre-treatment

Sediment samples were collected in May 1995 with a Gemini gravity corer, a box corer or a Van Veen grab.[1] A box corer (area 20 cm × 20 cm) was used at location 5 (see Fig. 1). The sample was sectioned by hand to correspond to depths of 0–2 cm, 2–4 cm and 4–7 cm. Six cores were collected using a Gemini corer at location 6. Cores of total length 4–7.5 cm were sectioned into 2 cm slices. Slices from the same vertical layers were pooled.

The lichen material was sampled in July 1995. The plots, 50 cm × 50 cm in size, were located on bedrock covered by soil layers and a lichen carpet. *Cladonia stellaris* (location A in Fig. 1) was separated from the bulk lichen sample for subsequent analyses and divided into horizontal sections.

In the laboratory the samples were dried and homogenised for high-resolution gamma spectrometry. The samples were divided into smaller subsamples which were counted separately. The measurement geometry was either 550 ml Marinelli containers or plastic jars of 100 ml and 35 ml. The samples containing radioactive particle(s) were repeatedly divided into two parts that were subsequently counted in order to identify the part containing the radioactive particle(s).

Preliminary identification of the presence of radioactive particles in the subsamples was performed as follows. The first measurement of the surface sediment sample collected in location 5 gave a ^{137}Cs concentration of 58 Bq kg^{-1}, whereas the other subsamples gave 5–6 Bq kg^{-1}. The first subsample was repeatedly divided into smaller parts and, after several divisions, a particle enhanced in respect to ^{137}Cs was finally located in a sample with a mass of 3.2 mg (mass of the original subsample 48.9 g). Particles containing enhanced levels of ^{137}Cs were similarly identified in the sample collected at location 6 (one particle from slice 4–6 cm, and one from slice 6–7.5 cm). The first gamma-ray analysis of the sample (mass 25 g) containing the top part of a *Cladonia stellaris* lichen gave concentrations of 285 Bq kg^{-1} for ^{137}Cs, 6.4 Bq kg^{-1} for ^{134}Cs, and 21.8 Bq kg^{-1} for ^{60}Co (dry weight). After subsequent divisions, the Cs concentrations remained at the same level, but the ^{60}Co concentration was found to be unevenly distributed in the fractioned samples. The mass of the final lichen sample from which the Co particles were isolated was 14 mg.

Analysis methods and results

Particle localisation, isolation and spectroscopic analyses

Localisation of the radioactive particles was performed using autoradiography in which an emulsion-coated autoradiography film (Kodak BioMax MR) was placed on the pretreated samples. The particles were isolated using consecutive autoradiograms, and were finally fixed on adhesive tape. After isolation, the activity of the particles was measured using a gamma-ray spectrometer and an alpha spectrometer. Since the particles are not massless, only an estimate of the total alpha activity is given.[8]

Exposure for 1 week in a lightproof cassette revealed the presence of 3 radioactive particles in the sediment samples (1 particle per sample) which were found to contain nuclides ^{134}Cs and ^{137}Cs (Table 1). No other artificial radionuclides were observed. No Cs was observed in the bulk of the samples from which the particles were separated. The particles were fragile since, during additional separations, two of the particles fragmented into smaller pieces (see Table 1).

In the case of lichen samples, three very tiny black spots were identified on the autoradiography film after 35 d exposure. The particles corresponding to the black spots were separated from the sample and only ^{60}Co was found (Table 2). The remaining lichen material contained a very small amount of ^{60}Co, but no additional efforts were made to isolate the remaining particles. No alpha-active materials were present in either type of particle.

Table 1 *Activities (or detection limits) of Cs particles identified in the marine sediment samples*[a]

	Gamma-ray analysis					Alpha analysis	
Code	Counting time/h	^{137}Cs/Bq	Unc. (%)	^{134}Cs/Bq	Unc. (%)	Counting time/h	$A_{\alpha,tot}$/Bq
Cs1	68	4	4	0.015	17	67	< 0.0005
	67	4.3	4	< 0.01			
Cs2	68	0.52	3	< 0.005		N.M.	
Cs2a	67	0.33	3	< 0.004		27	< 0.0007
Cs2b	67	0.16	6	< 0.006		27	< 0.0007
Cs3	68	0.38	5	< 0.006		N.M.	
Cs3a	16	0.075	8	< 0.01		74	< 0.0004
Cs3b	7	0.35	5	< 0.02		74	< 0.0004
Cs3ba	23	0.13	5	< 0.008		N.M.	
Cs3bb	N.M.					N.M.	
Cs3bc	66	0.11	4	< 0.005		N.M.	

[a] Activity analyses were performed using the GAMMA computer code[14] in summer 1997, and the uncertainties (Unc.) refer to 1 *s*. Some particles were counted several times with hyperpure germanium detectors of relative efficiency of 40% and 70%.[15] Energy resolution of the detectors is 1.8 keV in 1.33 MeV. Three particles were originally identified but, in subsequent isolation procedures, two of the particles (Cs2 and Cs3) fragmented into smaller pieces. The sum of the activities of daughter particles Cs2a + Cs2b and Cs3a + Cs3b are close to those of the parent particles Cs2 and Cs3. Particle Cs3b became further fragmented into 3 pieces. $A_{\alpha,tot}$ refers to the upper limit of the total alpha activity of the whole particle. N.M. = Not measured.

In some cases autoradiography can be used for activity analysis although the detailed composition of every beta-emitting nuclide is not known.[8,9] Particles on adhesive tape were placed in an exposure geometry for which beta dose rate coefficients for a water/water boundary[10] can be used. The detected size of the black spot compared with the calculated ('theoretical') value enabled the activity to be estimated by a factor of 2–3. In addition, the presence of high-energy pure beta emitters, such as $^{90}Sr/^{90}Y$, can be identified if their activity is not much lower than that of ^{137}Cs. However, no $^{90}Sr/^{90}Y$ was detected in the particles (Fig. 2). The upper limit for the activity of $^{90}Sr/^{90}Y$ in particle Cs1 was approximately 1 Bq.

Table 2 Activities (or detection limits) of Co particles present in the lichen samples[a]

	Gamma-ray analysis			Alpha analysis	
Code	Counting time/h	^{60}Co/Bq	Unc. (%)	Counting time/h	$A_{\alpha,tot}$/Bq
Co1	65	0.009	18	87	< 0.0003
	67	0.009	17		
	68	0.013	13		
Co2	67	0.015	12	N.M.	
Co3	65	0.037	7	73	< 0.0005

[a] Activity analyses were performed in summer 1997, and the uncertainties (Unc.) refer to 1 *s*. $A_{\alpha,tot}$ refers to total alpha activity detected from the whole particle. N.M. = Not measured.

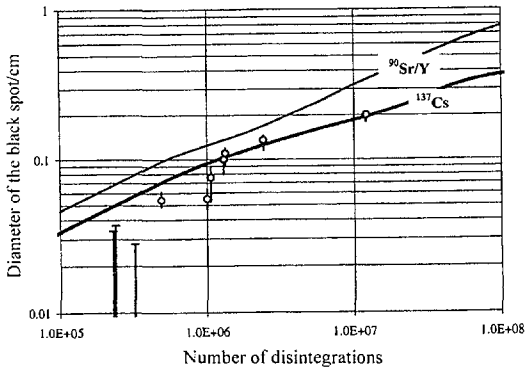

Fig. 2 Diameter of the black spots on autoradiography film produced by Cs particles as a function of the number of disintegrations (^{137}Cs or ^{90}Sr). The thick curve represents the 'theoretical' estimate[9] for ^{137}Cs, whereas the thin curve is that for ^{90}Sr. Measured values, obtained using several exposure times, are substituted in the figure. The size of the black spots cannot be determined accurately using a digital scanner when the diameter of the spot is smaller than about 0.5 mm.

SEM microanalysis of the particles

Electron micrographs of the particles on the adhesive tape were taken with a scanning electron microscope (SEM; Zeiss DSM 962) using either secondary electrons or backscattered electrons. X-ray spectra and X-ray maps were measured with an energy-dispersive spectrometer (Link ISIS) equipped with a thin window Si(Li) detector.

Identification of the radioactive particles from numerous non-active species (especially in the sediment samples) was a tedious task because the composition of the metallic background particles of artificial origin varied greatly, and the number of suspicious particles in a sample was very large. To avoid misidentification, the suspected radioactive objects were

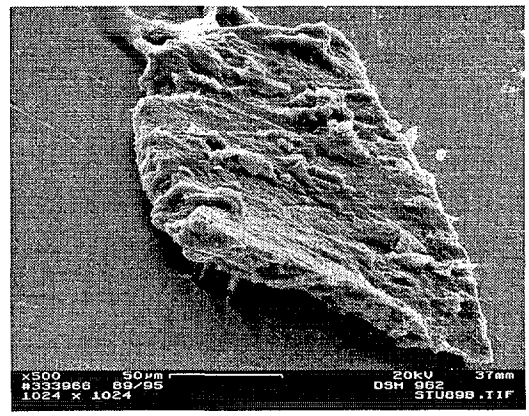

Fig. 3 Secondary electron-image of particle Cs1 (tilted 60°). The particle is lying on a steel plate. Remnants of the glue of the adhesive tape can be seen on the upper edge of the figure. Scale bar = 50 µm.

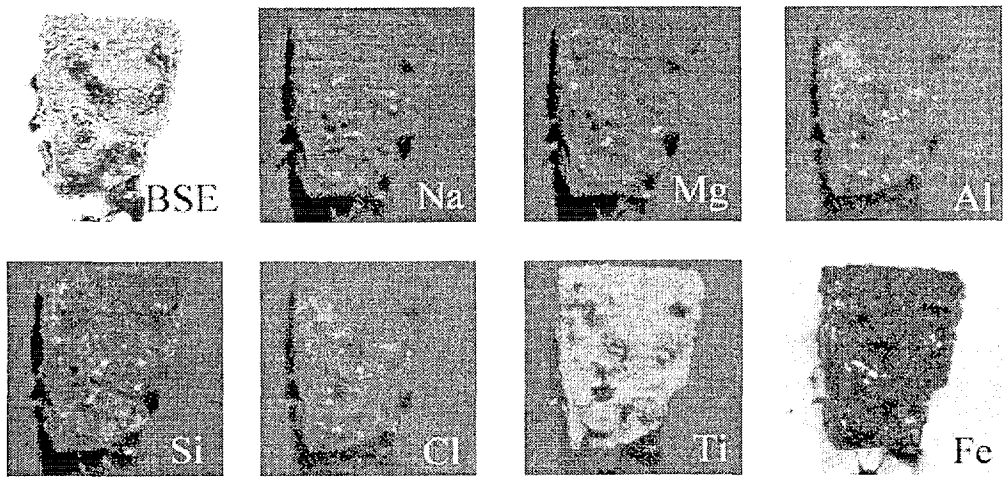

Fig. 4 Back-scattered electron image of particle Cs1 (no tilt, BSE) and X-ray maps for Na (K-line), Mg (K-line), Al (K-line), Si (K-line), Cl (K-line), Ti (K-line) and Fe (K-line). The brighter the X-ray map, the higher is the concentration of the respective element. Area of the images is 230 µm × 230 µm. Acceleration voltage was 20 keV.

remeasured using a gamma-ray spectrometer. Three particles (Cs1, Cs3bc and Co1) were unambiguously separated from the non-radioactive bulk particles.

Particle Cs1 (Fig. 3) was a flat rectangle-shaped object of about 30 μm × 160 μm × 200 μm in size and was hardly visible by the naked eye. X-ray maps showed the presence of numerous elements, as well as small agglomerated particles, heterogeneously distributed over the surface of the particle (Fig. 4). However, titanium (Ti) was rather evenly distributed on the particle surface. Ti is commonly used in paints. The structure of the particle Cs3bc (Fig. 5) was similar to that of Cs1, and it was composed of the same elements (Fig. 6).

The radioactive particles were very difficult to identify in the lichen samples although the number of inactive background particles was much smaller than that in the sediment samples. The reason for this was that the radioactive particles were very small and their activity very low. Thus, numerous time-consuming verification measurements were needed in a gamma-ray spectrometer. Particle Co1 was the only one that was definitely identified (Fig. 7). It consisted of small (< 1 μm) agglomerated particles, and its shape was very irregular. Because of the small size no other elements than Fe could be certainly identified. No U or transuranium elements were detected in the Cs and Co particles. The results of more detailed

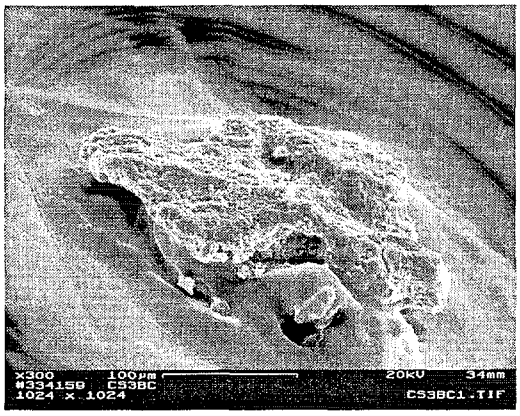

Fig. 5 Secondary electron-image of particle Cs3bc (tilted 60°). The particle is attached to adhesive tape. Scale bar = 100 μm.

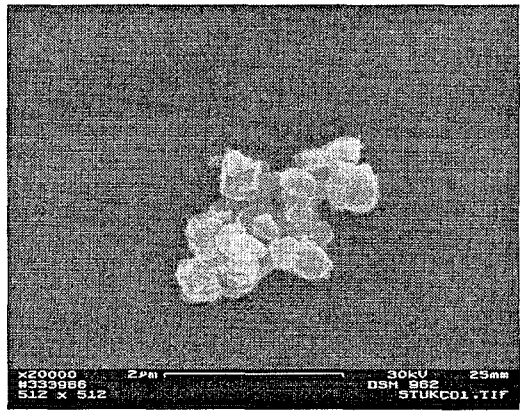

Fig. 7 Secondary electron-image of particle Co1 on adhesive tape. Scale bar = 2 μm.

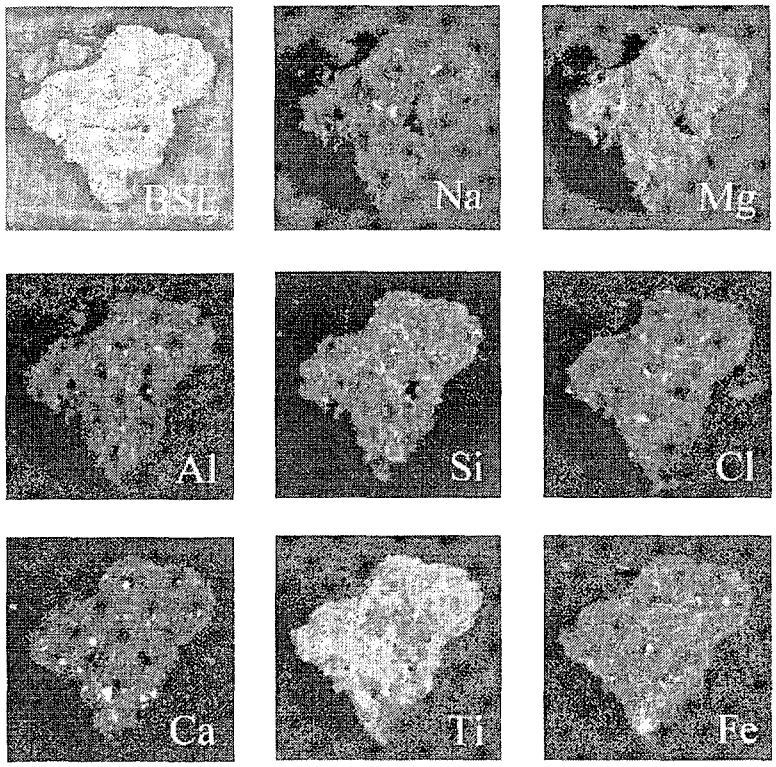

Fig. 6 Back-scattered electron image of particle Cs3bc (no tilt, BSE) and X-ray maps for Na (K-line), Mg (K-line), Al (K-line), Si (K-line), Cl (K-line), Ca (K-line), Ti (K-line) and Fe (K-line). Area of the images is 350 μm × 350 μm. Acceleration voltage was 20 keV.

analyses of particles Cs1 and Cs3bc are presented in the following.

Analysis of particle Cs1

Since particle Cs1 was relatively large and the composition and structure of its surface were heterogeneous, the question arises of whether the ^{137}Cs is homogeneously distributed in the particle or not. Particle Cs1 was embedded in resin (LX-112). After heat polymerization the hard block was sectioned into thin slices with an ultramicrotome (Leica Ultracut UTC) equipped with a glass knife.[11] The thickness of the slices was 3 μm and the total number of slices was approximately 60. The slices were transferred to glass plates (Fig. 8).

Autoradiography was carried out on the glass plates onto which the radioactive particle Cs1 was sliced. Exposure with light-multiplying layers[9] for two weeks revealed that the amount of ^{137}Cs was approximately equal in almost every slice (Fig. 9). Thus, ^{137}Cs was relatively evenly distributed either on the surface of the particle or within the particle. Electron micrographs of the slices were taken and X-ray maps showed that the bulk material of particle Cs1 was heterogeneous. Ti was clearly present.

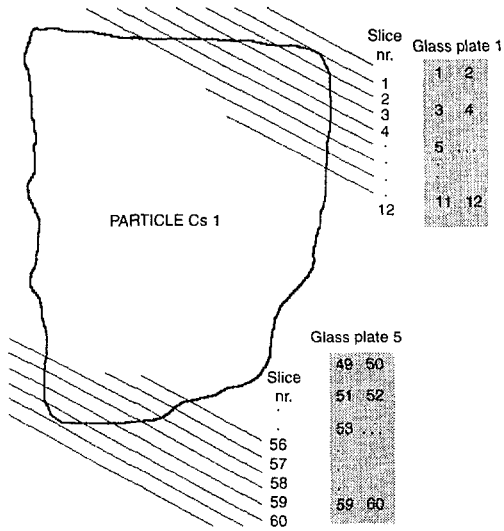

Fig. 8 Particle Cs1 was cut into 60 slices, which were subsequently transferred to 5 glass plates.

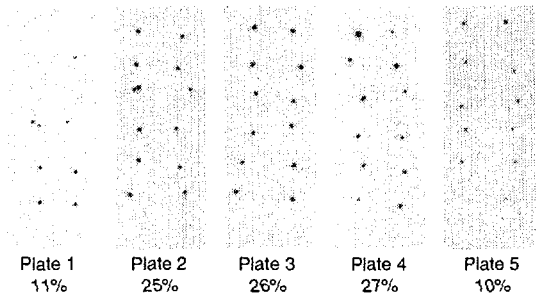

Fig. 9 Slices of particle Cs1 in autoradiography. The size of the black spots refers to the amount of ^{137}Cs in the slice. Percentages (counted using a gamma-ray spectrometer) refer to the proportion of ^{137}Cs out of the total activity. A few slices at the top of plate 1 and at the bottom of plate 5 do not include pieces of particle Cs1. Two slices may also be located adjacently (see for example plate 2) as a result of manual dislocation of the slices.

Since it was suspected that particle Cs1 was a piece of paint, an effort was made to use infrared (IR) spectroscopy to determine the chemical composition of the slices. Four slices of particle Cs1 were removed from the glass plates and were transferred onto KBr pellets for measuring the infrared absorption spectrum. The IR microscope (Spectra-Tech IR-Plan) revealed that the slices were greenish in colour. The IR spectra were measured using an FTIR spectrometer (Nicolet model 800) with a medium-band Hg–Cd–Te (MCT) detector.

The differences in the spectra of the different slices were small. The spectra were typical of polyester with inorganic components. The polyester was probably alkyd resin. Alkyd is a widely used resin in paints. The inorganic pigments were barium sulfate, ferriferrocyanide and an unidentified oxide. Ferriferrocyanide has long been used as a blue pigment in paints. The oxide might be titanium dioxide, but it could not be identified on the basis of the IR spectrum. One slice was burnt at 600 °C to remove the organic material. The white residue was mainly barium sulfate and an oxide. Ferriferrocyanide decomposes during the ignition process. Thus, particle Cs1 was most probably a fragment of paint.

Analysis of particle Cs3bc

Secondary ion mass spectrometry (SIMS) was used to verify the results of Cs3bc obtained by SEM. Another objective was to test the use of SIMS for nuclide and element analysis, since the method is not commonly used for radioactive particles. The analysis was carried out on a double-focusing magnetic sector instrument (Vacuum Generators IX70S).[12] Ga^+ ions of kinetic energy 14 keV and current 1.5 nA were used as primary ions. Element maps were taken of the positive secondary ions (Fig. 10).

The spatial resolution of SIMS is poorer than that of SEM. However, the detection limits in SIMS are several orders of magnitude lower than in SEM.[13] Small agglomerated particles on the surface of particle Cs3bc were also detected using SIMS. Comparison of the element maps produced by SIMS and SEM (Figs. 10 and 6) shows that the elements appear to be somewhat differently distributed over the particle surface. The differences arise from the different intensity ranges of the imaging software used in SEM and SIMS. Moreover, in SIMS the information about the concentration of elements comes from the very outermost surface layer of the particle, whereas in the case of SEM the information is obtained from depths of a few micrometres.

Discussion

The most difficult phase in determining the characteristics of the individual radioactive particles was their identification and separation from a bulk sample. This may be a simple task but, as in the present case, it is sometimes very tedious. The more active the particles, the easier is the isolation. However, the advantages of isolation are apparent. It is possible to achieve results that are otherwise not possible owing to the interference of non-relevant bulk particles in the sample.

The isolation of radioactive particles and subsequent analyses are not routinely performed on environmental samples. For routine particle analyses it is essential to develop some sort of 'cookbook', in which detailed procedures and methods of analysis are described. The manner in which different analysis techniques are used is highly dependent on the type of information needed in each case. It is evident that non-destructive analyses should be performed before destructive analyses. For example, the radiochemical separation of transur-

anium elements from a bulk sample prohibit subsequent analysis of individual particles.

The order in which the different phases of analysis are performed could be as follows (the list contains techniques that are not applied in the present paper).

(1) Identification, localisation and isolation of radioactive particles using a combination of gamma-ray spectrometry and autoradiography (or another method which is able to localise particles accurately). The particles can be fixed onto adhesive tape. In addition to gamma-ray measurements, preliminary activity analysis of individual particles can also be performed using autoradiography. The presence of pure beta emitters may then be revealed.[9]

(2) Gamma-ray analysis of isolated particles (if not performed in phase 1). The detection limits may be very low because of ideal point-source geometry and missing background radiation coming from the bulk sample.

(3) Alpha analysis of the entire particle. Only an estimate of the total alpha activity can be obtained because of the self-absorption of alpha particles.[8] However, the most energetic alpha-emitting nuclide can be identified on the basis of the maximum energy of the alpha spectrum.

(4) Identification of particle size and shape, and analysis of the elemental composition using (scanning) electron microscopy and X-ray mapping. Other X-ray fluorescence techniques and non-destructive mass spectrometry (such as SIMS) are also possible. These methods are intended for surface analysis of particles rather than for bulk particle analysis. However, concentration profiles can be measured as a function of depth using SIMS.

(5) Analysis of the beta spectrum emitted from the particle using a liquid scintillator. The beta spectrum may be too complicated for quantitative analysis if a large number of beta-active nuclides are present in the particle. In some cases $^{90}Sr/^{90}Y$ can be identified from the spectrum,[8] but point-source calibration is needed for quantitative results.

(6) Elemental composition of the bulk particle can be obtained by neutron activation analysis. In addition, infrared spectroscopy may also be applicable, as the present paper shows.

(7) The methods of analysis mentioned above are non-destructive (other methods not mentioned here also exist). A wide variety of destructive methods can be used in analysing the properties of bulk particles. For example, the radiochemical separation of certain elements and their subsequent analysis using an alpha spectrometer is a very sensitive method. Mass spectrometers, such as inductively coupled plasma mass spectrometry (ICP-MS), are adequate for analysing the nuclide composition.

A range of assay methods are needed for the complete characterisation of radioactive particles, and some of them were used in the present analyses. The possibility of making cross checks of the results between different methods gives an additional justification. It is clear that comprehensive analyses are not necessarily needed for every sample and for every particle. Radioactivity measurements are often sufficient. Because of the high costs of the analyses the need must be evaluated case by case.

It is clear that the particles were not from global fallout caused by nuclear explosion tests or the Chernobyl accident. The paint particles isolated from the sediment samples, and which contained radioactive Cs, might originate from the storage ships Lepse or Imandra lying in Atomflot. Some of the rusty storage containers are not necessarily leak-tight, and Cs-contaminated pieces of paint from the rusty storage ships may be washed into the Kola Bay. Unfortunately, in the present study it was not possible to verify this assumption. The origin of ^{137}Cs and ^{134}Cs in the paint particles is somewhat questionable,

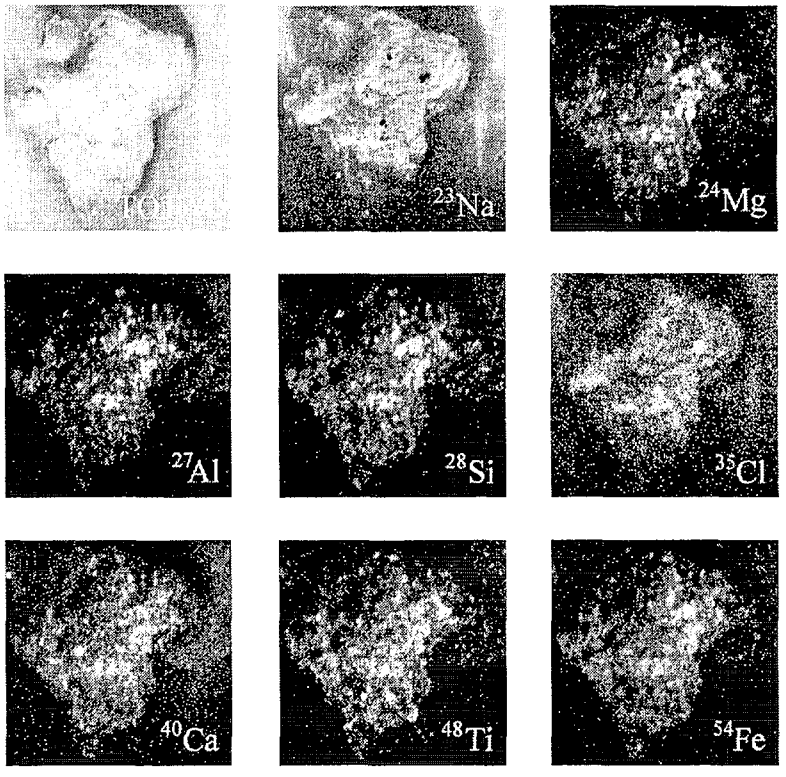

Fig. 10 The total ion image of particle Cs3bc taken by SIMS and element maps of ^{23}Na, ^{24}Mg, ^{27}Al, ^{28}Si, ^{35}Cl, ^{40}Ca, ^{48}Ti and ^{54}Fe.

but the presence of ^{134}Cs indicates that the Cs in the particles has been present in a nuclear reactor.

The particles isolated from the lichen sample and containing ^{60}Co probably originated from the Nerpa Shipyard in the Polarnyy area, where the maintenance and repair of nuclear-powered ships are performed. However, particle Co1 was so small that, in principle, it may have been transported also from distant areas.

Acknowledgements

This work was supported by the EC (Nuclear Fission Safety Programme, 1995–1999; Contract No. F14P-CT95-00335), by the Finnish Ministry of Foreign Affairs, by the Nordic Council of Ministers and by the Nordic Nuclear Safety Research (NKS-EKO-1).

References

1 K. Rissanen, T. K. Ikäheimonen, D. G. Matishov and G. G. Matishov, *Radiat. Prot. Dosim.*, 1998, **75**, 223.
2 K. Rissanen, T. K. Ikäheimonen, D. G. Matishov and G. G. Matishov, *Radioprot. Colloq.*, 1997, **32**, 323.
3 T. K. Ikäheimonen, K. Rissanen, D. G. Matishov and G. G. Matishov, *Sci. Total Environ.*, 1997, **202**, 79.
4 G. G. Matishov, D. G. Matishov, A. A. Namjatov, J. Carroll and S. Dahle, *J. Environ. Radioact.*, 1999, **43**, 77.
5 G. G. Matishov, D. G. Matishov, A. A. Namjatov, J. Carroll and S. Dahle, *J. Environ. Radioact.*, 2000, **48**, 5.
6 B. Salbu, *Radiat. Prot. Dosim.*, 2000, **92**, 49.
7 C. J. Zeissler, S. A. Wight and R. M. Lindstrom, *Appl. Radiat. Isot.*, 1998, **49**, 1091.
8 R. Pöllänen, T. K. Ikäheimonen, S. Klemola and J. Juhanoja, *J. Environ. Radioact.*, 1999, **45**, 149.
9 R. Pöllänen, A. Kansanaho and H. Toivonen, *Detection and analysis of radioactive particles using autoradiography*, Report on Task FIN A847 of the Finnish Support Programme to IAEA Safeguards, Finnish Centre for Radiation and Nuclear Safety, STUK-YTO-TR99, 1996.
10 W. G. Cross, N. O. Freedman and P. Y. Wong, *Radiat. Prot. Dosim.*,1992, **40**, 149.
11 P. C. Goodhew, in *Practical Methods in Electron Microscopy*, ed. A. M. Glauert, Elsevier, Amsterdam, 1985, vol. 11, pp. 117–123.
12 A. R. Bayly, M. Cummins, P. Vohralik, K. Williams, D. R. Kingham, A. R. Waugh and J. M. Walls, in *Secondary Ion Mass Spectrometry SIMSVI*, ed. A. Bennughoren, A. W. Huber and H. W. Werner, Wiley, New York, 1988, pp. 169–172.
13 M. P. Seah and D. Briggs, *Practical Surface Analysis, Ion and Neutral Spectroscopy*, Wiley, Chichester, 1992, vol. 2, p. 15.
14 K. Sinkko and H. Aaltonen, Calculation of the true coincidence summing correction for different sample geometries in gamma-ray spectroscopy, Finnish Centre for Radiation and Nuclear Safety, STUK-B-VALO 40, 1985.
15 A. Rantavaara, S. Klemola, R. Saxén, T. K. Ikäheimonen and M. Moring, Radionuclide analysis of environmental field trial samples at STUK, Report on Task FIN A 847 of the Finnish Support Programme to IAEA Safeguards, Finnish Centre for Radiation and Nuclear Safety, STUK-YTO-TR 75, 1994.

STUK-A reports

STUK-A188 Pöllänen R. Nuclear fuel particles in the environment - characteristics, atmospheric transport and skin doses. Helsinki 2002.

STUK-A187 Lindholm Carita, Simon Steve, Makar Beatrice, Baverstock Keith (Eds.) Workshop on dosimetry of the population living in the proximity of the Semipalatinsk atomic weapons test site. Helsinki 2002.

STUK-A186 Ammann M, Sinkko K, Kostiainen E, Salo A, Liskola K, Hämäläinen R P, Mustajoki J. Decision analysis of countermeasures for the milk pathway after an accidental release of radionuclides. Helsinki 2001.

STUK-A185 Sinkko K, Ammann M, Kostiainen E, Salo A, Liskola K, Hämäläinen R P, Mustajoki J. Maitotuotteisiin kohdistuvat vastatoimenpiteet ydinonnettomuustilanteessa. Helsinki 2001.

STUK-A184 Servomaa A, Parviainen T (toim.). Säteilyturvallisuus ja laatu röntgendiagnostiikassa 2001. Helsinki 2001.

STUK-A183 Sinkko K, Ammann M (eds.). RODOS Users' Group: Final project report. Helsinki 2001.

STUK-A182 Mäkeläinen I, Huikuri P, Salonen L, Markkanen M, Arvela H. Talousveden radioaktiivisuus - perusteita laatuvaatimuksille. Helsinki 2001.

STUK-A181 Jalarvo V. Suomalaisten solariuminkäyttö. Helsinki 2000.

STUK-A180 Salomaa S, Mustonen R (eds.). Research activities of STUK 1995 - 1999. Helsinki 2000.

STUK-A179 Salomaa S (ed.). Research projects of STUK 2000 - 2002. Helsinki 2000.

STUK-A178 Rantavaara A, Calmon P, Wendt J, Vetikko V. Forest food chain and dose model (FDMF) for RODOS. Model description. Helsinki 2001.

STUK-A177 Rantavaara A, Moring M. Puun tuhkan radioaktiivisuus. Helsinki 2001.

STUK-A176 Lindholm C. Stable chromosome aberrations in the reconstruction of radiation doses. Helsinki 2000.

STUK-A175 Annanmäki M, Turtiainen T, Jungclas H, Rausse C. Disposal of radioactive waste arising from water treatment: Recommendations for the EC. Helsinki 2000.

STUK-A174 Servomaa A, Parviainen T (toim). Säteilyturvallisuus ja laatu röntgendiagnostiikassa 2000. Koulutuspäivät 24. - 25.2.2000 ja 10. - 11.4.2000. Helsinki 2000.

STUK-A173 Hämäläinen RP, Sinkko K, Lindstedt M, Ammann M, Salo A. Decision analysis interviews on protective actions in Finland supported by the RODOS system. Helsinki 2000.

STUK-A172 Turtiainen T, Kokkonen P, Salonen L. Removal of Radon and Other Natural Radionuclides from Household Water with Domestic Style Granular Activated Carbon Filters. Helsinki 1999.

STUK-A171 Voutilainen A, Mäkeläinen I, Huikuri P, Salonen L, Arvela H. Porakaivoveden radonkartasto/Radonatlas över borrbrunnar/Radon Atlas of wells drilled into bedrock in Finland. Helsinki 1999.

STUK-A170 Saxén R, Koskelainen U, Alatalo M. Transfer of Chernobyl-derived 137Cs into fishes in some Finnish lakes. Helsinki 2000.

STUK-A169 Annanmäki M, Turtiainen T (eds.). Treatment Techniques for Removing Natural Radionuclides from Drinking Water. Helsinki 1999.

STUK-A168 Suomela M, Bergman R, Bunzl K, Jaakkola T, Rahola T, Steinnes E. Effect of industrial pollution on the distribution dynamics of radionuclides in boreal understorey ecosystems (EPORA). Helsinki 1999.

STUK-A167 Thorring H, Steinnes E, Nikonov V, Rahola T, Rissanen K. A summary of chemical data from the EPORA project. Helsinki 1999.

STUK-A166 Rahola T, Albers B, Bergman R, Bunzl K, Jaakkola T, Nikonov V, Pavlov V, Rissanen K, Schimmack W, Steinnes E, Suomela M, Tillander M, Äyräs M. General characterisation of study area and definition of experimental protocols. Helsinki 1999.

STUK-A165 Ilus E, Puhakainen M, Saxén R. Strontium-90 in the bottom sediments of some Finnish lakes. Helsinki 1999.

STUK-A164 Kosunen A. Metrology and quality of radiation therapy dosimetry of electron, photon and epithermal neutron beams. Helsinki 1999.

STUK-A163 Servomaa A (toim.). Säteilyturvallisuus ja laadunvarmistus röntgendiagnostiikassa 1999. Helsinki 1999.

STUK-A162 Arvela H, Rissanen R, Kettunen A-V ja Viljanen M. Kerrostalojen radonkorjaukset. Helsinki 1999.

A full list of publications is available from:

STUK— Radiation and Nuclear Safety Authority
P.O. Box 14
FIN-00881 Helsinki, Finland
Tel. +358 9 759 881

STUK

ISBN 951-712-528-3 (print)
ISSN 0781-1705

Edita Prima Oy, Helsinki 2002